Sabrine Kheriji

Design of an Energy-Aware Unequal Clustering Protocol based on Fuzzy Logic for Wireless Sensor Networks

Scientific Reports on Measurement and Sensor Technology

Volume 16

Prof. Dr. Olfa Kanoun (Editor)

Sabrine Kheriji

Design of an Energy-Aware Unequal Clustering Protocol based on Fuzzy Logic for Wireless Sensor Networks

TECHNISCHE UNIVERSITÄT
CHEMNITZ

Universitätsverlag Chemnitz
2021

Impressum

Bibliografische Information der Deutschen Nationalbibliothek

Die Deutsche Nationalbibliothek verzeichnet diese Publikation in der Deutschen Nationalbibliografie; detaillierte bibliografische Angaben sind im Internet über https://www.dnb.de abrufbar.

Titelgrafik: Chemnitz School of Metrology
Satz/Layout: Sabrine Kheriji

Technische Universität Chemnitz/Universitätsbibliothek
Universitätsverlag Chemnitz
09107 Chemnitz
https://www.tu-chemnitz.de/ub/univerlag

readbox unipress
in der readbox publishing GmbH
Rheinische Straße 171
44147 Dortmund
https://www.readbox.net/unipress/

ISSN 2509-5102 print - ISSN 2509-5110 online

ISBN 978-3-96100-130-9

https://nbn-resolving.org/urn:nbn:de:bsz:ch1-qucosa2-733031

TECHNISCHE UNIVERSITÄT
CHEMNITZ

Design of an Energy-Aware Unequal Clustering Protocol based on Fuzzy Logic for Wireless Sensor Networks

von der Fakultät für Elektrotechnik und Informationstechnik der
Technischen Universität Chemnitz

genehmigte

DISSERTATION

zur Erlangung des akademischen Grades

Doktor-Ingenieur
(Dr.-Ing.)

vorgelegt von

M.Sc. Dipl.-Ing. Sabrine Kheriji

Tag der Einreichung: 21. Juli 2020
Tag der Verteidigung: 18. Dezember 2020

Gutachter: Prof. Dr.-Ing. Olfa Kanoun (Technische Universität Chemnitz)
Prof. Dr.-Ing. Ines Kammoun (Universität Sfax)

Acknowledgments

One of the joys of completion is to look over the journey past and remember all the people who have helped and supported me along this fulfilling road.

First and the foremost, I would like to express my profound gratitude to my Doctor Mother Prof. Olfa Kanoun for providing me the opportunity to pursue my research towards completion of this PhD dissertation. Her wide knowledge and her logical way of thinking have been of great value for me. She was always available to meet and talk about my ideas, to proofread and mark up my papers, and to ask me the right questions, which helped me a lot to come forward in my work and to go through a lot of challenges. It was her enlightening supervision that inspired me to explore novel research areas and broadened my views in the research.

I would like to express my special appreciation and deep thanks to my supervisor Prof. Ines Kammoun who has supporting me with guidance and encouragement throughout my Ph.D. research. She helped me to go through all difficulties I encountered in my research work and thesis writing.

I would like to express my thanks to all my colleagues from the Energy Autonomous Systems (EASys) working group and all my colleagues at the Chair of Measurement and Sensor Technology (MST) at TU Chemnitz. Special thanks go to our group leader Dr. Christian Viehweger, Dr. Sonia Bradai, Dr. Slim Naifar, Dhouha El Houssaini, Ghada Bouattour and Meriem Ben Ammar for their cooperative and helpful feedback.

My sincere thanks also go to the German Academic Exchange Service (DAAD) and the InProTUC program, for the financial support during my thesis.

Last but not least, I express my strongest gratitude to my family, who experienced and shared all the ups and downs of my research. Their support and patience during these years were primordial to keep the motivation, the strength and the enthusiasm high.

Thanks for all your encouragement!

Sabrine Kheriji

Abstract

Energy consumption is a major concern in Wireless Sensor Networks (WSNs) resulting in a strong demand for energy-aware communication technologies. In this context, several unequal cluster-based routing protocols have been proposed. However, few of them adopt energetic analysis models for the calculation of the optimal cluster radius and several protocols can not realize an optimal workload balance between sensor nodes.
In this scope, the aim of the dissertation is to develop a cluster-based routing protocol for improving energy efficiency in WSN. We propose a Fuzzy-based Energy-Aware Unequal Clustering algorithm (FEAUC) with circular partitioning to balance the energy consumption between sensor nodes and solve the hotspot problem created by a multi-hop communication. The developed FEAUC involves mainly four phases: An off-line phase, a cluster formation phase, a cooperation phase and data collection phase. During the off-line phase, an energy analysis is performed to calculate the radius of each ring and the optimal cluster radius per ring. The cluster formation phase is based on a fuzzy logic approach for the cluster head (CH) selection. The cooperation phase aims to define an intermediate node as a router between different CHs. While, in the data collection phase, transmitting data packet from sensor nodes to their appropriate CHs is defined as an intra-cluster communication, and transmitting data from one CH to another until reaching the base station, is defined as an inter-cluster communication. The feasibility of the developed FEAUC is demonstrated by elaborating comparison with selected referred unequal clustering algorithms considering different parameters, mainly, the energy consumption, battery lifetime, time to first node shuts down (FND), time of half of nodes off-line (HND) and time to last node dies (LND).
Although, the developed FEAUC is intended to enhance the network lifetime by distributing the large load of CH tasks equally among the normal nodes, running the clustering process in each round is an additional burden, which can significantly drain the remaining energy. For this reason, the FEAUC based protocol has been further developed to become a fault tolerant algorithm (FEAUC-FT). It supports the fault tolerance by using backup CHs to avoid the re-clustering process in certain rounds or by building further routing paths in case of a link failure between different CHs.
The validation of the developed FEAUC in real scenarios has been performed. Some sensor nodes, powered with batteries, are deployed in a circular area forming clusters. Performance evaluations are carried out by realistic scenarios and tested for

a real deployment using the low-power wireless sensor node panStamp. To complete previous works, as a step of proof of concept, a smart irrigation system is designed, called Air-IoT. Furthermore, a real-time IoT-based sensor node architecture to control the quantity of water in some deployed nodes is introduced. To this end, a cloud-connected wireless network to monitor the soil moisture and temperature is well-designed. Generally, this step is essential to validate and evaluate the proposed unequal cluster-based routing algorithm in a real demonstrator. The proposed prototype guarantees both real-time monitoring and reliable and cost-effective transmission between each node and the base station.

Keywords: Wireless sensor networks, energy consumption, load balancing, optimal cluster radius, circular partitioning, fuzzy logic, test-bed implementation, fault tolerance, IoT.

Kurzfassung

Der Energieverbrauch ist ein Hauptanliegen in drahtlosen Sensornetzwerken (WSNs), was zu einer starken Nachfrage nach energiebewussten Kommunikationstechnologien führt. In diesem Zusammenhang wurden mehrere ungleiche clusterbasierte Routing-Protokolle vorgeschlagen. Allerdings verwenden nur die wenigsten energetische Analysemodelle für die Berechnung des optimalen Cluster-Radius, und mehrere Protokolle können keine optimale Auslastungsbalance zwischen Sensorknoten realisieren.
In diesem Zusammenhang ist es das Ziel der Dissertation, ein clusterbasiertes Routing-Protokoll zur Verbesserung der Energieeffizienz im WSN zu entwickeln. Wir schlagen einen Fuzzy-basierten Energy-Aware Unequal Clustering-Algorithmus (FEAUC) mit zirkulärer Partitionierung vor, um den Energieverbrauch zwischen Sensorknoten auszugleichen und das durch eine Multi-Hop-Kommunikation entstehende Hotspot-Problem zu lösen. Der entwickelte FEAUC umfasst hauptsächlich vier Phasen: Eine Offline-Phase, eine Clusterbildungsphase, eine Kooperationsphase und eine Phase der Datensammlung. Während der Offline-Phase wird eine Energieanalyse durchgeführt, um den Radius jedes Ringes und den optimalen Cluster-Radius pro Ring zu berechnen. Die Clusterbildungsphase basiert auf einem Fuzzy-Logik-Ansatz für die Clusterkopf (CH)-Auswahl. Die Kooperationsphase zielt darauf ab, einen Zwischenknoten als einen Router zwischen verschiedenen CHs zu definieren. In der Datensammelphase wird die Übertragung von Datenpaketen von Sensorknoten zu ihren entsprechenden CHs als eine Intra-Cluster-Kommunikation definiert, während die Übertragung von Daten von einem CH zu einem anderen CH bis zum Erreichen der Basisstation als eine Inter-Cluster-Kommunikation definiert wird. Die Machbarkeit des entwickelten FEAUC wird durch die Ausarbeitung eines Vergleichs mit ausgewählten referenzierten ungleichen Clustering-Algorithmen unter Berücksichtigung verschiedener Parameter demonstriert, hauptsächlich des Energieverbrauchs, der Batterielebensdauer, der Zeit bis zum Abschalten des ersten Knotens (FND), der Zeit, in der die Hälfte der Knoten offline ist (HND) und der Zeit bis zum letzten Knoten stirbt (LND).
Obwohl mit dem entwickelten FEAUC die Lebensdauer des Netzwerks erhöht werden soll, indem die große Last der CH-Aufgaben gleichmäßig auf die übrigen Knoten verteilt wird, stellt die Durchführung des Clustering-Prozesses in jeder Runde eine zusätzliche Belastung dar, die die verbleibende Energie erheblich entziehen kann. Aus diesem Grund wurde das auf FEAUC basierende Protokoll zu einem fehlertoleranten Algorithmus (FEAUC-FT) weiterentwickelt. Er unterstützt die Fehlertole-

ranz durch die Verwendung von Backup-CHs zur Vermeidung des Re-Clustering-Prozesses in bestimmten Runden oder durch den Aufbau weiterer Routing-Pfade im Falle eines Verbindungsausfalls zwischen verschiedenen CHs.
Die Validierung des entwickelten FEAUC in realen Szenarien ist durchgeführt worden. Einige Sensorknoten, die mit Batterien betrieben werden, sind in einem kreisförmigen Bereich angeordnet und bilden Cluster. Leistungsbewertungen werden anhand realistischer Szenarien durchgeführt und für einen realen Einsatz unter Verwendung des drahtlosen Low-Power-Sensorknoten panStamp getestet. Zur Vervollständigung früherer Arbeiten wird als Schritt des Proof-of-Concept ein intelligentes Bewässerungssystem mit der Bezeichnung Air-IoT entworfen. Darüber hinaus wird eine IoT-basierte Echtzeit-Sensorknotenarchitektur zur Kontrolle der Wassermenge in einigen eingesetzten Knoten eingeführt. Zu diesem Zweck wird ein mit der Cloud verbundenes drahtloses Netzwerk zur Überwachung der Bodenfeuchtigkeit und -temperatur gut konzipiert. Im Allgemeinen ist dieser Schritt unerlässlich, um den vorgeschlagenen ungleichen clusterbasierten Routing-Algorithmus in einem realen Demonstrator zu validieren und zu bewerten.Der vorgeschlagene Prototyp garantiert sowohl Echtzeit-Überwachung als auch zuverlässige und kostengünstige Übertragung zwischen jedem Knoten und der Basisstation.

Schlagwörter: Drahtlose Sensornetzwerke, Energieverbrauch, Lastausgleich, optimaler Clusterradius, zirkuläre Partitionierung, Fuzzy-Logik, Prüfstandsimplementierung, Fehlertoleranz, IoT.

Contents

CHAPTER 1

Introduction

1.1 Motivation and problem statement

Internet of Thing (IoT) is nowadays of high interest in several fields of science and technology including the smart home, precision agriculture and e-health [1–3]. In particular, Wireless Sensor Networks (WSNs), are thereby gaining importance as enabling technology for monitoring and decision making [4, 5]. With numerous sensors deployed and ubiquitous in various applications, WSNs become significantly complex as they integrate many functionalities aiming to satisfy the applications requirements. This includes the ability of sending and receiving data in real-time, which requires mainly sophisticated analysis tools as well as a sufficient amount of energy to ensure the communication within the network. A WSN is composed of a base station (BS) and a number of sensor nodes, where data is gathered and transmitted to the base station. Sensor nodes are maybe powered with limited energy sources, basically small batteries, which are difficult to recharge or to change, specially in a large field or in inaccessible positions such as underwater monitoring [6, 7].

In this context, various energy conservation techniques have been introduced as enabling technologies to boost the network efficiency and operability. The distributed capability of sensors is very important, since the data transmission presents the most consumed task in a WSN. Uploading data directly from a sensor node to the BS may result in long communication distances and degrades the energy of nodes. It is therefore interesting to use local processing as much as possible to minimize the data to be transmitted by each node to the sink.

For these reasons, hierarchical routing protocols have been introduced as energy efficient network protocols [8, 9]. They, basically, implement clustering approaches to organize nodes into sub-regions. As seen in Fig. 1.1, in each region, one node is selected as a cluster head (CH), which collects data packets from its cluster members and transmits them to the sink node or to the BS using single-hop or multi-hop communication schemes. By shorting the distance between the source and destination nodes, the energy consumption is reduced and the overall network lifetime is enhanced.

In several cluster-based routing protocols, the communication between a sensor node and its corresponding CH or between a CH and the BS is assumed to be a single-hop.

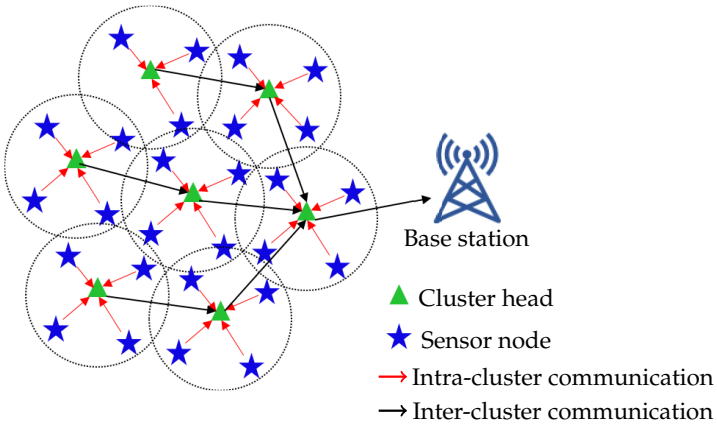

Figure 1.1: A cluster-based routing model.

This kind of communication is suitable only for a network with small area size or for a network with a few number of sensor nodes [10]. CHs far away the BS deplete their energy faster than others. To avoid this issue, multi-hop communication schemes can be applied [8, 11]. As seen in Fig. 1.1, CHs are used as intermediate nodes for other CHs. Since the energy consumption is proportional to the square of the distance, decreasing the distance between the source and destination nodes reduces the overall consumed energy significantly. In this case, the consumed energy between different CHs is balanced.

However, the CHs closer to the BS have an extra overload by an enormous traffic, since the data of the whole network is transmitted through them to the sink node. Thereby, they are prone to deplete their batteries earlier than other CHs, which is commonly defined as the hotspot problem. Furthermore, these nodes die early and the network can be isolated. For this reason, unequal sized clustering schemes, where the size of cluster is reduced from one hop to another from the BS, are advantageous in large area networks [8, 9]. To this end, the design of a new unequal clustering algorithm for WSNs, which can considerably balance the energy consumption among all clusters and achieve a noticeable improvement on the network lifetime is highly required. Thus, minimizing the intra-cluster communication, defined as the communication between a CH and its cluster members, can improve the bandwidth utilization and reduce the overhead.

The number of clusters is a promising factor affecting the energy efficiency of the unequal clustering. As the number of clusters becomes larger, the distance between CHs and their cluster members is shortened. Nevertheless, the energy consumed by the CHs increases proportionally to the number of clusters. Therefore, considering the optimal number of clusters is a key issue in a WSN, which is highly taken into account in this dissertation.

Additionally, WSNs are subject to different failures including hardware or software failures, power depletion, poor communication connectivity and harmful attacks. Thus, fault tolerant technique is introduced as another key issue in WSNs. Moreover, the most existing unequal cluster-based routing protocols support the fault tolerance technique by performing the re-clustering process, which consists on changing the CH at periodic intervals by fixing a threshold value. In this case, the additional communication overheads are reduced and the total number of transmitted packets is minimized leading to the extension of the network lifetime. For this reason, avoiding the re-clustering in some time has a great impact to conserve the consumed energy needed for the selection of CHs.

Numerous unequal clustering algorithms have been used in the literature to investigate the energy efficiency [12, 13]. However, there is a very limited research available on the practical implementations for cluster-based routing protocols. It is important to evaluate any proposed protocol on real hardware by considering real obstacles and real environment conditions.

1.2 Thesis focus and main contributions

The network lifetime is challenging due to the high demand of energy for the data transmission process. Thus, this work is mainly devoted to develop a novel energy-aware fuzzy-based unequal clustering protocol, to balance the energy consumption between different nodes in the network. In this respect, the main contributions of this thesis are summarized in the following points:

- An energy analysis model is developed aiming to determine the optimal number of clusters and the optimal cluster radius before the node deployment. To ensure a full coverage, the optimum unequal clustering (FEUAC) approach uses a circular partitioning model rather than a rectangular model.
- A non-probabilistic CH selection using a fuzzy logic system is used, where the node residual energy, node centrality and node density are considered to compute the fuzzy cost of CHs.
- An energy efficient cooperative communication method is developed to prevent long haul transmissions between CHs. A relay node is selected to forward the data from its appropriate CH to another CH within its transmission range.
- A real test-bed implementation for the developed FEAUC protocol is carried out. A comparison of the real implementation to simulation in terms of network residual energy and total received packets at the BS is investigated in this work.
- A dynamic autonomous energy consumption measurement circuit based on shunt resistor is designed to measure in real time the residual energy in each battery.
- Since sensor nodes are prone to faults, the developed FEAUC supports the fault tolerant technique. To this end, a backup CH is selected when the residual

energy of the primary CH is not enough to run the current round leading to reduce the consumed energy during the re-clustering process. Moreover, the inter-cluster fault tolerant technique consists on building a backup routing path in case of link failure between CHs from different rings.

- A smart irrigation system (Air-IoT) is designed as a proof of concept to validate the efficiency of the developed FEAUC in a real environment. A real-time IoT-based sensor node architecture to monitor both soil moisture and temperature is developed to adjust automatically the watering schedule.

1.3 Thesis outline

The thesis is structured in seven chapters as depicted in Fig. 1.2. In **Chapter 1**, the motivation of using unequal clustering protocols for energy balancing is described. This chapter introduces the problem statement, main contributions and focus of the entire thesis. Then, **Chapter 2** illustrates a detailed overview of energy constraints and available energy conservation techniques in WSNs. Cluster-based routing protocols are presented as a promising approach to improve the energy efficiency in WSNs. Indeed, a deep study of clustering approaches is provided including their objectives, attributes, challenging factors affecting them and performance metrics. The importance of the determination of the optimal size of a cluster is discussed.

Chapter 3 is intended as a survey of recent unequal cluster protocols, which are classified according to the CH selection to three categories, namely, random-based, deterministic-based and preset-based algorithms. A detailed description for each category is given with relevant related works. Afterwards, a comparative study to discuss different defined algorithms is provided.

Chapter 4 deals with the development of the novel fuzzy-based energy aware unequal clustering protocol, where the shape of the network is considered as circle. Aspects related to the FEAUC are explained, mainly the network model, the energy analysis and the working principle. Obtained results are elaborated and compared with some referred unequal clustering algorithms. A comparison with similar works in the literature is performed. In addition, a comparison between the elaborated FEAUC with and without applying the fault tolerant technique is illustrated.

A test-bed implementation of the developed unequal clustering protocol is carried out in **Chapter 5** to evaluate its efficiency on real hardware. Experimental results obtained with the wireless node panStamp are analysed and compared to the simulation results. Afterwards, to evaluate the proposed FEAUC in real cases, a smart irrigation system is designed in **Chapter 6**. A real-time IoT-based sensor node architecture is proposed to adjust automatically the watering schedule for some deployed nodes.

Finally, **Chapter 7** summarizes the main results of this work. In addition, conclusions and future trends are provided.

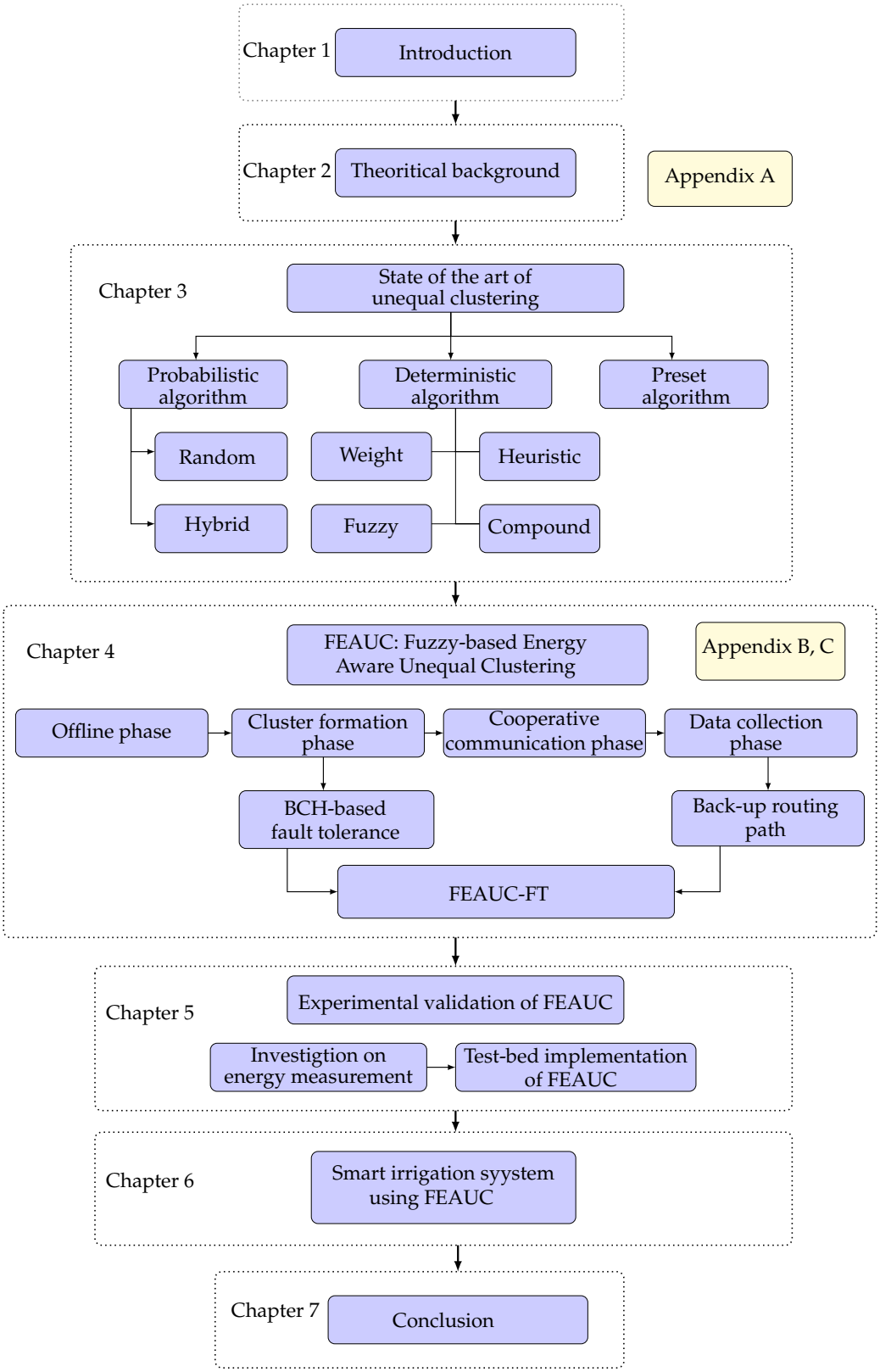

Figure 1.2: Thesis structure.

CHAPTER 2

Theoretical background

A wireless sensor node consists of a sensing unit for collecting physical data from surrounding and converting it to digital values, a processing unit used for data treatment and storage, a communication unit used for exchanging data packets between different sensor nodes or the end-user and a power unit used for supplying the sensor node [14]. Fig. 2.1 presents the general architecture of a sensor node.

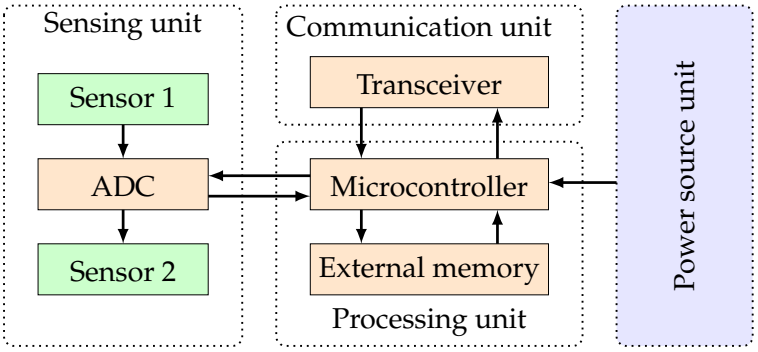

Figure 2.1: Sensor node architecture [15].

However, the main limitation of such architecture is the power source unit. Having a limited amount of energy can affect the network performance, lifetime and the Quality of Service (QoS) [16]. Changing batteries becomes difficult and even impossible in some scenarios such as in harsh environment [17, 18], where the accessibility and maintenance are costly and limited. For this reason, many efforts have been made to minimize the energy consumption of sensor nodes and extend their useful lifetime by adopting various approaches at different levels [8, 9, 15, 19, 20]. An auxiliary solution is to harvest the energy from the ambient or to use rechargeable batteries [21–24].

In this chapter, a detailed overview of energy constraints and available energy conservation techniques in WSNs is described. Cluster-based routing protocols are presented as a promising approach to improve the network energy efficiency.

2.1 Sources of energy losses during communication

Energy-constraint is a challenging feature for WSNs [15, 25, 26]. Generally, sensor nodes consume energy while sensing, processing, transmitting or receiving data.

This can be defined as useful power consumption. Fig. 2.2 illustrates an estimation-based energy consumption model for a wireless sensor node [27], which declares that the communication unit is the most energy consuming part. For this reason, it is crucial to develop energy saving methods during the communication process.

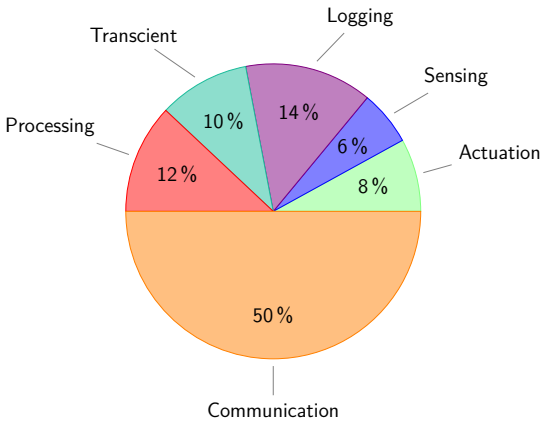

Figure 2.2: Components of energy consumption in WSNs.

However, nodes can consume the power in a inefficient way. To deal with the problem, major sources of energy dissipation need to be identified. Data are travelled from one node to another via the radio propagation, which is sensitive to various energy issues mostly the data collision, interference, idle listening and overhearing [15, 28, 29].

Data collision [15, 30–32] is considered as a primary source of energy dissipation during the data transmission. As shown in Fig. 2.3(a), this issue happens when two or more nodes attempt to send a data packet at the same time over the same channel. These packets have to be discarded and re-transmitted after certain time leading to energy loss and additional costs in terms of time execution and workload. In this context, it is important to define a scheduler to organize the transmission of packets between different nodes with a strict synchronization leading to reduce the number of communicated packets and therefore, the energy dissipated.

Another issue for energy losses during the data transmission is called overhearing [33], which is described in Fig. 2.3(b). It happens when a source node transmits a message and some nodes within its communication range can listen to the broadcast packet while they are not the intended recipient of the broadcast. As a consequence, neither the corresponding node receives the desired packet nor does the erroneous receiver get a coherent data. The packet should be re-transmitted to the right destination. Node dissipates effort in receiving a data packet destined for another node.

Data communication is based on radio signal propagation model, which is susceptible to various issues such as diffraction, wave attenuation and reflection. In this case, the affected signal needs to be re-transmitted many times via different paths until reaching the destination node, leading to additional energy utilisation. Nodes

can receive the transferred data packet, but they can not use it since they can not decode or extract it. This can be defined as an interference problem [34, 35], which is depicted in Fig. 2.3(c).

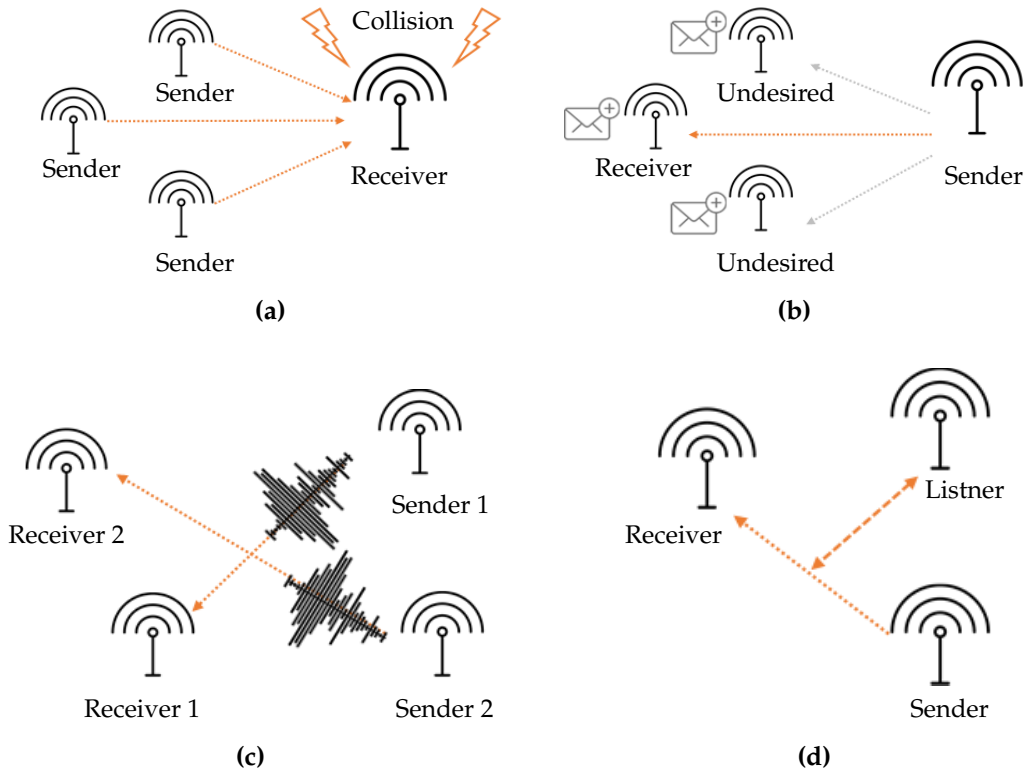

Figure 2.3: Energy consumption issues during data transmission: (a) Packets collision (b) overhearing (c) interference (d) idle listening.

As seen in Fig. 2.3(d), the idle listening occurs when a node is active but no data is transmitted, processed or received by the sensor node [36, 37]. To avoid that, the radio needs to be off when there is no data to send or to receive and it should be restarted as soon as the new packet is ready for the transmission. In this way, nodes switch between active (receive, transmit) and sleep states periodically. This can be defined as a state transition or duty cycle [38]. In fact, it can save the available amount of energy for each node and consequently extends the network lifetime.

According to this study, it is important to design intelligent and up-to date solutions to minimize the energy consumption of a node during the data transmission process in a way to conserve the energy consumption of the entire network as well as the network lifetime [36, 39, 40].

2.2 Energy saving techniques

After identifying the major sources of energy losses during the data communication, it is important to highlight the developed techniques used by numerous scholars to avoid such issues. A comprehensive review on energy saving schemes is described in

[15]. As depicted in Fig. 2.4, these techniques are mainly classified into four segments: Duty cycling, routing protocols, data-driven and mobility-driven approaches.

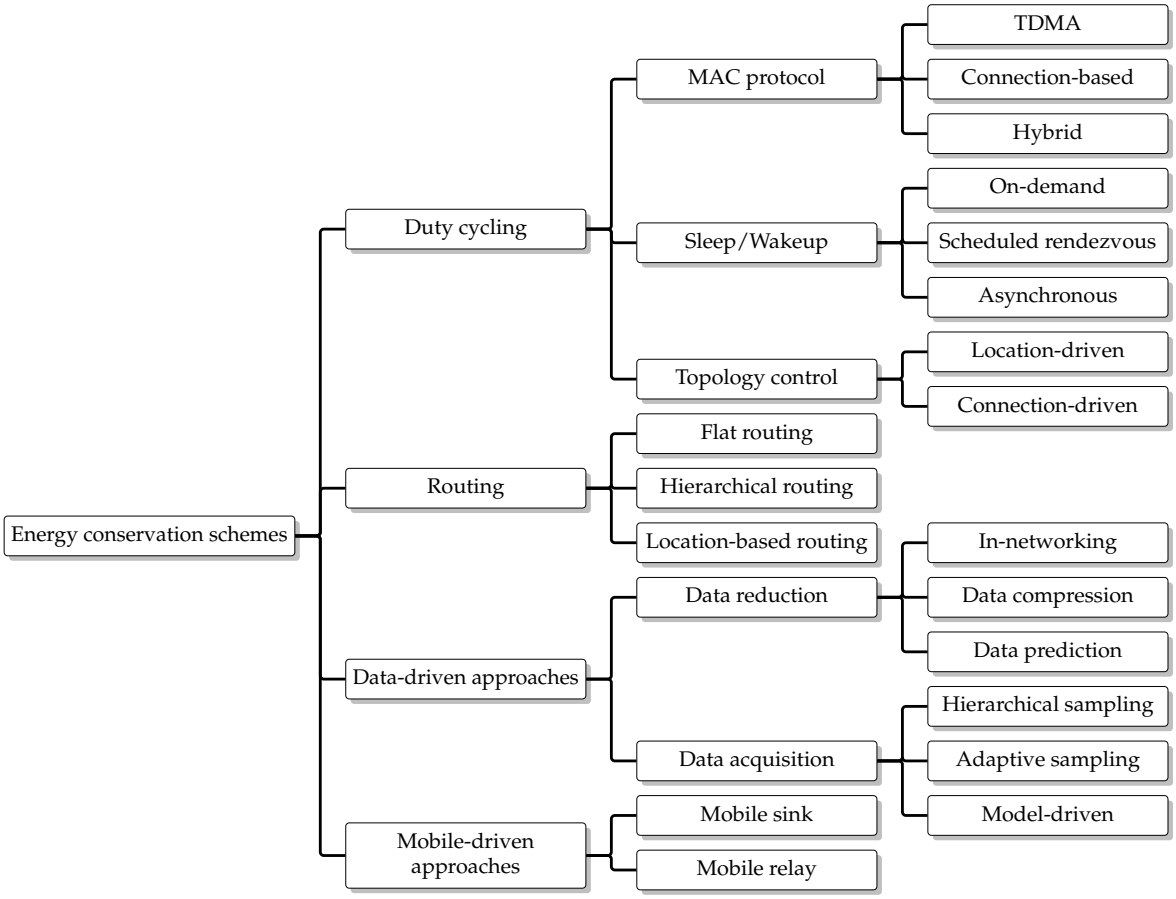

Figure 2.4: Energy saving schemes in WSNs.

Duty cycling techniques define the time during which a node is operating [38, 41]. They are used to manage the active and sleep states of a transceiver in order to check the power consumption during the transmission process. The non-structured transmissions and receptions lead to power losses. To manage and reduce that, the routes between nodes should be well-defined and monitored. A satisfactory routing protocol is highly required to extend the network lifetime. Data-driven techniques can decrease the number of messages to be sensed, treated and transferred to the destination node or to the BS. Mobility-driven approaches can provide, generally, a high amount of energy for a mobile node with specific capabilities leading to decrease the distance between different nodes in the network.

2.2.1 Duty-cycling

Duty cycling is introduced as one of the most energy efficient reduction techniques, which is based on turning off the node most of the time and wakes up it only if needed or at scheduled moments [38, 41]. Generally, this technique can be divided into three categories: Topology control, sleep/wake-up and MAC protocols [15].

The topology control technique can not only extend the network lifetime but also maintains the network connectivity by setting the density of nodes and the needed transmitting power to send or receive a data packet to another or from a node, respectively [42]. Herein, the number of deployed nodes is not well managed, which overloads the network in case of adding new or useless nodes. Moreover, this technique ensures the surveillance of message dissemination in an effective form by offering good modelling for energy efficient multi-casting and broadcasting. It can be divided into two classes: Location-driven and connectivity-driven. The location-driven approach determines the state of the node either in active or in sleep mode and assigns which node to wake up and when exactly depending on the location of such node, which is known previously. The connectivity-driven approach is used to activate and deactivate dynamically a sensor node to ensure a full coverage and maintain the network connectivity.

Sleep/wake-up protocols decrease basically the period that a radio still remains in the idle mode [43]. They can be divided into three categories: On-demand, scheduled rendezvous and asynchronous protocols [15]. In the case of on-demand protocols, a sensor node is turned on only if it receives a message from its neighbours. By using multiple radios with low data rate and transmission power, the sleeping node can be informed with possible nodes attempting to communicate with. For the scheduled rendezvous protocols, all the sensor nodes are periodically active for a determined interval of time, and then they are turned off until the upcoming rendezvous. All nodes need to be synchronized ensuring the interoperability at the same time. Asynchronous protocols present an alternative solution for the duty-cycling, which enable nodes to select their own time to wake-up and to sleep. Therefore, when a node is able to communicate with other nodes, it picks out a time to wake-up. This scheme allows each node to check independently its wake-up/sleep time frames.

The third category of duty-cycling technique consists on using efficiently the channel access. The Medium Access Control (MAC) protocols [44] are introduced to organize the communication between a node and each node in the same network or in other networks by fixing a transmission time for each node. The MAC protocol avoids the data collision by providing channel access and addressing mechanisms. The Time Division Multiple Access (TDMA) divides the time axis into different frames with specific size. Each frame is defined by a fixed number of time slots [45]. Slots are assigned to nodes for sending or receiving data, and when there is no activity, the node radio goes to sleep. A node can transmit data only in its pre-assigned time slot. Thus, this method avoids the interference from neighbouring nodes. Embedded channel access functionalities with a sleep/wake-up strategy is defined as contention-based protocols, which consist basically on the Carrier Sense Multiple Access (CSMA) or Carrier Sense Multiple Access/Collision Avoidance (CSMA/CA) [46]. In the CSMA, each node should listen to the channel before transmitting its data. When the channel is busy, the node has to delay its access and retry the same procedure until the channel becomes free. At this moment, it is able to transmit its

data. The use of the CSMA forces nodes to be awake to listen to the channel, which increases their energy consumption. This technique is not useful for the high density network. Hybrid MAC protocols combine TDMA and CSMA protocols admitting to variable traffic models [47]. They use some important information such as routing plans and the list of neighbours from superior layers to enhance their performance. These protocols eliminate the overhearing problem caused by the neighbouring nodes and control the channel access. Zebra Media access Control (Z-MAC) protocol presents an example of hybrid MAC protocols, which allows the network to work at low data load as in CSMA and at high network traffic as in TDMA [48].

2.2.2 Data-driven approaches

Data-driven schemes can be classified, depending on the issue that they address. Data reduction approaches are used in case of useless or redundant data, and data acquisition approaches are used to reduce the consumed energy during the sensing process [49]. Despite they have different principles, both approaches attempt to decrease the sent messages to the sink node.

Data reduction schemes reduce the size of data to be sensed, processed and transmitted to the sink node by converting it to a smaller entity, which can be decoded by the sink leading to decrease the energy consumption of the network. These schemes can be classified into three categories: Data compression, in-network processing and data prediction [50]. Data compression technique aims to compress the sensed data by the node itself or by an aggregator node. Then, only the needed data is transmitted to the destination. When the received data are decompressed by the sink node, various methods can be carried out such as Kalman filter, lossless compression and adaptive model selection [51–53]. The in-network processing technique performs data aggregation at the relay node, which is used to gather data from different nodes and deliver it to the sink node in a single packet. Thus, the amount of data is reduced and then the consumed energy is decreased. Data prediction technique focuses on the abstraction of the sensed data. It predicts the generated values from the sensor node within a certain error, and generates two instance models; one in the sink node and the other one at the related source node. Once the used prediction model is accurate, the sink can answer any query issued by the user, without communicating to the source node and has the exact value. In case of having inaccurate prediction model between sink and sensor nodes, the used model needs to be updated. Thus, using data prediction techniques can reduce the amount of message delivered from the source node to the sink and thus the required energy for the communication is reduced as well.

On the other side, data acquisition schemes are used to reduce the energy consumption during the sensing process by decreasing the data samples. These schemes are divided into three techniques: Hierarchical sensing, adaptive and model-based sampling [54]. In the first technique, sensor nodes need to be heterogeneous, i.e. equipped with different types of sensors. By selecting dynamically which class

to activate, this technique provides a balance between data accuracy and energy conservation. Adaptive sampling approaches minimize the amount of data packets to be acquired from the receiver node using spatial or temporal correlation. This approach is mostly used in centralized network, where the sink node needs a high computational effort to process all the received data from different sources. The third technique is based on model-driven approaches by building a model for the sensed event on a sample data to forecast the upcoming data. So, the amount of messages to be delivered to the sink node is reduced and thereby the consumed energy is decreased as well.

2.2.3 Mobility-driven approaches

Generally, the mobility of sensor nodes can be performed in two ways; either by placing the node in a mobile element or by installing a mobilizer in the node itself [55]. Since the mobilizer is energy consuming, adding the mobility in WSNs leads to a higher energy consumption. For this reason, the mobilizer can be installed only on nodes with less energy constrained compared to other normal nodes. In this case, the mobility is absolutely attached to heterogeneous network, where sensor nodes have different capabilities.

In the second case, all the sensor nodes in the network are putted onto mobile entities or a number of them are mobile and others are stationary. Therefore, both ways do not need extra energy consumption overhead because of adding the mobility aspect. However, it is necessary to consider the mobility pattern during the network planning and design.

Using the mobility of nodes in WSNs ensures a full network coverage and connectivity. For example, in a large scale area, mobile nodes can reach all isolated nodes. In case of hardware distortion and physical obstacles, deploying random nodes can be insufficient to cover a specific field as expected. For example, using aircraft can be a good solution to gather data and to cover all the nodes in the network. Besides, the mobility can be used, in some cases, to re-arrange the network and avoid the splitting, in a way that all nodes are well-connected. Therefore, the network lifetime is prolonged. Moreover, the mobility presents an efficient technique for minimizing the energy consumption. In fact, sensor nodes use multi-hop communication schemes to reach the sink node. So, the nodes closer to the sink are used as intermediate nodes. They are overloaded with several packets and their energy is depleted quickly. In this case, a mobile node can be used to collect data from normal nodes and then the consumed energy from different nodes can be uniformly distributed. The energy of ordinary nodes can be saved due to less contention overhead and link errors. In both cases, the mobile entity can be a mobile sink or a mobile relay. Generally, mobile sinks and relays are used to inform nodes with their new positions and to gather data from multiple sensors.

2.2.4 Routing

As a valuable energy conservation technique, routing protocols [56] aim to select the best reliable shortest path between the BS and nodes in the same network (inter-network) or between or across networks (intra-network). In a large scale network, some nodes are likely out of the transmission range of the sink node. Besides, the number of sensor nodes is not stable. Sometime, new nodes are added to the network and others are dead, thus can affect the network topology. So, routing a message through other nodes is essential to cover all the area. Depending on the design constraints for each network structure, different routing protocols can be developed including flat (data centric), hierarchical (clustering) and location-based (geographic) routing [57].

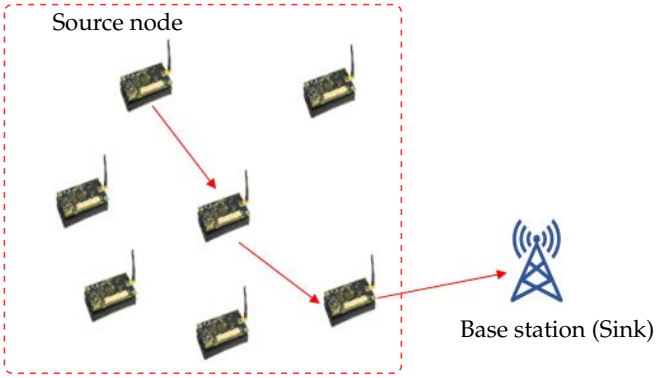

Figure 2.5: Flat-based routing process.

Flat routing protocols are called also data centric protocols [56] in where all nodes have the same role, and they communicate together to perform various sensing tasks. As seen in Fig. 2.5, the node source transmits its data packet to a specific node called sink. From the beginning, the sink node sends queries to nodes within the same sensing area and then still waiting for data from nodes located in the selected area. The intermediate nodes aggregate data from multiple sources within the deployment region and forward the collected data toward the sink. Thus, the transmission of data is reduced and the redundant data is avoided, and so, the energy of the whole network is saved. Numerous protocols are designed such as Sensor Protocol for Information via Negotiation (SPIN) [58], Direct Diffusion [59], Rumor Routing [60].

Location-based routing protocols, known also as geographic routing protocols, use the information about the location of nodes instead of its associated network address. As depicted in Fig. 2.6, each source node knows the geographic position of its destination and it is not provided with the position of the entire network. Generally, these protocols are used to locate the position of sensor nodes and, thus, calculate the distance between two known nodes. To compute the nearest neighbouring node distance, two techniques can be applied; either using the incoming signal strengths or the Global Positioning System (GPS) [61]. Then, the relative nodes coordinates can be determined via exchanging information between each others. Some query packets need to be transmitted to a precise region of interest. It helps to avoid the problem

of route discovery and therefore minimizing the routing overhead. Many protocols have been implemented in the literature including Geographical and Energy Aware Routing (GEAR) [62] and Greedy Perimeter Stateless Routing (GPRS) [63].

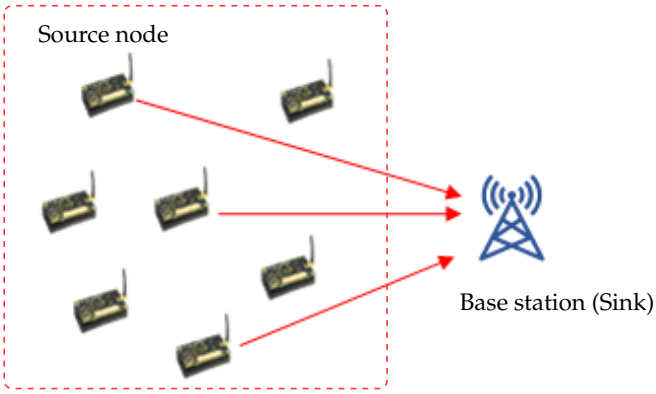

Figure 2.6: Location-based routing process.

The traditional routing protocols (flat and location-based) are not sufficiently optimal in terms of energy efficiency and load balancing [15, 57]. Hierarchical (cluster-based) routing is introduced as an energy-efficient communication protocol [8]. As presented in Fig. 2.7, it depends on three kind of nodes defined as follows: Normal Nodes (NN), CH and BS. In fact, NNs sense the environment, get data, and forward it to their associate CHs, which aggregates in its turn data from its cluster members. The main objectives of hierarchical routing is manage efficiently the energy consumption of the whole network. In addition, to minimize the amount of transmitted packets from the CH to BS, the clustering may include data aggregation and fusion techniques, which can reduce the overload as well as the packets loss.

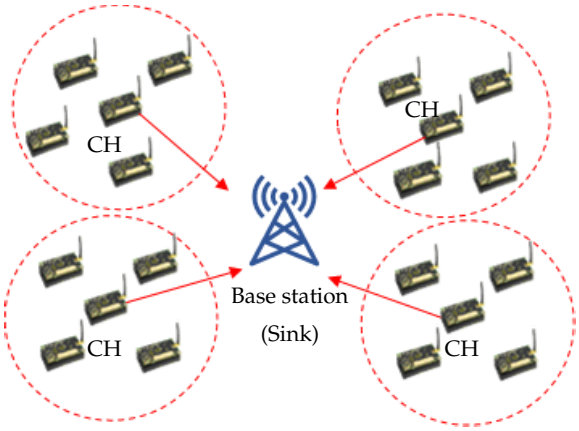

Figure 2.7: Cluster-based routing process.

2.3 Cluster-based routing protocols

After providing a deep review on the most energy conservation techniques in WSNs, this chapter focuses also on the theory and fundamentals related to the development

of cluster-based routing protocols as one of the most promising and effective solution for the network energy reduction. Their characteristics can be summarized in the taxonomy given in Fig. 2.8, including cluster attributes, challenging factors affecting clustering algorithms and their performance parameters.

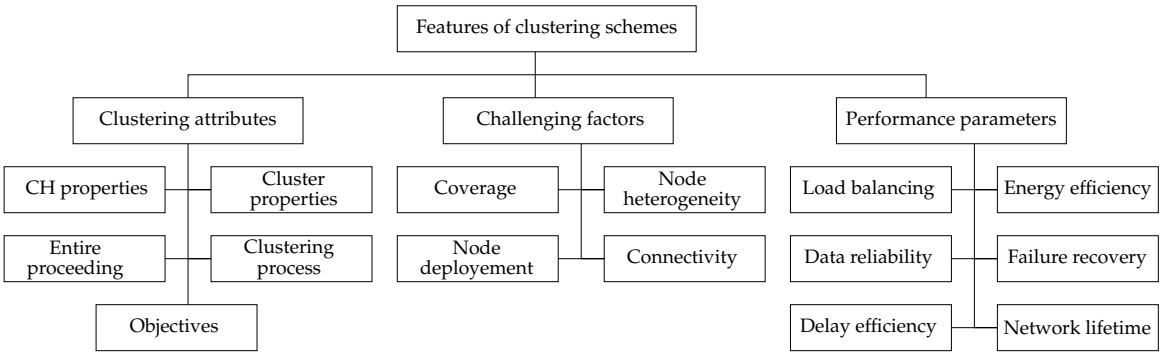

Figure 2.8: Features of cluster-based routing protocols.

2.3.1 Clustering attributes

As depicted in Fig. 2.9, clustering attributes can be divided into cluster properties, CH properties, clustering process characteristics and entire proceeding of the algorithm. A detailed description of different clustering attributes is discussed in this section.

- **Cluster properties**

Defining the properties of a cluster is important in the clustering process. As seen in Fig. 2.9, the characteristics of a cluster can be split into four subsets: Variability of the cluster count, uniformity of the cluster size, intra-cluster and inter-cluster routing.

Cluster count: The number of clusters can be fixed or variable depending on the application requirements. In some applications, the set of CHs are predetermined in advance and the number of CHs is fixed. In other applications, the CHs are selected randomly and so the number of these CHs are variable.

Cluster size: It can be classified into two categories: Equal or uniform and unequal or non-uniform size cluster. In equal clustering, all the formed clusters have the same size, while in unequal clustering, the size of cluster is variable and it is defined based on the distance to the BS. More details about the unequal clustering is given in section 2.4.

Intra-cluster routing: Transmitting a data packet from a cluster member to its corresponding CH is defined as an intra-cluster communication. It includes two classes: Single-hop and multiple-hop intra-cluster connectivity. For the single-hop, all the normal sensor nodes transmit its data directly to the associate CHs while in multi-hop, they use a relay node to forward data to the corresponding CH.

Inter-cluster routing: The inter-cluster communication involves the data transmission between different CHs. Every CH forwards the collected packets and its own

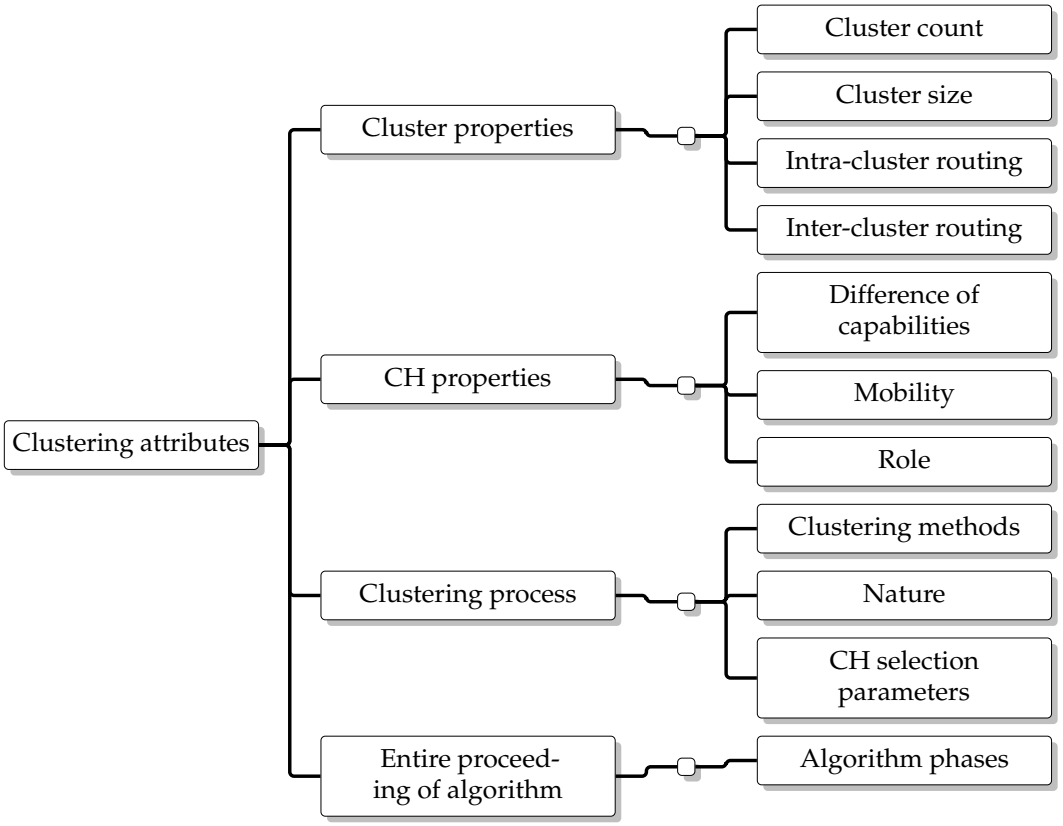

Figure 2.9: Taxonomy of clustering attributes in WSNs.

packet to the BS either directly, called single-hop communication scheme or through an intermediate CH, defined as a multi-hop communication scheme. Generally, multi-hop communication is used for large scale WSNs.

- **Cluster process properties**

Clustering methods: There are three methods of clustering, which are centralized, distributed and hybrid ones. In centralized techniques, the CH is selected by the BS or by a super node based on different parameters such as the residual energy, distance to the BS, number of hops. In this case, the number of CHs is pre-defined. Once a CH is selected, it remains static for the complete network lifetime. Generally, these approaches are used for small-scale networks. In distributed clustering methods, there is no central node, which controls the entire network operation. For each cluster, the node that satisfies specified conditions is selected as a CH independently of other nodes in the network. When another cluster member fulfils the requirements of being a CH, it announces itself as a new CH and the previous CH becomes a normal node. The selection of a CH is dynamic, which gives an equal chance for all nodes to be a CH, thus, the energy consumption of nodes in the network can be balanced. Hybrid methods present a combination of centralized and distributed approaches. In this case, distributed methods are used to ensure the coordination between CHs, while centralized methods are used to help CHs to establish individual clusters.

Nature: The clustering process can be proactive, reactive or hybrid. In proactive routing, also known as table-driven routing, each node continuously keeps directing information up-to-date to any other node in the network. The routing data is transmitted through the network building a routing table. The data transmission happens without delay, if the route was already in place before the arrival of the traffic. Otherwise, traffic packets needs to wait in the queue until the node receives the routing data that matches its destination. Different proactive protocols are developed such as Wireless Routing Protocol (WRP) [64], Cluster-head Gateway Switch Routing (CGSR) [65], Destination Sequenced Distance Vector (DSDV) [66] and Optimized Link State Routing protocol (OLSR) [67]. However, the table-driven routing protocols are not appropriate for wide-area networks, because each entry of a node needs to be managed in the routing table. This involves more overhead in the routing table, which increases the bandwidth usage.

In reactive protocols, also known on-demand routing protocol, a node starts a routing discovery or a routing activity at the network only when it needs to transmit a data packet to another node. Once the node builds a route to active destinations, a maintenance process is carried out to adjust the established route until it is no longer needed or the destination node can not be reached. Various reactive protocols are proposed such as the Ad-hoc On-demand Distance Vector routing (AODV) [68], Associativity-Based Routing (ABR) [69], Dynamic Source Routing (DSR) [70] and Signal Stability Routing (SSR) [71]. Hybrid routing protocols combine the merits of proactive and reactive routing protocols by getting data periodically as well as information about any threshold surpass. According to the application requirements, the route discovery fashion is assigned. Each path manner has some ups and downs. They are related to the time critical responses, data reports gathering, complexity, overhead, etc.

- **CH properties**

Difference of capabilities: Clustering methods can be homogeneous or heterogeneous. They called homogeneous, when nodes have the same capabilities such as the initial energy, transmission range, communication and computation resources. In this case, CHs are selected randomly or via defined criteria. While, in heterogeneous schemes, nodes have different performances and nodes with more capabilities are selected as CHs.

Mobility: Clustering methods can be stationary or mobile. In stationary clustering, CHs are placed in fixed positions and clusters are stables. However, in mobile clustering, CHs are mobile and cluster members are changed dynamically. Thus, a continuous maintenance of clusters is required.

Role: A CH receives data from its cluster members, aggregates the collected data and forwards it directly to the BS or via another CH or a relay node in case of the multi-hop communication.

- **Entire proceeding of algorithm**

In general, cluster-based routing algorithms often include four stages: CH selection, cluster formation, data aggregation and data transmission. The network schedule is split into different rounds of fixed periods. Each round includes two phases, namely, setup phase and steady-state phase. The CH selection process is performed during the setup phase. The steady-state phase attempts to aggregate data and ensures the data communication. For this reason, this phase is divided into different frames. In each frame, the sensor nodes transmit their data to the corresponding CH, which forwards it to the BS. The timing diagram of these two phases can be more explained in Fig. 2.10.

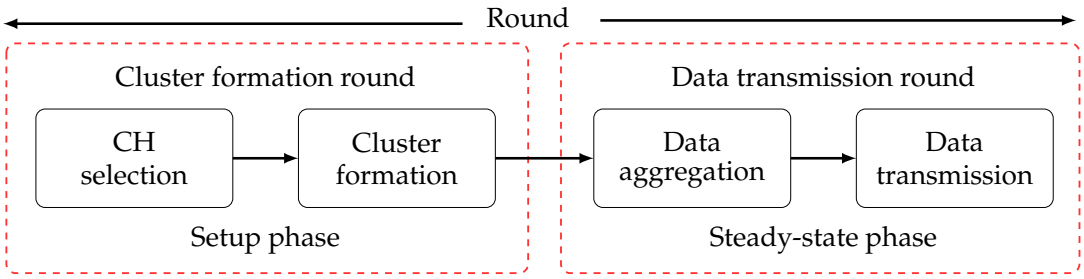

Figure 2.10: Phases of cluster-based routing in one round.

- **Objective of clustering**

Scalability: In a real-world scenario, sensor nodes can be deployed in a large number ranging from hundreds to thousands [2] depending upon the requirement of the application. Hierarchical architecture gives the adaptability in a large scale WSN by partitioning the detecting field into different layers and each layer is again partitioned into a number of clusters. This prompts to expand the scalability and decreases the extent of the routing table.

Data aggregation fusion: The main goals of this method is to reduce the number of data to be transmitted and avoid excess transmission. In cluster-based routing schemes, CH collects data from its cluster members and forwards it to the BS directly or through some relay nodes. Thus, the number of transmitted messages as well as the aggregate load of the system are reduced.

Increased lifetime: As sensor nodes are energy constrained, increasing the network lifetime is vital for real time applications. Selecting a CH with high capabilities can reduce the intra-cluster communication as well the consumed energy.

2.3.2 Challenging factors affecting cluster-based routing protocols

One of the most important aims behind designing a WSN is to ensure a successful data communication while involving the network longevity and preventing the degradation of the connectivity by using or developing energy efficient management methods. In this context, cluster-based routing protocols are considered as one of

the most significant techniques for the energy saving. For this reason, it is important to study the factors that influence the design of such protocols. These factors can be described in details in this section.

- Coverage

It can be defined as the number of nodes used to control an area by their sensing capabilities. Since sensor node has a short communication range, it can only cover a small area. For this reason, the network coverage can affect the network performance.

- Node deployment

The deployment of sensor nodes is defined by the requirement of the application and the available circumstances, which have effects on the productivity of a routing protocol. The node deployment can be either randomized or deterministic. In the random node deployment, an optimal clustering algorithm is important to prevent the connectivity abasement and to ensure a full network coverage. Indeed, the right position of the CH and the sink node can provide an energy efficient network operation. In deterministic deployment, nodes are manually placed at fixed positions and the routing paths are preset.

- Node/Link heterogeneity

In numerous cluster-based routing algorithms, nodes are assumed to be homogeneous, i.e, having the same communication range, initial energy and computation and processing capabilities. However, according to the application requirements, each sensor node is responsible for a specific function and can integrate multiple sensors. WSN can include sensor nodes with various characteristics. Different types of antennas and sensing devices result in various communication and sensing areas. Nodes have variant computing power, i.e, speed of microcontroller, size of memory. Some of them are battery-powered and other have unlimited power source. Several technical problems related to the data routing can be increased by the use of heterogeneous nodes.

- Connectivity

This factor depends on the random distribution of nodes. High node density precludes sensor nodes from being completely isolated from each other. Therefore, they are expected to be highly connected.

2.3.3 Performance parameters

To evaluate the efficiency of a cluster-based routing protocol, some performance metrics need to be considered as follows:

- Load balancing

It refers to divide the workload between two or more nodes in the network. Since the CH aggregates data coming from all nodes within the same cluster, it consumes more energy compared to cluster members. In homogeneous networks, where all

nodes are powered initially with the same amount of energy, selecting a new CH is required to balance the overall energy consumption. However, in heterogeneous networks, where CHs are powered with an external source or powerful batteries, it is useless to speak about the load balancing metric.

- Energy efficiency

The efficacy of a cluster-based routing protocol depends mainly on the energy efficiency parameter, which is crucial to maintain the network sustainability. To evaluate the performance of any clustering algorithm, it is important to determine the residual energy of the overall network or the consumed energy of each node. The most challenging issue in WSNs is how to reduce the consumed energy of a node while performing its assigned responsibilities and maintaining the network functionality.

- Data reliability

It refers to packet losses, which can be often affected by the multi-path fading, interference, etc. A major check for assessing the reliability is the amount of received data at the sink node [72]. Some applications related to the personal security such as medical and military applications [73] require a very high reliability. In contrast, agricultural applications may need a comparatively low network reliability. In this context, the success of any cluster-based routing protocol is depending on the transmission of data from the source node to the destination without any loss. Eq. 2.1 defines the packet losses ratio.

$$\text{Packet loss ratio} = \frac{\text{Number of lost packets}}{\text{Number of received packets}} \tag{2.1}$$

- Failure recovery

This characteristic is important, mainly, in critical applications. Some algorithms are equipped with CH failure recovery by using a backup CH to replace the primary CH in case of faults [74] and avoid the losses of sensed data. Although the addition of such kind of CHs can add extra costs, it is highly demanded in some applications [75] to have the precise data.

- Delay efficiency

Data need to be delivered within a certain period. This performance metric can be evaluated by the parameter "End to end delay", defined in eq. 2.2. It indicates the duration required by a source node to transmit a data packet to the receiver node.

$$\text{End to end delay (sec)} = \sum \frac{\text{Time to receive a packet-Time to transmit a packet}}{\text{Total number of packets}} \tag{2.2}$$

Multi-hop communication schemes can be used to shorten the distance between sensor nodes. Thus, for each hop, an aggregation delay is added. Reducing the energy can lead to extra delays, which is not appropriate for real-time applications.

- Network lifetime

The network lifetime is considered as one of the most critical performance factor, especially for unattended networks. Indeed, this metric depends significantly on the lifetime of an individual node. However, there is no general agreement for the definition of the network lifetime. It can be defined according to the number of alive nodes, coverage, connectivity and application requirements. One of these definitions is the time during which all nodes are alive. Authors in [76] consider three parameters to estimate the network lifetime, which are First Node Dies (FND), Half of the Nodes Die (HND) and Last Node Dies (LND). The FND factor considers the death of the first node as the end of the entire network lifetime. The HND metric emerges from the point that the death of the network is indicated by the energy drainage of the half of the nodes. The LND factor indicates all nodes in the network are dead. Another definition relies on the network coverage as a measure of how well the network is recognized by the deployed sensor nodes. However, even having a full coverage is not enough to ensure the operability of the network when the aggregated data are not transferred to the gateway. The network lifetime can be also defined based on the network connectivity, which indicates how well each sensor node is connected to other nodes.

2.4 Unequal clustering

This section is devoted to define in details the unequal clustering. Cluster-based routing protocols are designed to extend the overall network lifetime by reducing the number of exchanged messages and the distances between nodes to be overloaded by certain messages. Cluster members transmit their sensed data to the appropriate CH, which forwards the received packets to the BS using single-hop or multi-hop communication schemes. Therefore, CHs consume more energy than cluster members due to the additional load, leading to an uneven energy consumption in the network. As seen in see Fig. 2.11(a), when CHs communicate directly with the BS, a high amount of energy is consumed because the needed energy for the signal propagation increases proportionally with the square of the distance between the transmitter and receiver up to a defined threshold distance and after that it will be power of four.

On the other hand, several clustering protocols use the multi-hop communication as an energy efficient solution because it shortens the distance between CHs and the base station, which can balance the consumed energy between different CHs. However, as seen in Fig. 2.11(b), CHs closer to the BS have extra overload by enormous traffic, since the data of the whole network are transmitted through them. Thereby, they are prone to deplete their batteries earlier than other CHs, which is commonly defined as hot spot problem. Furthermore, these nodes die early and the network can be isolated.

To overcome this problem, unequal clustering algorithms are introduced. As depicted in Fig. 2.12, the size of cluster is reduced from one hop to another from the

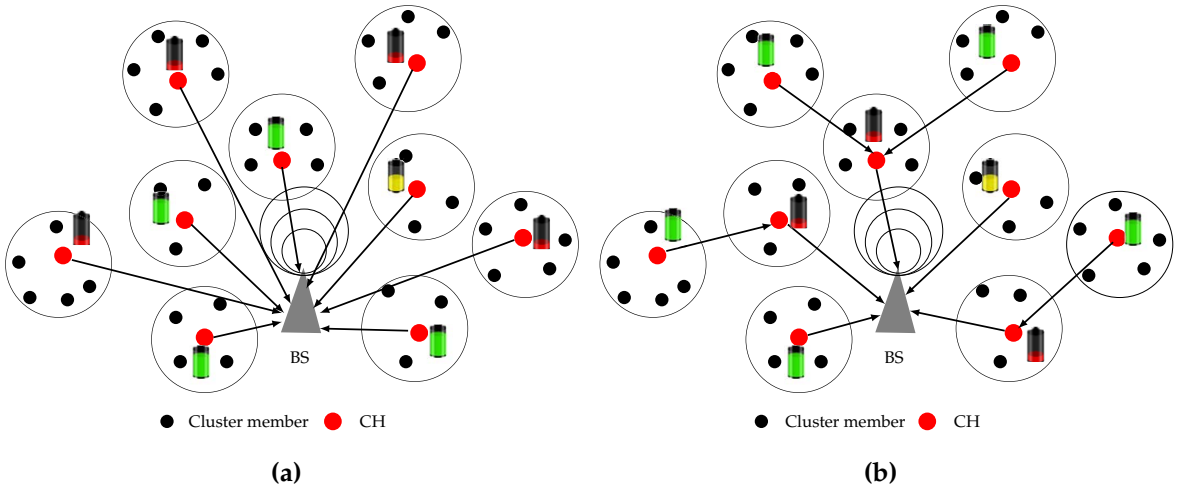

Figure 2.11: Inter-clustering: (a) Single-hop, (b) multi-hop.

BS. As equal clustering, unequal clustering aims to reduce the energy consumption of the deployed nodes, but it has some additional objectives such as load balancing and hotspot problem avoidance.

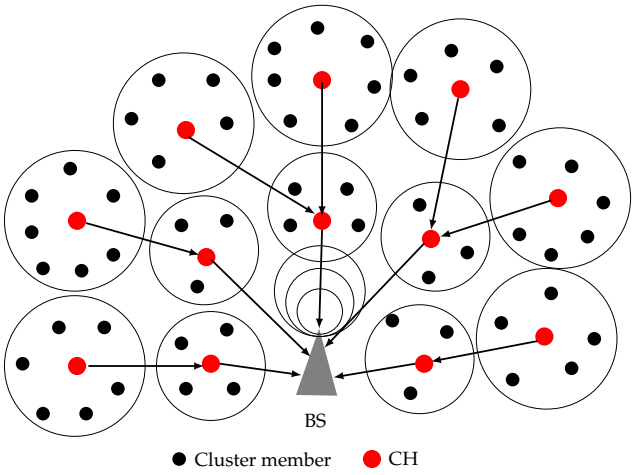

Figure 2.12: Architecture of unequal clustering.

The number of clusters is an important driver affecting the energy efficiency of the clustering process. As the number of clusters becomes larger, the distance between CHs and their cluster members is shortened. Nevertheless, the energy consumed by the CHs increases proportionally to the number of clusters. Therefore, considering the optimal number of clusters is a key issue in a WSN. For this reason, it is valuable to study this issue in section 2.5.

2.5 Determination of optimal number of clusters

Determining the optimal number of clusters in a deployed network is important to enhance the energy efficiency of the clustering scheme. However, some parameters,

presented in Table 2.1, can affect this process including radio model, network and clustering levels.

Table 2.1: Factors affecting optimal number of clusters

Level	Parameters
Radio model	Energy model Sensing model
Network	Node density Transmitter and receiver circuit Sensing field size BS location Single-hop and multi-hop
Clustering	CH and BS distance

2.5.1 Radio model level

The parameters affecting the determination of clusters number in the radio model are as follows:

- **Energy model**

The type of the used energy model can affect highly the optimal number of clusters in a network. It is significant to select the appropriate energy model. Generally, there are four models that can be used [77–80]. The most used one [77] is described in Fig. 2.13. In this model, the transmitter dissipates the energy to run the radio electronics in order to transmit and amplify the signal. While the receiver runs electronics' circuitry to receive signals. It consists of two different radio models: Free space and multi-path fading channel. When the distance between the sender and the receiver is less than the threshold value d_0, the free space model (d^2 power loss) is adopted. Otherwise, for large distance transmissions, the multi-path fading channel model (d^4 power loss) is used.

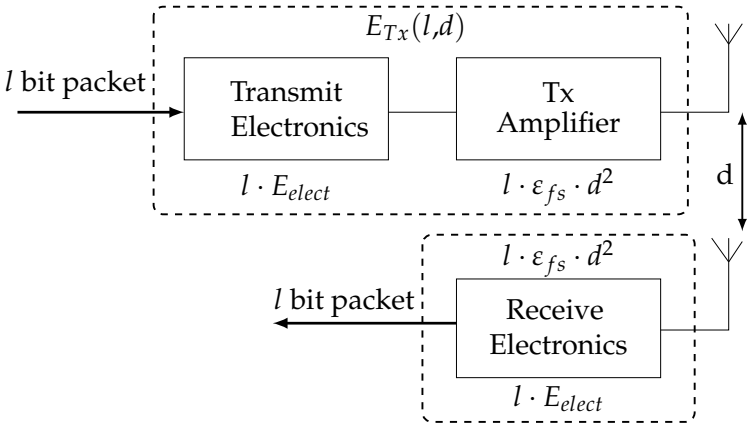

Figure 2.13: Radio energy dissipation model.

To transmit l bit message to a receiver over a distance d, the energy consumed by the transmitter $E_{Tx}(l,d)$ and by the receiver $E_{Rx}(l)$ are:

$$E_{Tx}(l,d) = \begin{cases} l \cdot E_{elect} + l \cdot \varepsilon_{fs} \cdot d^2 & \text{if} \quad d < d_0 \\ l \cdot E_{elect} + l \cdot \varepsilon_{amp} \cdot d^4 & \text{if} \quad d \geqslant d_0 \end{cases} \tag{2.3}$$

and

$$E_{Rx}(l) = l \cdot E_{elect} \tag{2.4}$$

where E_{elect} presents the energy required for one-bit to run over the transmitter's or receiver's circuitry. The parameters ε_{fs} and ε_{amp} are defined as the energy consumption factors for, respectively, free space and multi-path radio models. $d_0 = \sqrt{\frac{\varepsilon_{fs}}{\varepsilon_{amp}}}$.

- **Sensing model**

The distance between the BS and CH varies with the change of the sensing model. Generally, sensing models can be classified into deterministic disk and probabilistic disk models. In the first one, the sensing is carried out only in an area of a disk with a given radius R_s. In the second model, the probability $P(x_i,y_i)$ of detecting an event depends on the distance between the node S_i and the access point P with coordinates (x_i,y_i). As seen in Fig. 2.14, different sensing areas can be defined, where R_ε defines

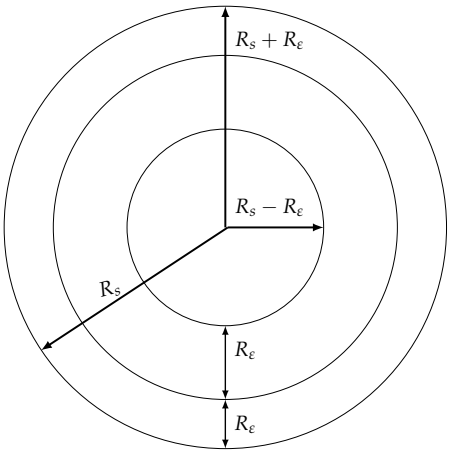

Figure 2.14: Probabilistic disk sensing model.

the uncertainty value in detection. The probabilistic coverage $C_{x_i,y_i}(S_i)$ of a point P is described in eq. 2.5

$$C_{x_i,y_i}(S_i) = \begin{cases} 1 \quad \text{if} \quad R < R_s - R_\varepsilon \\ exp(-w(d(S_i,P) - (R_s - R_\varepsilon))^\beta) \quad \text{if} \in [R_s - R_\varepsilon, R_s + R_\varepsilon] \\ 0 \quad \text{if} \quad R > R_s + R_\varepsilon \end{cases} \tag{2.5}$$

Based on the probability function defined in eq. 2.5, the distance between the CH and BS is easily determined.

2.5.2 Network level

In the network level, different parameters can affect the determination of the optimal number of clusters such as the node density, transmitter and receiver circuit, sensing field size, BS position and the type of communication schemes.

- **Node density**

Authors in [81] performed an experimental analysis to prove that lower densities ($\approx 250 - 375\,km^2$) results on larger cluster size. For higher densities ($\approx 400 - 500\,km^2$), the optimal cluster size is one-hop.

- **Transmitter and receiver circuit**

In [82], an analytical study shows that the optimal size of cluster is independent of the energy consumption of the transmitter circuitry E_{Tx}. However, it can be changed by the energy consumption of the receiver electronics E_{Rx}, which presents one of the major parameters to perform the clustering.

- **Sensing field size**

As mentioned in [82], the size of sensing field has no impact on the optimal number of clusters only under certain situations like the energy consumption of the transmitter circuitry is smaller than the one on the receiver, the BS is positioned inside the sensing area and the wireless communications depend on the free space radio propagation model. Otherwise, the optimal number of clusters can be greatly changed according to the number of sensor nodes $k_{opt} = f(N)$. When the shape of the network is square or circular, the optimal number of clusters is defined as $k_{opt} = \tau\sqrt{N}$, where $\tau \leq 1$.

- **Base station position**

When the BS is placed in the centre of the sensing area, the optimal number of clusters becomes large. However, when it is located outside the sensing field, the optimal number of clusters decreases dramatically.

- **Single-hop and multi-hop communication**

The single-hop communication has great influences on the determination of the optimal number of clusters because the energy consumption value during the data transmission is proportional to the square of the distance between the sender and receiver nodes.

2.5.3 Clustering level

Regarding the cluster level, the distance between the CH and BS influences the selection of the optimal cluster size. This distance depends on the type of sensing model and the size of the sensing area.

To conclude this section, the energy conservation is the primary problem in WSNs because of the limited available power supply to sensor nodes. As explained in this chapter, the clustering is an energy-efficient technique since it reduces the number

of sensor nodes involved in a long-distance communication. Nevertheless, sensor nodes are susceptible to failure due to various factors such as the energy limitation and environmental risks, which can degrade the network lifetime. Fault tolerance is therefore another long-term challenge for WSNs.

2.6 Fault tolerant WSN

This section is devoted to identify the sources and types of faults in WSNs, and define the techniques used to overcome such issue. Sensor nodes become faulty and problematic for various reasons including the hardware and software failure, environmental impacts and malevolent assaults. The faulty packet is transmitted to the sensor node or to the BS, which can reduce the precision of decisions taken by the BS.

2.6.1 Faults sources

Failures can occur for various reasons. Firstly, sensor nodes can fail because of the depletion of batteries or the destruction of the hardware due to certain external events such as the landslide or rainfall. Secondly, links are susceptible to faults [83], which cut down the connectivity between nodes in the network. Thus, the network topology is changed dynamically. This kind of faults happens either temporarily or permanently due to the occurrence of obstacles or objects between the transmitter and receiver nodes or to unattended environmental factors. Therefore, the received/-transmitted data packet can be damaged or lost. Thirdly, faults especially the packet loss arises when there is an error in the data transmission or network congestion. The congestion occurs when a sensor node has an insufficient bandwidth or the network has more data traffic than its capacity [84]. Therefore, the network service quality can be damaged, leading to the corruption of incoming data and the network partition.

2.6.2 Fault types

Several methods are defined to classify the fault types, which can be classified according to the time span, the inherent reason or the behaviour of the malfunctioning unit [83, 85]. Therefore, faults can be divided into two classes, as seen in Fig. 2.15, including the behaviour-based and time-based faults [85].

The behaviour-based fault can be split into two categories, namely hard and soft faults. The hard fault can be defined as a permanent fault in which the sensor node is unable to communicate with the rest of the network due to failures of some hardware modules such as the communication module, transceiver module and the energy depletion of the source unit [83]. In the case of soft faults, a sensor node can operate continuously generating random erroneous information. Therefore, it is difficult to detect or predict this kind of fault [86].

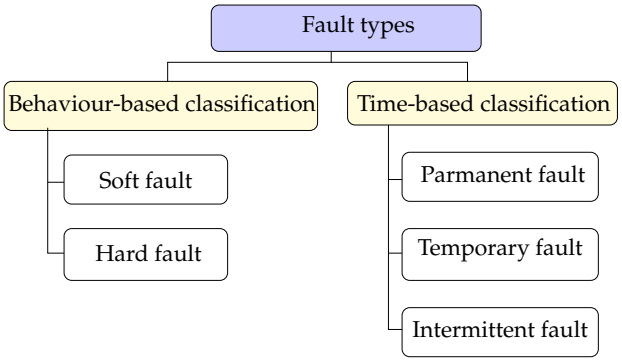

Figure 2.15: Faults classification.

For the time-based fault, faults can be categorized according to the time span as permanent, temporary or intermittent [87]. A permanent fault occurs when a fault intends to remain unchanged indefinitely. A temporary fault happens when a fault lasting for only a limited period. When a fault takes place at irregular intervals, not continuous or steady, it is called intermittent fault.

2.6.3 Fault tolerance techniques

Numerous fault tolerance techniques are developed to handle various kind of faults in different layers of the protocol stack [85, 88]. Therefore, through this section, the most existing techniques are introduced to build a clear overview about fault tolerant issues. To this end, two criteria are involved including the source of faults and the time at which this technique is activated. Therefore, those strategies can be classified as proactive and reactive techniques as seen in Fig. 2.16.

In the case of proactive technique, the sensor node uses its existing resources sensibly and proactively to prolong the network lifetime and avoid the occurrence of faults. Thus, the faults are detected before happening.

Depending on the source of faults, proactive techniques are divided into node-based

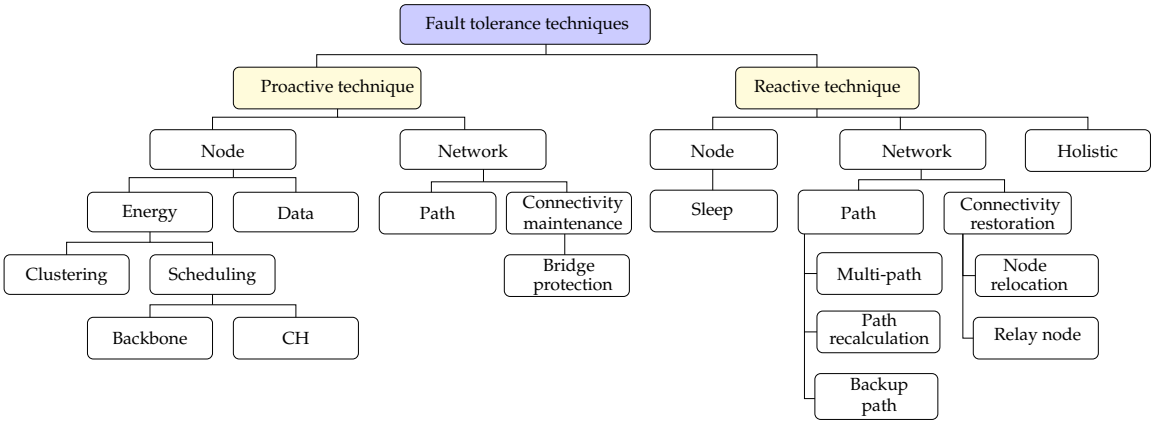

Figure 2.16: Taxonomy of fault tolerant techniques in WSNs.

and network-based categories [87]. The first category consists of energy-based and data-based fault methods. The energy-based fault aims to extend the network lifetime by involving clustering and scheduling algorithms. One of the most used data fault tolerance methods is the transmission of a data packet twice and then the received two packets are compared for error identification. For the network-based proactive technique, it includes the path and connectivity maintenance strategies. This method uses relay nodes to ensure the data transmission through different paths. Therefore, the data redundancy is increased and the network faults are prevented.

Reactive techniques wait the occurrence of the faults and once a fault happens, a recovery process is launched to treat the fault. Furthermore, these techniques can be divided depending on the fault source into node-based, network-based and holistic-based strategies. The first strategy is used to recover faults by turning off for example the backup node when a fault occurs. For the network-based reactive strategy, it uses multi-paths, backup paths or establishes new paths to recover the link or the network failure. In addition, some node can be relocated or some new extra nodes can be added to the network in order to restore the network connectivity. As for the holistic-based reactive strategy, it can handle both node and network-based faults. Therefore, it gives a full fault tolerance for different types of faults.

2.7 Measurement methods for node energy consumption

Since the energy consumption is the primary key of this dissertation, this section is devoted to describe the existing measurement methods for a wireless sensor node. To this end, several techniques can be applied to measure the energy consumption of a sensor node, namely simulation-based measurement, experimental-based measurement and software probe-based measurement [89–96]. Fig. 2.17 presents the taxonomy for the measurement methods.

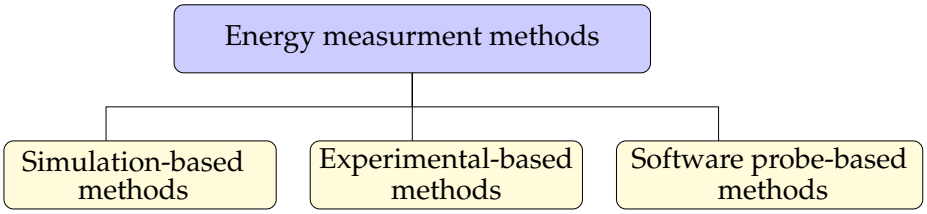

Figure 2.17: Classification of existing energy measurement methods.

The fundamental concept of the simulation-based measurement model is to use simulation tools including NS3 [90], TOSSIM [91], WSNet [92] to estimate and analyze the power consumption of the operating node (see Annex C). Indeed, this approach relies on certain parameters defined from the experiments. The simulations are performed under ideal circumstances, without considering external effects, such as weather and environmental conditions, that can affect the system's performance and lead to more energy dissipation. Thus, a small gap between the simulation and experimental results can be reported.

The experimental-based measurement model is carried out with an additional hardware circuit. It mainly consists on determining the operating current and voltage of a node in different states to estimate the power consumption. In this context, various tools can be used, including current mirrors [93], shunt resistors [94] and current probes [95]. The fundamental principle of the shunt resistance method is to measure the voltage drop through the resistance that is mounted in the supply circuit. This approach needs a precise adaptation of the resistors to guarantee an accurate measurement of the differential amplifiers. Besides, the current mirror method is a modification of the shunt resistance. It is based on the Wilson current mirror circuit, which is designed using four bipolar transistors. The circuit duplicates the current consumed by the device under test (DUT) and the derivation resistance. The mirror current is then measured with the ammeter. Another method is the introduction of a current probe. Indeed, it generates an output voltage as a linear function of the current through the clamp. It enables the high-bandwidth measurement around 50 kHz [97]. Nevertheless, the measurement is proper only for current measurements in milliamperes [96]. In most cases, experimental measurement methods are relatively simple to implement, but they usually need an oscilloscope to study the behaviour of a node. While it offers high sampling rates and high temporal resolution, the oscilloscope can not be used to control energy consumption in real time and as it is big and costly, it can not be used on a large scale.

For these reasons, the probe-based measurement software is introduced. It incorporates the additional hardware circuitry with an energy consumption code to control the dynamic behaviour of the current drawn by the battery. Different software probes are presented, including the SPOT (Scalable Power Observation Tool) [98], which offers a responsive and reliable micro-meter providing real-time monitoring of the power profiles of a wireless sensor node.

To conclude, this chapter provides a panoramic view of the cluster-based routing protocols and focuses on their overall features including challenges, objectives, attributes and performance parameters. Especially, unequal clustering is introduced as a promising technique to balance the network energy consumption and avoid the hotspot problem. In addition, fault tolerant techniques are described as a long-term issue for WSNs. Since the energy efficiency is the primary challenge in this dissertation, different energy measurement techniques are presented. In the next chapter, a detailed literature review about unequal clustering protocols is expounded and analysed.

CHAPTER 3

State of the art of unequal cluster-based routing protocols

For a large area network, CHs located closest to the BS are more overloaded than others, since the data of the whole network is transmitted through them to the BS. Thereby, they are prone to deplete the energy prematurely, which is commonly defined as the hot spot problem. To avoid this issue, unequal clustering protocols can be used leading to balance uneven energy consumption between different CHs [12, 99–104]. Therefore, the size of clusters increases with the increase of the distance between the CH and BS as seen in Fig. 3.1. Having a small size of cluster for nodes close to the BS denotes a reduced number of cluster members and a small amount of intra-cluster data communication. CHs consume more energy for the inter-cluster traffic. However, CHs far away the BS consume more energy for the intra-cluster communication since they are belonged to clusters with more cluster members.

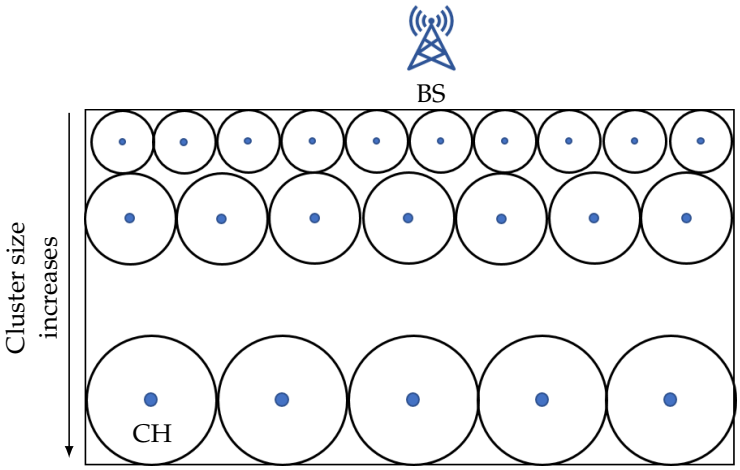

Figure 3.1: Unequal clustering concept.

This chapter is intended as a survey of recent unequal cluster-based routing protocols. It presents a review for the main existing unequal clustering protocols in the state of the art. As presented in Fig. 3.2, they can be divided into three categories: Pre-set, probabilistic, deterministic and protocols. A detailed description for each category is given in the following sections. Then, a deep comparison between the described algorithms is presented.

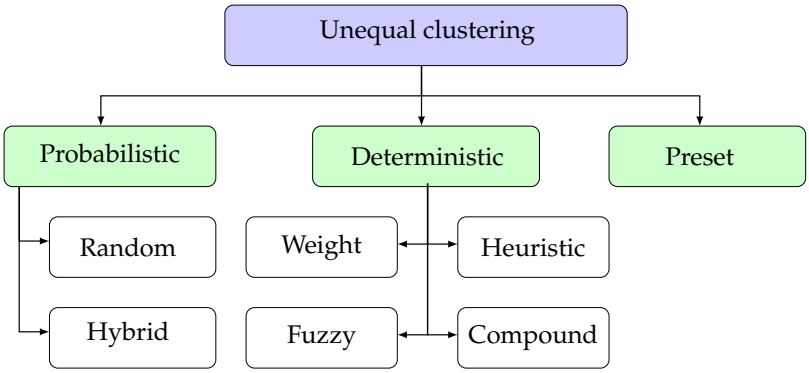

Figure 3.2: Taxonomy of unequal cluster-based routing protocols.

3.1 Preset unequal clustering protocols

In preset clustering protocols, the location of CHs, their number and the number of clusters are prearranged before the node deployment. However, the system conditions are not considered. In WSNs, the remote connection failure/node failure prompts the re-organization of the topology the most of the time. These algorithms are not appropriate for real applications.

Unequal Clustering Size (UCS) [99] protocol is considered as the first preset unequal clustering model, where the positions of CHs are defined a priory. The BS is disposed in the centre of the network and all CHs are placed symmetrically in concentric circles around it, which make the control of current sizes of different clusters very easy. The sensing area is assumed as circle and partitioned into two concentric circles, called layers. To simplify the theoretical analysis, the sensing field is taken as a pie shaped area with multiple layers as shown in Fig. 3.3.

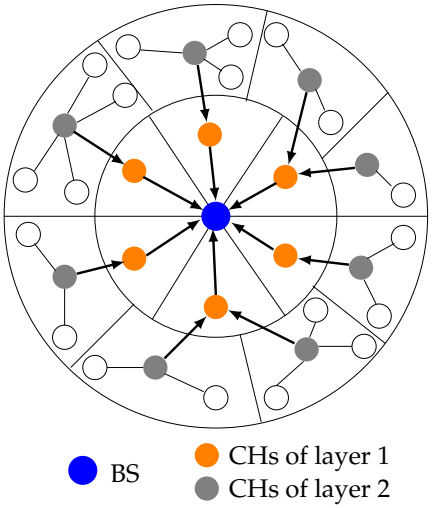

Figure 3.3: UCS: Pie shaped clusters arranged in two layers following [99].

All the clusters in the first layer have the same shape and size, but the clusters in the second layer are different in both shape and size. The overall energy consumption

of nodes that placed in the cluster is determined through the location of CHs within the cluster boundaries. Each CH has to be located at the centre of its cluster, which minimizes the total energy dissipation within the cluster. The radius of the first layer, R_{eq} is obtained in eq. 3.1, where R_a defines the network radius, m_1 and m_2 present, respectively the number of clusters in the inner and outer layers.

$$R_{eq} = R_a \frac{m_1}{m_1 + m_2} \tag{3.1}$$

The number of nodes is changed in each cluster considering the communication load, which maintains more uniform energy consumption of CHs. Moreover, the total dissipated energy of each CH is identical. With the use of two hops inter-cluster and the two layered network model, UCS outcomes a short average transmission distance. However, it is assumed that the network is heterogeneous and there is super nodes, which perform primary CHs all the time by deploying them at predefined positions. In addition, the key factor of this model is to place CHs in the centre of the cluster but it does not consider the residual energy. Since it uses only two hops for forwarding data from sources to the BS, the two hops inter-cluster routing is still not useful in large scale network, where a long distance communications is required.

3.2 Probabilistic unequal clustering protocols

This section describes in details the probabilistic protocols, which are partitioned into random and hybrid methods as shown in Fig. 3.2. In random approaches, a probability is assigned for each node, which is a number between 0 and 1. When this number is less than a predefined threshold, this node announces itself as a CH. These methods are simple and guarantee an optimal overhead. On the other side, hybrid approaches are used to legitimately adjust the clusters by consolidating irregular techniques with few parameters such as the residual energy and the distance to the BS. These methods are iterative-based, which generates both time and message complexities compared to the random approaches. Different probabilistic unequal clustering protocols are introduced and detailed in this section.

3.2.1 Random-based unequal clustering protocols

Probability-Driven Unequal Clustering (PRODUCE) is a randomized unequal clustering protocol [100]. It uses localized probabilities to form unequal clusters and a stochastic geometry to ensure the inter-clustering process. The main objective of PRODUCE is to provide a balanced coverage time and to extend the network lifetime. As seen in Fig. 3.4, sensor nodes are randomly deployed over a circle with a radius R. The network area is partitioned into some levels based on the distance between the BS and the node.

By sending a "Hello" message to all nodes in the network, each node estimates its distance to the BS based on the Received Signal Strength Indicator (RSSI) technique.

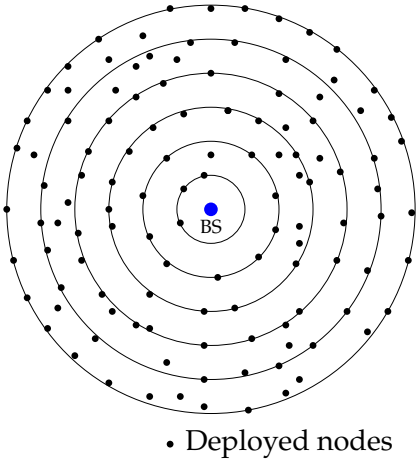

Figure 3.4: PRODUCE: Network topology following [100].

After the node deployment, the BS broadcasts a message to all nodes in the network including the number of nodes and the corresponding probability of a CH from the last level (P_{cross}). When a node receives this message, it calculates its probability P_{CH}, which varies between P_{cross} and P_{max} (the probability of a CH from the first level). P_{CH} is defined in eq. 3.2.

$$P_{CH} = P_{cross} + \frac{P_{max} - P_{cross}}{n-1}(n-i) \tag{3.2}$$

where i defines the level of a node, n_i is the number of the last level. However, using centralized approach to divide the network into some levels and calculate the probability of a CH make PRODUCE suffering from the scalability issue. Since the BS uses one-hop communication to compute its distance to all nodes, PRODUCE is not suitable for some real applications, where the network area is large due to the fact that limited communication range of the sensor node.

Another probability-based unequal clustering protocol is Location based Unequal Clustering Algorithm (LUCA) [101]. N nodes are deployed in a square area based on a Poisson process with density λ, where the BS is located in the centre. To avoid the hotspot problem, LUCA defines the optimal cluster size r by adopting the distance between the CH and the sink node. r is calculated in eq. 3.3.

$$r = \frac{1}{r_0}\sqrt[3]{\frac{3D}{\lambda\pi}} \tag{3.3}$$

where r_0 presents the transmission range. D defines the distance between the CH and the sink. Firstly, each sensor node sets its back-off time using a random value generator. After the node deployment, by measuring its distance from the sink node using a GPS, each node can determine the cluster size. When a node does not receive any advertisement after the expiration of its back-off time interval, it broadcasts

an advertisement message within its radius cluster. Otherwise, it joins the nearest cluster. Despite it uses a simple algorithm to uniformly generate CHs, LUCA can not be used for real applications because using GPS for all sensors is not affordable, as well as placing all nodes in areas with fixed geographic coordinates is not practical. Moreover, the choice of a relay CH is not considered in this work, which can degrade the network performance.

3.2.2 Hybrid-based unequal clustering protocols

The hybrid-based unequal clustering protocol combines the random approach with specific parameters such as distance to the BS or the residual energy. As an example of hybrid algorithms, an Energy Efficient Unequal Clustering (EEUC) has been proposed, which is considered as a mechanism for periodical data aggregation in WSNs [102]. As shown in Fig. 3.5, N nodes are deployed in a square area, where the BS is placed outside the network. Using the RSSI-based localization technique, sensor nodes recognize their distance to the BS.

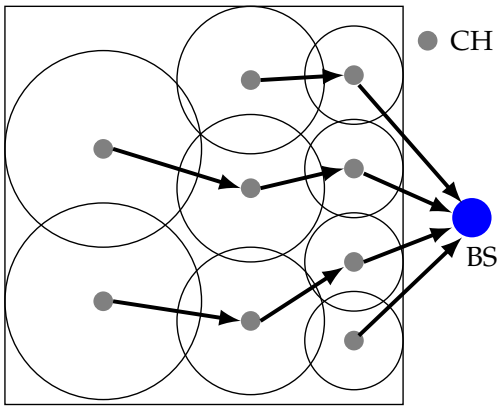

Figure 3.5: EEUC: Clustering formation following [102].

Two parameters are considered to select the suitable CH: Node residual energy and distance of node to the BS. The radius of each cluster is carried out in eq. 3.4, where $d(n_i,BS)$ defines the distance between a node n_i and the BS. d_{max} and d_{min} present, respectively, the maximum and the minimum distance of a node to the BS. R_0, a preset value, defines the maximum competition radius.

$$R_{comp} = (1 - \frac{d_{max} - d(n_i,BS)}{d_{max} - d_{min}})R_0 \tag{3.4}$$

However, this algorithm is suitable only for small area. Some nodes can be at the same time included in more than one cluster, leading to energy losses. Another limit of EEUC is the determination of cluster radius, which is inaccurate, since it depends only on the distance parameter. It does not consider the node energy as input for the cluster radius. In chapter 2, it is proven that considering the energy is crucial in the determination of the optimal cluster radius.

Another hybrid-based unequal clustering protocol is Constructing Optimal Clustering Architecture (COCA) [105]. The main objective of COCA is to build up an optimal cluster-based architecture to maximize the network lifetime. As seen in Fig. 3.6, the network area is partitioned into equal sized square units with an optimal size $l = d_0/\lambda$, where d_0 is a distance threshold and λ is a predefined constant equal to 1.088.

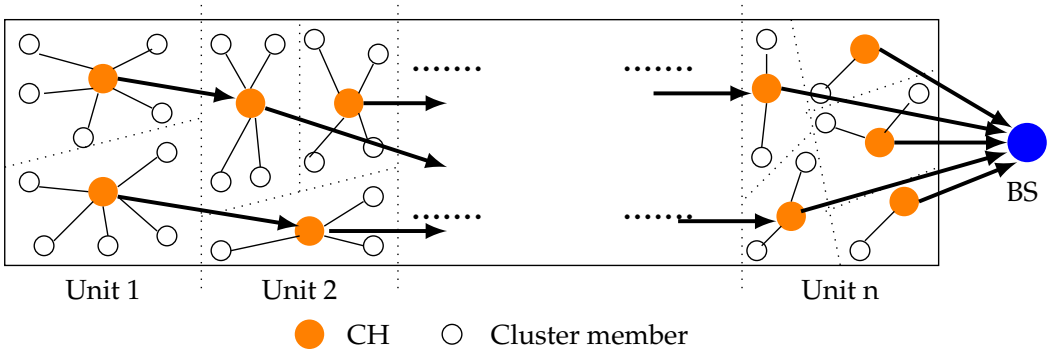

Figure 3.6: COCA: Network model following [105].

Firstly, the optimal number of cluster in the first level is $c_1 = \frac{1}{\lambda^2}\sqrt{\frac{\rho\varepsilon_f}{2\pi\rho\varepsilon_m}}$, where ρ is the distributed density of nodes, ε_f and ε_m present, respectively the amplifier coefficient for the free space model and two-ray ground model. Depending on c_1, the number of clusters in each unit, c_i, can be calculated as seen in eq. 3.5.

$$(c_{i+1} + c_i)(\alpha + \frac{\beta}{c_i c_{i+1}}) = \gamma \tag{3.5}$$

where $\alpha = 2qE_{elec}$, $\beta = \frac{nq\varepsilon_f l^2}{2\pi}$ and $\gamma = 2naqE_{elec} + naq\varepsilon_m l^4 l^4 > 0$. l is the optimal length of a unit. q is the size of a transmitted packet. E_{elec} is the energy spent by electronics. a is the aggregation ratio for all CHs. n is the number of nodes per unit. After the node deployment, COCA is divided mainly into two phases: Topology formation and data transmission. The first phase includes the CH selection, cluster formation and inter-cluster operations. Firstly, CHs per unit are identified randomly by the sink node. After a certain communication rounds, sensor nodes broadcast their residual energy within the unit they belong. The node with the highest energy value except the CH is selected as a CH and it broadcasts its status to all nodes within the same unit. Other nodes join one of the selected CHs based on the signal strength and the distance that separates it from the CH. After that, each cluster member transmits data to its corresponding CH, which collects all the received data and then forwards it to the CH from the adjacent unit until reaching the BS. A re-clustering process is carried out to select a new CH after a certain number of rounds, τ for better energy conservation. However, the period to select again a CH is randomly chosen. Since the selection of the relay node is arbitrarily, a CH can select another CH, which is about to die and all the data are lost.

A Multi Objective Fuzzy Clustering Algorithm (MOFCA) is proposed in [12], which uses local decisions to determine the node competition radius as well as to select both tentative and final CHs. As seen in Fig. 3.7, N nodes are deployed in a square area. Tentative CHs can be selected based on random approaches. The competition radius of such tentative CHs is estimated using three parameters, which are remaining energy, distance to sink node and density of the nodes.

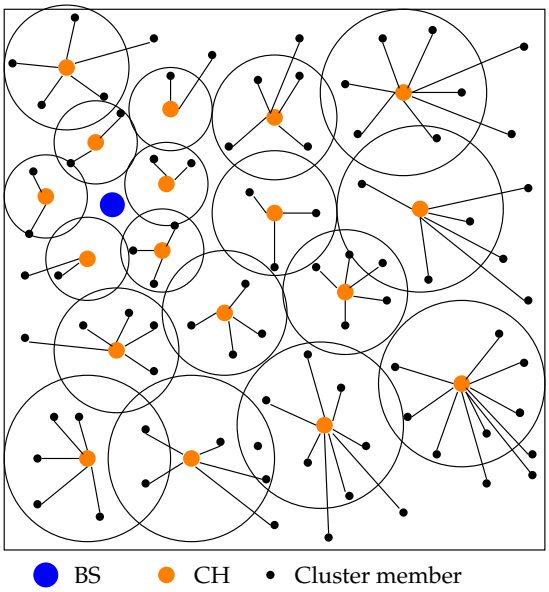

Figure 3.7: MOFCA: Clustering formation following [12].

Moreover, it uses a probabilistic model to select CHs by comparing a random number with the optimal threshold value. For the re-clustering process, MOFCA involves randomized periodical rotation. Here, the choice of the threshold value for being a CH is random, which can have impact on the right selection of the final CH.

3.3 Deterministic unequal clustering protocols

Deterministic approaches use standard metrics to select CHs including the node density, distance to the BS and the residual energy. This data is generally refreshed by trading message between its neighbours. The choice of CHs is more controllable. As seen in Fig. 3.2, these approaches can be further classified as weight-based, fuzzy-based, heuristic-based and compound-based unequal clustering algorithms.

In weight-based approaches, a weight is computed at every node in view of few measurements for example, node degree, distance to the BS, etc. The node with insignificant weight is chosen as a CH. In the other side, the fuzzy logic is used to choose CHs in circumstances, where there are more uncertainties. The CH is picked in view of fuzzy input parameters such as the residual energy, node degree, node centrality. The output fuzzy parameters can be either cluster size or node's chance to be a CH. Different optimization algorithms can be applied to perform heuristic-based approaches such as Ant Colony Optimization (ACO) [106], Particle Swarm

Optimization (PSO) [107], Genetic Algorithm (GA) [108], Artificial Bee Colony (ABC) [109]. Each algorithm defines various metrics in the fitness function to select the appropriate CH. These approaches are centrally-based, where the BS controls all the operations in the network [110]. The compound approaches use various concepts such as Sierpinski triangle [111] and connected graph [112] to achieve the clustering process.

3.3.1 Weight-based unequal clustering protocols

Arranging Cluster sizes and Transmission ranges algorithm (ACT) [103] is a cluster-based protocol proposed to decrease the size of clusters close to the BS. N sensor nodes with fixed positions are deployed in a rectangular area ($W \times L$), where the BS is located outside the sensing area as seen in Fig. 3.8.

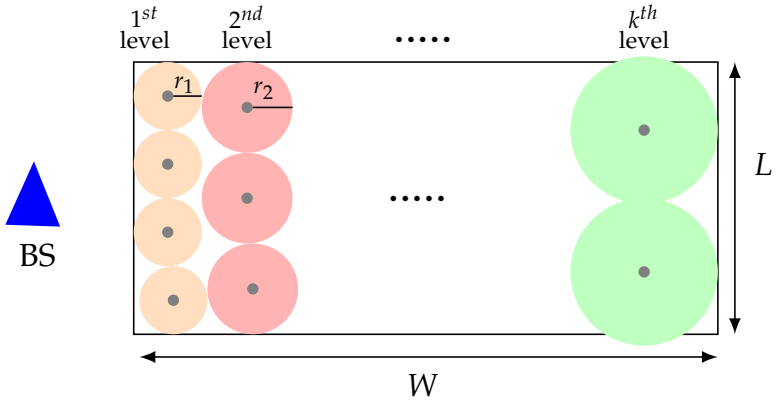

Figure 3.8: ACT: Network topology following [103].

As process, it includes three phases. Firstly, the cluster formation phase is performed to determine the hierarchical level of the network topology, calculates the cluster radius, establishes the cluster setup and builds CH-to-CH routing paths. The BS divides the area into a predefined number of k levels. Then, the radius of cluster r_i in the level i is determined as seen in eq. 3.6.

$$r_i = \sqrt{(r_1)^2 + (N_i)^2} \tag{3.6}$$

$$S = \frac{a_{i-1}}{a_i} \tag{3.7}$$

where r_1 is the radius of the first level and N_i is the vertical distance between a node and the BS, a_i and a_{i-1} are, respectively, the number of clusters in level i and level $(i-1)$. With the help of eq. 3.6 and considering eq. 3.7, the number of other clusters in each level can be calculated. When the network topology is established, the sensor node with the closet location to the theoretical location is selected as a CH. The second phase is the data forwarding phase including intra-cluster and inter-cluster data transmission operations. The third phase is the maintenance phase. It includes

the rotation of CHs and the cross-level data forwarding to the BS. When the residual energy of a CH is less than 15%, a new CH is selected. In fact, it helps to reduce efficiently the energy consumption of CHs around the BS and all CHs have the same energy dissipation. However, it is very difficult to implement it for a large area because the algorithm becomes complex with the increase of the area width. So, ACT is suitable only for a small scale network. Moreover, the CH is selected depending only on its location. It comes that a node close to the theoretical position is selected as a CH, but, it has not enough energy to run the round. The threshold value used for the re-clustering process is chosen randomly.

An Energy-Balancing Unequal Clustering Approach (EBUCA) [104] is a cognitive partition-based unequal clustering algorithm. The topological structure of the network is described in Fig. 3.9. It is presented as a graph $G = (V, E)$, where V defines the set of all nodes in the network and E indicates the set of edges between the nodes. After the node deployment, an energy balancing cluster formation phase starts. The BS divides the network area into n unequal partitions ($p_1, p_2, ..., p_n$), organized serially, where the size of partition increases as the distance between each partition and the BS increases. A CH is assigned for each partition. To this end, the BS selects a set of candidate CHs, having minimal weights. The node with minimum distance to the BS is selected as a CH for the corresponding partition.

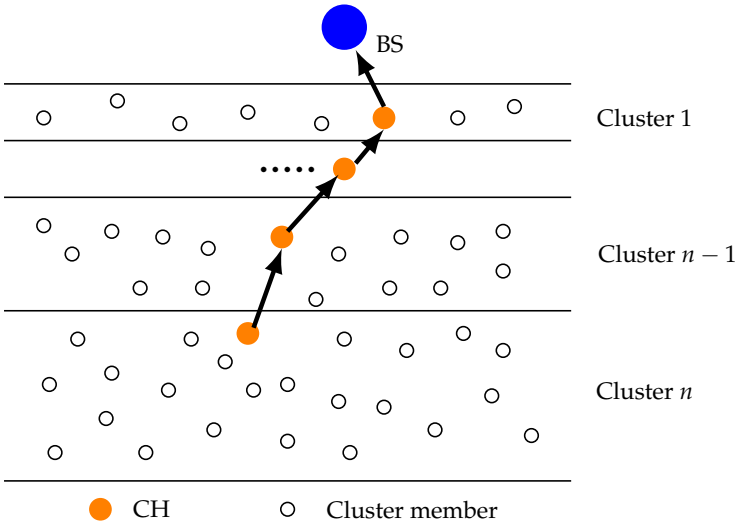

Figure 3.9: EBUCA: Network topology following [104].

However, each CH transmits the data traffic to the next CH towards the BS randomly. It comes that a relay CH node is unable to forward the received packets since it has insufficient residual energy. The size of partition does not consider the energy aspect. It depends only on the distance to the BS.

Another weight-based unequal clustering protocol is Improved Energy Aware Distributed Unequal Clustering for heterogeneous WSN (Improved EADUC) [113]. N nodes are deployed randomly in a square area, where the BS is placed far away the sensing field. Since nodes are not location-aware, they use the RSSI technique to

compute their distance to the BS. As presented in Fig. 3.10, the Improved EADUC includes two phases: Setup and steady-state. During the setup phase, each node broadcasts a discovery message including its ID and residual energy to collect information from its neighbours. The average residual energy per cluster is determined. Afterwards, the CH competition sub-phase takes place wherein three parameters are involved to assign the competition radii R_c to nodes, which are the residual energy, distance to the BS and number of neighbour nodes. R_c is defined in eq. 3.8.

$$R_c = [1 - \alpha(\frac{d_{max} - d(s_i,BS)}{d_{max} - d_{min}}) - \beta(1 - \frac{E_r}{E_{max}}) + \gamma(1 - \frac{S_{i(nb)}}{nb_{max}})]R_{max} \tag{3.8}$$

where α, β and γ are the assigned weight with a value between (0, 1). d_{max} and d_{min} define, respectively, the maximum and minimum distances to the BS. $d(s_i,BS)$ is the distance separating a node s_i and the BS. R_{max} presents the maximum value of the communication range. $S_{i(nb)}$ is the number of neighbour nodes and nb_{max} is the maximum possible number of neighbours of a node i.

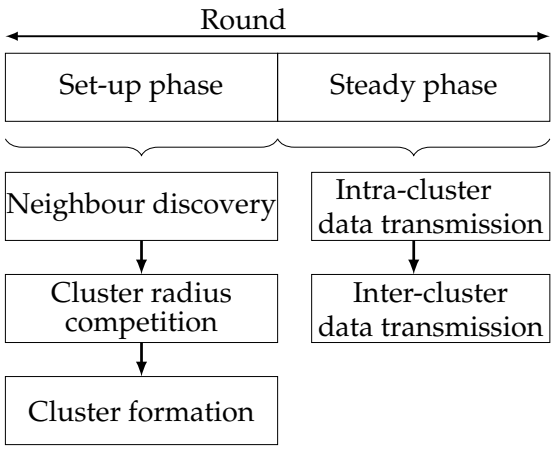

Figure 3.10: Improved EADUC: Operational process.

Afterwards, the cluster formation sub-phase starts aiming to choose the CH for each cluster. For this reason, the node residual energy and the ratio of average energy of neighbour nodes are used. Cluster members join the nearest CH. In the steady-state phase, the data transmission process occurs. Normal nodes transmit their data packets to their appropriate CHs considering their time schedule. CHs aggregate the received data into one packet and transmit it directly to the BS or via a relay node, which is a CH from the next hop. Improved EDAUC incorporates the energy and the distance between two CHs as important parameters to select the respective relay node. A new CH is selected after certain rounds.

However, the inter-cluster communication process is random. In some rounds, the relay CH has insufficient energy to forward the received packet. In this case, data are lost. To reduce the cluster overhead, the cluster formation step is retrained for a few rounds but this number is not scientifically fixed. It come sometime, that a CH is about to dead but there is no cluster formation till reaching the fixed round.

3.3.2 Fuzzy-based unequal clustering protocols

In fuzzy-based clustering protocols, to select CHs different fuzzy input parameters can be involved such as the residual energy, node density and distance to BS. The output of such fuzzy systems can be the chance of being a CH or the size of each cluster. A Distributed load balancing Unequal Clustering based on Fuzzy approach (DUCF) [114] is proposed. N nodes are deployed in a square area, where the BS is located at the centre. It is assumed that the distance between nodes is performed depending on RSSI techniques but it is not proved during the work. After the node deployment, each node transmits a "HELLO" message to the BS including its communication range. Using this information, the number of neighbours and the distance to the BS can be determined. DUCF includes mainly two phases, cluster formation and data collection phases. As presented in Fig. 3.11, the outputs of the first phase are the chance of a node to become a CH and the size of each cluster, i.e the maximum number of nodes that can be included in a cluster.

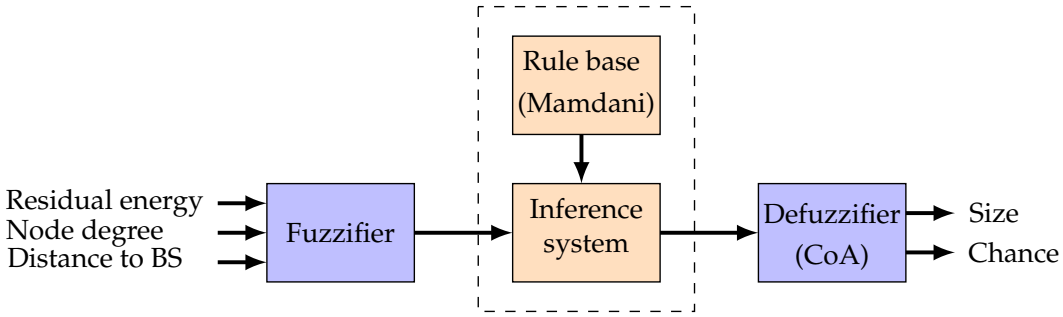

Figure 3.11: DUCF: Fuzzy inference system following [114].

To compute the two mentioned outputs, three fuzzy input variables are used, which are the distance to the BS, node degree and residual energy. Each node broadcasts a message to all neighbours within the same communication range including its ID and its chance value. Node with higher chance announces itself as a CH and inform their neighbours with its status. After the building of clusters, the collection phase starts. Each CH maintains a TDMA schedule and assigns the TDMA slots to cluster members. The nodes of the same cluster exchange their data with their CH in its pre-allocated time slot. Each collects the received data into a single packet and transmits it to the BS if it is close to the BS or via other CHs when it is far away. For the selection of CHs, a significant parameter like the node centrality is not considered, which can lead to the selection of a CH with distant neighbours. In this case, a CH spends more energy for intra-cluster traffic, which may affect the overall energy dissipation.

Authors in [13] proposed a Multi-Clustering algorithm based on Fuzzy Logic (MCFL). N nodes are randomly distributed in a square area, where the BS is positioned in the centre. It is assumed that nodes know from the beginning their positions and the position of all other nodes. As presented in Fig. 3.12, the network timeline includes three clustering algorithms. In the first round $i = 1$ and for all upcoming rounds,

where $i = i + 3$, the residual energy and the number of neighbours are used as fuzzy descriptors for the CH selection. Nodes with higher fuzzy output are selected as CHs. In the second round $j = 2$ and for all next rounds where $j = j + 2$, the same CHs remain as CHs in two consecutive rounds. In the third round $k = 3$ and for all next rounds where $k = k + 3$, the process of the CH selection is held and new CHs are chosen based on the node residual energy and its distance to the previous CH. By trusting CHs for at least few rounds, the number of received and sent messages is reduced while guaranteeing increased capacities to save energy within the network.

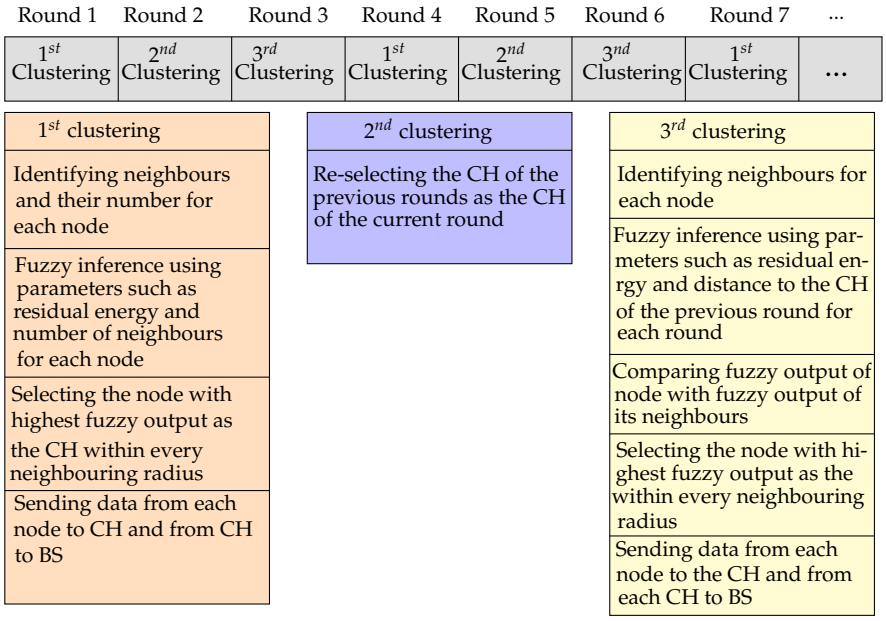

Figure 3.12: MCFL: Network timeline following [13].

However, it comes that a CH dies in the beginning of round, where the second clustering algorithm is applied. In this case, the transmitted data from cluster members to this CH are lost. Moreover, the node centrality parameter is not considered in the selection of CHs, which leads to the choice of a CH with distant neighbours. Thus, an extra intra-clustering communication is added affecting the overall energy dissipation. In addition, in MCFL, all CHs transmit the aggregated data directly to the BS, which is adequate only for a small area network.

3.3.3 Heuristic-based unequal clustering protocols

In heuristic-based clustering protocols, CHs can be selected using Ant Colony Optimization (ACO), Particle Swarm Optimization (PSO), Differential Evolution (DE), Simulated Annealing or Artificial Bee Colony Optimization (ABC). To get better performance, each approach describes different metrics to have the fitness function [110].

In [115], a Fuzzy and Ant Colony Optimization (ACO) based on MAC, routing, and unequal clustering cross-layer protocol (FAMCROW) is proposed. The network is

divided into layers, where the BS is positioned in the centre of the sensing field as seen in Fig. 3.13. Each node uses two-ray ground radio propagation model [116] to determine its distance to the BS. Each node broadcasts a packet within its communication range including its layer ID, its ID and its distance to the BS to discover the list of neighbours within the same layer.

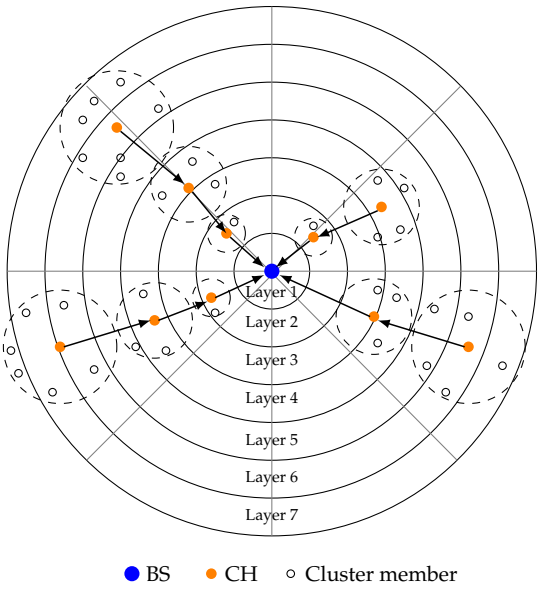

Figure 3.13: FAMACROW: Network topology following [115].

After that, in each layer the CHs are selected based on some fuzzy descriptors such as residual energy, node's neighbourhood nearness and link quality indicator. In order to decrease the intra-clustering communication, there are no clusters in the first layer. Nodes located in this layer transmit directly their data to the BS. CHs of outermost layers broadcast an advertisement message to cluster members within a radius R_{adv}, defined in eq. 3.9.

$$R_{adv}(Ch_i) = R_{max} \times [(1 - w\frac{d_{max} - d(CH_i,BS)}{d_{max} + d_{min}})(\frac{E_{current}(CH_i)}{E_{initial}(CH_i)})] \tag{3.9}$$

where R_{max} defines the maximum advertisement radius and w is a factor between 0 and 0.99 indicating the amount of inequality of cluster size. d_{max} and d_{min} are the maximum and the minimum distances of a node to the BS, respectively, while $d(CH_i,BS)$ is the distance of a CH_i to the BS. $E_{current}(CH_i)$ and $E_{initial}(CH_i)$ present the current and the initial energy of a CH_i. To establish routes from a CH to another CH, the ACO approach is used. However, the size of each layer is determined randomly without considering any parameter. The radius of a CH is calculated using only the distance between the tentative CH and BS. There no consideration of the energy consumption. As explained in Chapter 2, there is a great impact of the energy model in the determination of the optimal cluster radius.

A PSO-based Uneven Dynamic Clustering multi-hop Routing Protocol (PUDCRP)

[107] is proposed. The position of the BS is fixed at the boundary of the square area as seen in Fig. 3.14. Sensor nodes know their location based on the GPS technique. In the setup phase, the BS executes an improved PSO to find the circular area, where the candidate CH can be positioned. The radius of this circular area is given in eq. 3.10. Based on eq. 3.11, the optimal number of circles in the i^{th} layer can be determined.

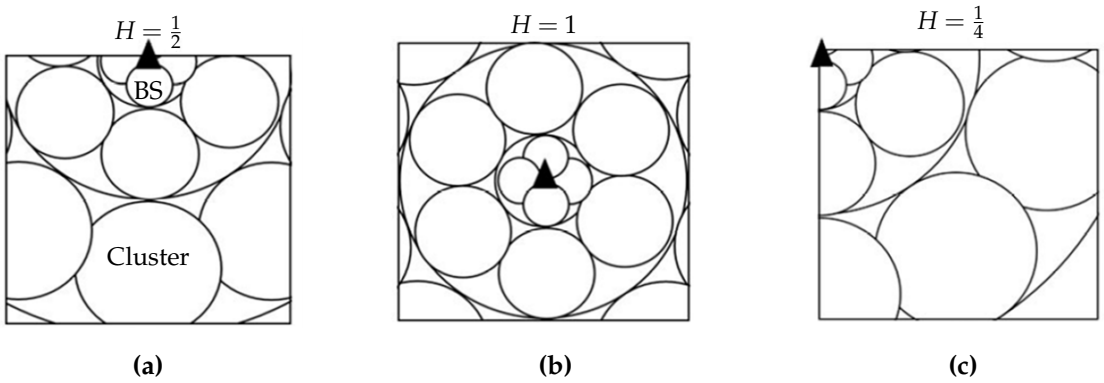

Figure 3.14: PUDCRP: The BS is located on the: (a) boundary of the monitoring area, (b) centre of the area, (c) vertex of the rectangle network area [107].

$$R_i = \frac{dis_i}{d_{max}}(R_{max} - d_1) + d_1 \tag{3.10}$$

$$A = \sum_{i=1}^{K} n_i \times \pi R_i^2 \tag{3.11}$$

where d_i is the distance between the BS and the centre of the circular area i^{th} and d_1 is the minimum radius of the circular area. R_{max} is the maximum radius and d_{max} is the maximum distance between the BS and circular area centres. After that, the selection of CH is carried out in each circle based on a multi-objective fitness function $Weight_{ij}$. As seen in eq. 3.12, such function uses the distance of nodes to the BS, the residual energy of nodes and the number of neighbours within the same communication range.

$$Weight_{ij} = w_1 \frac{E_{ij}}{E_0} + w_2 \frac{n_{nb_i}}{n} + w_3 \frac{d_{min_j}}{d_{s_i}} \tag{3.12}$$

where w_1, w_2 and w_3 are weight for each CH selection factor. E_0 is the initial energy, while E_{ij} is the residual energy of a node s_i in the circular area j. n_{nb_i} presents the list of neighbours. d_{min_j} is the minimum distance between nodes and the BS in the circular area j.

Then, the steady-state phase starts. When the distance between a non-CH and the BS is less than a fixed value d_0, this node transmits directly its own data packet to the BS. Otherwise, it sends the packet to the corresponding CH, which forwards it to the BS via single-hop communication or in multi-hop communication. Indeed, when

the distance between the CH and the BS is less than the distance d_0, CHs transmit directly their data to the BS. Otherwise, a connecting line aided route construction method is used to select the relay node. Thus, the energy dissipation from the multi-hop inter-cluster traffic is decreased. Despite its efficiency, PUDCRP does not consider the energy parameter in the determination of the circular area radius. Moreover, the choice of d_0 as a parameter for the inter-cluster communication is randomly fixed. There is no scientific reason behind this choice. In each round, the cluster formation phase is launched, which increases the clustering overhead.

3.3.4 Compound-based unequal clustering protocols

In compound-based unequal clustering algorithms, various metrics can be used for CH selection such as Sierpinski triangle and connected graph. In this context, an Energy Degree Distance Unequal Clustering Algorithm (EDDUCA) [111] is developed. It includes cluster formation, CH selection and data transmission phases. As seen in Fig. 3.15, in the cluster formation phase, Sierpinski triangle method is used to divide the network into equilateral triangles. By connecting the mid-points of its sides, each triangle is divided into small equilateral triangles. After that, the triangle in the centre is be removed and the other triangles repeat the same process.

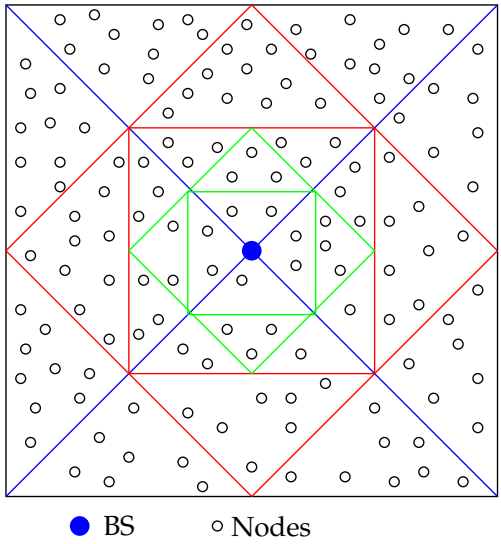

Figure 3.15: EDDUCA: Network deployment following [111].

The weight of each node, $Weight(i)$, is calculated in eq. 3.13. It is based on the residual energy, the node degree and the distance to the BS. For each triangle, the node having the minimal weight is selected as a CH. Then, each normal node transmits its data packet to its corresponding CH, which forwards the collected data to its upper CH until reaching the BS.

$$Weight(i) = \frac{1}{Deg(i)} + \frac{E_c(i)}{E_n} + \frac{DiscC(i)}{DiscC_{max}} \tag{3.13}$$

where $Deg(i)$ is the degree of a node i, i.e the number of neighbour nodes. $E_c(i)$ is the consumed energy during the communication, while E_n is the initial energy. $DiscC(i)$ defines the distance to the cluster centre and $DiscC_{max}$ is a defined maximum distance. However, EDDUCA does not consider the node centrality in the selection of CHs. It comes that a CH is located far away all other nodes, more energy is needed to be communicated with their cluster members. Moreover, the path length connecting the CHs to the BS and the energy factor are not considered.

Authors in [112] proposed an energy-efficient routing algorithm based on Unequal Clustering theory and Connected GRAph theory (UCCGRA). N nodes are distributed randomly in a square area as shown in Fig. 3.16. A vote method is used to select the CH, which is based on three parameters, namely, the network topology, the residual energy and the power transmission.

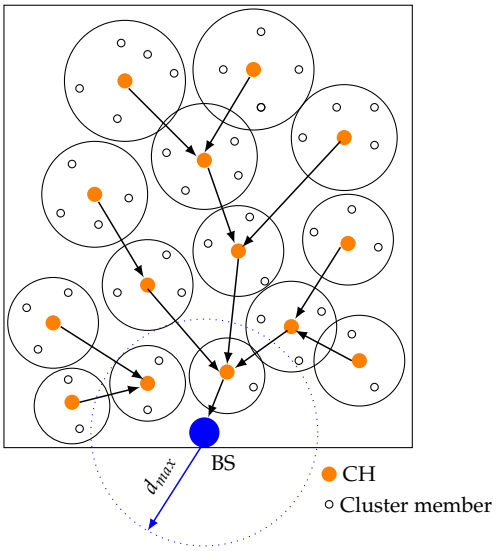

Figure 3.16: UCCGRA: Network model following [112].

Each sensor node i casts a vote to other nodes, $v_{i,j}$ defined in eq. 3.14.

$$v_{i,j} = \begin{cases} \dfrac{E_i}{\sum\limits_{d_{ik} \leq R_i} E_k} & \text{if} \quad d_{ij} \leq R_i \\ 0 \quad \text{if} \quad d > R_i \end{cases} \tag{3.14}$$

where E_i is the residual energy of a node i, d_{ij} is the distance between node i and node j. R_i is the distance of a node i to the BS. The vote of a node $vote(i)$ is the sum of votes received from its neighbours. Based on this vote, an announcement A_i is calculated in 3.15.

$$A_i = \frac{vote(i)}{\sum\limits_{k=1}^{n} \dfrac{(d_{ik})^2}{n}} \tag{3.15}$$

where n is the total number of neighbours for a node i. A node with maximum announcement value is selected as a CH. When a node has more than one CH within its radius cluster, it selects to join the CH with the highest residual energy. After the selection of CHs, a connected graph-based multi-hop routing method is developed to establish the inter-clustering data transmission. A link path is constructed between the BS and the CHs. All CHs establish a connection between them based on their geographical positions. However, UCCGRA does not consider the optimal parameters for energy minimization. In addition, the periodic vote method and the theory of connected graph generate an energy overhead and high complexity.

3.4 Comparison and discussion

This section presents a comparison of different unequal clustering protocols, which are categorized, basically, into three classes: Preset, probabilistic and deterministic. In preset approaches, the location of either clusters or CHs is pre-assigned before the deployment in a physical environment. Since clusters are formed as pre-assigned information, the main disadvantage of this approach is that it is static and the network changes or the node conditions are not considered. Probabilistic methods are known for their easy to use and energy-saving nature. They can be divided into two classes, namely random-based and hybrid-based approaches. The random-based approach selects CHs without considering the various lifetime parameters such as energy level, number of neighbour nodes, intra and inter cluster distance. Despite its simplicity, it leads to the selection of non suitable nodes as CHs, which affects the lifetime of the WSN. The hybrid-based approach are competitive-based, thereby raising the overall complexity in terms of both communication and time.

In contrast to probabilistic-based methods, the deterministic approaches use a variety of criteria to select CHs. They are more accurate and manageable than probabilistic methods. Basically, they are classified into four categories, namely weight-based, heuristic-based, fuzzy-based and compound-based approaches. In the case of weight-based approach, the CHs are selected using the above said parameters. When the nodes are not uniformly deployed over the Region-Of-Interest (ROI), the same nodes are selected as CH frequently. It leads to premature death of that higher weight nodes and affects the overall network lifetime. In the most of the literature survey, it is found that the algorithms, which blend both probabilistic approach and weight-based approach gives better results than using one of them separately. In heuristic approaches, a global information is required by the BS to control all operations in the network. In many applications, where there is insufficient information or nodes are deployed far away the BS, heuristic methods are unrealistic to cover a large scale area.

Fuzzy logic is an important tool for decision making, even if there is insufficient information. Using fuzzy logic in unequal cluster-based routing protocols can process a large number of input data, which can be imprecise or incomplete by

modelling their reaction and behaviour rules. Moreover, this approach is known by its interoperability and simplicity as it uses simple logic relation to estimate the output values, which reduces the computational complexity of the system. In fact, fuzzy controller can automatically refine an initial approximate set of fuzzy rule, when new data or rules are added to the system, then no need to re-train the system once again.

In this chapter, various unequal clustering protocols for balancing the consumption of energy among CHs are analysed. Unequal clustering helps to overcome hotspot problem and prolong the network lifetime. Since preset clustering protocols are not dynamic, in case of inconsistent network conditions its performance is impractical. Hence, this method is not suitable for real-time application. Probabilistic-based clustering algorithms are popular for its simplicity and low energy consumption. Non-probabilistic or deterministic clustering protocols are more robust and reliable than probabilistic protocols.

Table 3.1: Comparison of unequal clustering routing protocols in WSNs

Algorithm	Clustering process		Input parameters				Re-clustering	Simulation standards			
	Clustering methods	Radius calculation	Residual energy	Density	Centrality	Others		BS location	Node number	Evaluations' parameter	Filed shape
UCS [99]	Preset	Pie shape	-	-	-	-	Not mentioned	Center	400	-Energy -Network lifetime	Circular, $R = 200\,m$
PRODUCE [100]	Random	preset	-	-	-	Probability	random	centre	400 to 5000	-Number of alive nodes -Coverage time	circle
LUCA [101]	Random	-Network density -Distance to BS	-	-	-	Probability	random	Centre	500	Energy consumption	Square
EEUC [102]	Hybrid	distance to BS	✓	-	-	distance to BS	Each round	outside	400	-Energy consumption -FND	Square
COCA [105]	Hybrid	Energy	✓	✓	-	Distance to BS	Each round	inside	100	-Residual energy -Alive nodes	square
MOFCA [12]	Hybrid	Based FL: -Distance to BS -Residual energy -Density	-	-	-	Probability	Each round	Outside (250,250), center	100	-Energy -Network lifetime (FND, HND)	Square $200\,m \times 200\,m$
ACT [103]	Weight	Distance to BS	-	-	✓	-	Residual energy of CH $\leqslant$ 15 %	Outside	96 nodes	-Energy consumption -Number of node alives	Rectangle $80\,m \times 120\,m$
EBUCA [104]	Weight	-Total number of events occured in area -Energy- deviation -Distance between nodes	-	-	-	Weight function	Each round	Outside (100, 50)	300	-Network lifetime -Energy consumption	Rectangular $80\,m \times 120\,m$
CUCA [117]	Weight	Distance between BS and the closet and farthest nodes	✓	-	-	Coverage	Each round	center (0, 0)	60-100	-Coverage -Network lifetime	Square $40\,m \times 40\,m$
Improved EADUC [113]	Weight	-Residual energy -Distance to BS -Number of neighbours	✓	-	-	Ratio of average energy	After few rounds	Outside (250, 100)	100	-Energy -Network lifetime	Square $200\,m \times 200\,m$
DUCF [114]	Fuzzy logic	based fuzzy logic	✓	✓	-	Distance to BS	Each round	Center	100	-Energy -Total number of transmitted packets -Network lifetime (FNd, HND)	Square $200\,m \times 200\,m$
MCFL [13]	Fuzzy logic	NA	✓	✓	-	-	After (2i+1) rounds, where i=0..N	center, outside	100	Network lifetime (FND, HND, LND)	Square $200\,m \times 200\,m$
FAMACROW [115]	Heuristic	Distance to BS	✓	✓	-	Quality of communication link	Each round	Center	1000	-Energy -Network lifetime -Data received at BS	Circle $1000m \times 1000m$
PUDCRP [107]	Heuristic	Distance between BS and the center of circular area	✓	✓	-	-	Each round	Outside	100 to 500	-Network lifetime (FND, HND, LND) -Energy -Number of packets	Square $200\,m \times 200\,m$ or Square $400m \times 400m$
EDDUCA [111]	Compound	Sierpinski triangle	✓	✓	-	Distance between nodes	Each round	Center	300	-Energy -Network lifetime	Square $200\,m \times 200\,m$
UCCGRA [112]	Compound	Distance between node and BS	✓	-	-	-Network topology -Transmission power	Each round	Outside (250, 500)	200	-Number of clusters -Network lifetime (FND)	Square $500\,m \times 500\,m$

3.5 Novel approach of developing unequal cluster-based routing protocol

Although there are several unequal cluster-based routing protocols aiming to reduce the network energy consumption, some problems remain not solved including:

- The determination of optimal cluster radius using an energy analysis model
- The determination of the ring width for the circular partitioning considering energetic aspects
- The real implementation of the developed protocols
- The integration of relay nodes considering the energy parameters

In this work, we propose to design a deterministic unequal cluster based routing protocol using fuzzy logic to:

- Balance the load of CHs by defining the optimal radius of clusters considering an energy analysis model
- Select the optimal CHs using three parameters, namely, the residual energy, density and centrality
- Reduce the long-haul transmission between distant CHs using the distance and energy parameters
- Avoid the re-clustering process by fixing a threshold value
- Measure the node energy consumption in real-time
- Implement the developed protocol in real-hardware

Thereby there are several open questions concerning:

- The amount of energy needed for transmitting a data packet
- The threshold value for the re-clustering process
- The number of nodes per cluster

CHAPTER 4

FEAUC: Fuzzy-based Energy-Aware Unequal Clustering

This chapter deals with the development of the novel Fuzzy-based Energy Aware Unequal Clustering protocol (FEAUC), where the shape of the network is considered as circular. The circular partitioning, as depicted in Fig. 4.1, is selected because its independency of the network dimension. The aim is to have an energy efficient, adaptable and scalable unequal clustering protocol, which can be applied in different territories (area shape) and for various network size (short-scale and large-scale networks).

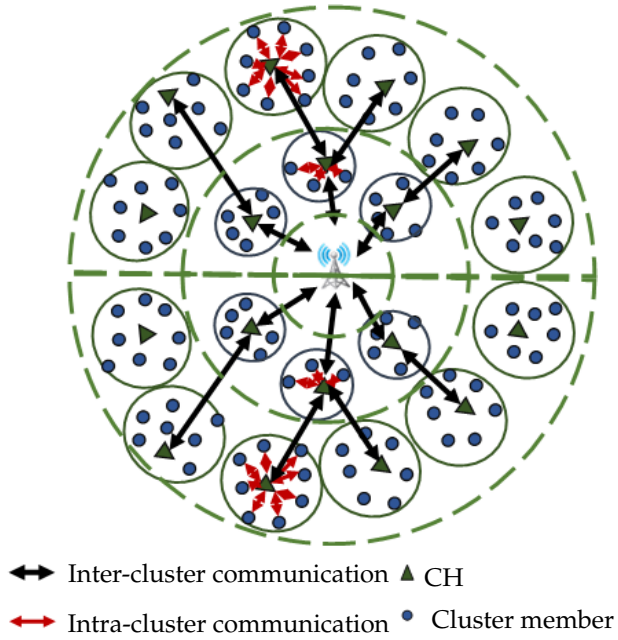

Figure 4.1: FEAUC: Network topology.

In the following, a detailed description of the developed cluster-based routing protocol is provided. Aspects related to the FEAUC are then explained, mainly the network model, the energy analysis and the working principle. Obtained results are presented and compared to main existing unequal clustering protocols in terms of energy consumption and network lifetime. To avoid the energy consumed for the re-clustering process in some rounds, a FEAUC-based fault tolerant algorithm (FEAUC-FT) is developed. To this end, a backup CH is selected when the residual

energy of the primary CH is not enough to run the current round. At the end, a conclusion with a comparative study is presented.

4.1 Network model

Before describing the developed FEAUC protocol, it is important to highlight the used network model. To this end, this section is devoted to explain the reasons behind using circular partitioning. Different network partitioning models are introduced to facilitate and monitor communication efforts such as rectangular and circular partitioning. Generally, various unequal clustering algorithms define the network as rectangular area, which is then, divided into equal sub-area equidistant to the BS as depicted in Fig. 4.2. However, based on the studies done in [82, 118], this partitioning remains efficient only in case of small network. While in large scale case, such partitioning shape could not cover all the network.

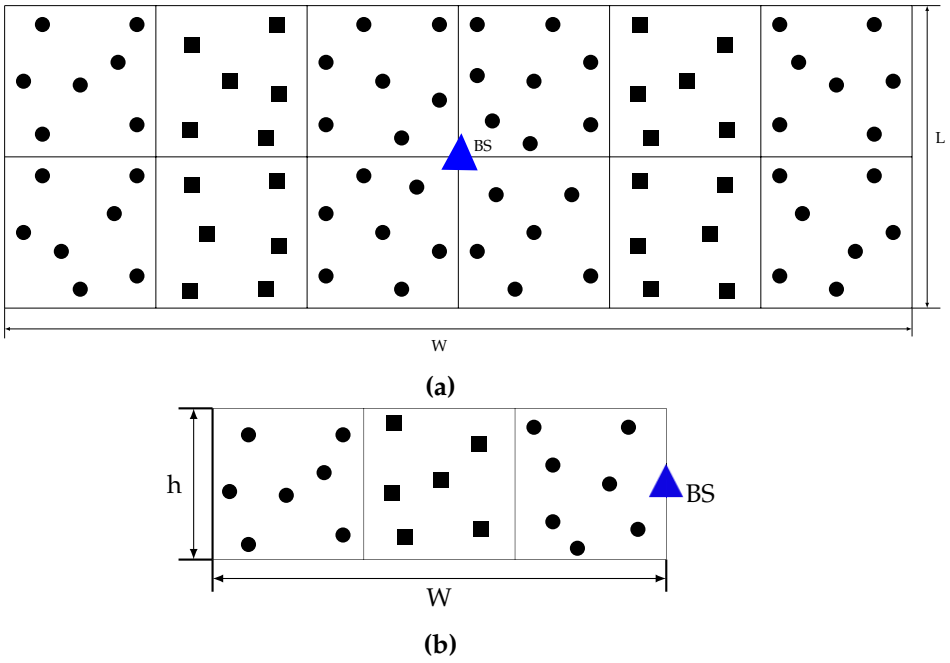

Figure 4.2: (a) Schematic presentation of a rectangular network partitioning, (b) partitioning rectangle into regions.

For a rectangular area with a length L and a width W, the network area is partitioned into some small rectangular regions with a length h as shown in Fig. 4.2(b). The maximum difference distance from the BS of a region, Δ_{BS} can be calculated in eq. 4.1.

$$\Delta_{BS} = d_{toBS_{max}} - d_{toBS_{min}} = \sqrt{(h/2)^2 + w_i^2} \tag{4.1}$$

$d_{toBS_{max}}$ presents the distance that separates the BS to the farthest point, placed on the upper left or lower left edge. $d_{toBS_{min}}$ presents the closet point to the base station. As seen in eq. 4.1, Δ_{BS} increases with increasing the width of a region h.

In case of a circular partitioning, the complete network is considered as a circle with a radius R as depicted in Fig. 4.3(a). The network is then, partitioned into circles, where the BS is placed in the centre. The defined circles are created according to the angular deviation α and radius r as presented in Fig. 4.3(b). Then, a piece, or a region i is considered as shaded area with radius $(i-1)r$ as the right border and ir as the left border.

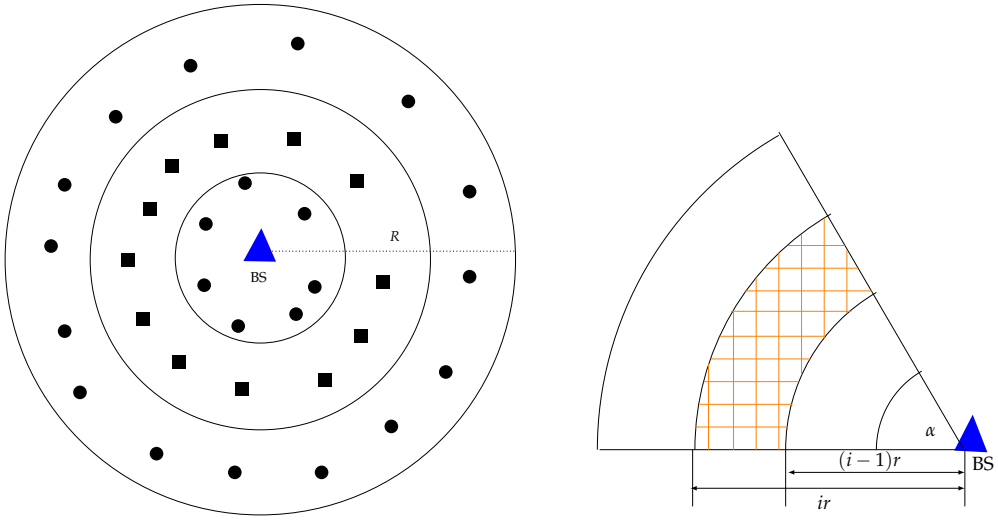

Figure 4.3: (a) Schematic presentation of circular network partitioning, (b) dividing rings into regions.

The maximum difference distance from the BS, Δ_{BS}, is formulated in eq. 4.2. Considering this equation, Δ_{BS} remains constant, despite the variation of the area's radius r.

$$\Delta_{BS} = ir - (i-1)r = r \tag{4.2}$$

The choice of the partitioning model is critical in order to enhance the network stability. Hence, a comparison between both models is carried out in term of maximum distance to the BS. Fig. 4.4 draws out a comparison between the square and the circular partitioning for different values of region width. Obtained results confirm that the circular partitioning is independent of the network dimension, as the maximum distance to the BS, it remains stable compared to the square partitioning scheme. From Fig. 4.4, it is proved that circular network model has a better accuracy in term of energy consumption compared with rectangular partitioning scheme. The use of rectangular network is inaccurate for the variable dimensions compared to the circular partitioning scheme.

For this reason, the circular model is considered in this dissertation. The network is assumed, then, as a circle, where the BS is in the centre. The whole area is then partitioned into a defined number of rings with specific radii. Initially, all nodes have the same energy. Moreover, sensor nodes are randomly deployed in an uniform distribution with a density λ. The choice of using uniform random deployment is

based on the comparative study given in [119] on different deployment topologies in term of k-coverage, which proves that the uniform random deployment outperforms the Poison distribution and the grid in terms of energy consumption and cost. Indeed, it is known as a cost-effective deployment strategy because the installation of nodes is easy.

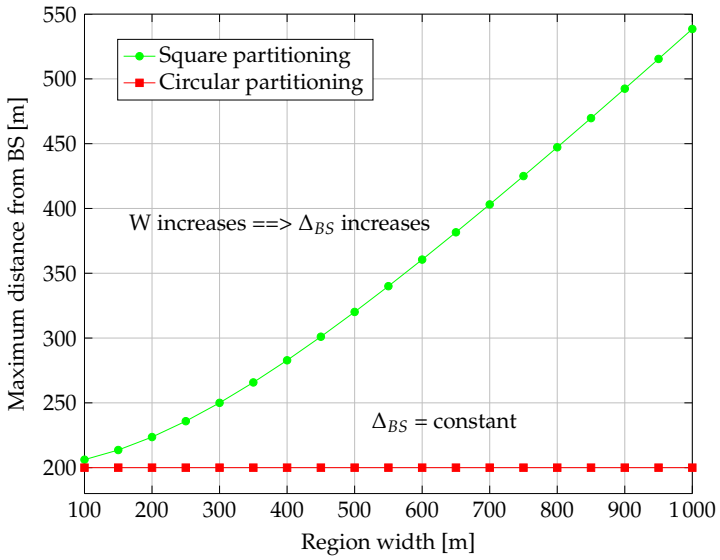

Figure 4.4: Comparison between square and circular partitioning.

Another major contribution and characteristic of the chosen model lies primarily in its ability to be implemented in the most diverse territories (circular, square, etc) (see Fig. 4.5(a), Fig. 4.5(b), Fig. 4.5(c), Fig. 4.5(d)), which ensures a certain portability and adaptability. Indeed, for each area, the BS is located at the centre and from this highest point the distance is chosen as far as possible so that the radius is equal to the maximum distance between the centre and the border. This is done to ensure a full coverage of the area.

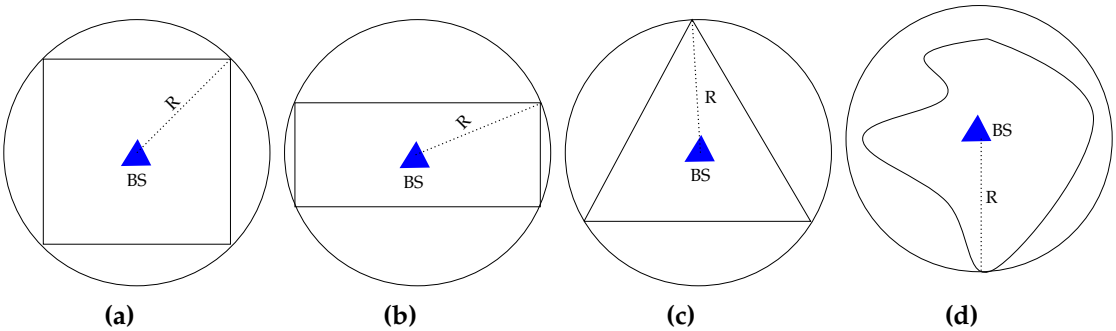

Figure 4.5: Different possible shapes: (a) Square, (b) rectangular, (c) triangle, (d) random.

4.2 Developed unequal cluster-based routing protocol

This section is devoted to describe deeply the working principle of the novel unequal clustering protocol. As seen in Fig. 4.6, FEAUC is divided into four phases: Off-line, cluster formation, cooperation and data collection. During the off-line phase, an energy analysis is performed to calculate the radius of each ring and the optimal radius for each cluster. The cluster formation phase calls out a fuzzy logic approach for the CH selection. It uses the residual energy of a node, its density and centrality as input parameters for the fuzzy system. The cooperation phase aims to define an intermediate node as a router between different CHs. In the data collection phase, transmitting a data packet from sensor nodes to their appropriate CHs is defined as an intra-cluster communication. While transmitting data from one CH to another until reaching the BS, is defined as an inter-cluster communication.

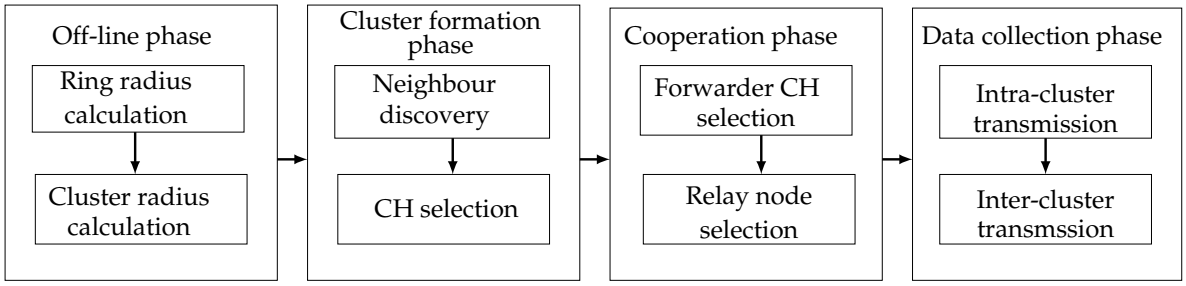

Figure 4.6: Operational process of FEAUC.

The network timeline of the developed unequal clustering protocol is depicted in Fig. 4.7. In the first round, nodes define the list of their neighbours within the cluster radius resulting from the off-line phase. Then, a CH selection step is launched to identify the adequate CH for each cluster. After that, since the multi-hop communication scheme is used, the routing path between the CH and BS is established by using an intermediate node. This later can be a CH from the upper ring, namely forwarder CH, or a relay node, which will be defined in details later. After establishing routes between different CHs from various rings, data is aggregated and forwarded to the BS. A detailed description for each phase is provided in the following subsections.

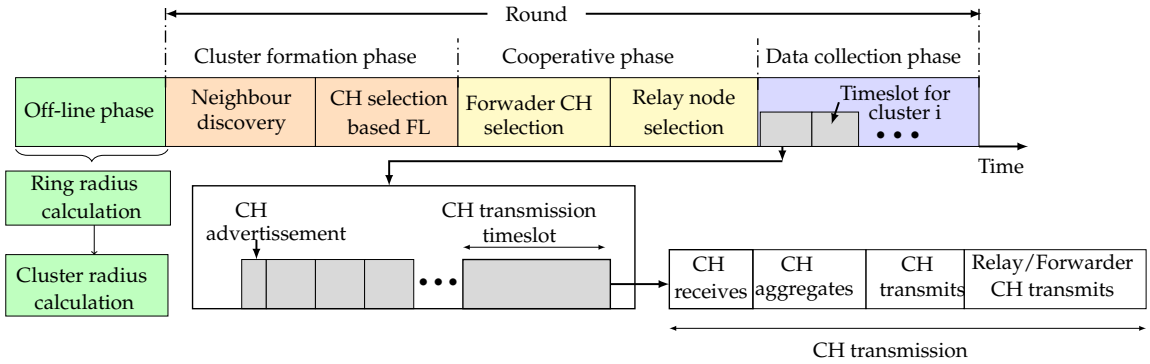

Figure 4.7: Timeline diagram of FEAUC.

4.2.1 Off-line phase

An energy analysis is carried out to efficiently calculate the optimal number of rings in the network, the number of nodes in each ring and the optimal radius of each cluster. The creation of an optimum number of clusters in the network is a significant feature, which has a considerable impact on the energy consumption. It is proven in [82] that if clusters are not formed in an optimal distribution, the total energy consumption of the network increase significantly. So, if the number of clusters built exceeds/inferior the optimal number of clusters, an added amount of energy is consumed. In the same way, an optimal number of nodes are expected to be CHs (c_{opt}). When the number of CHs is less than c_{opt}, a considerable number of nodes have to transmit their data over extremely large distances to access the CH, leading to a high overall energy drain across the whole network. On the other hand, when the number of CHs is more than c_{opt} CHs, then fewer data is aggregated at the local level and a great amount of transmissions is needed to control the whole coverage field.

- Ring radius calculation and network deployment

The network is assumed to be circular, where the BS is located at the centre as depicted in Fig 4.8 (a). The output of the presented sub-phase is to determine the optimal radius of a ring and the optimal number of nodes within a ring.

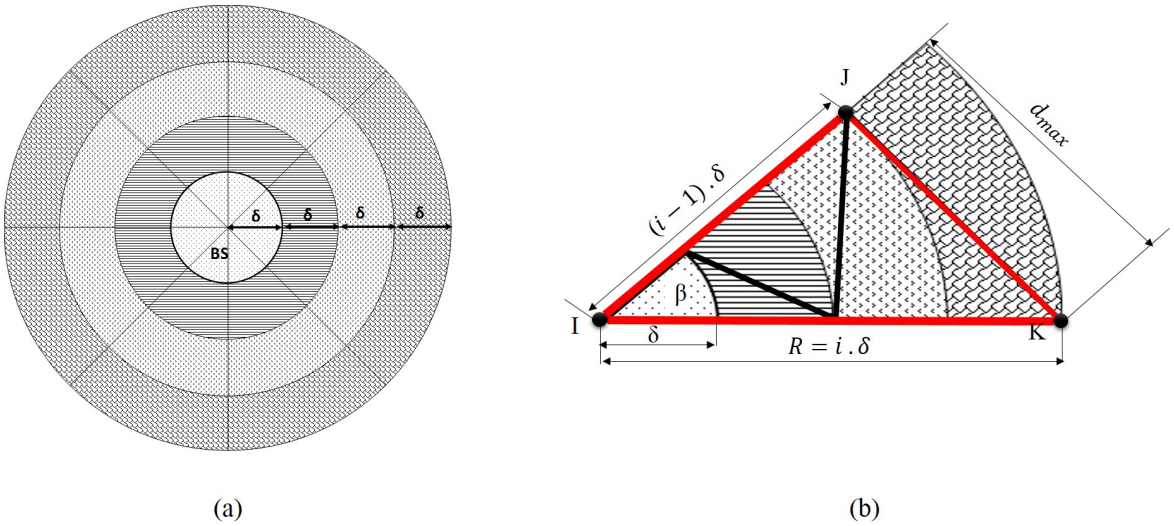

Figure 4.8: Definition of the network model: (a) Cluster distribution in a circular network with BS at centre, (b) geometric presentation of ring radius calculation.

The network area with radius R is partitioned into L rings. To calculate the optimal number of rings, the circle is divided into pies with a given angle, β, as depicted in

Fig. 4.8 (b). The width of a ring δ is obtained by solving eq. 4.3:

$$\begin{cases} min\ (E_{path}) \\ s.t \\ 0 \leqslant \delta \leqslant \frac{R}{2} \end{cases} \tag{4.3}$$

E_{path} is the energy needed to transmit one bit from the node having the longest distance to the BS. Depending on eq. 2.3, the required energy to transfer one bit data via a selected route can be obtained in eq. 4.4:

$$E_{Tx}(l,d_i) = \begin{cases} l \cdot E_{elect} + l \cdot \varepsilon_{fs} \cdot d_i^2 & \text{if} \quad d_i < d_0 \\ l \cdot E_{elect} + l \cdot \varepsilon_{amp} \cdot d_i^4 & \text{if} \quad d_i \geqslant d_0 \end{cases} \tag{4.4}$$

d_i is measured by applying a geometric Pythagoras relation on the formed triangle IJK as depicted in Fig. 4.8 (b). It is defined by the length of JK side, which can be calculated as in eq. 4.5.

$$\begin{aligned} d_{max} = d_i = \left\| \overrightarrow{JK} \right\| &= \sqrt{IK^2 + IJ^2 - 2IK \cdot IJ \cdot cos\beta} \\ &= \sqrt{(i\delta)^2 + ((i-1)\delta)^2 - 2i\delta(i-1)\delta cos\beta} \end{aligned} \tag{4.5}$$

where i defines the number of the ring. By solving eq. 4.3 and eq. 4.5 the ring radius δ is obtained.

The network radius is defined by $R = L \times \delta$. The optimal number of CHs in a ring k is m_k, with $k = 1..L$. Here, N is the total number of nodes deployed in the whole network. On average, the total number of nodes N_k in ring k is:

$$N_k = \frac{\pi(k\delta)^2 - \pi((k-1)\delta)^2}{\pi R^2} N = \frac{2k-1}{L^2} N \tag{4.6}$$

After determining the optimal number of nodes in each ring, those nodes are assumed to be uniformly distributed.

- Calculation of the optimal cluster radius

After the network deployment, the optimal number of clusters in each ring and the optimal radius of each CH are determined. The expectation of the squared distance between CH of k-th ring and the BS $E[d^2_{CH_k,BS}]$ is obtained in eq. 4.7.

$$\begin{aligned} E[d_{CH_k,BS}] = \int_0^{2\pi} \int_{(k-1)\delta}^{k\delta} \frac{r^2}{\pi(k\delta)^2 - \pi((k-1)\delta)^2} dr d\theta \\ = \frac{2[k^3 - (k-1)^3]}{3(2k-1)} \delta \end{aligned} \tag{4.7}$$

The expected distance of a CH from a sensor node within the same cluster of k^{th} ring, $E[d^2_{CM,CH_k}]$, can be calculated in eq. 4.8:

$$E[d^2_{CM,CH_k}] = \int_0^{2\pi} \int_{(k-1)\delta}^{k\delta} \frac{r^3}{\pi(k\delta)^2 - \pi((k-1)\delta)^2} dr d\theta = \frac{k^2 + (k-1)^2}{2}\delta^2 \tag{4.8}$$

The expectation of the squared distance between the CH in the k-th ring and the CH of ring $(k-1)$ can be calculated as in eq. 4.9.

$$E[d^2_{CH_k,CH_{k-1}}] = E[(d_{CHk} - d_{CH_{k-1}})^2] = \frac{42(k-1)^2 - 17}{9(2k-1)(2k-3))}\delta^2 \tag{4.9}$$

Due to multi-hop communications, distances used by single-hop schemes are relatively short. As assumption, the distance between all sensor nodes is less than the critical distance d_0 ($d_0 = 70\,m$ in this work). The total energy consumed by the whole network can be expressed as in eq. 4.10, having E_{DA} as the energy for the data aggregation.

$$\begin{aligned} E_{Cluster_k} &= lE_{Rx}(\frac{N_k}{m_k} - 1) + lE_{DA}\frac{N_k}{m_k} \\ &+ l\frac{\sum_{i=k+1}^{L} m_i}{m_k}(E_{Rx} + E_{Tx} + \varepsilon_{fs}E[d^2_{CHk,CH(k-1))}]) \\ &+ l(E_{Tx} + \varepsilon_{fs}E[d^2_{CH_k,CH_{k-1})}]) \end{aligned} \tag{4.10}$$

Even from the perspective of energy consumption, the average consumed energy of a CH from the first ring should be equal to the average consumed energy of the CH from the (k-1)-th ring.

$$E_{Cluster_k} = E_{Cluster_1} \tag{4.11}$$

In the first ring, the energy consumption of each cluster can be obtained by eq. 4.12.

$$\begin{aligned} E_{Cluster_1} &= E_{CH_1} + (\frac{N_1}{m_1} - 1)E_{non-CH} \\ &\approx E_{CH_1} + (\frac{N_1}{m_1})E_{non-CH} \end{aligned} \tag{4.12}$$

where E_{CH_1} is the energy consumption of a CH from the first ring, E_{non-CH} is the energy consumption for an individual node from the first ring, N_1 is the optimal number of nodes in a cluster and m_1 is the optimal number of cluster in the first ring.

The total energy consumed by all clusters in the first ring is equal to

$$E_{Total_1} = m_1 E_{Cluster_1} = l(E_{Rx} + E_{DA})N_1 + lm_1\varepsilon_{fs}d_{CH_1}^2 + l\sum_{i=2}^{n_{cluster}} m_i(E_{Rx} + E_{Tx} + \varepsilon_{fs}d_{CH1}^2) + N_1 lE_{Tx} + \frac{N_1}{2m_1}l\varepsilon_{fs}\delta^2 \tag{4.13}$$

The energy consumption of each cluster in the k-th ring can be obtained by eq. 4.14.

$$\begin{aligned} E_{Cluster_k} &= E_{CH_k} + (\frac{N_k}{m_k} - 1)E_{non-CH} \\ &\approx E_{CH_k} + (\frac{N_k}{m_k})E_{non-CH} \end{aligned} \tag{4.14}$$

with E_{CH_k} and E_{non-CH_k} are the energy consumption in a ring k of a CH and normal nodes (non-CH), respectively. The total energy spent by all nodes in a ring E_{Total_k} is

$$E_{Total_k} = m_k E_{Cluster_k} \tag{4.15}$$

To obtain the optimal number of CHs $m_{k_{opt}}$, eq. 4.13 should be differentiated with respect to m_k as follows:

$$l\varepsilon_{fs}\frac{42(k-1)^2 - 17)}{9(2k-1)(2k-3)}\delta^2 - \frac{N_k l\varepsilon_{fs}(k^2 + (k-1)^2)}{2m_k^2}\delta^2 = 0 \tag{4.16}$$

With resolving eq. 4.15, the optimal number of clusters in each ring is obtained:

$$m_{k_{opt}} = \frac{9N_k(k^2 + (k-1)^2)(2k-1)(2k-3)}{2(42(k-1)^2 - 17)}. \quad k = 2,..,L \tag{4.17}$$

The optimal radius of a cluster in a ring k is therefore described in eq. 4.18.

$$R_{(CH_k)opt} = \delta\sqrt{\frac{2k-1}{m_{kopt}}}, \quad k = 2,..,L \tag{4.18}$$

After determining the radius of each ring, all nodes within the same ring are placed at the same radius relative to the BS, which differs from one ring to another. The output of the off-line phase are the ring's width, the optimal cluster radius and the optimal number of nodes in each ring.

4.2.2 Cluster formation phase

After the uniform random node deployment, a cluster formation is initiated. This phase involves neighbour discovery and CH selection sub-phases as depicted in Fig. 4.7.

- Neighbour discovery

Each node uses a TDMA protocol to broadcast a NODE_INFO message including its ID, ring ID, position and residual energy within a communication range equal to the optimal radius determined in eq. 4.18. When a node receives a NODE_INFO from its neighbours, it saves the information in its routing table, adds this node in its neighbour list and calculates its distance to all neighbouring nodes. Thus, the routing table of each node includes the node ID, ring ID, positions, list of neighbours, distance to each neighbour and residual energy.

- Fuzzy-based CH selection

After determining the neighbours list, each node has to calculate independently its chance to be a CH by applying a fuzzy logic system (see annex A). As described in Fig. 4.9, the fuzzy logic consists basically on three blocks including the fuzzifier, fuzzy decision block and defuzzifier. Since the inputs' data are crisps, a fuzzification block is required, which converts these crisps into linguistic values. A set of fuzzy rules that describes the system behaviour is generated by the rule base. The Mamdani [120] fuzzy rule-based system is considered. The linguistic values and the fuzzy IF-THEN rules are used by the inference system. The Center of Area (CoA) technique is applied for the defuzzification of the competition radius.

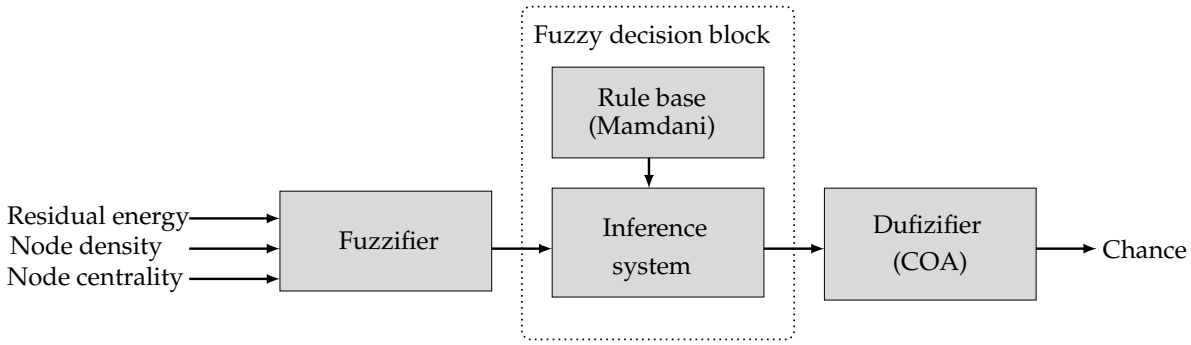

Figure 4.9: Fuzzy system of the developed FEAUC protocol.

The three input parameters are the residual energy, density and centrality. As explained follows, these parameters are chosen because of their importance for extending the network lifetime.

(1) Residual energy: The residual energy defines the remaining energy of each node at a defined time. The more residual energy contained in the node, the more its lifetime is longer, the more data is transmitted and the more stable the network is.

(2) Density: The density presents the number of neighbour nodes for a tentative CH. It is more reasonable to select a CH having more neighbours. For example, a node i is placed in a such cluster belonging to a such ring. Its density, $Density_i$ can be calculated using eq. 4.19.

$$Density_i = \frac{\text{Number of neighbors node}}{\text{Total node number in the ring}} \tag{4.19}$$

(3) Centrality: It presents how central the node is among its neighbours. The more central the node is to a CH, the less distance to its cluster members. As the energy needed for transmission is generally proportional to the square of the distance between the transmitter and receiver. Having a higher value of centrality implies less energy is needed by surrounding nodes to deliver data to the candidate CH. For example, a node i is deployed in a such cluster belonging to a such ring. Its centrality, $Centrality_i$ can be calculated using eq. 4.20.

$$Centrality_i = \sqrt{\frac{\frac{\sum_j dist^2(i,j)}{|nbr(i)|}}{\text{Cluster radius}}} \tag{4.20}$$

where, j is the node neighbour of a node i, $nbr(i)$ is the list of neighbours and $dist$ is the distance between two nodes.

Table 4.1: Fuzzy rules for the CH selection

Rule No.	Residual energy	Node density	Node centrality	Chance
1	Low	Low	Close	w
2	Low	Low	Adequate	w
3	Low	Low	Far	vw
4	Low	Medium	Close	w
5	Low	Medium	Adequate	w
6	Low	Medium	Far	w
7	Low	High	Close	lw
8	Low	High	Adequate	w
9	Low	High	Far	vw
10	Medium	Low	Close	lh
11	Medium	Low	Adequate	m
12	Medium	Low	Far	w
13	Medium	Medium	Close	h
14	Medium	Medium	Adequate	m
15	Medium	Medium	Far	lw
16	Medium	High	Close	h
17	Medium	High	Adequate	lh
18	Medium	High	Far	lw
19	High	Low	Close	lh
20	High	Low	Adequate	m
21	High	Low	Far	lw
22	High	Medium	Close	h
23	High	Medium	Adequate	lh
24	High	Medium	Far	m
25	High	High	Close	vh
26	High	High	Adequate	lh
27	High	High	Far	m

Very weak (vw), Weak (w), Little weak (lw), Medium (m), Little high (lh) High (h), Very high (vh)

Most of the existed clustering algorithms based on fuzzy logic used the residual energy and density or the residual energy and centrality or the density and centrality but none of them used the combination of these three parameters [13, 114, 115, 121,

122]. This work proposes to combine the three mentioned parameters. Table 4.1 describes the fuzzy rules and the corresponding chances for being a tentative CH.

The input variables of the residual energy, the node density and centrality are described in Fig. 4.10(a), Fig. 4.10(b) and Fig. 4.10(c), respectively. The only fuzzy output variable is the chance of a node to be a CH, which is presented in Fig. 4.10(d).

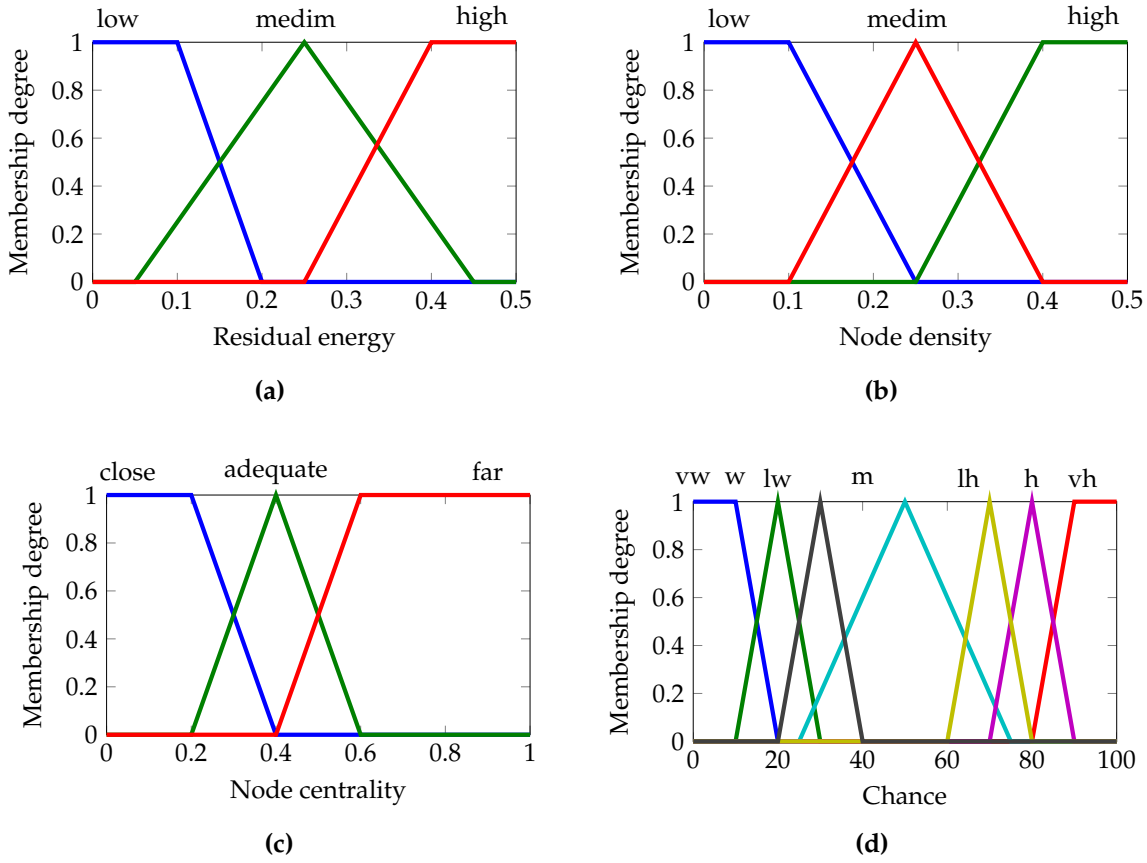

Figure 4.10: Membership function for input variable: (a) Node remaining energy [J], (b) node density, (c) node centrality, (d) membership function for output variable 'chance'.

Algorithm 1 summarizes the operation process of the cluster formation phase. As seen in algorithm 1, sensor nodes transmit their input parameters, including residual energy, density and centrality, to the fuzzy deduction engine, which calculates the chance of each node to be a CH. After that, the node compares its individual chance to the chance of its neighbours within the same cluster. The node having the highest chance is selected as a CH and transmits an announcement message to its members informing them about its status. The nodes receiving this message transmit a joint message to the respective CH. If a node receives more than one final CH message, it chooses the final CH with the highest cost to join it. If a node finishes the clustering process and does not receive any final CH message, it announces itself as a final CH.

Algorithm 1: Cluster formation phase

N: total number of sensor nodes in the network
N_j: total number of sensor nodes in a ring j
n_j: a sensor node in a ring j
a: number of rings
x_i and y_i: coordinates of a node i
$E_{res}(i)$: residual energy of a node i

1. Do neighbouring discovery
2. Calculate the chance of being a CH
   for $k \leftarrow 1$ *to* a **do**
   for $h \leftarrow 1$ *to* N_j **do**
   h.Neighbors=number of nodes within the same communication radius
   h.Energy=residual energy of a sensor node
   h.Density=density of a sensor node
   h.Centrality=centrality of a sensor node
   h.chance=fuzzy(h.Energy,h.Density,h.Centrality)
   end
   end
3. Select the CH for each cluster
   for $l \leftarrow 1$ *to* N **do**
   send (l.chance, l.h.Neighbors)
   if *(l.chance=best(chance))* **then**
   $l.status \leftarrow finalCH$
   $send(l.status, l.Neighbors)$
   else
   $l.status \leftarrow member$
   join_cluster()
   send(l.data)
   end
   if $(l.Neighbors = \emptyset)$ **then**
   $l.status \leftarrow finalCH$
   end
   end

return (List of CHs)

4.2.3 Cooperation phase

In this stage, a CH is selected for each cluster. Since a multi-hop communication scheme is used to communicate the CHs with the BS, a cooperative phase is initiated. In this phase, the intermediate node is selected to establish the route between the transmitter CH and BS. To this end, as seen in Fig. 4.7, a forwarder CH or a relay node can be selected.

- Forwarder CH selection

This step performs the route between CHs from different rings. After the formation of clusters, each CH from ring (k) tries to select the adequate CH from ring (k-1) as a relay to forward data to the BS. To this end, each CH from ring (k) broadcasts an advertisement message to CHs from ring (k-1). This message includes its ID, ring ID, residual energy and position. Each CH from ring (k-1) receiving the transmitted message defines itself as a candidate forwarder CH and sends a join message to the transmitter CH including its ID, residual energy and position.

Since minimizing the energy consumption is the key objective of this work, the residual energy as well as the distances between CHs from different rings (successive rings) are highly recommended. This is because the consumed energy for the transmission increases proportionally with the square of the distance between the sender and receiver. To select a CH_i from the next ring as a forwarder CH, this CH_j should calculate the ratio of residual energy of CH_i , $E_{res}(CH_i)$, and the distance between CH_i and CH_j, $d_{CH_i\,to\,CH_i}$, as expressed in eq. 4.21.

$$ratio(E_{res},d_{CH_itoCH_j}) = \frac{E_{res}(CH_i)}{d_{CH_itoCH_j}} \tag{4.21}$$

The candidate forwarder node having the maximum ratio rate is selected as a final forwarder CH. In the most relevant clustering algorithms, the selection of the forwarder CH is made randomly or based only on the residual energy or the shortest distance. In this work, the ratio of residual energy and nodes distance is applied. This enables to select the right relay node having the highest energy and shortest distance to the transmitted CH. Considering only the residual energy can cause some issues because it comes that a CH has the maximum energy but it is far away from the source CH. Thus, the CH source energy is depleted promptly since it needs more energy to transmit data packets. Considering also only the shortest distance between the two CHs may cause some problems because the CH that is closest to the source CH is not necessarily having the power to receive this packet. For this reason, one of the contribution of the presented work is to combine the residual energy and the distance to select efficiently the forwarder CH.

- Relay selection using cooperative communication

Although the energy consumed during the transmission is substantially higher than during the reception, some scenarios are distinguished by a relatively low energy level that is proportional to the energy required for the reception E_{RX}. Therefore, to benefit from this potential energy reduction, a cooperative communication system should be set up to improve the network performance and to ensure a certain balance between the transmission and reception. The importance of this approach is the use of relay nodes as intermediate nodes, whereby the energy consumption is proportional to the square of the distance, and therefore decreasing the distance between the source and the destination reduces the energy considerably. As WSNs are battery-powered, there is a strong need to design an efficient transmission rule for clustered networks that reduces the energy transmission between any source CH in the cluster while maintaining the required level of reliability. Furthermore, a cooperative routing approach is developed that guarantees a reliable and energy efficient packet transmission by selecting the optimal relay node in the routing mechanism.

Algorithm 2 briefly explains the procedure of the relay selection sub-phase to reduce the transmission range of primary CHs.

Algorithm 2: Relay node selection process.

Result: (Relaynode)
CH_T,CH_R,$E_{res}(CH_T)$,$E_{res}(CH_R)$, $d_{CH_T toCH_R}$,n_j
$i \leftarrow 1$
count=1
if $E_{res}(CH_T) > E_{res}(CH_R)$ **then**
  CH_T sends Relay_Candidate_Signal packet to CH_R
  repeat
    if *(Relay_Candidate_Signal packet received = true) and* $(n_j \in CH_R)$ **then**
      $count \leftarrow count + 1$;
      $chance[j] = E_{res}(n_j)/d_{n_j toCH_T}$
      $i \leftarrow i + 1$;
    end
  until *i=count*;
  Relay_Chance $\leftarrow \max(chance)$
  Relaynode $\leftarrow (n_j(Relay\_Chance))$
  Start cooperative transmission
else
  CH_T transmit its packet directly to CH_R
end
return (Relay node)

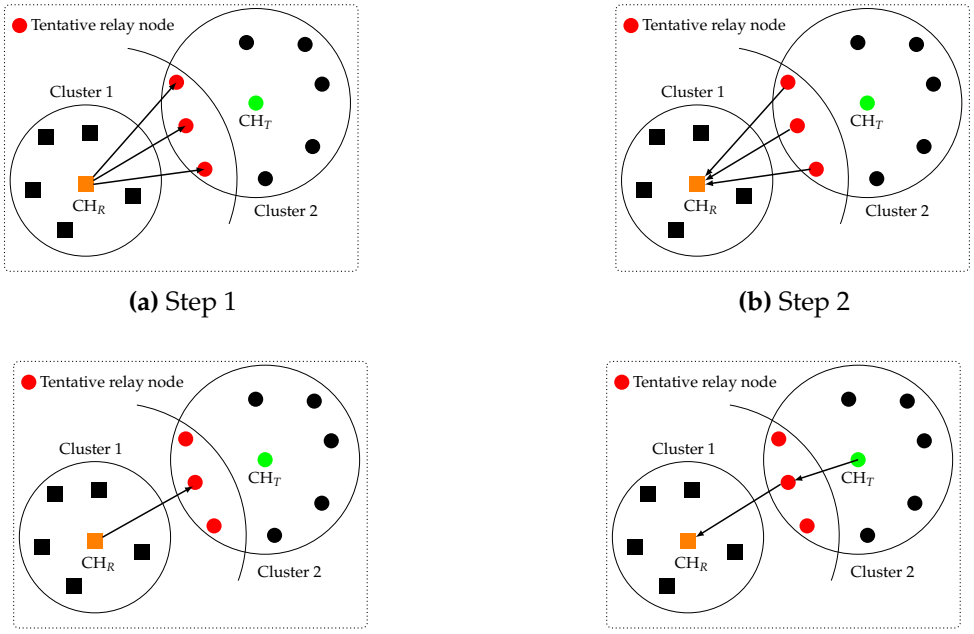

(a) Step 1 **(b)** Step 2

(c) Step 3 **(d)** Step 4

Figure 4.11: Relay candidate selection process.

As depicted in Fig. 4.11, a transmitter CH, CH_T, transmits its data to the receiver CH, CH_R, directly when its residual energy is higher than the residual energy of the CH_R or via a relay node of the CH_T itself in the other case. When performing the inter-cluster transmission, a selected relay node can cooperate with its CH to reduce the transmission range of CHs. CH_R broadcasts a relay candidate signal packet within a certain range, which presents its distance to CH_T. If a node from cluster T receives this relay candidate signal packet, it becomes a relay node for the CH_R. This node transmits an acknowledgement message to the CH_R to confirm the reception of

a relay candidate packet. The CH_R gathers information from all candidate members and transmits a data packet to the CH_T including the residual energy of each node (n_j) and its position. Then, the CH_R calculates for each candidate node its chance to be a relay node by dividing the residual energy of node (n_j) and its distance to CH_T ($d_{n_j toCH_T}$). The node having the higher chance, $ratio(E_{res}, d_{CH_T toCH_R})$, is selected by CH_R as a relay node, which will forward the data received from CH_T to CH_R.

To select a CH_i from the next ring as a relay, the CH_j calculates the ratio of the residual energy of CH_i, $E_{res}(CH_i)$ and the distance between CH_i and CH_j, called $d_{CH_i toCH_j}$, as expressed in eq. 4.22.

$$ratio(E_{res}, d_{n_j to CH_T}) = \frac{E_{res}(n_j)}{d_{n_j to CH_T}} \tag{4.22}$$

To conclude, when the transmitter CH has more residual energy than the receiver CH, it transmits its data packet directly without using a relay node. Otherwise, it applies the relay selection algorithm to select the optimal relay node that cooperates and assists the CH transmitter by minimizing the distance of transmission. Fig. 4.12 summarises the cooperation phase process.

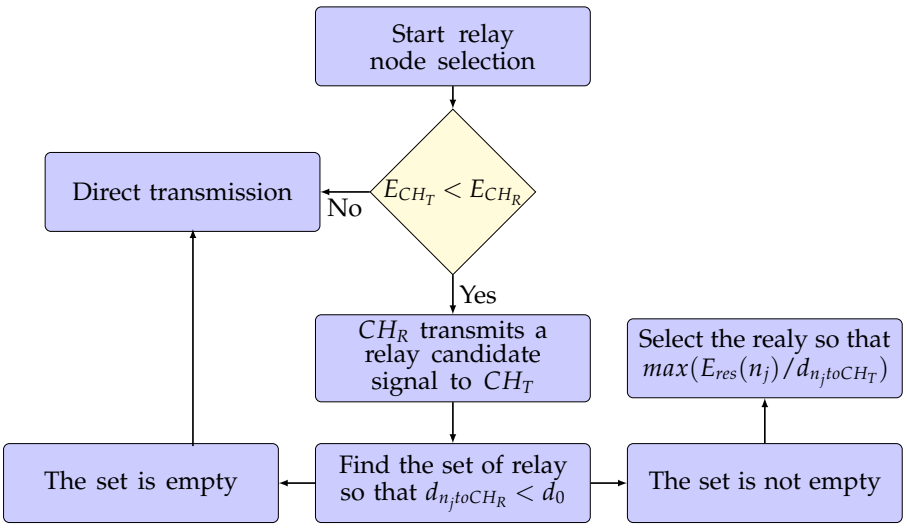

Figure 4.12: Flowchart of the transmission strategy.

4.2.4 Data collection phase

At this stage, all routes between the sensor nodes and the BS are well-established. Data gathered from nodes are transmitted to the BS via their own CH. Then, the collected information by each CH is transmitted to another CH from the previous ring or to a relay node until reaching the BS. Fig. 4.13 describes in details the working principle of the data collection phase. As presented in algorithm 3, The data collection phase comprises two steps: Intra-clustering transmission step and inter-clustering transmission step.

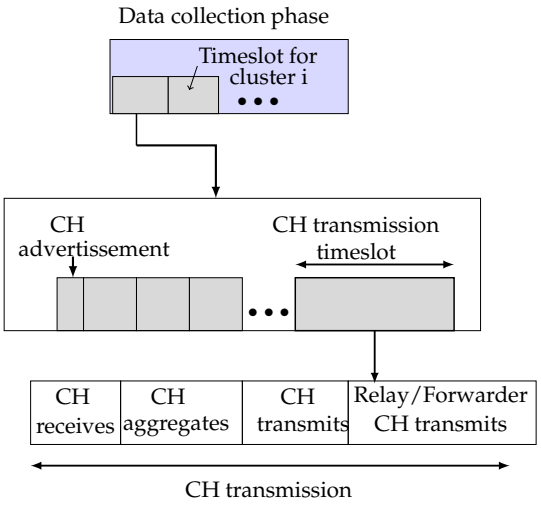

Figure 4.13: Data collection phase process.

- Intra-clustering transmission

In this step, normal nodes except relay nodes, transmit their data packets to their appropriate CHs. For each cluster, the CH transmits to its cluster members the appropriate parameters for the schedule, which is divided into TDMA frames. An example of a CH with two cluster members is illustrated in Fig. 4.14, where further interest to the concept of TDMA-based schedule is given. A synchronization between the CH and its cluster members should be respected to avoid the problem of clock drift and packets collision. Indeed, after receiving the schedule from their respective CH, each cluster member knows its timing and the timings of other nodes. They sense the environment periodically and save the last sensed value. Their radios are turned off, when it is not their time slot and wakes-up when their respective time slot starts. They send the last data saved in their memory to the CH. Therefore, an amount of energy can be saved in this case. The energy consumed by each CH should be updated and recalculated for each round.

- Inter-clustering transmission

At the end of each TDMA frame, every CH forwards the collected data packets and its own packet to the BS either directly, if the CH is from the first ring, or via another CH from previous level or via a relay node. In the case of using a relay node between the transmitter CH, "CH_T", (i.e CH from ring (k)) and the receiving CH, "CH_R", (i.e CH from ring (k-1)), the relay node aggregates the received data from the transmitter CH with its own data packet and forwards it to its respective CH.

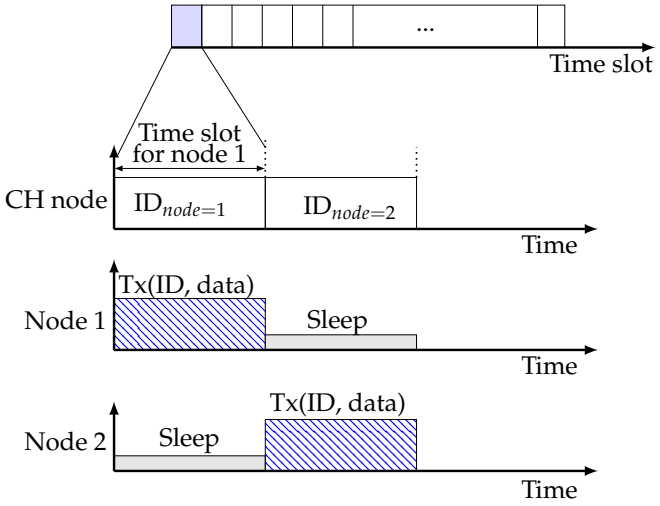

Figure 4.14: Intra-scheduling concept.

Algorithm 3: Data collection phase

1. **Intra-clustering transmission**
   This step is applied for each sensor node except for relay nodes
   a) Sense environment parameters
   b) Save sensed values
   c) Sleep until its time slot starts
   d) Transmit a packet to its own CH
2. **Inter-clustering transmission**

This step is applied for CHs and for relay nodes.
Each CH collects the received data as well as its own data
if $E_{res}(CH_T) \prec E_{res}(CH_R)$ **then**
  if *a relay node of* CH_T *is selected* **then**
    1. CH_T transmits the aggregated data packet to the relay node
    2. Relay node aggregates its own data with the received packet from CH_T
    3. Relay node forwards collected data packets to CH_R
  end
else
  CH_T forwards its data packet to CH_R
end

4.3 Simulation set-up and comparative results

The operation of network is illustrated in Fig. 4.7. After the node deployment, the cluster formation phase aims to select the CHs using the fuzzy logic system with the residual energy, number of neighbouring nodes and centrality of node among its neighbours. While the clustering process is finished, a cooperation phase is carried out to establish the routes between CHs from the ring n to CHs from the ring $(n-1)$.

Moreover, during this phase, the relay node considering its residual energy and its distance from current CH is selected. Finally, a data collection phase is performed, where various CHs aggregate data from cluster members and forward it to the BS via an intermediate CH or a relay node.

4.3.1 Communication/message complexity analysis

In this section, the complexity analysis of the developed FEAUC protocol, in term of total number of transmitted messages is described. Sensor nodes are assumed to have the same features. In total, there is N nodes deployed in the network. Every node broadcasts a message to discover its neighbours. For that, N messages are exchanged. After calculating its chance to be a CH, N messages are broadcast for the CH selection. From these N nodes, $M(< N)$ nodes announce themselves as CH and M messages are transmitted to their cluster members. Afterwards, $(N - M)$ nodes send joint messages to corresponding CHs. The total number of transmitted messages, (N_{CL}), during the cluster formation phase is equal to $(3N)$.

After that, the cooperative phase starts. $H(< M)$ CHs from ring $(k - 1)$ select CHs from ring (k) as forwarder nodes. Thus, H joint request messages are broadcast. $(M - H)$ messages are transmitted from the candidate forwarders. After selecting the optimal forwarder node, H messages are sent asking for joining. Thus, H other joint messages are transmitted from the CHs of ring (k). Among these H CHs, $L(< H)$ nodes have a residual energy less than the forwarder CH energy. For this reason, L relay candidate messages are broadcast to their cluster members. From these L nodes, $J(< L)$ CHs have empty sets of candidate relay nodes. Hence, no message is transmitted. $(L - J)$ messages are broadcast from the relay nodes. After the selection of intermediate nodes, $(L - J)$ messages are sent to optimal relay nodes. The total number of transmissions in the cooperative phase, (N_{CO}), is defined in eq. 4.23.

$$N_{CO} = i(M - H) + H + L + 2j(L - J) \tag{4.23}$$

Where $i(< M - H)$ and $j(< L - J)$ are, respectively, the number of joint request sent by the forwarder CH and relay candidate.

For the data collection phase, $(N - M)$ are transmitted as packets from cluster members to corresponding CHs. $(H - L)$ are transmitted from CHs of ring (k) having higher residual energy than forwarder CHs of ring (k-1) or having no candidate relay nodes. $2(L - J)$ are sent from relay nodes to transmitter CHs. The total number of transmissions, (N_{DC}), in this phase is equal to $(N - M) + (H - L) + 2(L - J)$. At the end, the number of message transmissions, N_{total}, for the FEAUC protocol is expressed in eq. 4.24.

$$\begin{aligned} N_{total} &= N_{CL} + N_{CO} + N_{DC} \\ &= 3N + N - M + H + (2j+1)(L-J) + i(M-H) \\ &= 4N + (i-1)(M-H) + (2j+1)(L-J) \\ &= \mathcal{O}(N) \end{aligned} \tag{4.24}$$

From eq. 4.24, the order of the control message transmission for the developed FEAUC protocol is 1. It has the same order of the first simple developed, LEACH protocol [123]. This is the highly recommended property in the majority of WSN applications. In the worst case, when i is equal to $(M-H)$ and j is equal to $(L-J)$, the message complexity N_{total} is equal to $\mathcal{O}(N^2)$.

4.3.2 FEAUC simulation

In this section, simulations are performed with the network simulator, NS3, to study the energetic aspect of the developed FEAUC as well as to compare it to other existing algorithms. Since the energy is the first objective of the presented work, performance metrics such as the node's residual energy, network lifetime, consumed energy per iteration and number of packets received at the BS are highlighted. The network lifetime can be measured per round until the first node dead i.e. it runs out of its energy. The network lifetime is analysed through the FND, HND and LND metrics.

Here, the developed FEAUC is analysed step by step. The offline phase starts by determining the value that gives the minimum E_{path}, calculated in eq. 4.3, which can be obtained by varying the number of rings in eq. 4.15. The curve of E_{path} that varies with the number of rings for five different values of area radius is shown in Fig. 4.15(a). The number of rings that gives the minimum value of E_{path} is illustrated in Fig. 4.15(b).

Table 4.2: Configuration parameters: 200 nodes

Parameter	Value
Network size	200 m × 200 m
Number of sensor nodes	200
Initial energy	1 J
Data packet size	4000 bits
Circuit energy consumption (E_{elect})	50 nJ/bit
Multi-path channel parameter (ε_{amp})	0.0013 pJ/bit/m^4
Free space channel parameter (ε_{fs})	10 pJ/bit/m^2

After calculating the optimum number of hops, the step of node deployment starts. By applying eq. 4.6, the number of nodes in each ring can be determined. As seen in Table 4.2, 200 nodes need to be deployed in an area of 200 m × 200 m, where the BS is located in the centre of the network. The radius, R is equal to 50 meters as depicted in Fig. 4.16(a).

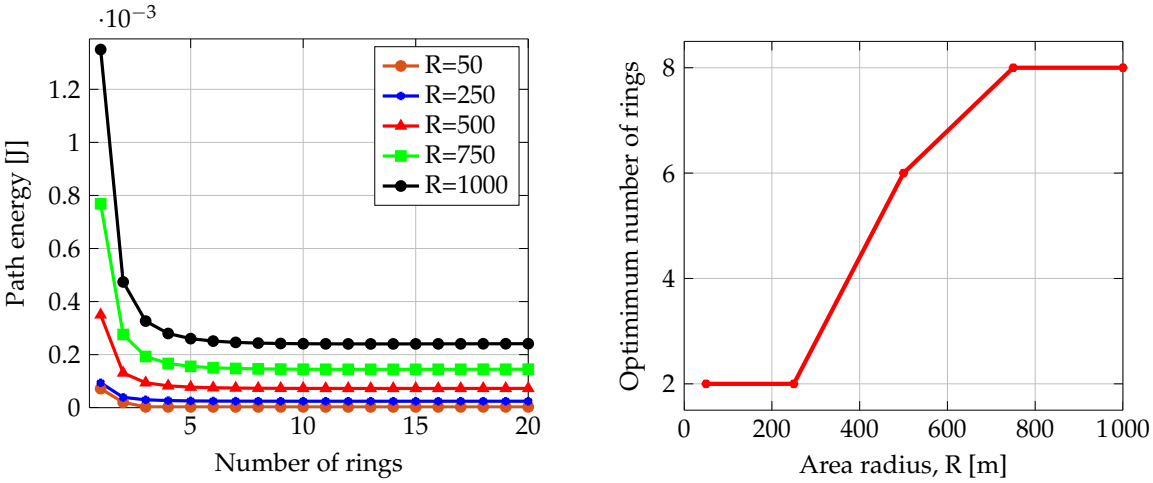

(a) **(b)**

Figure 4.15: (a) Path energy for various number of rings and network radius, (b) number of rings that gives the optimal path energy for different radius.

In the first ring, the optimal number of nodes are 50, while in the second ring, it is 150 nodes. The nodes are then distributed randomly in each ring. Before starting the selection of CHs, the step of the optimal cluster radius calculation is launched. By applying eq. 4.18, for the first ring, the optimal radius of each cluster is equal to 29.82 m and for the second ring, the cluster radius is about 38.5 m.

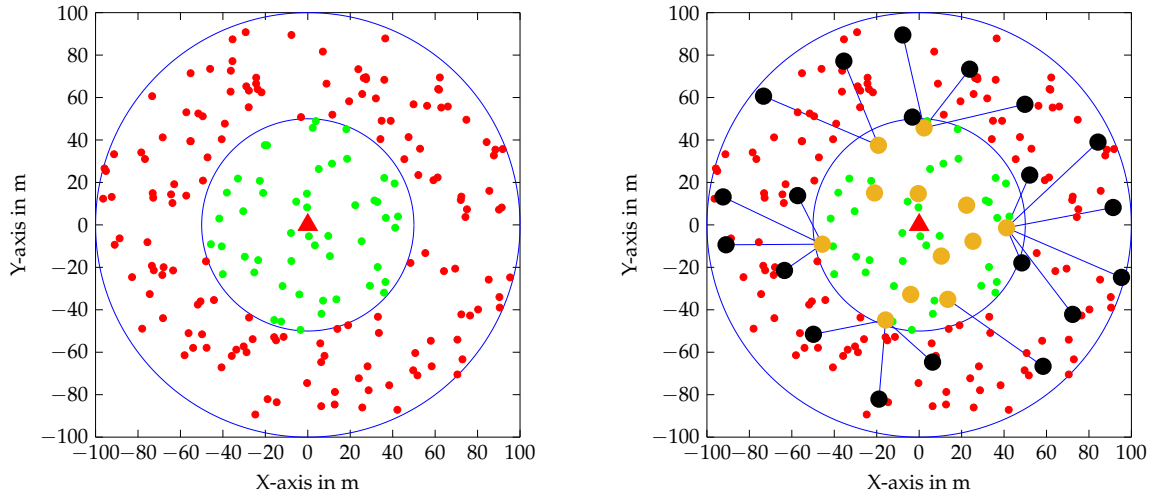

(a) **(b)**

Figure 4.16: (a) Deployment of 200 nodes in 200 m $\times$ 200 m network, (b) data communication during the first round.

Fig. 4.16(a) presents the dispersion of the sensor nodes in the field, the intra-clustering and inter-clustering process is illustrated in Fig. 4.16(b).

After finishing the offline phase, the cluster formation phase starts by exchanging a neighbouring discovery message between nodes within their cluster radius. Then, the process of CH selection is initiated. As discussed in section 4.2.2, the developed FEAUC considers three inputs fuzzy variables: Node residual energy, node density and node centrality. The evaluation of cluster formation is done based on the following three fuzzy membership functions illustrated in Fig. 4.17(a), 4.17(b) and 4.17(c). The residual energy is taken between 0 and 1 Joule because the initial energy of each node is 1 Joule and after running process, it decreases until being 0 Joule, which means the node runs out of energy.

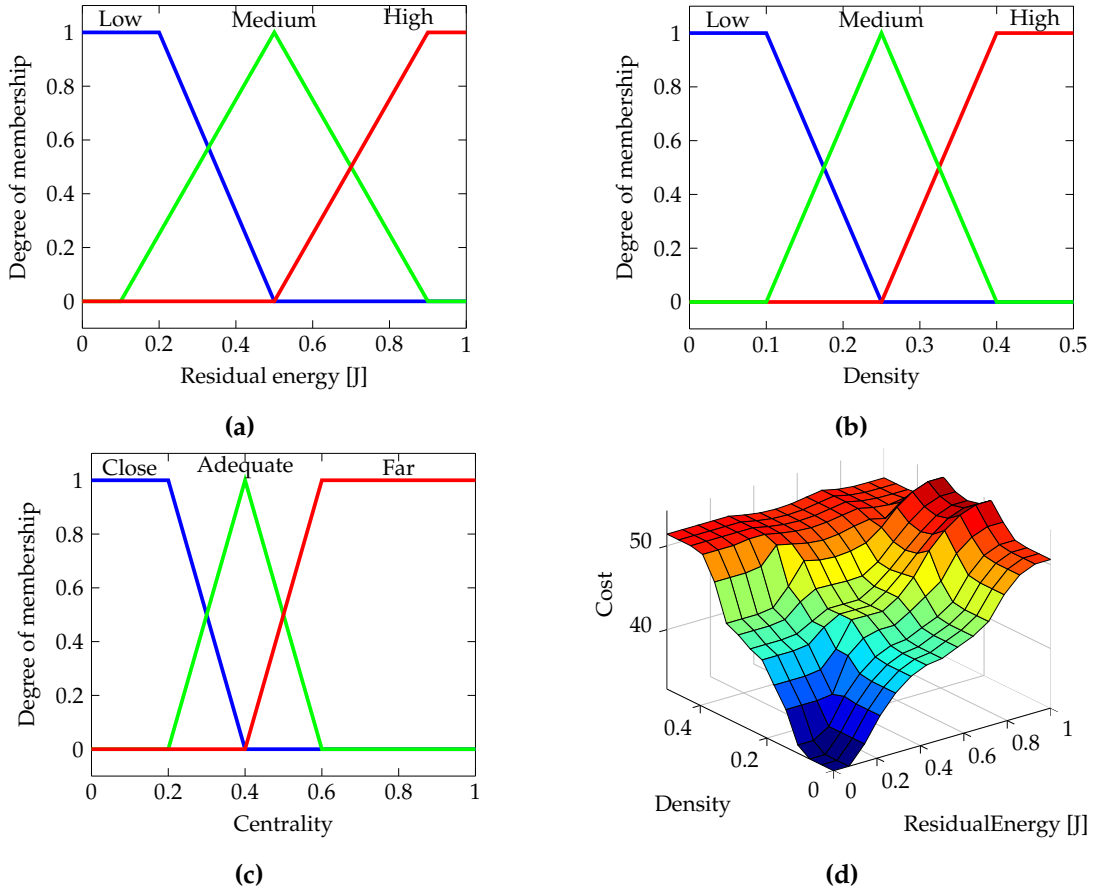

Figure 4.17: Membership function for input variable: (a) Node remaining energy [J], (b) node density, (c) node centrality, (d) membership function for output variable "chance".

As seen in Fig. 4.16(b), for 50 nodes, the number of CHs of the first ring are 12, while 20 CHs are selected in the second ring for a total number of 150 nodes. Indeed, 24% of nodes are selected as CHs in the first ring, while only $\simeq$ 13% of nodes are used as CHs in the second ring.

As conclusion, the number of CH increases when near to the BS compared to the total number of nodes in each ring. Since CHs from the first ring are responsible to collect data from their cluster members and forward the received packets form the second ring, it is important to have more number of CHs. It can be seen also, that

having a lot of CHs can reduce the number of cluster members, so that the energy can be balanced between CHs from different rings.

4.3.3 Comparison to the state of the art

This section is devoted to compare the developed FEAUC algorithm with some existing algorithms in terms of total network remaining energy, FND, HND and LND metrics. Two scenarios are adopted during simulations. One for small density (100 nodes) and the second one for a large density (1000 nodes). In the first scenario, FEAUC is compared with Fuzzy Logic [121], MOFCA [12], DUCF [114] and MCFL [13]. While, in the second scenario, it is compared with FAMACROW [115] and IFUC [124].

- First scenario: Small density

As seen Fig. 4.18, the BS is located in the centre of the network, where 100 nodes are deployed in an area of 100 m $\times$ 100 m. Different unequal clustering algorithms are evaluated according to simulation results presented in Table 4.3.

Table 4.3: Configuration parameters for small and large densities

Parameter	Scenario 1	Scenario 2
Network size	100 m $\times$ 100 m	1000 m $\times$ 1000 m
Number of sensor nodes	100	1000
Initial energy	0.5 J	0.5 J
Data packet size	4000 bits	6500 bits
Circuit energy consumption (E_{elect})	50 nJ/bit	50 nJ/bit
Multi-path channel parameter (ε_{amp})	0.0013 pJ/bit/m^4	0.0013 pJ/bit/m^4
Free space channel parameter (ε_{fs})	10 pJ/bit/m^2	10 pJ/bit/m^2

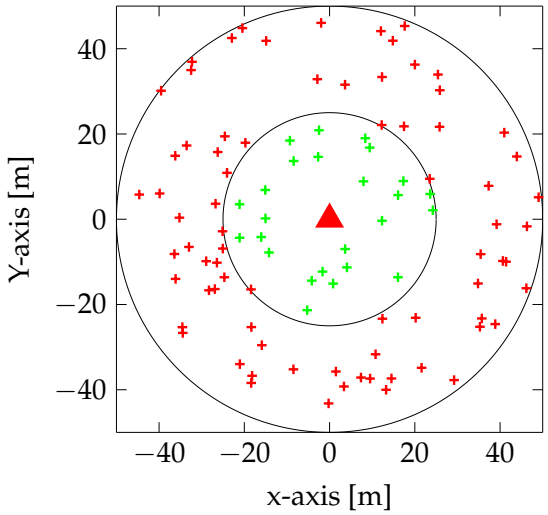

Figure 4.18: Nodes deployment in 100 m $\times$ 100 m network (scenario 1).

The value that gives the minimum E_{path} can be obtained by varying the number of rings in eq. 4.15. The curve of E_{path} that varies with the number of rings for five different values of half area length R is shown in Fig. 4.15(b).

For the first scenario and with a length R equal to 50 m, the number of rings that minimizes the value of E_{path} is two rings. So, the ring width can be simply calculated by dividing R by the optimum number of hops, with γ = 25 m. For the first iteration, in the first ring, we have 25 nodes with four CHs and the cluster radii is 29.82 m, while in the second ring, we have 75 nodes with 8 CHs and a cluster radii of 38.5 m.

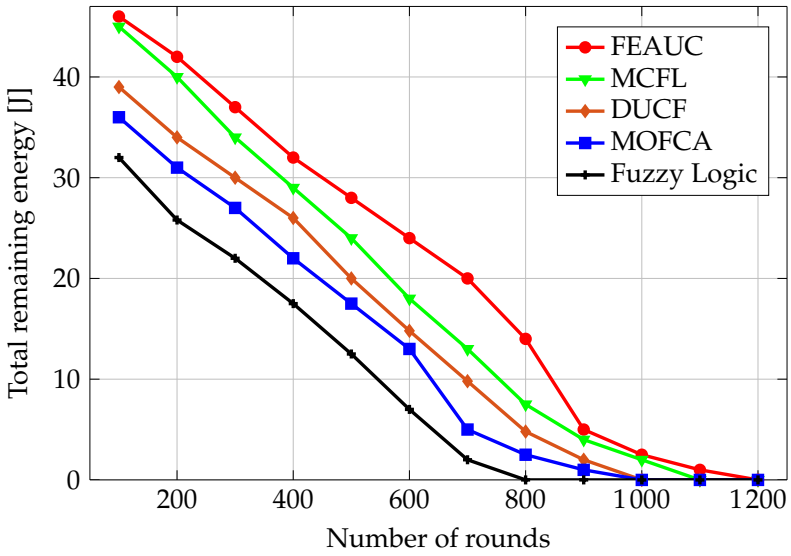

Figure 4.19: Network remaining energy of different protocols in each round.

Fig. 4.19 illustrates the evaluation of the remaining energy for the whole network. FEAUC outperforms the other protocols in term of energy consumption. After 600 rounds, the residual energy in the developed FEAUC algorithm is approximately equal to 24 joule. FEAUC is about 25% more energy efficient than MCFL, about 38% more energy efficient than to MOFCA and about 70 % more energy efficient than the Fuzzy Logic algorithm.

Simulations, illustrated in Fig. 4.20, show that the developed FEAUC outperforms the Fuzzy Logic, MOFCA, DUCF and MCFL algorithms in terms of FND, HND and LND metrics. Considering the FND metric, the proposed algorithm is more efficient than Fuzzy Logic algorithm by 36%, MOFCA by 16%, DUCF by 13% and MCFL by 5%. According to HND metric, the proposed algorithm is more performant than Fuzzy Logic algorithm by 18%, MOFCA by 14%, DUCF by 12% and MCFL by 2%. For the LND metric, FEAUC is more efficient than Fuzzy Logic algorithm by 13%, MOFCA by 8%, DUCF by 2% and MCFL by 1%.

As explanation for the results shown in Fig. 4.19, Fig. 4.20 and Fig. 4.21, it is noticed that the Fuzzy Logic algorithm does not use unequal clustering, which generates the hot spot problem and reduces the number of data packets received at the base station. Through the selection of a relay CH to transmit data packet to the BS from the first CH, the MOFCA algorithm outperforms the fuzzy-based clustering algorithm [121]. Varying the cluster size of CH nodes, DUCF ensures good results in terms of energy consumption and network lifetime. Because of the use of fuzzy logic for

the determination of the optimal node radius for each cluster, MOFCA outperforms DUCF algorithm. Reducing the number of CHs selection and reducing the repeated sending of messages, MCFL increases the network lifetime.

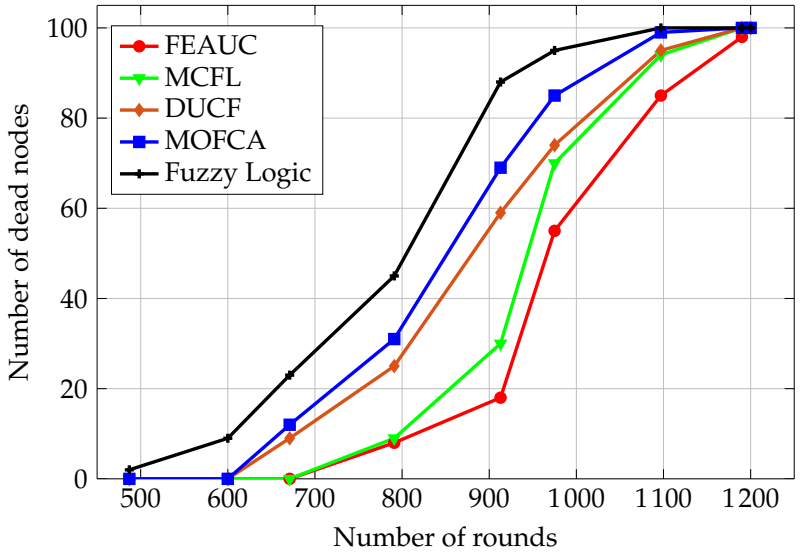

Figure 4.20: Number of dead nodes of different protocols over rounds.

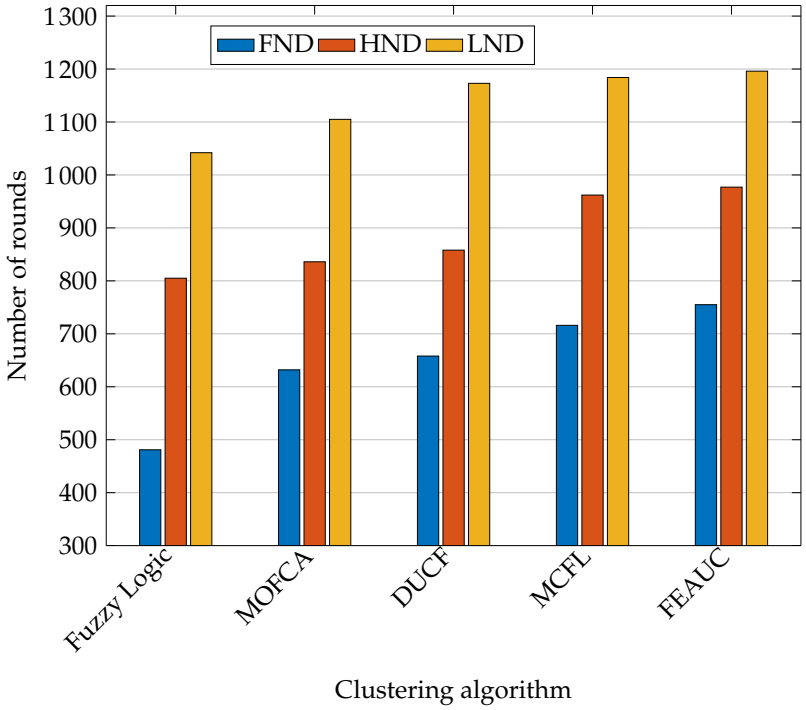

Figure 4.21: Comparison of FND, HND and LND of each protocol.

The performance of the developed algorithm is better than existing algorithms, since the selection of CHs with maximum number of neighbouring nodes decreases the overall intra-cluster communication cost and selection of nearby relay CH decreases

the inter-cluster communication cost. This fact enables to reduce the overall energy consumption of the network. Moreover, calculating the optimal radius of a CH is very important for saving energy.

- Second scenario: Large density

In the second scenario, comparisons are made based on simulation parameters given in Table 4.3. The BS is located in the centre of the network. As seen in Fig. 4.22, 1000 nodes are deployed in an area of 1000 m $\times$ 1000 m.

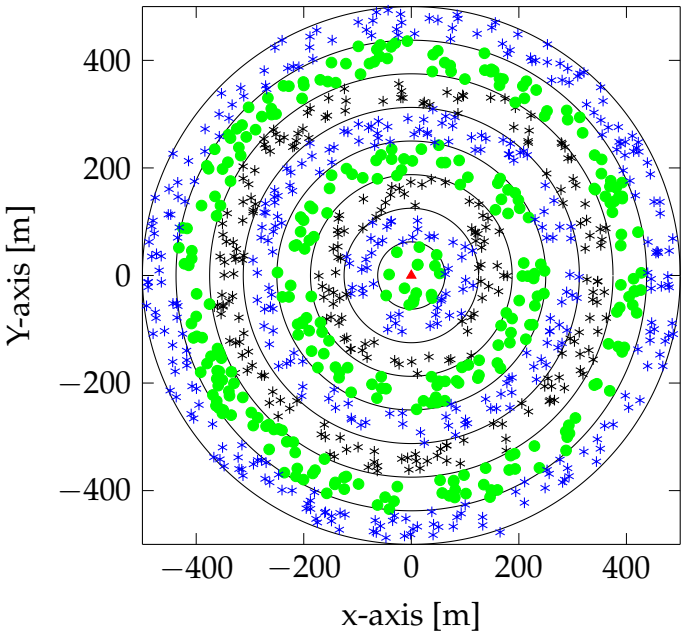

Figure 4.22: Nodes deployment in 1000 m $\times$ 1000 m network (scenario 2).

As shown in Fig. 4.15(b), for this scenario and with a length R equal to 500 m, the number of hops that minimizes the value of E_{path} is 8 hops. So, the ring width can be simply calculated by dividing R by the optimum number of hops, with γ equal to 62.5 m. To investigate the energy efficiency of unequal clustering algorithms, the sum of residual energy of nodes is measured and traced in Fig. 4.23 every 20 rounds. After 300 rounds, the residual energy in the developed FEAUC is approximately equal to 260 joule. FEAUC is about 8% more energy efficient than FAMACROW and about 48% more energy efficient than to the IFUC.

Considering the FND metric, the developed FEAUC algorithm is more efficient than IFUC by 96% and FAMACROW by 92%. According to HND metric, the proposed algorithm is more performant than IFUC by 58% and FAMACROW by 34%. For the LND metric, FEAUC is more efficient than IFUC by 53% and FAMACROW by 36%.

As explanations for the results shown in Fig. 4.23 and Fig. 4.24, it is noticed that the energy consumption of IFUC is maximum and the network lifetime is minimum.

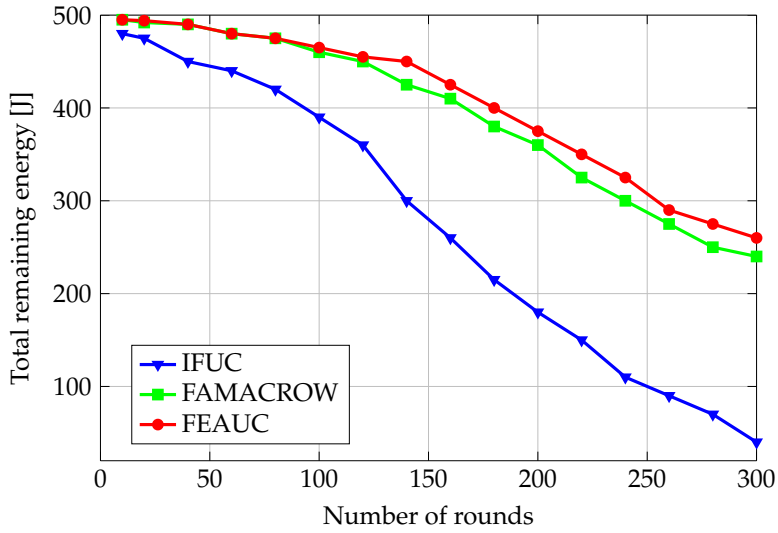

Figure 4.23: Network remaining energy over rounds.

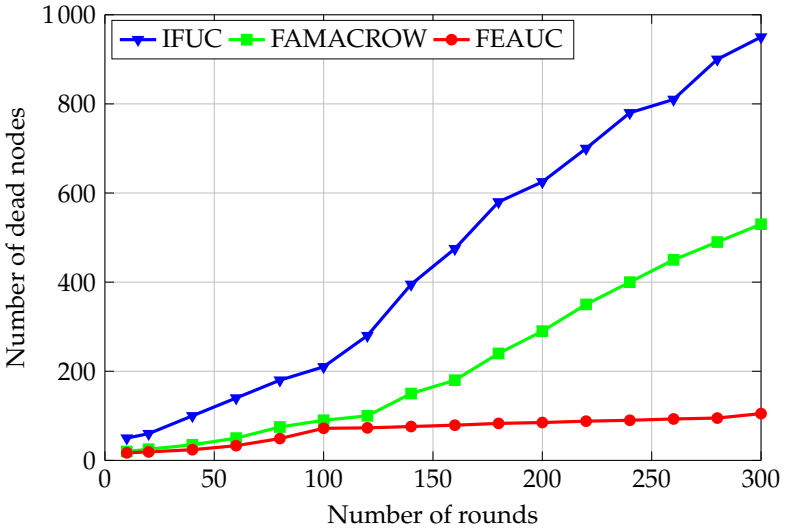

Figure 4.24: Number of dead nodes over rounds.

This is explained by the fact that, some nodes can be included in more than one cluster at the same time. Hence, the overlapping problem is increased dramatically leading to the energy depletion. FAMACROW protocol shows an improved lifetime ratio and a reduction of energy consumption of nodes because of using the fuzzy logic approach for the CH selection and ACO for inter-cluster routing and for diffusing data to the BS. So, FAMACROW outperforms IFUC protocol. Nevertheless, the developed protocol, FEAUC, shows better performance in terms of energy consumption and network lifetime. Indeed, FEAUC is based on the cluster radius calculation, ring radius competition and CH selection with maximum number of neighbouring nodes. This enables to reduce the overall intra-cluster communication

cost and the selection of nearby relay CH decreases the inter-cluster communication cost. As a result, the overall energy consumption of the network is decreased. Moreover, the network lifetime is extended by keeping clusters fixed and rotating CHs after the first round.

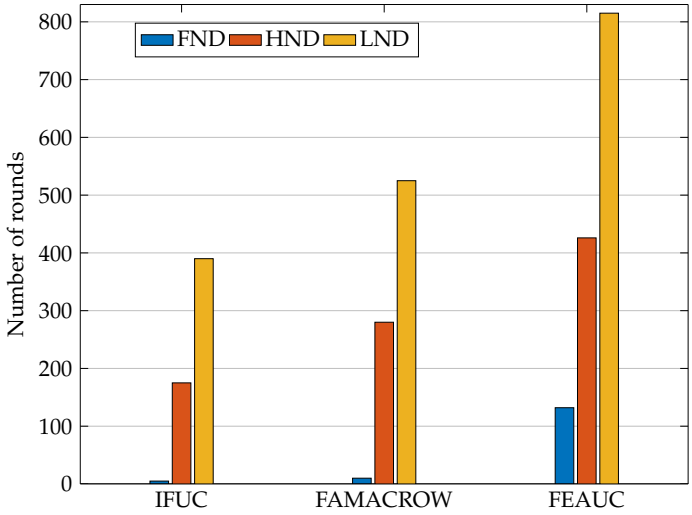

Figure 4.25: Comparison of FND, HND and LND for each protocol.

Results illustrated in section 4.3.3 are given by rotating CHs every round. FEAUC selects a new CH in each round; nevertheless, it outperforms the most relevant unequal clustering protocols. Although, the re-clustering is intended to enhance the network lifetime by distributing the large load of CH tasks equally among the normal nodes, running the clustering process in each round is an additional burden, which can significantly drain the remaining energy. For this reason, it is important to alleviate the problem associated with the re-clustering as well as leveraging the potential benefits of round-based clustering techniques. To this end, an energy-based threshold method is used to trigger the re-clustering process. In the following, a description of the developed fault-based algorithm is detailed.

4.4 Energy efficient fault tolerant recursive clustering protocol

This section is devoted to describe the FEAUC based fault tolerant algorithm (IFEAUC-FT). It supports both intra-cluster and inter-cluster fault tolerance. To avoid the re-clustering process in each round, a backup CH is selected only when the residual energy of the primary CH is not enough to run the current round. This is defined as intra-cluster fault tolerance. Each round includes the three phases of the developed FEAUC. Indeed, only CHs having less residual energy than the defined threshold will trigger the cluster formation phase and the same process used in the first round is carried out. Others CHs complete the round normally without running both cluster formation and cooperative phases. Sensor nodes have limited energy constraints and are highly prone to failure as they have many functions.

Malfunctioning nodes affect both data transmission and also reduce connectivity and network life. For this reason, inter-cluster fault tolerant technique consists on building a backup routing path in case of link failure between CHs from different rings.

Algorithm. 4 describes in details the overall working process of the developed FEAUC-FT algorithm.

Algorithm 4: FEAUC-FT algorithm

N: total number of sensor nodes in the network
$E_{res}(i)$: residual energy of node i
$E_{initial}$: initial energy
$threshold$: fixed threshold value
$list\_BCH$: list of BCH for a primary CH i
$TTL = \frac{1}{max(\frac{E_{res}}{E_{max}}), d_{max}}$
Intra-cluster fault tolerant based BCH
Start round by cluster formation phase
if $E_{CH} \geqslant Threshold\, E_{initial}$ **then**
  CH completes the round normally.
else
  Send a SoS message to the set of the BCH.
  while $(list\_BCH \neq \emptyset)$ **do**
    i=1;
    if $E_{BCH(i)} < Threshold E_{initial}$ **then**
      node BCH(i) becomes a CH;
      Broadcasts an update message to cluster members;
      Complete the round normally;
      $i \leftarrow i + 1$;
    else
      Set threshold $new\, threshold = last\, threshold - 10$;
      if $Threshold \geqslant 0$ **then**
        Start round by cluster formation phase ;
      else
        Check the energy availability of the concerned CH;
        if $If\, energy\, is\, enough\, to\, run\, the\, round$ **then**
          Complete the round normally;
        else
          Stop;
        end
      end
    end
  end
end
Inter-cluster fault tolerant based backup routing path
if *(No ACK received at* CH_i *from ring k and TTL=0)* **then**
  Select a new CH from ring (k-1)
  $send\,(data\_packet\,(CH_k)\, to\, new\, CH_{(k-1)})$
end

4.4.1 Intra-cluster fault tolerant based backup CH

Here, a description of the developed solution for avoiding the re-clustering process is given in details. To this end, T_{CL}, T_{CO} and T_{CN} are considered, respectively, as the clustering time, cooperation time and data collection time for the entire network. The network lifetime can be introduced as $i(T_{CL} + T_{CO} + T_{CN}) + j(T_{CO} + T_{CN})$, where i presents the number of times that the clustering operation is performed and j is the number of times that the network works without clustering process. Therefore, a

total time of $i(T_{CL})$ is used for the clustering operation. Reducing the T_{CL} time leads to reduce, significantly, the energy consumption of the whole network. To do so, a backup CH is selected. Since each clustering phase is followed by a cooperative phase, switching the primary CH by a BCH requires also the selection of both forwarder and relay nodes. In this FEAUC-FT algorithm, only CH having a residual energy less than the threshold energy will trigger the switching operation. Other CHs complete the round normally by launching only the data transmission phase. The time needed to switch from a primary CH to a BCH is shorter than the re-clustering time. Therefore, reducing the re-clustering occurrence can reduce significantly the energy consumed in certain clusters.

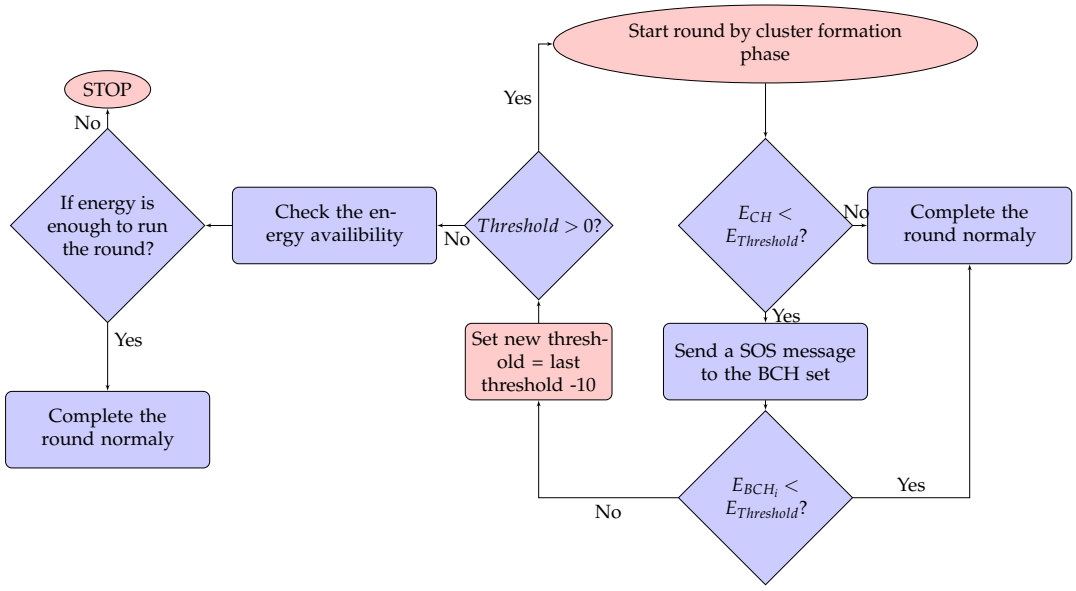

Figure 4.26: Flowchart of the fault tolerant based BCH.

As seen in Fig. 4.26, from the beginning of a round, each CH builds a ranked set of BCHs including all members according to their chance to be a CH. Then, it checks its residual energy. If it is still more than the defined threshold, it continues to work as a CH and complete the round normally. Otherwise, it verifies if the first node of the BCHs list has more or equal energy than the preset threshold. If so, it transmits a SOS message to the nominated BCH to become the primary CH for this round, which will continue working as a CH. The selected BCH broadcasts therefore, an update message to all cluster members including the previous CH informing them with its new status. Then, these nodes will send a join message to the new nominated CH. After that, the cooperative phase is launched, where the new CH selects the forwarder CH. If the first nominated BCHs does not fit the condition, the primary CH will looks in the ranked list to the next nodes till having one who has a residual energy equal to more than the defined threshold. Otherwise, a new clustering process is launched and a new threshold value is assigned, which is less than the previous one.

4.4.2 Inter-cluster fault tolerant based backup routing path

In case of successful inter-cluster data transmission, a CH from ring (k) receives an acknowledgement (ACK) from a CH of ring (k-1) informing it that it receives successfully the transmitted packet. However, when a CH from ring (k) gets failure to transmit its data packets to the CH of the previous ring as seen in Fig. 4.27, then it instantaneously uses its backup routing path, which needs to be the same for the incoming data packet transfer. Therefore, the number of dropped packets can be decreased. If a CH from ring (k) waits for a certain Time-To-Live (TTL), as expressed in eq. 4.25, and do not receive any acknowledgement, then it sends a health message to all the CHs from ring (k-1) within its transmission range informing them to forward its data packet.

$$TTL = \frac{1}{max(\frac{E_{res}}{E_{max}}), d_{max}} \tag{4.25}$$

where E_{res} is the current remaining energy of the transmitted CH, E_{max} defines the maximum energy related to a full battery and d_{max} is the distance between the transmitter and receiver CHs.

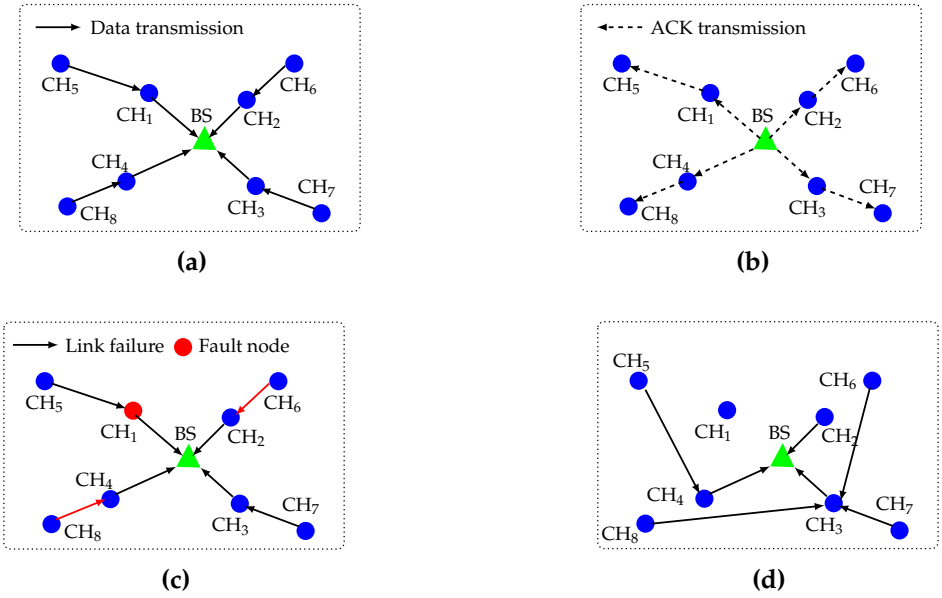

Figure 4.27: (a) Data transmission policy, (b) acknowledgement transmission policy, (c) fault identification, (d) fault recovery technique.

4.4.3 Simulation and performance analysis

A group of sensor nodes are deployed randomly in a 100 m $\times$ 100 m field. They are static after the deployment. The BS is placed at (0, 0) (marked with red triangle in Fig. 4.28). Fig. 4.28 presents the dispersion of the sensors in the field and the chosen CHs from the first of data collection cycle.

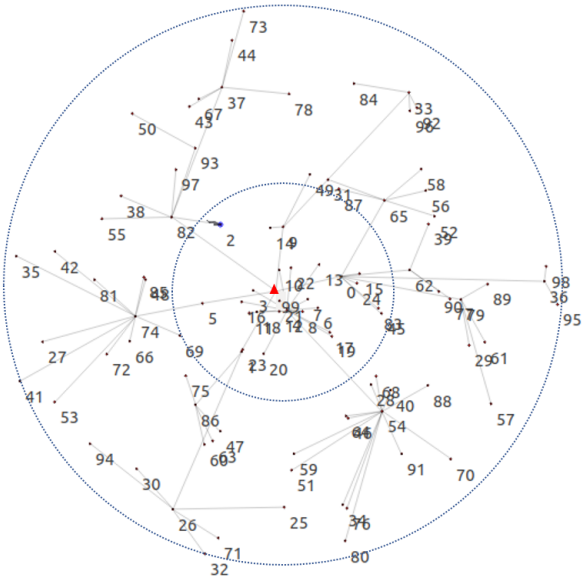

Figure 4.28: Network partitioning into clusters.

25 nodes are deployed in the first ring and 75 nodes are dispersed in the second ring. Detailed configuration is illustrated in Table. 4.4

Table 4.4: FEAUC-FT: Configuration parameters

Parameter	Value
Network size	100 m × 100 m
Number of sensor nodes	100
Initial energy	1 J
Data packet size	4000 bits
E_{elect}	100 nJ/bit
ε_{amp}	0.0013 pJ/bit/m^4
ε_{fs}	10 pJ/bit/m^2
Threshold	50 % of residual energy

Simulation results are carried out using the network simulator NS3. The values are expressed in term of rounds, which defines the data collection cycle. To evaluate the performance of the developed FEAUC based fault tolerant algorithm (FEAUC-FT), some parameters such as the network's remaining energy, the number of dead nodes in each round, the FND, HNd and LND metrics are considered.

The first evaluated parameter is the total residual energy of the whole network as seen in Fig. 4.29. Since each node has one Joule as initial energy, the total energy of all the network is 100 J at the beginning of the algorithm. The battery of each sensor node depletes proportionally with the increase of the number of round. For example, at round 500, DUCF has the lowest residual energy, which is approximately 24 J. FEAUC has about 30 J. MACHFL-FT has 40 J as energy level. On the other side, the developed FEAUC-FT algorithm has the highest remaining energy, about 57 J.

Since the developed FEAUC-FT algorithm avoids the selection of CHs in each round by fixing an energy threshold value, the energy consumed for the re-clustering

process increases significantly. Since DUCF repeats the clustering process in each round, then it consumes more energy. As proved in the given simulations, DUCF is the most consumed energy algorithm compared to others. To detect the packet transmission failure between two CHs form different rings by using a back-up routing path process, an amount of energy is consumed. FEAUC-FT normally consumes more energy than FEAUC, but since it uses a fixed threshold value to select a new CH, then the total number of exchanged packets decreases and thus the total residual energy is saved. By fixing a threshold, the MACHFL-FT algorithm avoids the re-selection process of CHs. So, the number of messages is reduced leading to save the total network energy. Despite, adding a routing back-up path process to detect packets loss in the inter-data transmission sub-phase, the developed FEAUC-FT outperforms the MACHFL-FT algorithm in term of energy consumption.

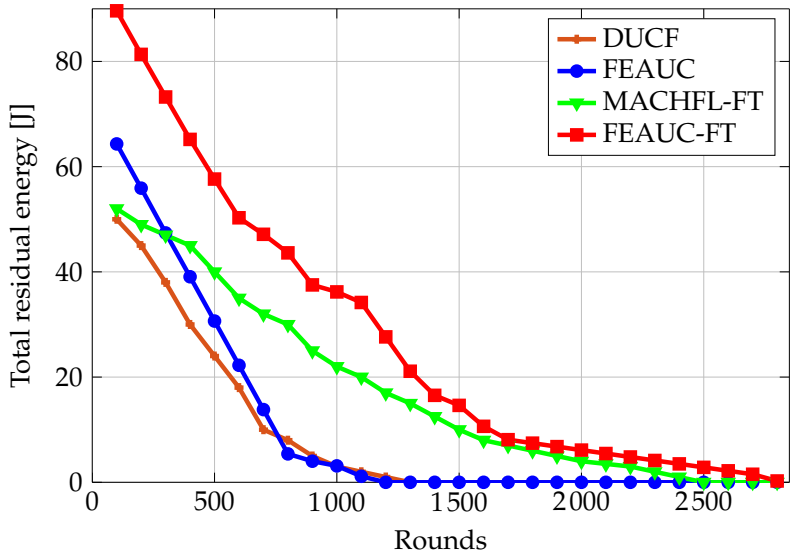

Figure 4.29: Network remaining energy of different protocols over rounds.

Fig. 4.30 presents a comparison of the proposed FEAUC-FT algorithm with other ones in term of network lifetime. Thus, only few nodes leave the network after successive rounds.

Simulations, illustrated in Fig. 4.31, prove that the FEAUC-FT algorithm outperforms DUCF, FEAUC, and MACHFL-FT in terms of FND, HND and LND. Respecting to the FND metric, the proposed algorithm is more efficient than DUCF by 21%, FEAUC by 8% and MACHFL-FT by 4%. Similarly, the proposed algorithm with respect to the HND metric is 18% more performant than the DUCF, 54% more efficient than FEAUC and 29% more performing than MACHFL-FT. Considering the LND metric, the developed FEAUC-FT algorithm is more efficient than DUCF by 54%, FEAUC by 57% and MACHFL-FT by 9%.

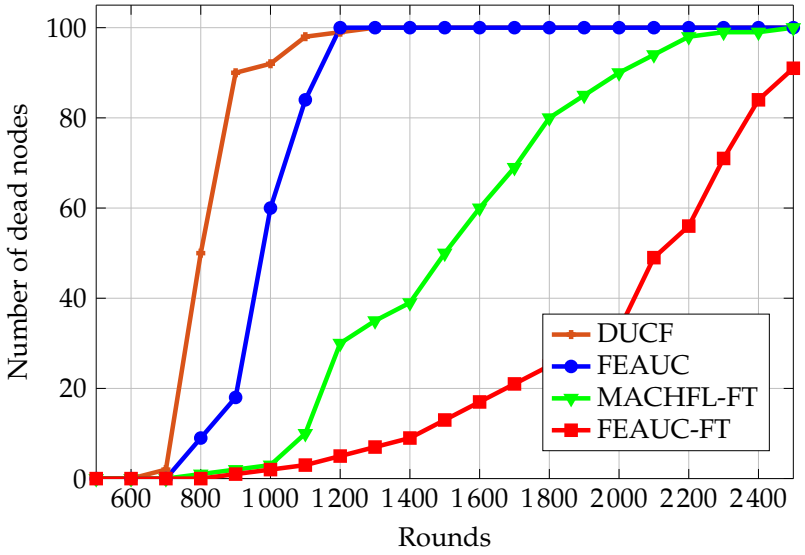

Figure 4.30: Number of dead nodes in each protocol over rounds.

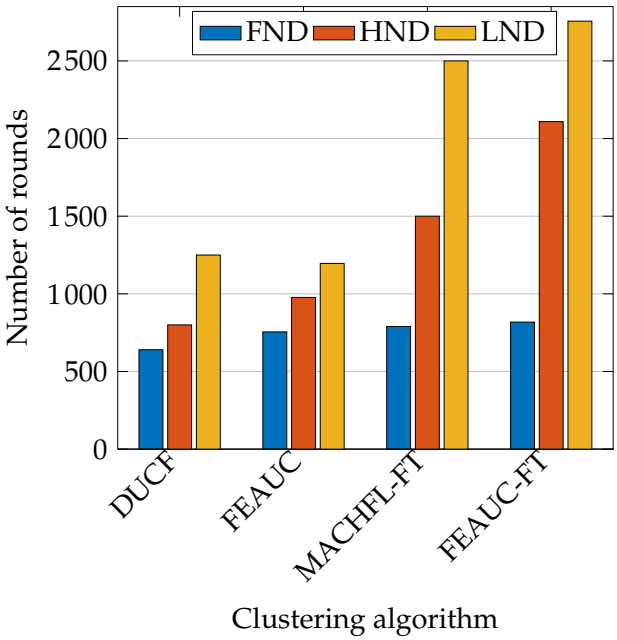

Figure 4.31: Comparison of FND, HND and LND metrics.

As explanation for the results illustrated in Fig. 4.29, Fig. 4.30 and Fig. 4.31, since the transmission and reception of packets between nodes within same cluster in the clustering process increase the total consumed energy, avoiding the re-clustering process in some rounds by using a preset threshold can save the network' total energy. An amount of energy can be added when building a back-up routing path between CH from ring (k) and a CH from ring (k-1). Despite this, the proposed

algorithm outperforms other algorithms, which do not consider the recovery of failed routing paths between different CHs. This can be explained by the choice of the input parameters of the fuzzy logic system to select the CH and the determination of the optimal number of nodes in each ring and the optimal cluster radius per ring as seen in [8].

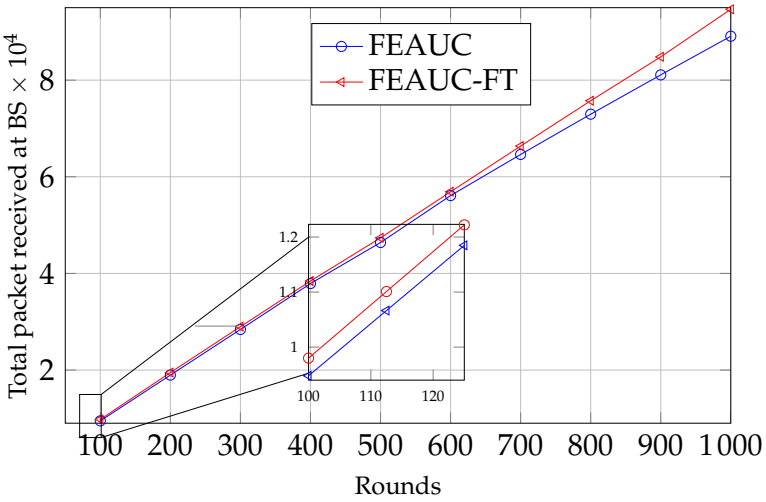

Figure 4.32: Number of received packet at the BS over rounds.

Fig. 4.32 illustrates the performance of the developed FEAUC based fault tolerant algorithm compared to the the FEAUC [8]. The number of packets received on the BS increases from one round to another. By building a backup routing path in case of link failure between CHs from different rings, the packet loss will be decreased and so more packets will be transmitted to the BS. For example, at round 100, around 500 messages are lost using FEAUC.

4.5 Characteristics analysis of the developed FEAUC Protocol

To conclude this chapter, the major characteristics of the novel FEAUC protocol can be summarized in the following points:

- The network is assumed as a circle, where the BS is located in the centre. As seen in Fig. 4.33, the whole area is partitioned into defined number of rings with specific radii. This helps to ensure a full coverage compared to the rectangular partitioning model.
- The circular partitioning model enables the protocol to be implemented in the most diverse territories and tested for different network scale.
- The optimal cluster radius and the ring width are determined through an energy analysis model. This helps to balance the network energy consumption and avoid the hotspot problem created by the multi-hop communication.

- CHs are selected using the fuzzy logic system, where the node residual energy, density and centrality are considered to calculate the chance of a node to be a CH. Combining these three parameters helps to choose the optimal CH.
- The relay metric is considered using the ratio of the transmitter CH and its distance to the tentative forwarder CH. This helps to prevent the long haul transmission between CHs and balance the overall energy consumption by selecting the optimal path to transmit data to the BS.
- The FEAUC-FT algorithm is developed to reduce the clustering overhead by selecting a BCH when the primary CH has an amount of energy less than a fixed threshold value. This decreases the number of transmitted data between cluster members and reduces the total consumed energy.
- A backup routing path is built between CHs from different rings to re-transmit the lost data packets in case of link failure. This ensures a higher data throughput.

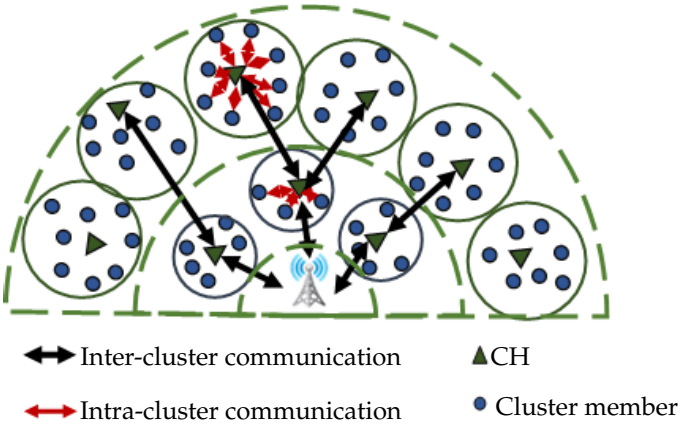

Figure 4.33: Data transmission for the developed FEAUC protocol.

CHAPTER 5

Experimental validation of the developed unequal clustering protocol

In this chapter, a test-bed implementation of the developed FEAUC protocol is carried out to evaluate its efficiency on real hardware. Some sensor nodes, powered with non-rechargeable batteries, are deployed in a circular area forming clusters. Since the residual energy is a primary factor in the developed protocol, a low power cost-efficient circuit is designed to measure the current consumption, which is later used to calculate the consumed power of the sensor node during different operations. The the energy consumption of the deployed nodes, their lifetime relative to the transmitted packets to the BS are evaluated in real time. Afterwards, a comparison between simulation and experiment is conducted in terms of energy consumption and total packets received at the BS.

5.1 Real-time implementation of the developed FEAUC protocol for large-scale applications

A brief overview on the network topology and node deployment is provided in this section. Besides, the selected wireless sensor node is introduced. To characterize the energy consumption of the node, the four-wire measurement method is used.

5.1.1 Node deployment and network overview

The test-bed includes a number of sensor nodes placed in a circular-partitioned area. Besides, as depicted in Chap 4, the shape of the field is assumed as a circle, where the BS is located in the centre. The entire area is partitioned into a specific number of rings with a defined radii. After the deployment of nodes, they broadcast their RSSI values to discover the list of the associated neighbours. Added to that, it is assumed that the nodes and the BS are stationary and all nodes have an equal initial energy. Once nodes are deployed and the network is established, each node executes a fuzzy logic-based algorithm, gathering an output giving it a chance to be a CH.

5.1.2 Characterization of nodes status

One of the most effective solution to save energy is to switch on the radio transceiver only when sending the information. Preferably, the power is turned off when there

is no data to send and it should be restarted as soon as a new data packet is ready for the transmission. This method saves significantly the energy. Depending on the network activity, nodes can switch from the active state to sleep state. This practice is commonly referred as a state transition or duty cycling. As depicted in Fig. 5.1, the sleep and wake-up scheduling algorithms are required for any duty-cycling scheme. Several scientific works [125], [126] have used this technique in order to extend the sensor node lifetime. In [125], the author demonstrates that with those techniques, 30 to 33% of saved energy can be guaranteed.

In the presented work, the state transition differs from one node to another considering its nature i.e, a normal node or a CH. For the normal node, it has four states: Off, sense, transmit and sleep. Each state has a specific function. After the booting of the node, the state changes from off to sense. In the sense state, the sensor node collects data from its environment and sends it to the microcontroller for processing. The radio of each node wakes up periodically from the sleep mode and listens for the incoming packets without interacting with the MCU. When the time schedule for this node is ready, the transmit state is launched. The node sends the sensed data to the corresponding CH following its time schedule. The time duration of this mode can be determined in eq. 5.2. If there is no data to be sent, the sensor node goes to the sleep mode. In case of hardware or software failures or battery drainage, the node goes to the off state.

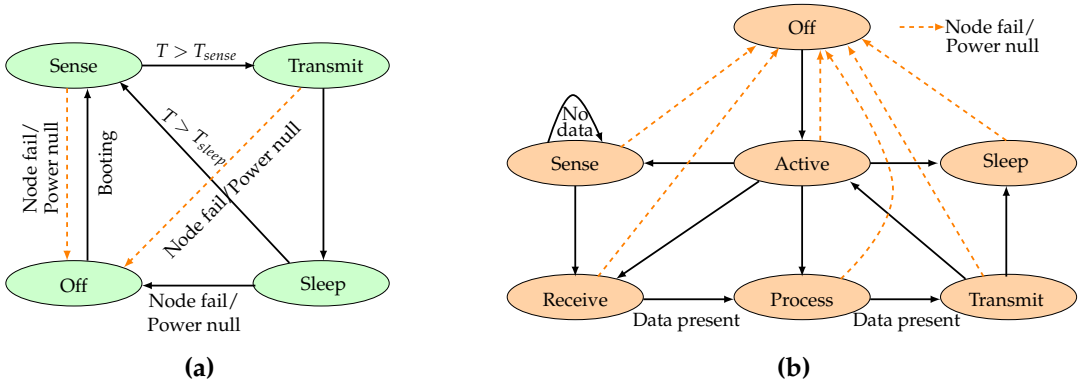

Figure 5.1: State transition: (a) Normal node (b) CH node.

The state transition of the CH is described in Fig. 5.1(b), which includes seven states. After the node booting, the state varies from off to active. During the active mode, the CH broadcasts a message to its cluster members informing them with its status or requests data from them if available or send to them their schedule time or other information. Then, the CH goes to the sense mode. After receiving data from the normal nodes, the CH state changes from receive to process. During the process state, the CH collects data from its cluster members and goes to the transmit state. Therefore, it transmits the aggregated data packet directly to the BS if it is located in the first ring, otherwise to another CH. Then, the CH goes to the active mode again in case of no data received, it goes to the sleep state.

5.2 Energetic investigation of wireless sensor node

Due to limited resources of sensor node hardware, power consumption is a crucial characteristic. Therefore, the choice of low power physical components helps to improve the energy consumption of the overall network. For this reason, the low power wireless platform panStamp NRG 2.0 (see Annex A) is used in this dissertation. It is based on the popular CC430F5137 SoC, including MSP430 microcontroller and CC11XX radio chip, which operates at 433 and 868-915 MHz. All nodes i.e the BS, the CH and the normal node are equipped with a PanStamp NRG 2.0. The BS is responsible for the data collection and then displaying it via a serial monitor (or a simple user interface). The data can be also uploaded to a server or a real time database (Firebase).

5.2.1 Black box based energetic model

To measure the energy consumption of a sensor node, the white box-based energy model is used in several research papers [8], which uses the distance between the transmitter and receiver nodes. To transmit l bits over a distance d, the consumed energy by the transmitter E_{Tx} and the receiver E_{RX} can be described in eq. 4.4, which is defined in Chap 4. In this model, different required parameters need to be available in the datasheet of panStamp NRG 2.0. However, some useful information are not provided in the datasheet of the used radio including the electrical energy of the circuit needed to transmit or to receive a message E_{elect}, the energy consumption factor for free space ε_{fs} and the energy consumption factor for multi-path radio model. Therefore, the aforementioned energy model can not be used in the real implementation.

Since panStamp is a SoC, it can be viewed in terms of its inputs and outputs without knowing its internal workings. That is why the used energy model is called black box. This model has to be accurate enough to predict approximately the real network lifetime by considering the state of a sensor node: Sleep, Transmit, Receive, etc. The energy consumed of each node, E_{state}, can be described in eq. 5.1.

$$E_{state} = \sum_{state} V_{state} \cdot I_{state} \cdot \Delta t_{state} \tag{5.1}$$

where V_{state} is the supply voltage in volt, I_{state} presents the consumed current in each state, in Ampere and the Δt_{state} presents the state duration in seconds. The chosen energy model is primarily based on these three parameters. Nevertheless, the most important one is time spent in each state, as this parameter affects the consumed energy giving different current values. The transmission rate is about 38.4 kbps. The energy needed to transmit one bit can be calculated using the method introduced in [127]. The time needed to send or receive 1 bit $\Delta t_{Tx/Rx}$ is described in eq. 5.2.

$$\Delta t_{Tx/Rx} = \frac{\text{Packet size}}{\text{Data rate}} \tag{5.2}$$

According the node's role, its total consumed energy $E_{consumed}$ is the sum of the consumed energy in each state (eq. 5.3).

$$E_{consumed} = \sum_{i} E_i \tag{5.3}$$

where E_i presents the energy consumption of a node in each state in Joule, and i is the state i.e. transmission state (Tx), receiving state (Rx), sleep state, and even a switch state has been considered in order to provide a precise and realistic energy consumption model.

Depending on the used data rate and the packet size during the transmission and reception, in each state, the consumed energy can be calculated given its state duration. Calculating the remaining energy in batteries requires two parameters as shown in eq. 5.4.

$$E_{remaining} = E_{initial} - E_{consumed} \tag{5.4}$$

The consumed energy of a sensor node in Joule $E_{consumed}$ has been calculated in eq. 5.3, while, the initial energy, $E_{initial}$, is given from the battery's datasheet [128]. With 1150 mAh of battery capacity and 1.5 V as voltage, each battery has 6210 J of initial energy calculated in eq. 5.5. Using two batteries for one sensor to reach 3 V as a power supply, that initial energy needs to be multiplied by 2. It means finally, each sensor has 12420 J as initial energy.

$$E_{initial} = \text{Voltage} \cdot \text{Capacity of battery} \tag{5.5}$$

5.2.2 Battery-driven power supply

The residual energy can be easily estimated using the battery voltage, which can be read by the ADC. However, these values are not constant. In fact, the voltage value is steady as long as the node is off. When the node is turned on, the voltage starts to fluctuate around the original value. When the radio is active, the voltage decreases, otherwise it is increased. In [125], [126], it is assumed a constant value of supply voltage due to the hard approximation or measurement. In [129], a battery model is used in which the discharge curve of the battery is approximated as a linear curve. The battery capacity depends also on temperature and the initial capacity of the battery. Based on the linear model of the discharge curve, the capacity equation of the battery can be introduced. This method has not been measured experimentally. Hence, estimating or measuring the supply voltage is challenging due to the variation of current, initial energy and temperature impacts.

5.2.3 PanStamp energy characterization using four-wire energy measurement method

Accurate power estimation at early design stage is a key ingredient for a successful design methodology at system level. The measurement instrument used is a Keysight Technologies E5270 8-channel Precision Measurement Mainframe [97]. It supports a

high-resolution Source/Measure Unit (SMU). The SMU applies a voltage to the force connection and measures it over the device under test (DUT) with a sense interface. The controller automatically adjusts the supply voltage to match the voltage drop that is caused by the parasitic resistances of the force wires. The current profile is measured using the integrated ammeter in series with the force connection. The thereby introduced voltage drop is eliminated by the feedback-controlled 4-wire-setup.

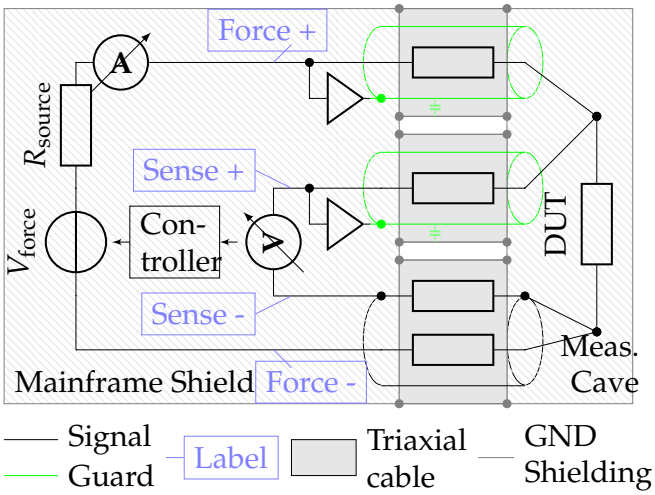

Figure 5.2: Four-wire measurement setup involving a Keysight technologies E5270 8-channel precision measurement mainframe following [97] guarding and shielding using a source measurement unit (SMU).

Fig. 5.2 shows the measurement setup including the measurement device on the left side and the Faraday cage containing the microcontroller as device under test on the right side. Both are connected by three triaxial shielded and guarded cables to minimize errors caused by wire resistance.

It is important to determine the maximum transmission range of a node to configure its sending power. For this reason, real outdoor measurements are carried out to define the maximum distances in each configuration. These measurements are later used to calculate the consumed current of a sensor node according to the transmitted payload size. In real environmental conditions, deployed nodes can face various obstacles and external issues coming from the weather or environment, which can limit the transmitting-receiving range. For this reason, as seen in Fig. 5.3, a field test of experiments is carried out in a park having different types of hurdles such as trees, plants, persons moving.

As shown Fig. 5.3(a), the transmitter node is positioned directly in the grass. On Fig. 5.3(b), a receiver node is connected to a laptop to examine received data packets. The first tests, radio sensor nodes are configured in Tx low power. Second one, radio motes are configured in Tx high power. Distance measured between nodes are made with precise laser-powered BOSCH GLM 80 device.

Figure 5.3: Outdoor field test for: (a) Transmitter node, (b) receiver node.

Table 5.1 shows experimental results based on maximum distance determined approximately when the first data packet is lost.

Table 5.1: Measured distance according to power transmission

Power transmission configuration [dBm]	Measured distance [m]
Tx low power: 0	70
Tx high power: +12	110

In Fig. 5.4, a proof of the concept for the presented energy estimation approach is carried-out for experimental evaluation. Different test beds are necessary to fill in a complete survey of measurements. Table 5.2 provides the average consumed current for different payload size (8 bytes, 16 bytes and 32 bytes) for each operation cycle.

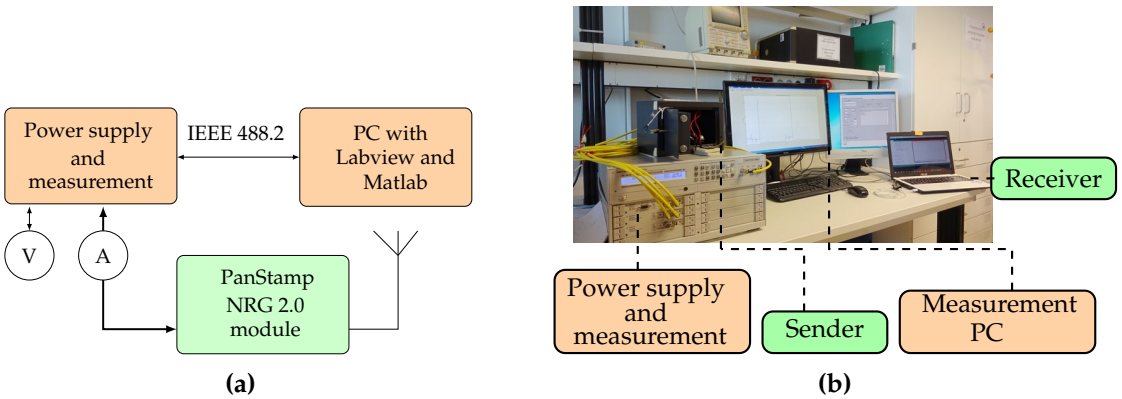

Figure 5.4: Outdoor field test for: (a) The transmitter node, (b) the receiver node.

The CC1101 [130] contains a specific packet structure provided in Fig. 5.5 with a total size n_{total}. The preamble pattern is an alternating sequence of ones and zeros

(10101010...). The minimum length of the preamble is programmable through the value of MDMCFG1·NUM_PREAMBLE. When enabling Tx, the modulator starts transmitting the preamble. When the programmed number of preamble bytes n_{pream} are transmitted, the modulator sends the synchronization word and then the stored data available in the Tx First In First Out (FIFO) buffer.

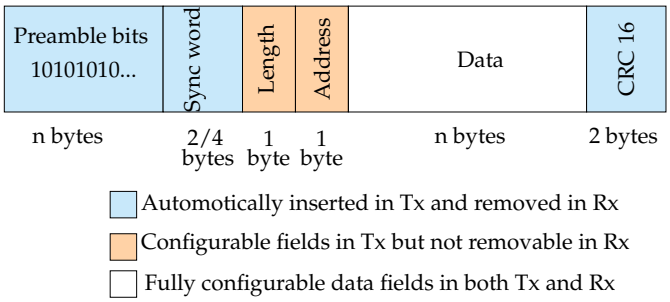

Figure 5.5: CC1101 packet structure.

If the Tx FIFO is empty, the modulator continues to send preamble bytes until the first byte is written to the Tx FIFO. The synchronization word is used to identify networks and make them "unique". It is presented by four-byte values at maximum. It is an initial 2 bytes with 2 bytes value transmitted by most radios to synchronize timings between nodes.

Table 5.2: Drained current for different node operations and different payload size.

Mean current	Datasheet [mA]	8 bytes [mA]	16 bytes [mA]	32 bytes [mA]
WOR	NA	2.69	2.57	2.51
Tx	36 max	20.12	19.69	18.2
Rx	18 max	12.21	12.19	12.09
Sleep mode	1-2 10^{-3}	0.46	0.36	0.41
Tx to Sleep transition	NA	2.81	2.85	2.72

The operation cycle of the sender is presented in Fig. 5.6 including Wake On Radio (WOR), transmit (Tx), switch from Tx to sleep mode and sleep modes. This node is supplied by 3.3 V and it transmits 8 bytes as payload.

The data bytes are transmitted as shown in Fig. 5.7. The number of samples recorded during the transmission are around 3, 5 and 8 for 8, 16 and 32 bytes respectively. From this figure, the time required to transmit x bytes can be calculated as illustrated in eq. 5.6,

$$time = 0.103x + 0.884 \tag{5.6}$$

As seen from the table 5.3, the energy required for the transmission of one byte is higher when the total data bytes transmitted are less. The energy required per byte transmission for 8 bytes is more compared to 32 bytes. Thus, it can be noticed that, the more the data bytes are transmitted, the less the energy per byte is consumed. The current required to transmit a data packet between two nodes decreases when the size of payload increases as seen in table 5.3.

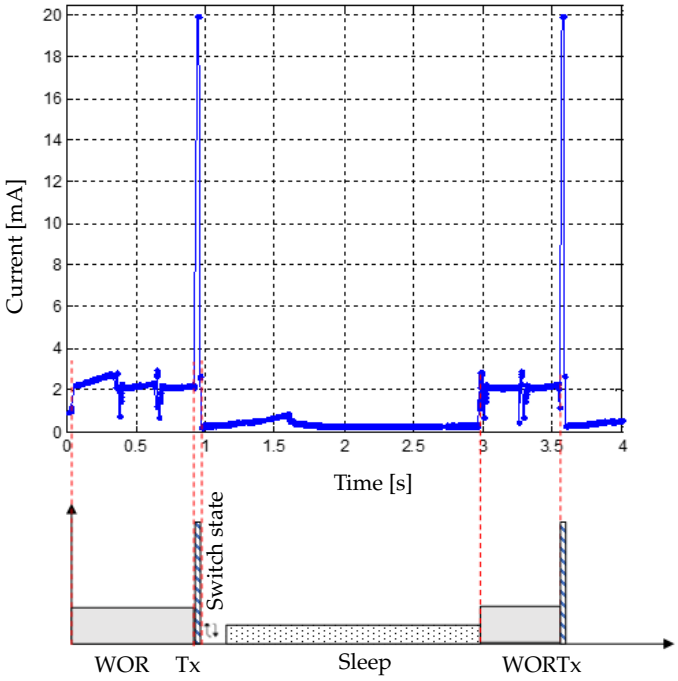

Figure 5.6: Dynamic current consumed drawn from the panStamp during 8 bytes in low power transmission mode.

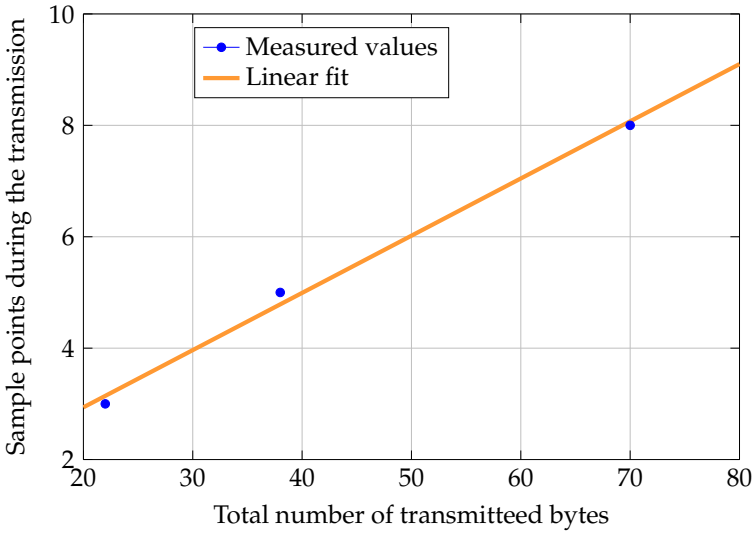

Figure 5.7: Measurement of the number of points per bytes.

Investigating radio datasheet and some official online documentation of panStamp NRG 2, depending on the state of the sensor node and in power transmission, different current consumption values can be used. However, the distance can be included with exploring the power transmission. Two radio configurations can be set up. The first one is called Tx high power configuration, which represents +12 dBm as power transmission in the documentation. The second one is called in Arduino

Table 5.3: Summary of the energy consumption for different payloads

Payload bytes	Total number of transmitted bytes	Number of points	Energy per payload byte [μJ]	Sampling period [ms]
8	22	3	21.7	1.2
16	38	5	21.3	1.2
32	70	8	18.5	1.2

Tx low power configuration, which represents 0 dBm as power transmission. Due to these possibilities,the distance can be included as from now on, passing by the first configuration to a second one, current consumption values are changed and that can affect consumed energy when sensor nodes are differently deployed in terms of distance. Switching between two configurations depends on distances between nodes and their capability to send data without any data loss. Definitely, using 0 dBm as a power transmission enables to save more energy compared to the current consumption values of the second configuration.

5.3 Design of a dynamic autonomous energy consumption measurement circuit

The available integrated circuits on the market are not intended to meet the dynamic range and sampling demands of the developed FEAUC protocol. For this reason, in this work, a new electronic circuit that can measure the power consumption of a wireless node in a real time is designed. This section describes in details the designed circuit for the energy consumption measurement.

5.3.1 Experimental setup of the proposed electric circuit

An electric circuit with low energy consumption that helps to measure the consumed current while transmitting or receiving a data packet is designed and presented in Fig. 5.8. The output of the circuit is connected to an analog pin of the transmitter node to read the output voltage of the circuit and measure the current consumption of the sensor nodes. Then, it sends the data to the receiver node, which is connected via USB cable to the computer.

The developed measurement setup is presented in Fig 5.8. It is acting as a load to measure the current and power consumption at different states and lifespan of the wireless sensor nodes. The developed circuit is connected to the transmitter node and the receiver node is connected to the laptop via serial communication to monitor the results of the consumed energy consumption by the transmitter.

The working principle of the circuit can be described within this section. As seen in Fig. 5.8, the current comes from the battery supply of $\pm 3\,V_{DC}$ flowing through a shunt resistor R_2 of 0.2 Ω and panStamp. The shunt resistor is connected to the input of the LT1637 precision amplifier with supply voltage of 3 V_{DC}. The current flows through R_1 then into the MOSFET BS [131]. The BS 170 N channel enhancement

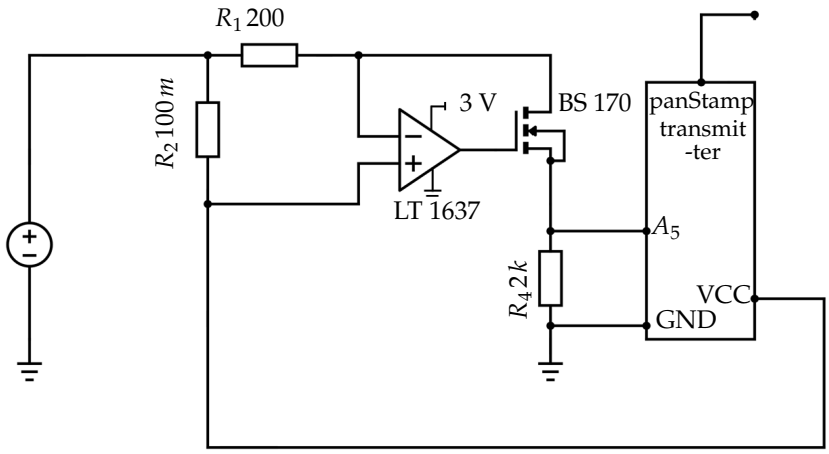

Figure 5.8: Experimental setup of the designed circuit.

mode field effect transistor is produced using Fairchild's proprietary. This transistor provides reliable, rugged, high switching performance and designed to reduce the on-state resistance. It is suitable for low voltage and low current applications.

The output voltage signal of the LT1637 controls the base of the MOSFET in a way that current from I (R_1) can pass through T1 and R_4. So, R_2 converts the load current into a voltage. The transduction of the current to a voltage is necessary. That is why, it could be read by the ADC later on. Further, the load current derived from the designed circuit can be described in eq. 5.7:

$$I_{load} = \frac{V_{out} \cdot R_1}{R_2 \cdot R_4} \tag{5.7}$$

where V_{out}, R_1, R_2 and R_4 are defined in Fig. 5.8. The precision amplifier LT 1637 [132] is selected to design the current measurement circuit as it fits for battery monitoring and current sensing with the single supply input range from -0.4 V to 44 V.

For all measurements, as power supply, an AAA alkaline battery with a voltage of 1.5 V and a capacity of 1150 mAh is considered [128]. In order to build a compensation model, an error analysis is carried out. In Fig. 5.9, the error (I_{out_err}), defined as the difference between the real value (I_{out_re}) and the experimental value (I_{out_exp}) by LTSpice. $I_{out\_err} = I_{out\_re} - I_{out\_exp}$ is plotted versus I_{out_re}. This analysis can help to build a compensation model.

As seen in Fig. 5.9, the error is linear and goes from 10.8 μA to 118 μA. This means that it is possible to build a linear compensation model to ameliorate the performance of the overall circuit. This leads to eq. 5.8.

$$I_{out\_re} = \alpha I_{out\_exp} + \beta \tag{5.8}$$

where α and β are the coefficients of the linear model. Those two values can be calculated by linear regression of the experimental values I_{out_exp} to the theoretical value I_{out_th} as shown in Fig. 5.10.

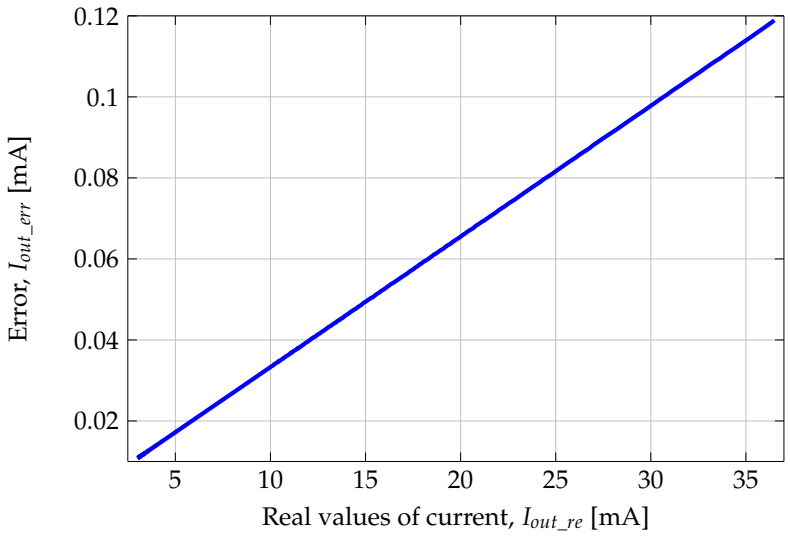

Figure 5.9: Variation of the error relative to the current consumption of load for circuit LT 1637 with MOSFET transistor.

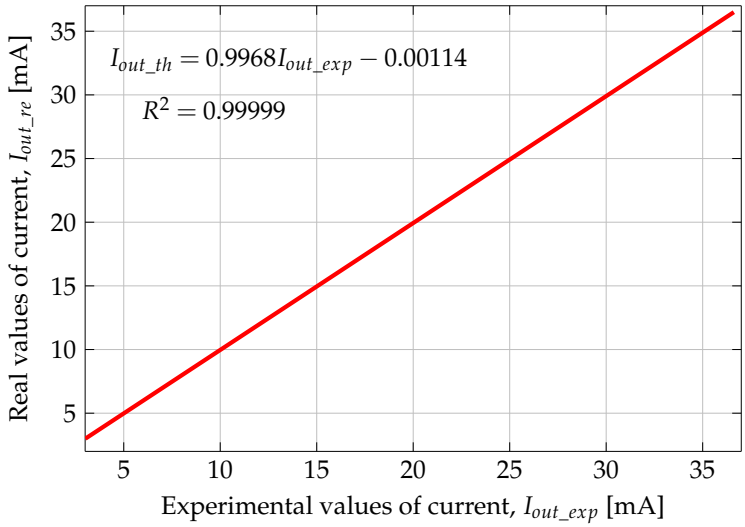

Figure 5.10: Variation of the real values relative to experimental values for circuit LT 1637 with MOSFET transistor.

These coefficients are determined and equal to $\alpha = 0.9968$ and $\beta = 0.00114$. R^2 is evaluated to explain how far the determined data are close to the expected values within the fitting. The coefficient of determination R^2 is calculated using the function linear regression analysis of experimental and theoretical values for both the circuits to find the goodness of fit out of the designed circuit. Thus, R^2 is close to one for the circuit LT1637 with MOSFET configuration.

The relation between the current and the output voltage is depicted in Fig. 5.11. Measurements are carried out using Keysight E5270B precision IV analyser [97].

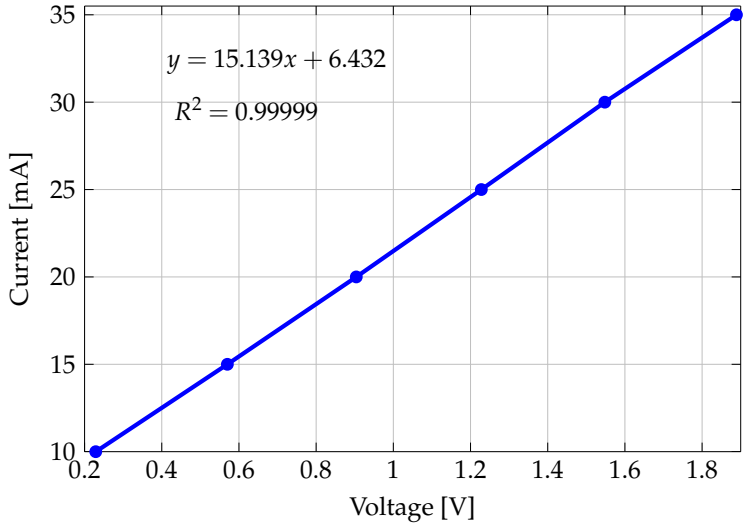

Figure 5.11: Current measurement device output in function of the output voltage.

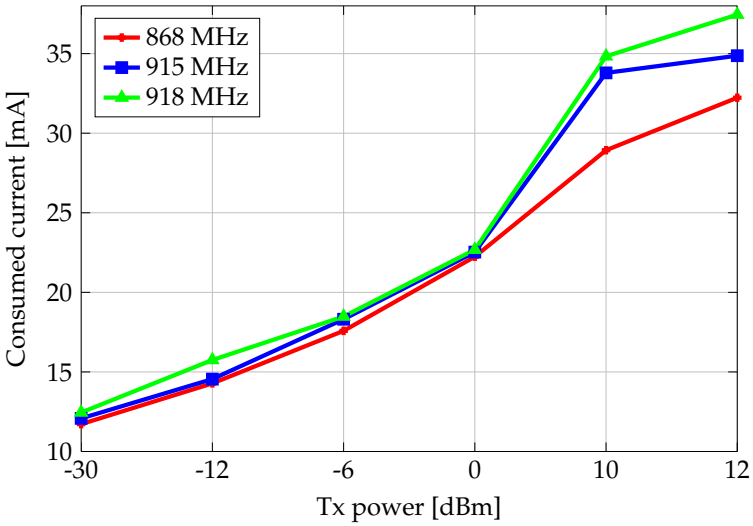

Figure 5.12: Current consumption of panStamp during data transmission at 868 MHz, 915 MHz and 918 MHz.

Fig. 5.12 shows the influence of the radio frequency on the current consumption for the transmitter side at different sending power. A higher frequency leads to an increased power consumption, due to the fact that a higher frequency leads to a higher processing speed.

For the second experiment and as seen in Fig. 5.13, the transmitter node is initialized at low Tx power 0 dBm. The measurements are carried out at different payload size of 8 bytes, 16 bytes, 24 bytes and 32 bytes and at different frequencies: 868 MHz, 915 MHz and 918 MHz. The current consumption for the increase of the packet

size is plotted in Fig. 5.13. It can be seen that increasing the payload size leads to the increase of the current consumption because longer packets involves longer transmission times.

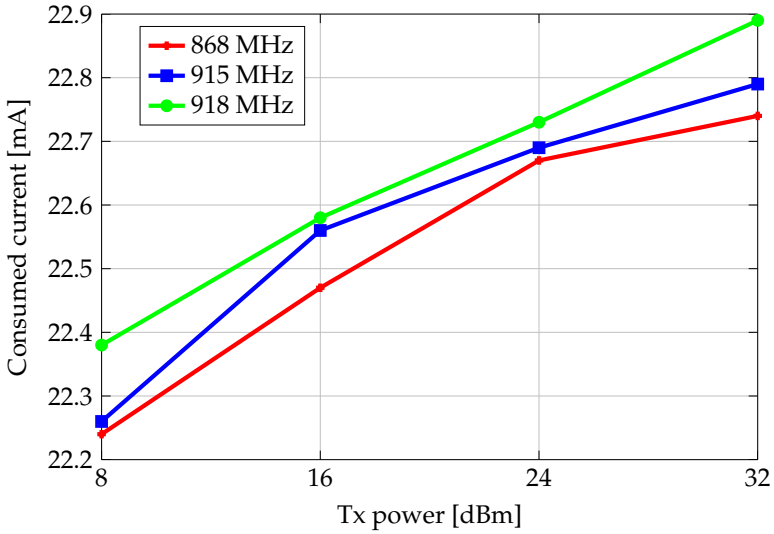

Figure 5.13: Current consumption during transmission of different payload.

In the next step, the amount of energy consumed by the transmitter during transmission at low Tx power of 0 dBm and high Tx power of 12 dBm is measured at different time intervals.

From table 5.4, it can be noticed, as expected, that the energy consumption of the sensor node is extremely high at +12 dBm transmission power and low at the 0 dBm transmission power. In order to maximize the life span of sensor node, the low transmission power should be selected to reduce the energy consumption. The transmission power of sensor node has to be chosen according to the required distance between the sender and receiver. A normal node is consuming almost 47.28 Joule/Day for continuous operations, where the transmitter sends 1 byte to the receiver at low Tx power and a frequency of 868 MHz.

Table 5.4: Energy consumption of the transmitter node during low and high transmission at different time intervals

Time [Hour]	Low Tx at 0 dBm [J]	High Tx at +12 dBm [J]
0.5	1.41	3.56
1	1.97	4.34
1.5	3.29	5.48
2	4.03	5.94
2.5	4.59	6.45
3	5.83	8.39

5.4 Case studies

To evaluate the performance of the developed FEAUC in terms of network lifetime, energy consumption and number of packets received at the BS, experimental setup is carried out in a small area. Seven panStamp sensor nodes are deployed, including the BS, and the energy consumption is evaluated. As seen in Fig. 5.14, three nodes are placed in the first ring as well in the second ring.

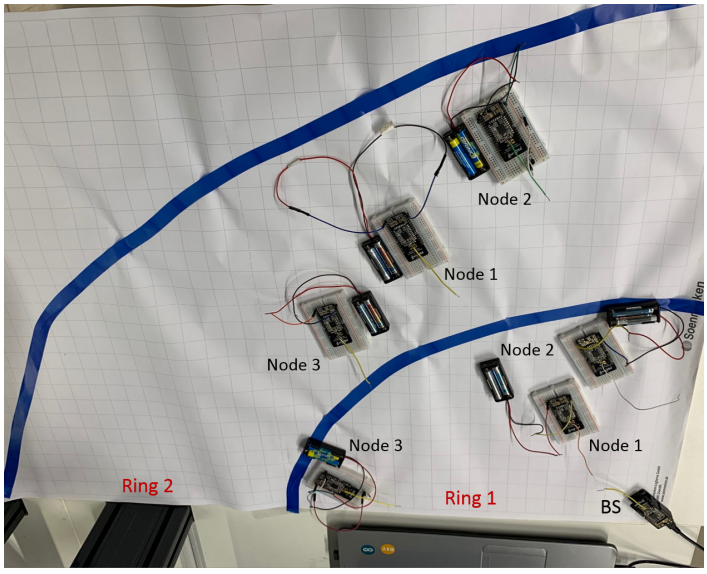

Figure 5.14: Cluster formation prototype

Starting with the off-line phase, since the wireless nodes are deployed in static positions, the respective geographical coordinates are estimated with a RSSI-based localization algorithm. In fact, in the first, step nodes communicate their RSSI values, which are then converted into distances. These estimated distances are, therefore, used to estimate the position of installed nodes via the trilateration technique.

To this end, the BS broadcasts a "HELLO" message to nodes within the distance $\delta = 70\,m$. Each node receiving this message replies an unicast message to the BS including the RSSI value. In fact, RSSI values are measured at the receiver node with respect to the path loss model of the radio signal, as presented in eq. 5.9.

$$P_r(d)[dbm] = P_r(d_0) - 10 \cdot \eta \cdot \log_{10}(\frac{d}{d_0}) + X_\sigma \tag{5.9}$$

where $P_r(d)$ and $P_r(d_0)$ indicate the received signal power at the real distance d and the reference distance d_0, respectively. η is the attenuation factor. X_σ denotes a Gaussian distributed random variable with zero mean and variance σ^2. In this experiment, the reference distance is assumed to be one meter.

Once the received signal is measured, the distance between the BS and the three nodes of the first ring is computed as in eq. 5.10.

$$d = 10^{\frac{RSSI_0 - RSSI}{10 \cdot n}} \tag{5.10}$$

where $RSSI_0$ indicates the offset value of RSSI at the reference distance d_0, which is basically defined by the hardware datasheet. Afterwards, a trilateration technique is carried out to estimate the position of the node of interest.

$$\begin{aligned} d_1^2 &= (x_1 - x_U)^2 + (y_1 - y_U)^2, \\ d_2^2 &= (x_2 - x_U)^2 + (y_2 - y_U)^2, \\ d_3^2 &= (x_3 - x_U)^2 + (y_3 - y_U)^2. \end{aligned} \tag{5.11}$$

$$A = \begin{bmatrix} x_2 - x_1 & y_2 - y_1 \\ x_3 - x_1 & y_3 - y_1 \end{bmatrix}, \quad U = \begin{bmatrix} X_U \\ Y_U \end{bmatrix}, \quad b = \begin{bmatrix} x_2^2 + y_2^2 - d_2^2 - (x_1^2 + y_1^2 - d_1^2) \\ x_3^2 + y_3^2 - d_3^2 - (x_1^2 + y_1^2 - d_1^2) \end{bmatrix}$$

$$U = (A^T A)^{-}1 A^T b \tag{5.12}$$

At this stage, the estimated positions of the three nodes of the first ring are respectively, (22.2 39.23), (17.65 60.21) and (59.9 15.46). After that, these three nodes are considered as anchor nodes (reference nodes), which broadcast a packet to nodes within a distance $\delta = 70\,m$. The trialiration technique is applied to determine the position of each node from the second ring, which have as locations (51.95 91.96), (36.55 116.17) and (64.2 70.5), respectively. The duration of this process is approximately one minute and it is executed only one time.

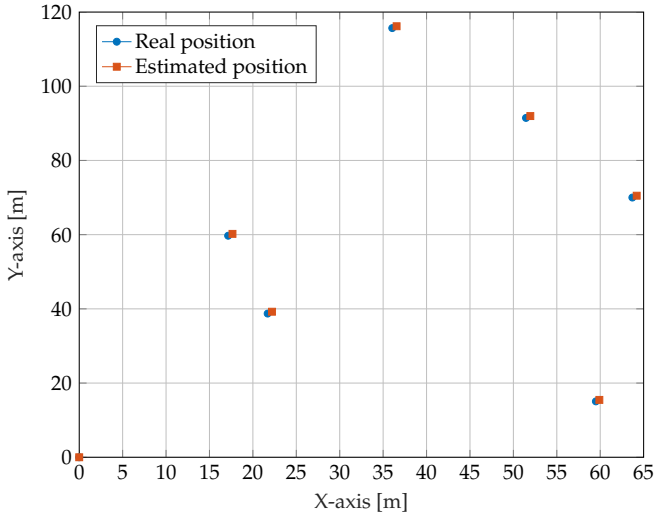

Figure 5.15: Random distribution of wireless nodes in a 100 m $\times$ 100 m network

Obtained results are depicted in Fig. 5.15, where a small deviation between real and estimated positions, around 0.5 m.

After estimating their positions, all nodes are considered at first as simple nodes, and execute the same steps. To avoid data collision, each node is programmed to transmit its message in a defined time equal to 20 seconds, while other nodes are in the receiving mode. Each node broadcasts a data packet including its ID, ring ID, position and residual energy with a communication range equal to the optimal radius determined, $r_{optimal}$, in eq. 4.18 ($r_{optimal} = 29.82$ for the first ring and $r_{optimal} = 38.5$ for the second ring). When a node receives this data packet, it checks, firstly, if it belongs to the same ring. Then it calculates the distance that separates it to the transmitted node. If this distance is less or equal to the defined radius, it considers this node as a neighbour node. The node routing table is updated including its ID, ring ID, positions, distance to each neighbour, list of neighbours and node residual energy. The process of neighbouring takes 2.4 ms for each node from the first ring and 3.6 ms for each node from the second ring.

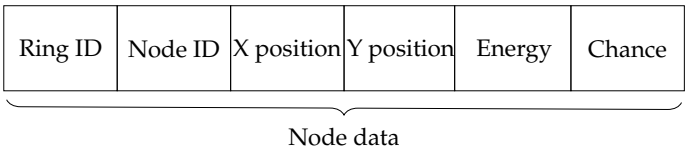

Figure 5.16: Structure of packet transmitted from a cluster member to other node

Afterwards, each node executes the developed FEAUC protocol to gather a decimal value defining its chance to be a CH. Once the chance is calculated, the node transmits this data to the other nodes within the same cluster. The packet structure is presented in Fig. 5.16. Node with the highest chance is selected as a CH and it informs its neighbours with its status. In this case study, two clusters are formed in the first ring, where the first one includes two nodes (node 1, node 2) and the second cluster includes only one node (node 3). In the second ring, one cluster including three nodes is built (node 1, node 2 and node 3). Table 5.5 includes the position of each node, list of neighbours and its chance for being a CH.

Table 5.5: Node parameters in the routing table

Ring 1				
Node	ID	(x, y)	Neighbours	Chance to be a CH
Node 1	1	(22.2 39.23)	[2]	53.73
Node 2	2	(17.65 60.21)	[1]	51.67
Node 3	3	(59.9 15.46)	∅	50.63
Ring 2				
Node	ID	(x, y)	Neighbours	Chance to be a CH
Node 1	1	(51.95 91.96)	[2, 3]	58.35
Node 2	2	(36.55 116.17)	[1, 3]	50.80
Node 3	3	(64.2 70.5)	[1, 2]	51.78

The node having the maximum self chance announces itself as a CH. From Table 5.5, it is noticed that for the first ring, node 1 is selected as a CH for the first cluster. Since node 3 has not any neighbour, it defines itself as a CH for the second cluster. However, in the second ring, node 1 announces itself as a CH because it has the highest chance. Cluster members transmit their data packet, depicted in Fig. 5.17, and repeat this process every 20 seconds. The CH waits the arrival of sent data from its cluster members or other CHs.

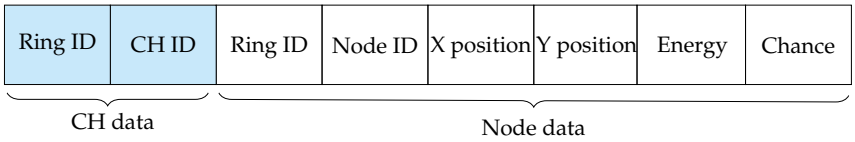

Figure 5.17: Structure of packet transmitted from a cluster member to the CH.

5.4.1 Energy consumption

This section is devoted to analyse the energy consumption of the deployed nodes, presented in Fig. 5.14, by applying the developed FEAUC protocol in this work.

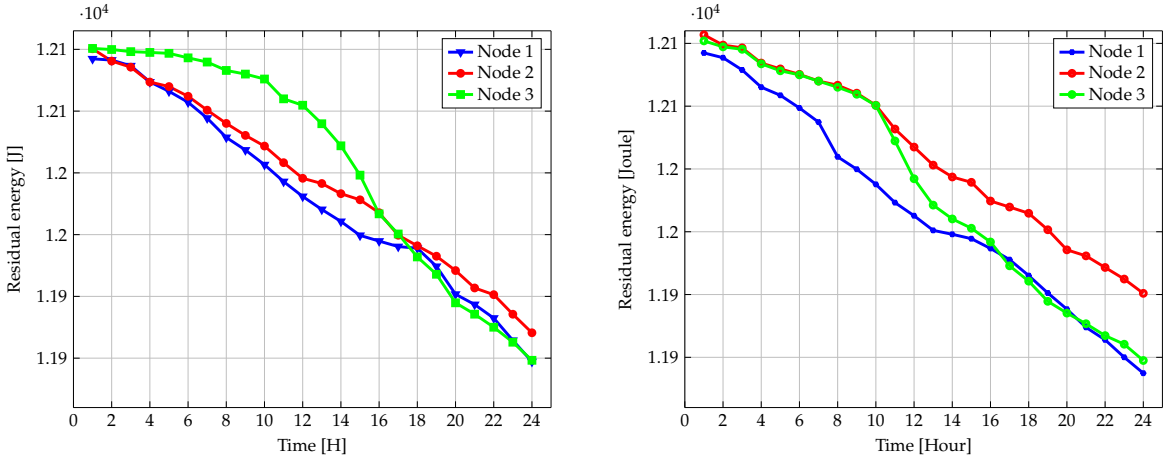

(a) **(b)**

Figure 5.18: Residual energy of nodes: (a) Ring 1, (b) ring 2.

Fig. 5.18(a) illustrates the energy consumption profile of the network after one day, of continuous operations. Two clusters are formed in the first ring. One of them includes two nodes and the second cluster contains only one node. Since the node 1 is selected as a CH for the first cycle, it consumes more energy than node 2 (node 1 consumes approximately 0.053 J during 20 s, while node 2 consumes only 150.3 μJ). After one hour of processing, the node 2 is selected as a CH for the first cluster. It remains working as a CH for approximately three hours. At time equal to four hours and 40 s, the node 1 becomes a CH and still working as a CH till time equal to 18 h and 120 s. After that, the role of CH is given to the node 2 till the end of the day. After one day, 245 J are consumed from node 1, while, approximately 225 J are consumed from node 2 of the first ring.

The implemented FEAUC protocol balances the energy consumption between nodes within the same cluster. Node 3 has no neighbour nodes, it becomes directly a CH for the second cluster. Since it transmits only its corresponding data packet to the BS, it consumes less energy than CH from the first cluster. The equation of the energy consumption of this node is linear (consumes about 4.5 J per hour). After 13 hours, node 3 is selected as intermediate node from the CH of the second ring to forward the data to the BS till the time equal to 20 h and 20 s. For this reason, the residual energy decreases significantly and the energy consumed is about 25 J per hour. After one day, the node 3 consumed almost 252 J. To conclude, the developed FEAUC balances the energy consumption between nodes in the same ring.

As seen in Fig. 5.18(b), in the second ring, the node 1 is selected as a CH. In addition to receiving data from its cluster members, it forwards the received packet to the CH form the first ring. For thus, it consumes about 14 joules more than the node 2 and about 10 Joule more than node 3. It remains working as a CH until the time equal to 13 hours. During this period, it consumes about 129 joules. The node 2 and node 3 have closer energy consumption since they transmit only their packets to node 1 and go to the sleep mode. After 13 hours, the node 3 is selected as a CH. It transmits the collected data from node 1 and node 2 and forwards it to node 3 of the first ring. It remains as a CH until the time equal to 21 hours. After that, the node 1 becomes again a CH. After 24 hours, the consumed energy of node 1, node 2 and node 3 from the second ring is equal to 256 J, 205 J and 254 J, respectively.

Based on the results illustrated in Fig. 5.19, the energy consumption is balanced between nodes in the same cluster or nodes from the same ring and nodes from different rings because of the implemented FEAUC protocol.

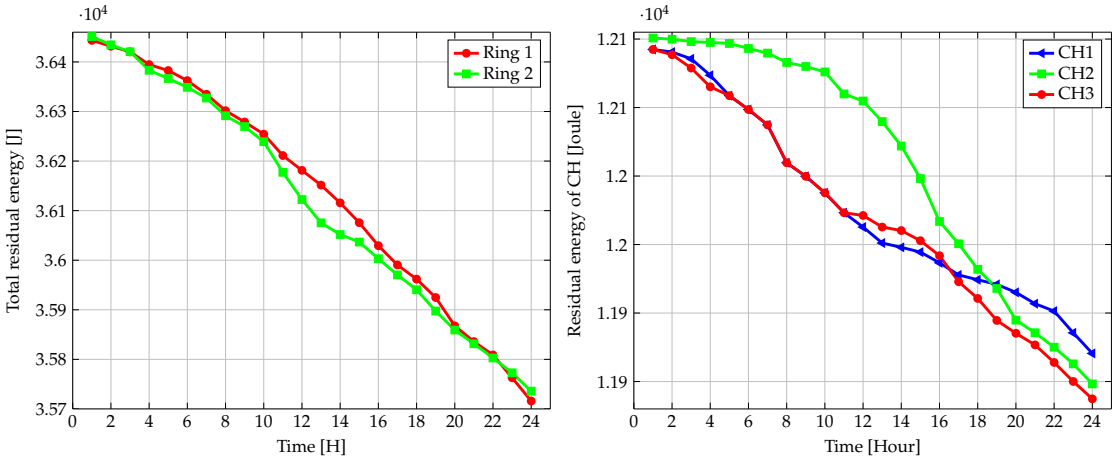

(a) **(b)**

Figure 5.19: Residual energy of:(a) Total number of nodes, (b) of CHs.

From Fig. 5.19(a), nodes from the first and second rings have approximately the same residual energy. The range of difference varies from 0.11 J to 58 J. Thus, the energy consumption is balanced. After 24 hours of continuous operations, the consumed energy of the first ring is equal to 727.58 J, while 715.42 J for the second ring.

The first CH (CH1 denoted in Fig. 5.19(b)) of the first ring has one neighbour. It is responsible of receiving data from its cluster member and the collected data coming from the CH of the second ring (CH3 denoted in Fig. 5.19(b)). CH3 receives data packets from two neighbours and forwards it to the CH1. For this reason, CH1 and CH3 consume approximately the same amount of energy. The difference between them occurs at the time equal to 13 hours, when the CH of the second ring is changed. Before being an intermediate CH for the second ring, the second CH of the first node (CH2 denoted in Fig. 5.19(b)) consumes less energy than the other CHs (CH1 and CH3). By changing the CH, the consumed energy is equal.

To conclude this section, the developed FEAUC balances the energy consumption between nodes in the same cluster, between nodes in the same ring, between nodes in different rings and between all selected CHs.

5.4.2 Network lifetime

The network lifetime is an important metric to evaluate the performance of the developed FEAUC. To this end, Fig. 5.20(a) illustrates the number of dead nodes. As mentioned in section 5.4, the nodes execute continuous operations (repeating cycle every 20 seconds). A node is considered as a dead node if its residual energy reaches out 7038 Joules. As seen in Fig. 5.20(a), the first node dead after 21 days (FND = 21 days). After 22 days, the batteries of three nodes are depleted (HND = 22 days). Another node is dead two days later. The whole network stops working at the day 26 (LND = 26 days). From Fig. 5.20(b), the six nodes die in near days. By changing the CH, when its residual energy is 5% from its initial energy, the consumed energy between nodes is approximately equal leading to have closely lifetime.

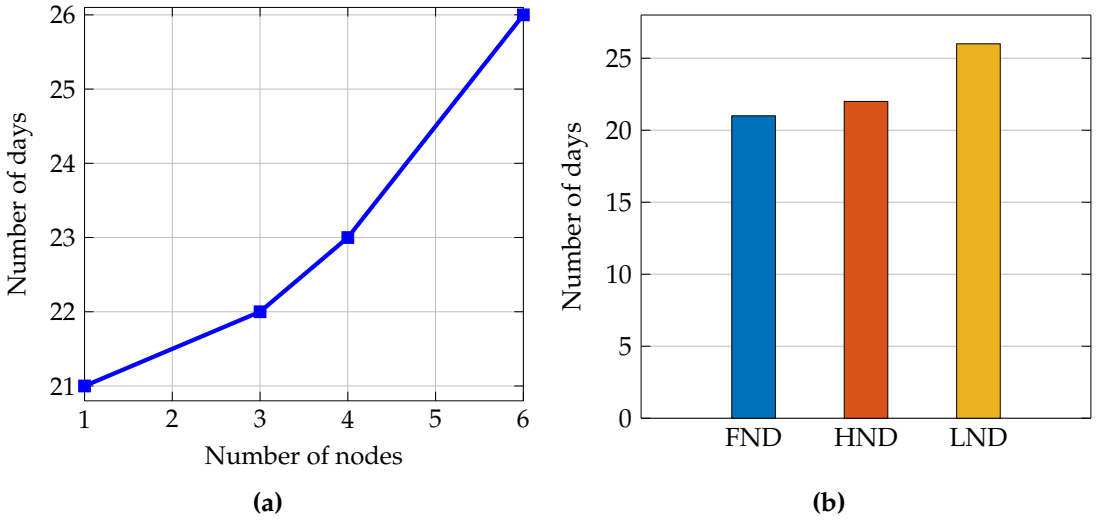

Figure 5.20: Network lifetime: (a) Number of dead nodes over days, (b) comparison of FND, HND and LND.

5.4.3 Number of transmitted packets

As seen in Fig. 5.21(a), for the first ring, the total number of packets exchanged between nodes in the same cluster is less than the data packets of the inter-cluster. However, in the second ring, the total number of packets of intra-cluster is higher than the number of exchanged packets between nodes within the same cluster. It is explained by the fact that the cluster of the first ring has only one neighbour, while the cluster of the second ring has two neighbours, leading to have more packets exchanged in the second cluster compared to the first one (50 %). Since the CH of the first ring is responsible to forward the received packet from the other cluster in addition to its packet to the BS, the number of packets for the inter-cluster is higher 68% compared to the second cluster. Fig. 5.21(b) illustrates the total number of packets exchanged between nodes in the network including, transmitted/received data between nodes in the same ring, from different rings and the transmitted packets to the BS. The range of difference is from 1 to 537 packets.

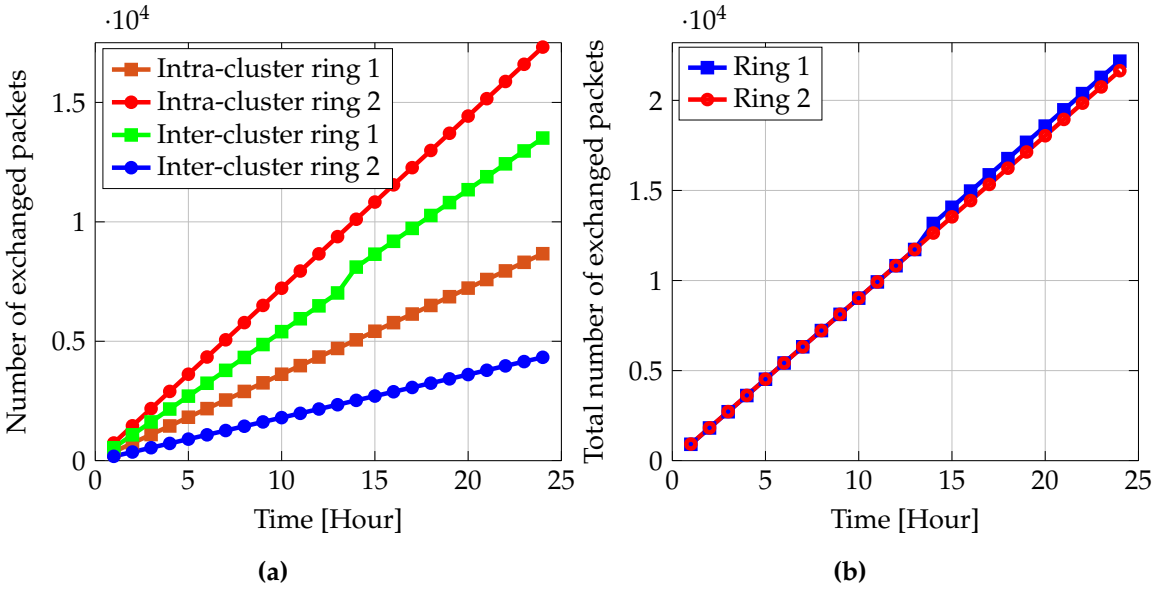

Figure 5.21: Exchanged packets between nodes.

5.5 Comparison to simulation results

In this section, a comparison between the simulation and experimental results in terms of energy consumption and number of packets received at the BS is conducted to underline the importance of the test-bed implementation. Fig. 5.22 presents the variation of the total residual in the network. A difference between the experimental and simulation results is shown and varies from to 102.82 J to 288.88 J. This is due to the fact that simulations are running under ideal circumstances without taking into account external factors, including surrounding environment and obstacles, which reduce potentially the network performance of the system and and thus lead to a loss of energy.

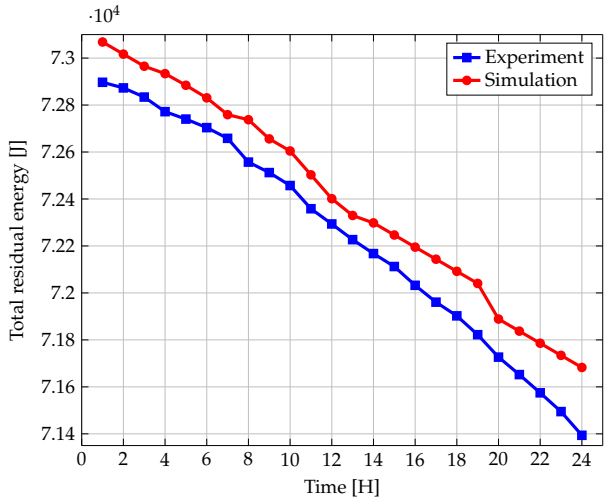

Figure 5.22: Total residual energy variation by the time.

The number of packets received on the BS increases over time. Fig. 5.23 presents a comparison between the simulation and the actual implementation in terms of the total number of packets received at the BS. A difference between the two results, which varies from 20 to 478 packets is depicted. The explanation for this is that in the simulation, all transmitted packets are immediately received because the simulation works on the optimal environment without any external effects. However, in the real implementation, some issues such as the data collision or overhearing can happen. Therefore, some nodes (CH or cluster member) do not reach their destination. A new packet is retransmitted increasing the number of packets received at the BS.

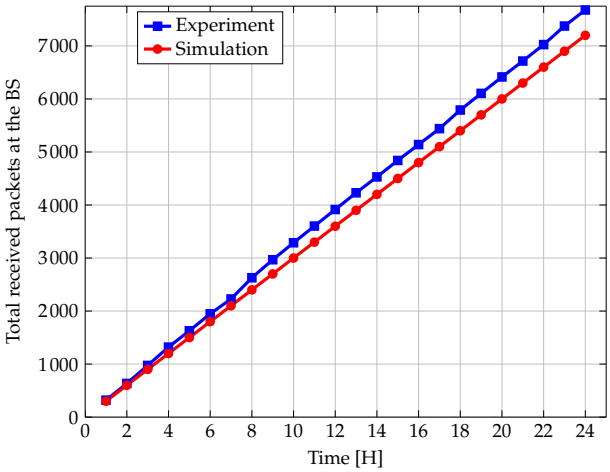

Figure 5.23: Comparison of experiment and simulation results for the total number of received data in the BS.

During the simulation, external disturbances are not considered, such as weather impact, environment definition and obstacles. Thus, the main contribution of this work is to implement and test the developed algorithm on a real hardware, in order to

investigate its performance under real conditions and with hardware consideration. Therefore, in this chapter, the developed FEAUC is mapped on an Arduino-based sensor node and tested in the real field. Results show the performance of the proposed protocol in terms of energy consumption and data received packets at the BS. Furthermore, an automated irrigation system is designed as a real demonstrator. During the real-field test, it is noticed that some nodes fail to transmit or receive data packets from other nodes. In some cases, the CH is unable to communicate with its cluster members because of some hardware or software limitations. Thus, it is important to identify the source of fault and recover it for better network connectivity, lifetime and QoS. In the next chapter, a real-time IoT-based sensor node architecture is designed to evaluate the performance of the proposed FEAUC, where a smart irrigation system is the target application.

CHAPTER 6

Real application to specific uses cases

WSNs have a significant role in real-time decision-making systems, which are mainly related to different environmental and physical parameter monitoring. In this context, modern agricultural systems are, nowadays, based on WSNs to have a complete and real time overview about the changes in the field and the crops state. There is plenty of agricultural activities, which can be significantly improved through the use of WSN technologies. One of these activities is to irrigate automatically cultivated lands. This chapter proposes a real-time IoT-based sensor node architecture to control the quantity of water in some deployed nodes. The developed automated irrigation-based IoT system is called Air-IoT. Thereby the lifetime of the deployed sensor nodes is important for reducing the duration of maintenance intervals. One of the decisive factors for this is the routing protocol, which decides about the number of messages in the network and the necessary sending power. In this chapter, the developed FEAUC protocol is applied to reduce the power consumption for data transmission. The proposed prototype guarantees both real-time monitoring, reliable and cost-effective transmission to communicate each node with the BS.

6.1 WSNs enabled IoT for agricultural applications

The use of new and innovative technologies to boost the performance, quantity and quality of agricultural outputs is crucial in today's modern agriculture. In fact, new advances in the fields of Information Technology (IT), microelectronics and sensors have made it possible to create small, low-cost sensors that greatly facilitate the deployment phase in different scenarios, such as crop and yield surveillance and animal and forestry control [133].

The IoT paradigm has led to a digital revolution that has disrupted decades of progress in electronics and computing, with unprecedented levels of low-cost data storage [134], artificial intelligence [135], mobile computing [134], software as a service (SaaS) [136] and cloud computing [137]. The IoT is fuelled by an alliance of key assets, including the massive proliferation of smart devices, the confluence of low-cost technologies such as sensors, wireless networks, large amount of data (Big Data) and high performance computing capabilities (HPC), ubiquitous connectivity and significant data volumes [138]. The increasing of the number of connected

devices is driven by emerging applications and business models and mainly, WSN, which emerged as a promising technology due to its advancements in wireless technology and digital electronics [19].

The growing popularity of internet and communication technology leads towards a society, where everything need to be connected. The number of IoT devices is currently in its peak of inflated expectations predicted to increase by 21% between 2016 and 2022 to around 18 billion [139]. IoT devices with cellular connections is projected to reach 1.5 billion in 2022 or around 70% of wide-area IoT category. The main concept of IoT [140] is to embedded communication technologies such as Radio-Frequency Identification (RFID) tags with electronics such as sensors, actuators and connectivity capabilities. The IoT retrieves data from the environment in which it is deployed and interacts with the physical world. It leverages also pre-existing internet standards to deliver efficient and high-quality smart services for both date transfer and analysis, applications, and communications.

Consequently, a taxonomy of agricultural applications on the basis of WSN can be derived in Fig. 6.1.

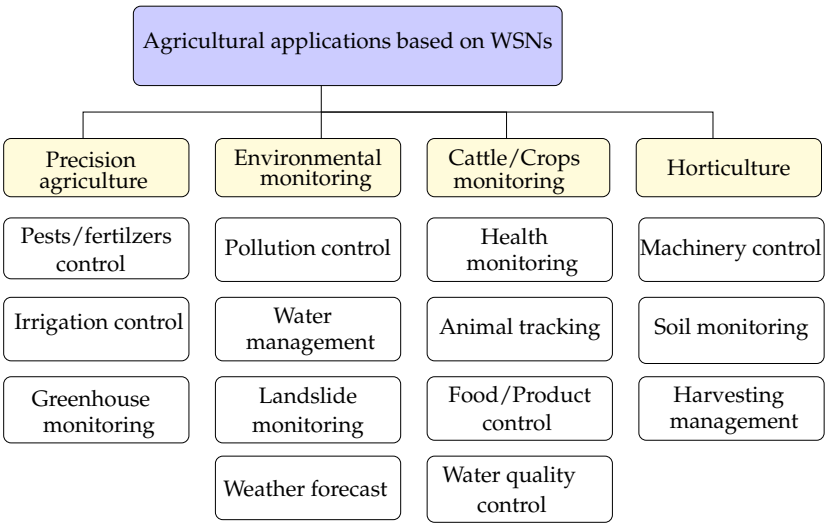

Figure 6.1: Taxonomy of agricultural applications using WSNs and IoT.

Generally, agricultural applications-based WSN and IoT can be classified into four main classes: Precision agriculture, environmental monitoring, cattle/crops monitoring and horticulture. According to this taxonomy, it is noticed that the water is one of the most challenging aspect, which needs to be considered since it is involved mostly in all agricultural application categories. In precision irrigation applications, the control of irrigation is highly recommanded to reduce the over-use of water. In some environmental applications, it is interesting to apply different water management policies, which help to determine the upcoming irrigation expectations. Controlling the water quality is a critical practice because it affects directly the plant nutrition. Sometimes, water can not dissolve properly fertilizer resulting a problem in the plant growth. In addition, calcium salts in water may produce a white crust of calcium

carbonate. Such layer causes the rapid formation of stones, which can block the irrigation system. For this reason, the focus on this chapter is on the irrigation.

In this context, WSNs are scalable in their use, reliable in difficult situations, provide a full control in a closed-loop operation and offer more coverage with a high time and space resolution. A further feature of the use of sensor nodes is to minimize the amount of work involved, thereby reducing the costs associated with the deployment, operation and maintenance. In other words, WSNs provide real-time monitoring of field evolution and crop conditions that support the precision agriculture by controlling parameters and yielding cyclical data [141].

The wireless communication reduces the total cost of the network by approximately 80% compared to hardwired alternatives [142]. WSN-based systems for agricultural purposes are expected to be user-friendly, straightforward to design, maintain and update. Thus, if each node is supplied with a battery, it becomes hard to recharge or change the batteries from one time to the next, especially for a large network. For long-term uses, extending the lifespan of wireless sensor nodes through the energy conservation is an area of concern that needs to be highly considered. This is the reason for investigating on the development of energy efficient techniques including routing and data aggregation protocols. As discussed through previous chapters, the main aim of the presented dissertation is to conserve the energy consumption of the whole network by developing an unequal-based clustering protocol. The overall architecture of the proposed paradigm can be implemented to monitor agricultural applications as presented in Fig. 6.2.

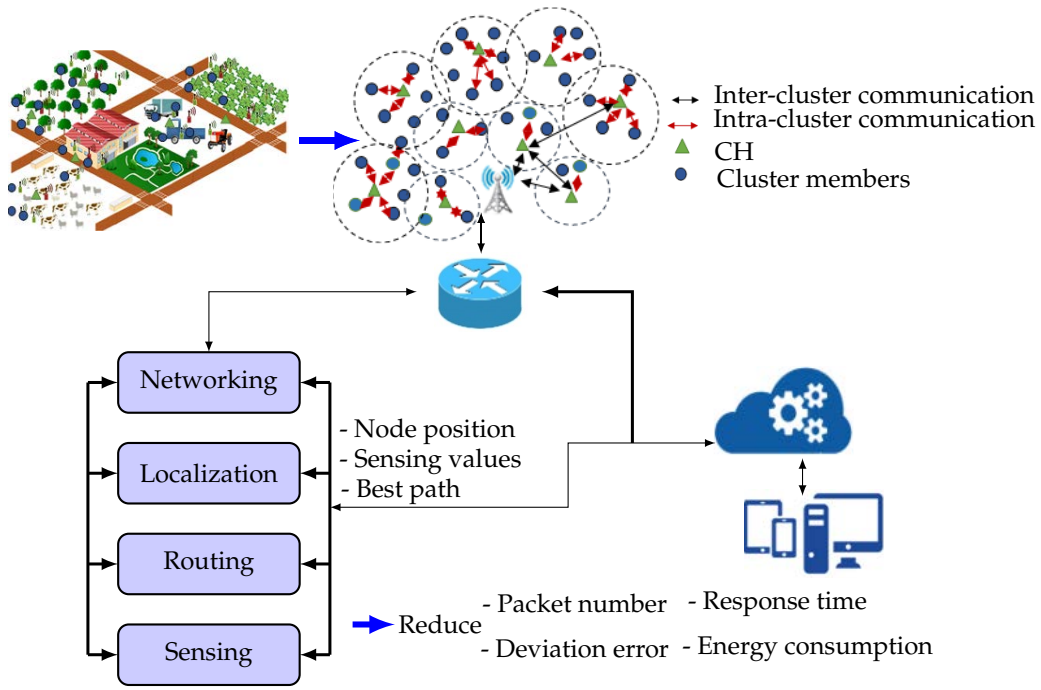

Figure 6.2: General architecture of a monitoring system-based on WSNs for agricultural applications.

The developed architecture of the agricultural monitoring system provides a comprehensive overview of the deployed system, where critical information collected in the field is effectively communicated between installed nodes. Nodes are deployed randomly. Then, a clustering algorithm is performed to organize these nodes into different groups. Each cluster contains a CH, with a predefined position and a number of nodes. All information are collected in the BS and transmitted to a network gateway. At this stage, the data processing and decision-making are applied, such as location, routing detection and data networking. Once the necessary decisions have been made, the results are again communicated to the installed nodes. As a result, an increasing number of reported data packets are being created, which increases both the energy consumption of deployed nodes and thus affects the network's energy balance. In fact, the main challenge is to develop low-cost, low-power, fail-safe components with simple operation and high reliability.

6.2 Discussion about existing automated irrigation systems

The climate change has a great impact on the irrigation as a result of the increased prevalence of extreme events and unpredictability of weather patterns. The new scenario of drying up of water tables, rivers, and tanks present a critical need for the proper use of the water. Many research works focus on the field of automated irrigation and different studies aims to reduce the inefficient water consumption.

Different controlled irrigation techniques, such as sprinkler irrigation and drip irrigation, are recommended to solve the inefficiency of water uses [143]. The quality and quantity of the yield are strongly affected by coping with the water shortage, as uneven irrigation. In some cases, the water overflowing can reduce the soil nutrition and leads to various microbial diseases. It is not easy to estimate precisely the amount of the water needed by crops because many parameters can be involved to take the decision of watering such as the type of soil, type of crop, rainfall and irrigation technique. To this end, the existing irrigation systems can be improved by adopting IoT technologies. Take the example of the irrigation management using the crop water stress index, which can significantly improve the crop quality and quantity [144].

Authors in [145] propose a smart irrigation system-based on IoT devices to control the use of the water in agricultural fields. A cloud farming surveillance system has been developed to help the farmer to check the soil status. The watering system includes mainly three units: Sensor and actuator, cloud and user application. Sensors are responsible ot measure the air temperature and the soil moisture. The actuator is used to manage the irrigation flow. A gateway node is used to transmit the collected data from sensor nodes to the cloud platform using the HTTP protocol.

In [146], an automated irrigation system is designed including, mainly, the sensing and data storage units. The first unit is responsible for sensing the soil criteria such as the moisture, temperature and luminosity. Depending on the soil parameters, an automated operation is carried out by switching the motor on and off using the

threshold values incorporated in the code. The status of the latter is alerted on the home screen by means of GSM messages. Indeed, The GSM module is interfaced with the open source, Arduino, to establish a cellular communication between the system and user.

A mobile-integrated smart irrigation management and monitoring system is presented in [147]. The key aim is to control the water supply and monitor plant's parameters involving the soil moisture, air humidity and temperature. The irrigation operation depends on a threshold value of the soil moisture. In fact, the system uses the Raspberry Pi, which monitors the sensed data and stores them in the cloud. A smartphone is connected to the Raspberry Pi through a Bluetooth to turn on and off the motor.

An IoT-based automated agricultural monitoring and control system is implemented in [148]. It uses a network of several NodeMCUs (ESP8266) microcontrollers to monitor and control multiple systems over the cloud. A raspberry Pi is used as a gateway node, where a local Message Queuing Telemetry Transport (MQTT) broker is installed to connect all microcontrollers to the cloud. The NodeMCUs constantly monitor the respective states of various elements of the farm and report the data to the central control unit. The user can then take appropriate actions from analysing this data, i.e. assign their desired tasks to each of microcontrollers separately by using a mobile or web application.

In [149], an automated irrigation system is designed. To control the amount of water, threshold values of the soil temperature and moisture are fixed on the gateway side, which processes sensed data, activates the actuators and forwards the data to a web-based application. Solar panels are used to power the entire system. Moreover, the system provided a two-way communication link using a mobile internet interface, which ensures the data verification and the watering via a website. A wireless sensor unit uses the ZigBee technology to send sensed data to the wireless information unit. This later is equipped with a GPRS module to transfer the data to a web server.

A Smart Water Management Platform (SWAMP) employs various IoT-based approaches to design a precision irrigation system in four different countries [150]. Various crop conditions such as the size of crops and their growth stage and different weather parameters such as the rainfall, air temperature are involved to estimate the accurate amount of water depending on the location of yield and the type of crops. Moreover, SWAMP is intended to ensure the ability of used high-tech devices to work in different circumstances and to be easily reproduced in various places and environments.

A comparative analysis of some referred smart irrigation systems is described in Table 6.1 using some attributes such as the selected hardware, the wireless communication standard and the programming language. All the described irrigation systems do not consider the energy consumption issue. They focus either on the real-time water monitoring or on the reduction of water dissipation. However, no one of them aims to save the consumed energy. One of the main contributions of this chapter is

to design a low-cost, real-time automated irrigation system that helps farmers to irrigate its crops in an efficient way.

Table 6.1: Comparison of existing smart irrigation systems

Work	Plant	Hardware			Communication technology	Programming language
		Sensors	Microcontroller	Other		
[145]	Peach tree	Soil moisture, weather forecast	MSP430F2274	Electrovalve	ZigBee, IEEE 802.15.4, HTTP, GPRS, GPS	JSON, Model-View-Controller
[146]	Groundnut	Moisture, light temperature	ATMEGA328	Pump	GSM, Bluetooth, Wi-Fi	Sprakfub
[147]	Not mentioned	Temperature, soil moisture	Raspberry Pi	pump, motor	Bluetooth	Python
[148]	Not mentioned Not mentioned	Temperature soil moisture	ESP8266	Raspberry Pi pump, solar cell	MQTT, Wi-Fi	node.js
[148]	Not mentioned Not mentioned	Temperature soil moisture	ESP8266	Raspberry Pi pump, solar cell	MQTT, Wi-Fi	node.js
[149]	Organic sage	Temperature soil moisture	Pic24FJ64GB004	Photovoltaic panels	GPRS, Zigbee	SQL server, C#

6.3 Air-IoT: Developed automated irrigation system

A real-time IoT-based sensor node architecture to monitor both the soil moisture and temperature is developed to control the quantity of water and presented in Fig. 6.3.

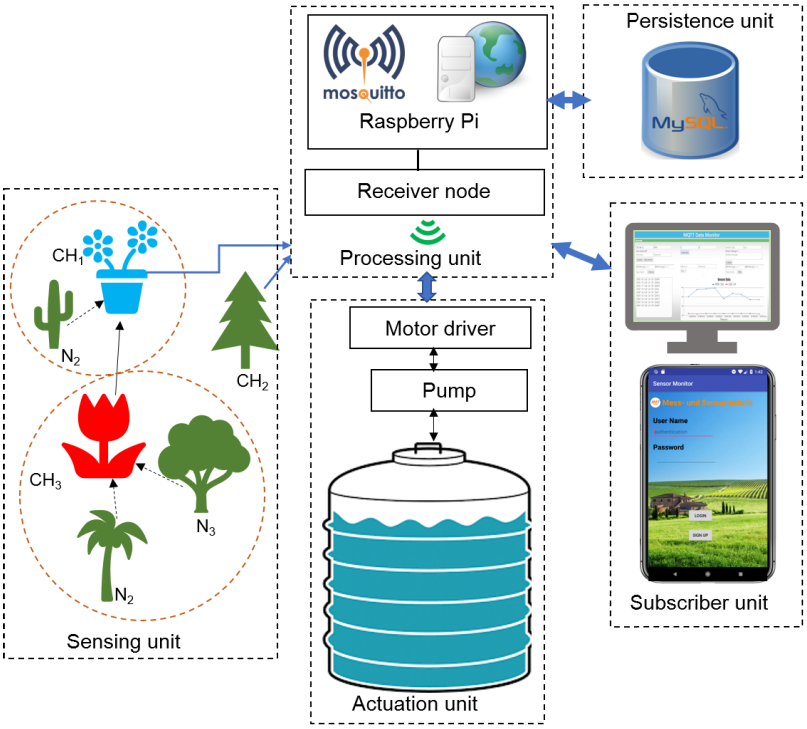

Figure 6.3: Air-IoT system architecture.

The developed solution includes five units: Sensing, processing, front-end, actuation and persistence. The sensing unit is composed of a number of wireless nodes integrating the soil moisture and temperature sensors. A processing unit consists on a receiver node, serially, connected to a Raspberry Pi. In fact, the sensed data are sent from the receiver to the gateway using the MQTT communication protocol. A python

script is written to implement the publisher client to transmit data using MQTT protocol to specific topics handled by Mosquitto broker [151]. On the subscriber unit, a graphical web interface and a mobile application are designed and implemented, which enable the user to monitor the data in a real time. The web interface pages are implemented in HTML/CSS and JavaScript, hosted on the Raspberry Pi and served using a lightweight framework called Flask [152].

When the soil moisture level falls below the threshold, the user can view the information in the application and take prompt action to give control to the motor through the mobile application, thus reducing water and energy dissipation. A persistence unit based on the MySQL database is used to store data directly from the publisher end. It can be also accessible via both web interface and mobile application. Later, in the following subsections, each unit is discussed in details as well as the implementation of the back-end and front-end functionalities.

6.3.1 Sensing unit using the developed FEAUC protocol

To control the level of water on the soil, the sensing unit compromises the resistive-based soil moisture sensor, namely, SEN-13637 [153], the soil temperature, namely DS18B20 [154] and the wireless node or mote, called panStamp [6]. The soil moisture sensor is composed of two pads, together acting as a variable resistor. The more water that is in the soil means the better the conductivity between the pads is, resulting in a lower resistance.

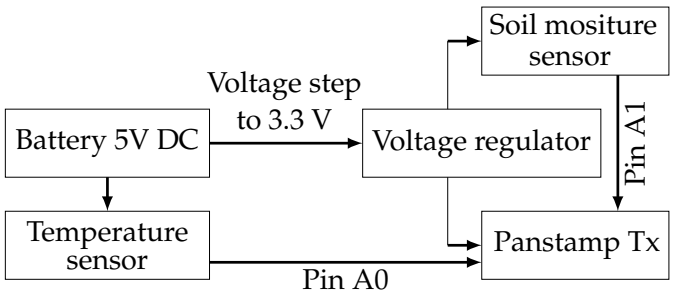

Figure 6.4: Sensing unit block diagram.

As presented in Fig. 6.4, the panStamp transmitter and the integrated sensors are powered by a battery 5V DC and the grounds are commonly connected. The soil moisture sensor signal pin is interfaced with analog pin of the panStamp. The temperature sensor has an operating range of -55 °C to +125 °C.

In this unit, as an example, the network includes six nodes, where three of them are CHs. Sensors for the soil temperature and moisture are integrated in each node. The developed FEAUC algorithm is applied in this stage to route the sensed data between cluster members and the gateway as described in Fig. 6.3. After defining the list of neighbours for each node, the CH selection step is launched to identify the adequate CH in each cluster. Every node calculates its chance for being a CH using the fuzzy logic system. The node having the highest chance is defined as a

CH for this cluster. Then, depending on the ring where it belongs, a forwarder CH selection sub-phase is started. For the uses case presented in this chapter, CH_3 selects the CH_1 as a relay node to transfer its data to the BS. After the data sensing, each cluster member transmits its data packet to the corresponding CH. CH_3 collects the received data from its cluster members and forwards it to the CH_1, which in its turn aggregates the received data with its own information and forwards the collected data to the gateway. Cluster members are set in the sleep mode and they are awake in every five minutes for measurements.

6.3.2 Processing unit using the MQTT protocol

In the processing unit, the panStamp receiver node receives sensed data from remote nodes and forwards it to the gateway (Raspberry Pi). This embedded board is used in the developed prototype because of its large usage in IoT applications and its low cost. The gateway should be fast enough to collect data from multiple sensor nodes, run algorithms to exchange messages with the cloud. To this end, the choice of the appropriate messaging protocol among considerable protocols such as the MQTT, CoAP, AMQP and HTTP is highly recommended. The MQTT protocol is distinguished by its short message transmission capability and low bandwidth usage, which makes it suitable for Machine to Machine (M2M) communications of the connected object type [155].

A MQTT network consists of publisher nodes, topics, subscriber nodes and a broker. Publisher nodes send messages over the topics, which are received by the broker. The broker plays the role of a central unit in every MQTT network and forwards the data to the subscribed clients for the topic. The MQTT allows devices to concretely send information on a given subject to a server that functions as a message broker. The broker pushes this information to the subscribed customers. An open source lightweight broker, Mosquitto, is selected because it is suitable for low power single board computers such as raspberry pi. With the MQTT, all customer devices that need to communicate with each others have to interoperate with the same broker. The broker stores the received messages from the sending entities (publishers) and relays them to one or more receivers (subscribers). Messages are sent via a given information channel (or topic). As a result, when the broker receives a published message, it broadcasts it to all subscribers. Only those who have subscribed to the given information channel are able to receive it.

To select the right server for the developed system, three options are considered: Flask [152], Lighttpd [156] and Nginx [157]. Lighttpd is the most lightweight web server, which makes it an ideal candidate for embedded systems. When compared between Flask and Nginx, both offer a wide range of features such as the load balancing, fault tolerance and auto-indexing. However, Flask is the most widely used as a web server for different development purposes and offers a better community support. Flask is generally considered as a micro-framework that comes with built-in development server and fast debugger. Moreover, Flask is compatible with other

web servers such as Apache. For these reasons, Falsk is considered to be used in this presented work.

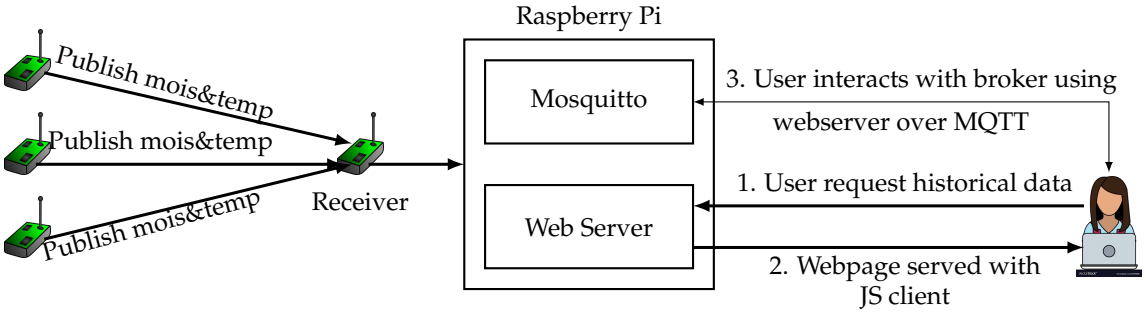

Figure 6.5: Communication flow in the processing unit.

The most vital part of designing a web interface is to give the user the ability to interact with the broker in a simplified way. Any interaction requires a connection from a client with the broker. For this purpose, the web server comes into the picture. All the web pages will be hosted on the web server. So, the Raspberry Pi is used as a web server and Mosquitto server. As presented in Fig. 6.5, the idea is that the user can fetch the web pages from the server using a normal HTTP request method. Once it has the webpage, it can communicate with the Mosquitto broker through the MQTT protocol. The MQTT client is implemented using Paho Mqtt JavaScript library enabling the interaction with the MQTT from the browser using web-sockets.

6.3.3 Subscriber unit using the Mosquitto broker

After the implementation of the core functionalities of the system, the next task is to design and implement a web interface for the subscriber. This gives the user the ability to either subscribe or publish to topics, monitor data in a log form, visualize data in a plot with historical data in tabular and plot form. The core architecture of the web interface is based on HTML and CSS, whereas Python has been selected for running operations on the web server. JavaScript is used to leverage the functionality of web sockets in Mosquitto. Eclipse Paho project provides open source client implementation of MQTT. The libraries are available in JavaScript too, which provides a simpler platform to interface with Mosquitto. Apart from that, JavaScript provides better user experience and more control on the browser end. Once the user provides the broker name, port, user name and password the information is sent to the Mosquitto broker to verify the identity of the subscriber.

6.3.4 Actuation unit using the water pump

In the actuation unit, as presented in Fig. 6.6, a 12V DC water pump integrated with a motor driver is attached to the Raspberry Pi. In fact, the 12V DC motor operates with the motor current of 200-300 mA. It has 2 silicone tubing used for pumping. One tube is used for fetching water from the tank and another tube is used for watering the plants. It has a flow rate of 100 mL/min. A dual H-bridge motor driver, L298N

[158], is used to control, simultaneously, both speed and direction of the DC motor, which uses a power supply from 5V DC to 46V DC with a peak current up to 2A.

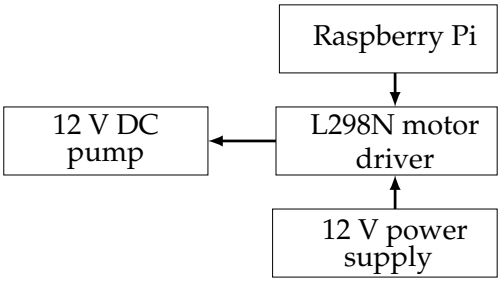

Figure 6.6: Actuation unit block diagram.

The sensed values are transmitted to the server through the Raspberry Pi. When the user logins to the mobile application, the real time graphs of the soil moisture and temperature sensor data can be viewed. When the soil moisture is low, the user can switch the motor to the ON state from the mobile application remotely. This command is received by the server. When the Raspberry pi detects the 'ON' state, it sends a signal to the motor driver to turn on the motor and waters the plants. The user can turn 'OFF' the motor when the soil has enough moisture content. When the gateway detects the 'OFF' state, it transmits a signal to the motor driver to turn off the motor.

6.3.5 Persistence unit using the MySQL database

After transmitting the data from wireless nodes to the subscriber node over MQTT, the next milestone is to store data packets in a database for further access. This process is depicted in Fig. 6.7. There is a variety of databases, each with its own specification, strengths and limits. In this developed system, MySQL has been selected. It is a well-known large-scale and open-source relational database. It consists of server/client architecture, which requires a multi-threaded SQL server. Moreover, MySQL supports multi-user features, which along with its scalability makes it a perfect candidate for distributed applications.

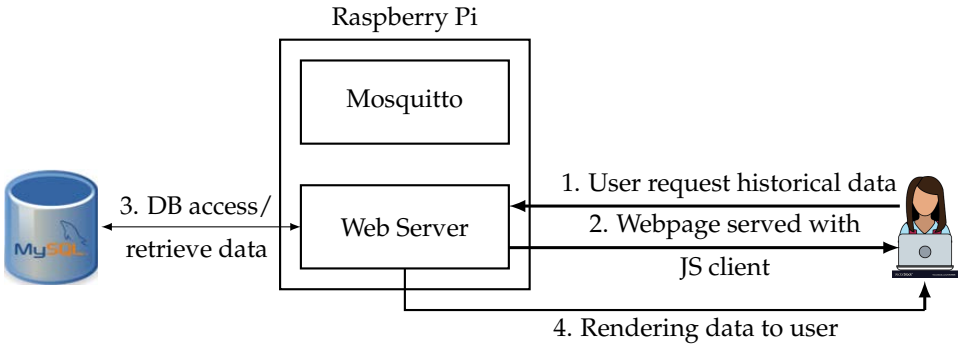

Figure 6.7: Database access steps.

6.3.6 Results of the Air-IoT architecture deployment

The web interface enables the user to monitor the historical data of any node in tabular and plot forms. In this system, the latency issue is not taken into consideration. For this reason, the HTTP protocol is used to provide a request to the web server, which in its turn sends the query to the database and gives the response back to the user. To fetch data the user does not need to be connected to the Mosquitto broker because this functionality is directly dealing with the web server.

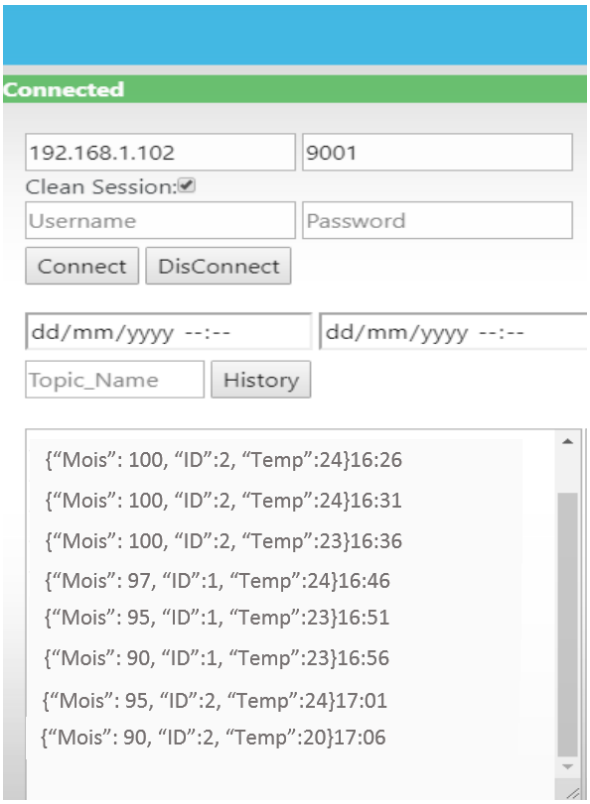

Figure 6.8: Real-time data monitoring in a log form.

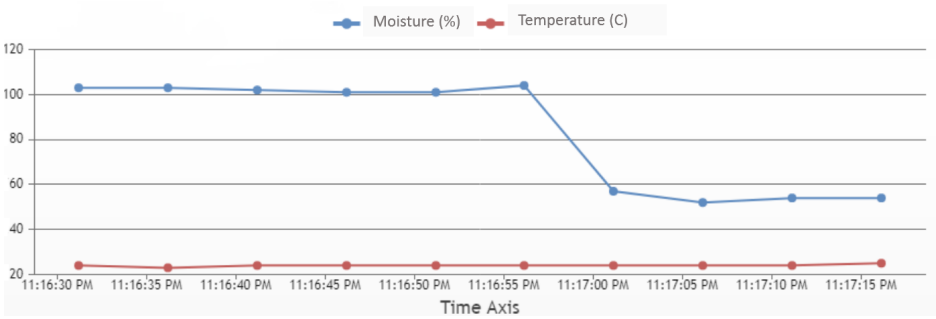

Figure 6.9: Real-time data monitoring in a plot form.

As seen in Fig. 6.8 and Fig. 6.9, the sensed data can be monitored regularly through the web application. Fig. 6.9 shows the soil moisture and temperature in real time. Thus, the user can turn on/off the motor in the field through the application from

a remote location. By turning on or off the device state, the web server is updated. Another important activity is 'show weekly graph' button, which directs the user to the weekly graphical representation of the sensor value to determine the changes in the behaviour of each sensor. This activity is shown in Fig. 6.10(b). A google map is implemented to check the location of the node.

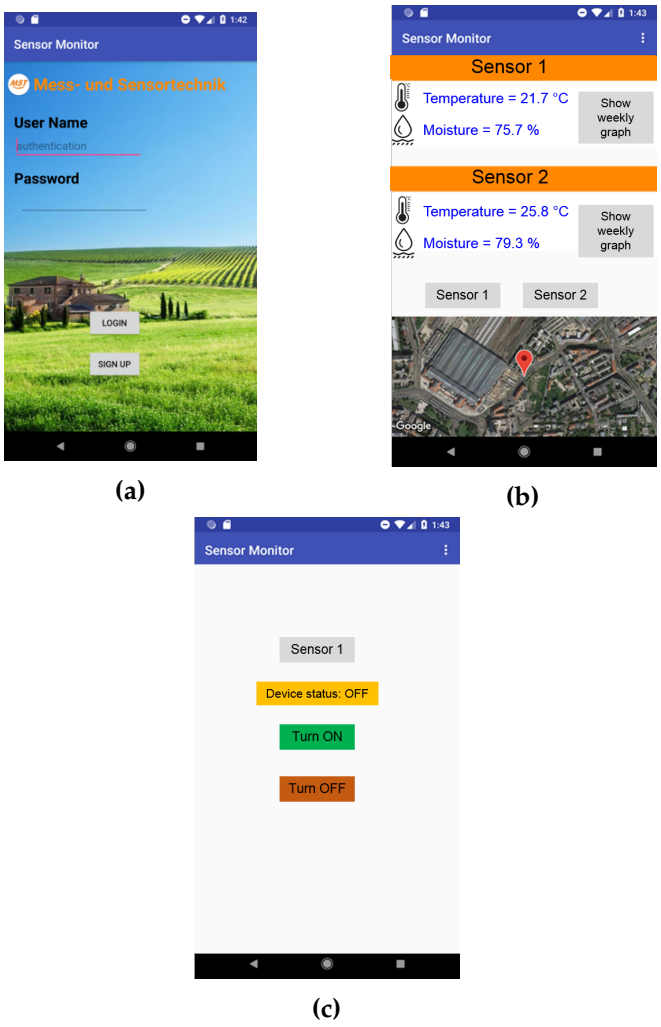

Figure 6.10: Illustration of the end-user interfaces: (a) User authentication layout, (b) graphical presentation of sensed data,(c) controlling the motor from the android application.

The water management is a key challenge in the agriculture since its availability is a worldwide issue for the forthcoming decades. Therefore, the precision irrigation is introduced, as a cutting edge method, to increase the crop productivity and manage the over-use of the water with the help of advanced technologies, including WSNs, cloud computing and IoT. This chapter highlighted the importance of the precision irrigation in agricultural applications. Moreover, the challenging factors affecting the need of crops for water is described to identify the most essential sensors that can be used in such irrigation systems. The most common wireless technologies as

well as the general architecture of IoT-based irrigation systems are discussed. The key objective of designing smart irrigation solutions on the basis of IoT and WSN is to save the water consumption and reduce manpower, time and money. For this reason, a cost-effective, real-time IoT-based automated irrigation system is designed using soil temperature and moisture sensors. Sensed data are forwarded to the processing unit (Raspberry Pi), presented as a central node in the system. To collect data from multiple sensor nodes, the lightweight publisher/subscriber messaging transport protocol, MQTT, is used. Mosquitto has been used as a message broker, which implements the MQTT protocol. When the moisture level of the soil is less than the threshold level, the user can visualize them and takes an immediate action to give the control to the motor through the mobile application thus reducing the water dissipation.

CHAPTER 7

Conclusions and future research directions

Since the data communication is one of the most energy consuming tasks in WSNs. Therefore, energy efficient routing protocols are significantly important for organizing data packet circulation and extending the network lifetime. Cluster-based routing is one of the most interesting energy-aware techniques that minimize simultaneously the number of transmitted messages and the distances between nodes to be covered by a certain message. In this chapter, a summary of the proposed protocol and experimental results are discussed. Then, directions for future works are provided.

7.1 Conclusions

Because of the energy restriction of battery-powered sensor nodes, energy reduction techniques pose challenges for WSNs. There is a considerable demand for the development of energy-efficient strategies. In this dissertation, different contributions to overcome the energy constraint challenge are provided. Firstly, a comprehensive review of energy constraints and available energy saving techniques in WSNs is described. Cluster-based routing protocols are presented as a promising approach to improve the energy efficiency in WSNs. An unequal clustering protocol FEAUC with a partitioned circular network model is developed to balance the energy consumption among all sensor nodes and to enhance the network lifetime.

The developed FEAUC is split mainly into four phases: Off-line phase, cluster formation phase, cooperative phase and data collection phase. The off-line phase is performed to calculate the region width of the circular cluster and to determine the optimal number and size of each cluster. The cluster formation phase ensures the building of clusters and the selection of CHs. The proposed protocol uses the fuzzy logic with the residual energy of a node, its centrality and density. The cooperative phase prevents long haul transmissions by selecting a relay node considering its residual energy and its distance to the current CH. The data collection phase consists of intra-cluster and inter-cluster data transmission.

Extensive simulations in different scenarios are carried out to evaluate the proposed solution. Simulation results show that the developed FEAUC outperforms Fuzzy Logic, MOFCA, DUCF, EEUC, IFUC, FAMCROW and MCFL algorithms in term of

energy consumption leading to improve the network lifetime. Considering the FND metric, the proposed algorithm is more efficient than the fuzzy Logic algorithm by 36%, MOFCA by 16%, DUCF by 13% and MCFL by 5%. According to HND metric, the developed FEAUC is more efficient than Fuzzy Logic algorithm by 18%, MOFCA by 14%, DUCF by 12% and MCFL by 2%. Considering the residual energy metric, after 700 rounds, the total residual energy in FEAUC is about 20 J, 13 J for MCFL, 9.8 J for DUCF, 5 J for MOFCA and only 2 J for the Fuzzy Logic protocol.

The proposed network in this work is designed considering more than one round and for this purpose the fault tolerant based unequal clustering algorithm (FEAUC-FT) is developed. It avoids the selection of CH in each round by selecting a backup CH, that takes the role of the primary CH in case of fault of having an amount of energy less than a fixed threshold value. Hence, the number of transmitted data packets between cluster members is decreased significantly and so the total consumed energy is reduced. Moreover, a backup routing path is built between CHs from different rings to re-transmit the lost packets in case of link failure. Therefore, the data losses is decreased and then the data network connectivity is improved.

Simulation results prove that the FEAUC-FT outperforms the FEAUC protocol in terms of energy consumption and network lifetime. For example, at round 500, FEAUC has approximately 30 J, while the FEAUC-FT has about 57 J. Moreover, considering the FND performance metric, the optimized version is 8% more efficient than FEAUC. Similarly, the developed FEAUC-FT with respect to the HND metric is 54% more efficient than FEAUC.

A real implementation of the proposed FEAUC is carried out to evaluate its efficiency on real hardware. Results comparison between the simulation and experiment is conducted to highlight the importance of such test bed implementation. Both results show the efficiency of the proposed clustering algorithm in terms of energy consumption, battery lifetime and transmitted packets. Besides, a low power cost-effective electric circuit is designed to monitor the current consumption to calculate the residual energy of the batteries. The measurement setup is based on a shunt resistance between the power supply and sensor node. Together with the precision amplifiers, the shunt resistance provides a good environment for current measurement with less interference.

For the demonstration of the novel protocol, a smart irrigation system, called Air-IoT, is designed as a prototype to validate the efficiency of the developed FEAUC in a real environment. FEAUC is applied to reduce the power consumption during data transmission. To this end, a real-time IoT-based sensor node architecture to monitor both soil moisture and temperature is developed to control the quantity of water. Indeed, the sensor data is collected and stored in the cloud. The data can be retrieved and visualized in the smartphone application. When the moisture level of the soil reaches below the threshold level, the user can visualize them in the application and take immediate action to give control to the motor through the application thus reducing the wastage of water and energy.

7.2 Future lines of research

As a future work, to overcome the problem of inaccurate choice of threshold, a threshold-based energy analysis model needs to be developed and implemented. Although many cluster-based routing algorithms have been developed to extend the network lifetime using well-selected scenarios, nodes drain their energy and eventually fail at a certain time. Harvesting energy from external resources presents a promising solution to avoid the problem of limited power. Nodes can be powered from the surrounding environmental sources and have a self-powering feature.

In addition, we envisage to apply the Compressive Sensing (CS) techniques for the data aggregation, which has the benefit of having a low traffic cost. The fundamental milestone to perform the CS is to build a measurement matrix according to the network structure and to give a unique column vector of the measurement matrix for each node.

A Wireless sensor nodes

WSNs consist of a number of autonomous and spatially-distributed sensor nodes deployed to monitor, control and record surrounding physical parameters such as the temperature, humidity and pressure. These sensors are deployed over a certain area, communicating wirelessly together in order to achieve a specific application such as the health, military, smart home and agriculture [159]. The general structure of a WSN is presented in Fig. A.1.

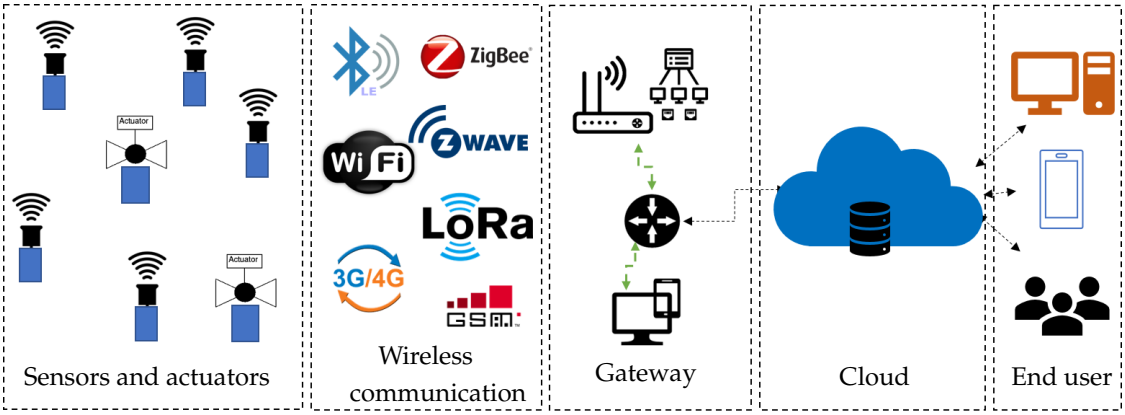

Figure A.1: General structure of WSNs.

The protocol stack of sensor nodes is presented in Fig. A.2, which integrates the power management with the routing efficiency. It combines the data delivery and networking protocols. In addition, it transfers the power using the wireless medium. Most common architectures for WSNs follows the OSI model, including five layers, namely application, transport, network, data link and physical layers [160].

(1) Application layer: It includes a variety of applications, services and interfaces. Indeed, it provides the interface that connects the platform to run the deployed software. Every service, task and other background application needed for the network connectivity and data analysis operates at this layer.

(2) Transport layer: It is in charge of providing the reliable data required by the application layer. It maintains the flow of data from the application layer to the network layer.

(3) Network layer: It is responsible for the data routing from the transport layer by directing the process of the selection paths along which to send the data in the network. This layer is mainly charged with the multiplexing of the data stream, the transmission and reception of data frames, media access and error control.

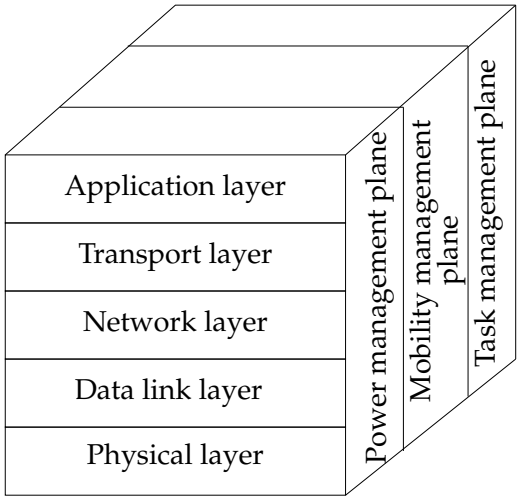

Figure A.2: Protocol stack for WSNs.

(4) Data link layer: It creates the link between the software and medium. It is responsible for the data stream multiplexing, data frame detection, medium access and error control providing reliable data transmissions.

(5) Physical layer: It is used to convert bit streams from the data link layer to signals, which can be transmitted over the communication medium. To this end, it has to address a variety of related issues, including the choice of transmission medium and frequency, carrier frequency generation, data encryption, and signal modulation and detection. Furthermore, this layer is involved in the design of the underlying hardware and numerous electrical interfaces.

A.1 Commercial wireless Sensor nodes

This section describes some existing wireless sensor nodes as follows.

Mica2 and MicaZ: They use Atmega128L as microcontroller embedded with a CC1000/CC2420 RF module, respectively. They integrate some sensors such as humidity, temperature and light sensors enabling motes to measure barometric pressure, acceleration/seismic activity, etc. The motes are powered from external 2 AA batteries with an operating range of 2.1 to 3.6 V DC.

TelosB Motes: It is a platform produced by the American company Crossbow as a prototype intelligent sensor. It uses a 16-bit Texas Instruments MSP430 microprocessor with 8 MHz clock frequency and 2.4 GHz radio link. As current, the TelosB consumes 0.7 mA in the idle mode and 200 mA in the active mode. A set of sensors are integrated in this mote including temperature, relative humidity, visible and infrared light. The mote works on an open source TinyOS operating system. It is powered from external 2 AA batteries with an operating range of 2.1 to 3.6 V DC.

IRIS: It offers a high communication range, which is approximately near to 500 meters. It is based on the low power microcontroller ATmega1281. It uses TinyOS

operating system and a 2.4 GHz IEEE 802.15.4 as wireless module. This mote can support external boards using a standard 51-pin expansion connector. The consumed current during the transmission varies from 10 to 17 mA. For indoor applications, the transmission range reaches up to 50 meters and more than 300 meters for outdoor applications.

Waspmote: It is introduced by Libelium as an open source node for IoT applications. It uses an IEEE 802.15.4 compliant radio module. It has Atmega1281 running at 8 MHz as a microcontroller and XBee module as a wireless communication unit operating at 2.45 GHz.

Panstamp NRG 2: It is a small low-power wireless sensor mote programmable from the Arduino IDE [6]. It uses an MSP430 core embedded with an CC1101 RF transceiver, which forms CC430F5137 SoC. These modules communicate over the free 868-900-915 MHz bands. For outdoor applications, the communication range reaches to 200 meters.

A.2 Wireless sensor system communication standards

Different communication protocols have been developed in recent decades with the rapid growth of WSN technologies and IoT devices. Each protocol has its own specifications considering many parameters including the transmission range, bandwidth, frequency band, data rate, power consumption and cost. This section describes some existing wireless sensor system communication standards [160]. Then, a comparison between them is provided in table A.1.

Bluetooth is a low power, low cost wireless technology and low latency used to transmit data over short distances up to 10 meters. It uses a short wavelength ultra high frequency (UHF) radio waves in the ISM band from 2.4 to 2.485 GHz. It provides a data rate up to 24 Mbps.

Zigbee is an ultra low power consumption wireless communication technology created by Zigbee Alliance in 2002. It uses the IEEE standard 802.15.4. This technology supports a small range of communication, which is between 10 to 20 meters. The Zigbee can be applied for ad-hoc, decentralized and mesh network deployments. A typical Zigbee network includes mainly three devices, which are coordinator, router and end devices. The coordinator is responsible for the network formation, information storage and the selection of the communication channel. The router enlarges the network area coverage by routing traffic between different nodes. The end devices are responsible for the data sensing or actuation. They can transmit or receive data but they can not make a route traffic.

WiFi is a wireless local network (WLAN) standard, which uses the radio wave (RF) enabling the exchange of information between two devices and the connexion to the Internet. It runs on the IEEE standard 802.11. WiFi uses both the global 2.4 GHz UHF and 5 GHz super high frequency (SHF) ISM radio bands. This technology provides a communication range up to 35 meters for indoor applications and up to 100 meters

for outdoor applications. WiFi enables the connexion of heterogeneous architectures over an ad-hoc network and it allows cheaper deployment of LAN networks.

General Packet Radio Service (GPRS) stands on the GSM communication, which can complement some existing services like the circuit switching cellular phone connections. It is standardized by the European Telecommunications Standard Institute (ETSI) as a 2.5 G networks. Moreover, the GPRS can support X2.5 connections, Internet protocol (IP) and Point-to-Point Protocol (PPP). It provides a high data transfer speeds at a rate up to 171 Kbps. Using the packet switching mechanism, the data are transmitted from many terminals in the network across different channels. The GPRS facilitates the usage of Internet applications over mobile networks.

Simple Wireless Abstract Protocol (SWAP) is developed to provide the M2M interoperability between simple wireless devices. Moreover, SWAP relies on the long distance capability of CC11XX radio frequency front-ends. This protocol can be implemented in a few kilobytes of flash memory. SWAP can be applied for star network, peer to peer network. It provides data transfer speeds at a rate up to 600 kbps. It can offer a data range communication up to 200 meters in outdoor applications.

WIMAX is defined as Worldwide Interoperability for Microwave Access. Indeed, this wireless communication technology runs on the inter-operable implementations of the IEEE 802.16 standards. It provides data transfer speeds at a rate of 30 to 40 Mbps. It can offer a data range communication up to 50 km. Since, it provides a long-range and high speed communication features, WiMAX presents a good choice for many applications, which needs a large scale networks.

LoRaWAN is a low-power, long-range network technology. It is a spread spectrum modulation technique derived from Chirp Spread Spectrum (CSS) technology and uses the ISM frequency band.

Table A.1: Comparison between different communication technologies

Wireless technology	Communication standard	Frequency band	Data rate	Transmission range
Bluetooth	IEEE 802.15.1	2.4 GHz	1-24 Mbps	8-10 m
Zigbee	IEEE 802.15.4	868/915 MHz 2.4 GHz	20-250 kbps	10-20 m
WiFi	IEEE 802.11a,b,g,n	2.4 GHz	2-54 Mbps	10-200 m
WIMAX	IEEE 802.16.a,e	2-66 GHz	0.4-1 Gbps 50-100 Mbps	$\geq$ 50 km
GPRS	NA	900-1800 MHz	up to 171 kbps	1-10 km
SWAP	NA	433/868/905 915/918 MHz	up 600 kbps	200 m
LoRaWAN	IEEE 802.11ah	868 MHz-915 MHz	0.3-50 kbps	5-10 km

B Fuzzy Logic

Different computational intelligence techniques such as the fuzzy logic, particle swarm optimization, artificial neural network are used to address various problems. In particular, the fuzzy logic system can process a large number of input data, which can be imprecise or incomplete by modelling their reaction and behaviour rules. In addition, it does not require any extra hardware, which makes it ideal as a cost effective solution. The fuzzy logic technique is known by the interpret-ability and simplicity aspects as it uses a simple logic relation to estimate the output values. Thus, the computational complexity of the system is reduced. In fact, the fuzzy controller can automatically refine an initial approximate set of fuzzy rules. When new data or rules are added to the system, it is no need to re-train the system again.

Firstly, the fuzzy logic concept was introduced by Professor Lotfi Zadeh in 1965 [161, 162]. Indeed, it was initialized to provide an approach to handle the data by authorizing the partial set membership instead of the crisp set membership. Fuzzy logic can be defined as a multi-valued logic, which extends the conventional evaluations (Boolean) such as YES/NO, TRUE/FALSE. Other notions such as small or very large can be defined using mathematics formulas and processed using computers by applying the concept of degrees of membership. In other words, the main objective behind using the FL system is to apply a more human-like way of thinking in the programming of computers [162].

B.1 Basic architecture of fuzzy logic systems

The most important part of the FL system concept is the Fuzzy Inference System (FIS). The FIS has mainly four components: Fuzzifier, fuzzy rules, fuzzy inference engine and defuzzifier. The architecture of the mentioned model is shown in Fig. B.1. The fuzzifier is a module, which transforms the system inputs and crisp numbers into fuzzy sets. It is performed via the fuzzification function. By implementing the inputs and IF-THEN rules, the inference engine can simulate the human reasoning process. The fuzzy knowledge base is used to store IF-THEN rules. The defuzzifier is responsible to transform the fuzzy set obtained by the inference engine into a crisp value.

FIS is the collection of a set of fuzzy IF-THEN rules and can be defined as a database for the membership functions of linguistic variables. It is developed also to establish a very complex and non-linear relationships between crisp inputs and crisp outputs. Sugeno [163], Mamdani [164] and Tsukamoto [165] are presented as the most implemented FIS in many applications. The aggregation and defuzzification processes are different from one type of FIS to another.

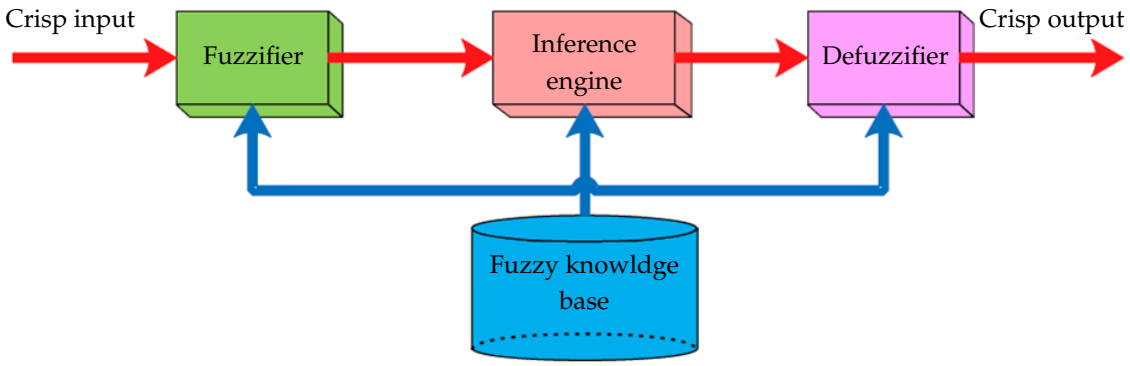

Figure B.1: Fuzzy logic system architecture.

B.2 Working principle of fuzzy logic systems

The fuzzy operation involves the use of fuzzy sets and membership functions. Each fuzzy set is a presentation of a linguistic variable defining the possible state of outputs. The membership function is the function of a generic value in a fuzzy set. Based on the principle of IF-THEN rules, the degrees of membership of the generic value determines the output. The memberships are assigned according to the assumption of outputs with the help of inputs and their rate of change. Thus, the membership function is basically a graphical representation of the fuzzy set.

To define the working principle of the fuzzy logic system, a value x such that $x \in X$ for all interval [0,1] and a fuzzy set A, which is a subset of X are considered. The membership function of the membership value x in the subset A is defined as $\mu_A(x)$. The graphical representation of fuzzy sets is given in Fig. B.2. While the x-axis denotes the universal set, the y-axis denotes the membership degrees. The shape of membership functions can be triangular, trapezoidal, singleton or Gaussian.

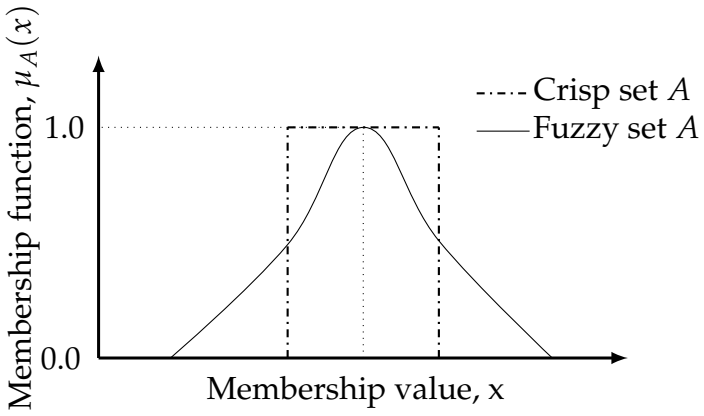

Figure B.2: Graphical representation of fuzzy sets.

B.3 Fuzzy logic: Example

This section describes in details the implementation of the Mamdani technique in the developed FEAUC protocol. Indeed, it explains the process of using the FIS to define the chance of a sensor node to be a CH. To this end, an example is described as follows. As an assumption, the CH has an $energy\,level = 0.2\,J$, $density = 0.35$ and $centrality = 0.35$.

Step 1: Input of crisp value and fuzzification: Firstly, the inputs, which are crisp values are forwarded to the FIS. The intersection point between the value of the used parameter with the degree of membership function forms the value of membership function, which are presented in Fig. B.3(a), Fig. B.3(b) and Fig. B.3(c), respectively.

Step 2: Rule evaluation: After the step of fuzzification, the obtained membership values are used as inputs for IF-THEN rules to define the new fuzzy output set. The inputs of fuzzy IF-THEN rules are the three variables defined previously and the operator "AND", which chooses the minimum of the three membership variables to obtain a single number as seen in Table B.1.

Table B.1: Fuzzy rules for the CH selection

Rule No.	Residual energy	Node density	Node centrality	Chance
1	Low (=0.37)	Low (=0)	Far (=0.27)	vw (min=0)
2	Low (=0.37)	Low (=0)	Adequate (=0.74)	w (min=0)
3	Low (=0.37)	Low (=0)	Close (=0)	w (min=0)
4	Low (=0.37)	Medium (=0.34)	Far (=0.27)	w (min=0.27)
5	Low (=0.37)	Medium (=0.34)	Adequate (=0.74)	w (min=0.34)
6	Low (=0.37)	Medium (=0.34)	Close (=0)	w (min=0)
7	Low (=0.37)	High (=0.67)	Far (=0.27)	vw (min=0)
8	Low (=0.37)	High (=0.67)	Adequate (=0.74)	w (min=0.37)
9	Low (=0.37)	High (=0.67)	Close (=0)	lw (min=0)
10	Medium (=0.67)	Low (=0)	Far (=0.27)	w (min=0)
11	Medium (=0.67)	Low (=0)	Adequate (=0.74)	m (min=0)
12	Medium (=0.67)	Low (=0)	Close (=0)	lh (min=0)
13	Medium (=0.67)	Medium (=0.34)	Far (=0.27)	lw (min=0.27)
14	Medium (=0.67)	Medium (=0.34)	Adequate (=0.74)	m (min=0.34)
15	Medium (=0.67)	Medium (=0.34)	Close (=0)	h (min=)
16	Medium (=0.67)	High (=0.67)	Far (=0.27)	lw (min=0.27)
17	Medium (=0.67)	High (=0.67)	Adequate (=0.74)	lh (min=0)
18	Medium (=0.67)	High (=0.67)	Close (=0)	h (min=0)
19	High (=0)	Low (=0)	Far (=0.27)	lw (min=0)
20	High (=0)	Low (=0)	Adequate (=0.74)	m (min=0)
21	High (=0)	Low (=0)	Close (=0)	lh (min=0)
22	High (=0)	Medium (=0.34)	Far (=0.27)	m (min=0)
23	High (=0)	Medium (=0.34)	Adequate (=0.74)	lh (min=0)
24	High (=0)	Medium (=0.34)	Close(=0)	h (min=0)
25	High (=0)	High (=0.67)	Far (=0.27)	m (min=0)
26	High (=0)	High (=0.67)	Adequate (=0.74)	lh (min=0)
27	High (=0)	High (=0.67)	Close (=0)	vh (min=0)

Very weak (vw), Weak (w), Little weak (lw), Medium (m), Little high (lh)
High (h), Very high (vh)

Step 3: Aggregation of the rule outputs: The conjunction of all outputs obtained from applying the 27 rules of the FIS model forms the aggregation process. To collect all the used rules, this step tries to involve the "OR" fuzzy logic operator. This operator selects the maximum of rule evaluation values to produce the new

aggregate fuzzy set, which can be defined in the next step. Fig. B.4 provides the aggregation output of the rules.

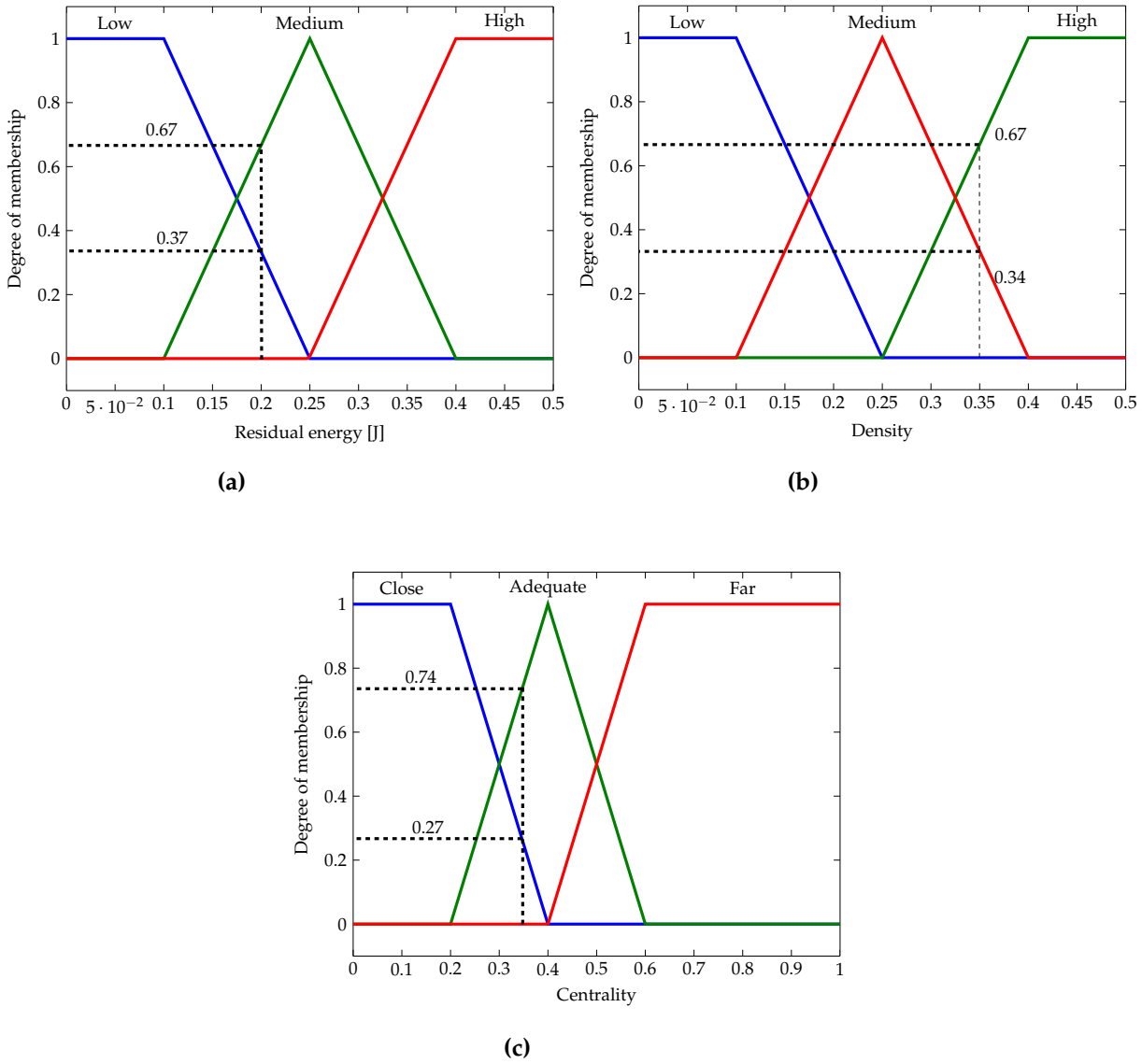

Figure B.3: Fuzzification of crisp node: (a) $Energy\,level = 0.2\,J$, (b) $density = 0.35$, (c) $centrality = 0.35$.

Step 4: Defuzzification The last step is called defuzzification, which has as output the chance value. To this end, a Mamdani technique and a centroid defuzzification method (CoA) are used. The CoA can be expressed by the eq. B.1:

$$CoA = \frac{\int \mu_A(x) x dx}{\int \mu_A(x) dx} \tag{B.1}$$

where $\mu_A(x)$ is the degree of membership function of a set A. By applying the values

obtained from step 3 and with calculating the integration given by eq. B.1, the chance value is obtained, which is equal to 23.17. This value is approximately equal to the value given by applying the FIS. As seen in Fig. B.5, the centroid point is well determined.

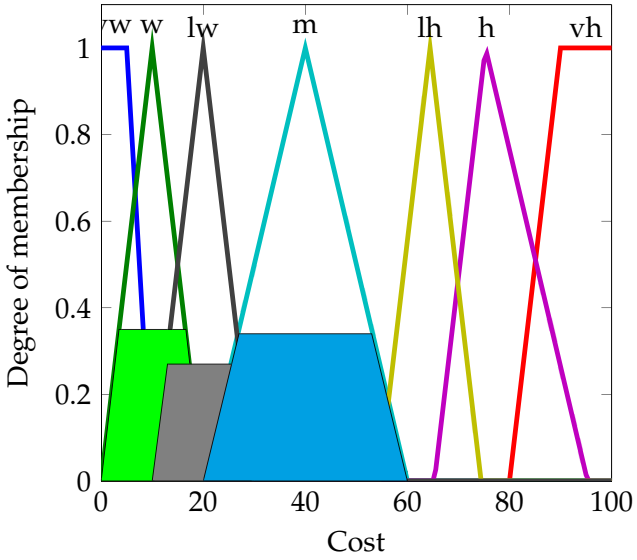

Figure B.4: Output of evaluation of Fuzzy IF-THEN rules.

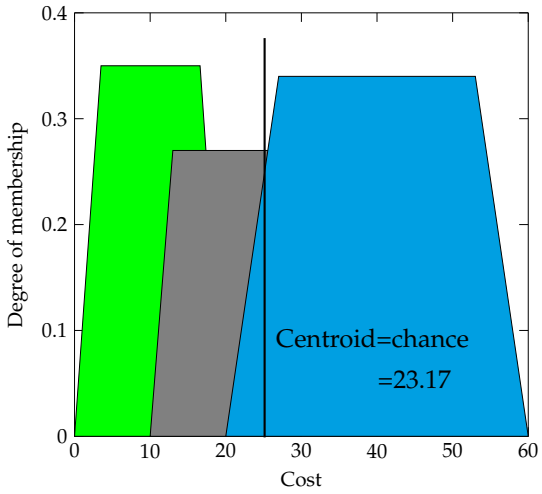

Figure B.5: Presentation of the centroid point.

C WSN Simulation environments

Different simulation tools are used to test protocols or applications for WSNs. When using simulation, it is always a concern that the results do not reflect a specific behaviour. For this reason, it is important to study the strengths and limits of the well-used simulators, including NS2, NS3, OMNeT++, QualNet, J-Sim, OPNET and TOSSIM.

C.1 General overview of simulators

NS-2 is the shortened form of the Network Simulator variant two, which has been initially created in 1989 as the real network simulator [166]. Currently, NS-2 is supported by Defense Advanced Research Projects Agency and National Science Foundation. It is an open source and discrete event network simulator worked in Object-Oriented expansion of Tool Command Language (OTCL) and C++. It can run on Linux OS or on Cygwin. NS-2 can be used for wire and remote territories. As a non-particular network simulator, NS-2 can support a significant scope of protocols in all layers. Moreover, the online documentations permit the clients effortlessly to change and enhance the codes.

NS-3 is the abbreviation of Network Simulator version three. It is targeted primarily for research and educational uses as it is an open source simulator. It was launched in June 2008 [167]. In NS-3, all programs are written in C++ with optional python links. In NS-2, there is no graphical tool, which is the case in NS-3. Nevertheless, graphical outcomes can be interpreted using the open software, NetAnim. It defines a model of working procedure of packets. It provides, also configurable libraries including wired and WSNs, and various types of routing protocols. It supports simulations for the TCP, UDP, ICMP, IPv4, P2P communications and CSMA protocols, energy models and etc. It offers multi 802.11 models providing an efficient MAC-level implementation. In addition, NS-3 enables simulations with large-scale networks.

OMNeT++ (Castalia) is designed especially for low power embedded devices. It is currently being used by researchers to simulate algorithms and protocols in real-time wireless channels [168].

QualNet is the abbreviation of Quality Networking [169]. It is a commercial network simulator that incorporates routers, switches, servers, access points, radios, antennas, computers and other equipment, as well as various protocols to allow packet movement over the network. Windows and Linux are the major operating systems supported by QualNet.

MATLAB is well-known commercial software used in almost all engineering fields thanks to its rich features as a computation and visualization tool [170]. MATLAB provides a communication toolbox set to build a complete system model for WSNs. The simulation procedure consists of building the hardware architecture of transmitting nodes, modelling the communication channel and receiving node structure. However, this software is not specific for WSNs.

J-Sim is the abbreviation of Java Simulator. J-Sim has a Script Interface, which facilities the execution of numerous script totally based on languages like Perl, TCL or Python [171]. J-Sim is used to implement three protocols of WSNs including the localization, Geographic Routing (GR), and Directed Diffusion (DF). This simulator has numerous benefits in terms of the execution time, memory allocation, and scalability. Furthermore, it affords a great platform to carry out large-scale WSN simulations with more than a thousand nodes.

OPNET is an object oriented network simulator [172]. It was released, initially, for military purposes. OPNET can be used as a research and network design/analysis tool. Recent versions supports the ZigBee compatible 802.15.4 MAC. The strength of OPNET in WSN simulations is the accurate modelling of the radio transmission. Different characteristics of physical link transceivers, antennas are provided. However, only a few ready models for recent wireless systems are existing.

TOSSIM is a network simulator for TinyOS sensor networks [91]. It provides several mechanisms for interacting with the network including the monitoring packet traffic, statically or dynamically injecting of a packet into the network and invocation of TinyOS call. It has different mechanisms for detailed visualization of a running simulation. The default models supplied are simple. However, TOSSIM is used only for the wireless sensor nodes supporting TinyOS like TelosB or IRIS.

C.2 Comparison between existing simulators

Table C.1 summarizes various types of network simulators by classifying them according to some criteria. At first sight, the specificity to WSNs is considered as the pillar of the presented classification. The second criteria is the availability of the energy model. Therefore, it is important to select a simulator having the capability to predict energy consumption, especially in large-scale deployments. Additional criteria can be as well considered the likes of software's license, simulation time and personal programming skills. Besides, the software popularity and documentation are useful when implementing a new protocol.

Table C.1: Comparison between different network simulators

Simulator	Licence	Platform	Langauge	Advantages	Limits
NS-2	Free	Linux Windows (Cygwin)	C++/OTCL	- Supports various protocols - Network topology setting in nodes	- Limited documentation - Not oriented to energy consumption - Sensing model does not exist - Unrealistic energy model, packet formats, and MAC protocols - Simulating less than 100 nodes
NS-3	Free	Windows (Cygwin)	C++/Python	- Oriented to energy consumption -Various protocols, existence of sensing, radio and energy models - High accuracy - Large-scale networks - Flexible designing of network protocols	- Limited in some libraries protocols
Castalia	Free	Linux Windows	C++	- Various MAC and routing protocols - Advanced radio model for low power communication	- Not oriented to energy consumption - Not a specific sensor platform
QualNet	Commercial	Linux Windows	C++	- Large-scale networks - Various protocol models - High accuracy	- Not oriented to energy consumption - Expensive licence
MATLAB	Commercial	Linux Windows	C/Java	- Simulation includes building the hardware architecture of nodes S/N ratio, attenuation, interference are considered	- Not specific to WSN - Expensive licence
J-Sim	Free	Linux Windows	Java	- Large-scale networks (more than 1000 nodes) - Can simulate radio channels and power consumption	- Limited in protocols - Long simulation - Complex
OPNET	Free	Linux Windows	C++	- Node model and configuring packet formats - Defines the communication network topology	- Limited node architecture - Complex for componenents between 210 and 290 nodes
TOSSIM	Free	Linux Windows	Python/ NesC/C++	- Large-scale networks	- Need of commercial software to simulate power consumption

Bibliography

1. YADAV, DEVENDRA KUMAR et al.: 'Critical review on slope monitoring systems with a vision of unifying WSN and IoT'. *IET Wireless Sensor Systems* (2019), vol. DOI: 10.1049/iet-wss.2018.5197.
2. KHRIJI, SABRINE et al.: 'Precision irrigation based on wireless sensor network'. *IET Science, Measurement & Technology* (2014), vol. 8(3): pp. 98–106. DOI: 10.1049/iet-smt.2013.0137.
3. KHRIJI, SABRINE et al.: 'Precision Irrigation: An IoT-Enabled Wireless Sensor Network for Smart Irrigation Systems'. *Women in Precision Agriculture, Women in Engineering and Science*. Springer Nature Switzerland AG, 2021. DOI: 10.1007/978-3-030-49244-1_6.
4. BOUBICHE, SABRINA et al.: 'Big data challenges and data aggregation strategies in wireless sensor networks'. *IEEE Access* (2018), vol. 6: pp. 20558–20571. DOI: 10.1109/ACCESS.2018.2821445.
5. FARHAN, LAITH et al.: 'Towards green computing for Internet of things: Energy oriented path and message scheduling approach'. *Sustainable Cities and Society* (2018), vol. 38: pp. 195–204. DOI: https://doi.org/10.1016/j.scs.2017.12.018.
6. KHRIJI, SABRINE et al.: 'Measuring Energy Consumption of a Wireless Sensor Node During Transmission: panStamp'. *2018 IEEE 32nd International Conference on Advanced Information Networking and Applications (AINA)*. IEEE. 2018: pp. 274–280. DOI: 10.1109/AINA.2018.00050.
7. AISSA, YOUSRA BEN et al.: 'On Feasibility of Multichannel Reconfigurable Wireless Sensor Networks Under Real-Time and Energy Constraints'. *IEEE Transactions on Systems, Man, and Cybernetics: Systems* (2019), vol. DOI: 10.1109/TSMC.2019.2897166.
8. KHRIJI, SABRINE et al.: 'A Fuzzy Based Energy Aware Unequal Clustering for Wireless Sensor Networks'. *International Conference on Ad-Hoc Networks and Wireless*. Springer. 2018: pp. 126–131. DOI: https://doi.org/10.1007/978-3-030-00247-3_12.
9. KHRIJI, SABRINE et al.: 'Energy-Efficient Routing Algorithm Based on Localization and Clustering Techniques for Agricultural Applications'. *IEEE Aerospace and Electronic Systems Magazine* (2019), vol. 34(3): pp. 56–66. DOI: 10.1109/MAES.2019.2905947.

10. YAACOUB, ELIAS et al.: 'Multihop routing for energy efficiency in wireless sensor networks'. *Wireless Sensor Networks-Technology and Protocols*. InTech Press, 2012: pp. 165–186. DOI: 10.5772/39221.

11. SAJWAN, MOHIT et al.: 'CAMP: cluster aided multi-path routing protocol for wireless sensor networks'. *Wireless Networks* (2019), vol. 25(5): pp. 2603–2620. DOI: https://doi.org/10.1007/s11276-018-1689-0.

12. SERT, SEYYIT ALPER et al.: 'MOFCA: Multi-objective fuzzy clustering algorithm for wireless sensor networks'. *Applied Soft Computing* (2015), vol. 30: pp. 151–165. DOI: https://doi.org/10.1016/j.asoc.2014.11.063.

13. MIRZAIE, MOSTAFA et al.: 'MCFL: An energy efficient multi-clustering algorithm using fuzzy logic in wireless sensor network'. *Wireless Networks* (2018), vol. 24(6): pp. 2251–2266. DOI: https://doi.org/10.1007/s11276-017-1466-5.

14. BEN-MOSHE, BOAZ et al.: 'Long-range and energy-efficient optical networking for tiny sensors'. *Wireless Networks* (2018), vol.: pp. 1–18. DOI: https://doi.org/10.1007/s11276-018-1668-5.

15. KHRIJI, S. et al.: 'Energy-efficient techniques in wireless sensor networks: Technology, Components and System Design'. *Energy Harvesting for Wireless Sensor Networks*. DE GRUYTER, 2018: pp. 287–304. ISBN: 978-3-11-044505-3. DOI: 10.1515/9783110445053-017.

16. TAKALE, SACHIN B et al.: 'Quality of Service Requirement in Wireless Sensor Networks: A Survey'. *2018 IEEE Global Conference on Wireless Computing and Networking (GCWCN)*. IEEE. 2018: pp. 34–38. DOI: 10.1109/GCWCN.2018.8668636.

17. GIRI, PRAPTI et al.: 'Wireless Sensor Network System for Landslide Monitoring and Warning'. *IEEE Transactions on Instrumentation and Measurement* (2018), vol. (99): pp. 1–11. DOI: 10.1109/TIM.2018.2861999.

18. BOUDRIGA, NOUREDDINE et al.: 'Measurement and security trust in WSNs: a proximity deviation based approach'. *Annals of Telecommunications* (2019), vol. 74(5-6): pp. 257–272. DOI: https://doi.org/10.1007/s12243-018-0675-y.

19. CHÉOUR, RYM et al.: 'New combined method for low energy consumption in Wireless Sensor Network applications'. *SIMULATION* (2018), vol. 94(10): pp. 873–885. DOI: https://doi.org/10.1177/0037549718759432.

20. OBEID, ABDULFATTAH MOHAMMAD et al.: 'A survey on efficient power consumption in adaptive wireless sensor networks'. *Wireless Personal Communications* (2018), vol. 101(1): pp. 101–117. DOI: https://doi.org/10.1007/s11277-018-5678-5.

21. YASIN, SANA et al.: 'A Parametric Performance Evaluation of Batteries in Wireless Sensor Networks'. *Recent Trends and Advances in Wireless and IoT-enabled Networks*. Springer, 2019: pp. 187–196. DOI: 10.1007/978-3-319-99966-1_17.
22. BRADAI, S et al.: 'Electromagnetic vibration energy harvesting for railway applications'. *MATEC Web of Conferences*. Vol. 148. EDP Sciences. 2018: p. 12004. DOI: https://doi.org/10.1051/matecconf/201814812004.
23. NAIFAR, SLIM et al.: 'Evaluation of multiple transducers implementation in a magnetoelectric vibration energy harvester'. *tm-Technisches Messen* (2018), vol. 85(9): pp. 580–589. DOI: 10.1515/teme-2017-0080.
24. VIEHWEGER, CHRISTIAN et al.: 'Modellbasierte Bestimmung der zeitabhängigen Eingangsleistung von Solarzellen für das Energiemanagement drahtloser Sensorsysteme'. *tm-Technisches Messen* (2016), vol. 83(9): pp. 503–510. DOI: https://doi.org/10.1515/teme-2015-0111.
25. CHAMMAS, MICHEL et al.: 'An efficient data model for energy prediction using wireless sensors'. *Computers & Electrical Engineering* (2019), vol. 76: pp. 249–257. DOI: https://doi.org/10.1016/j.compeleceng.2019.04.002.
26. SACHAN, VIBHAV KUMAR et al.: 'Energy-efficient communication methods in wireless sensor networks: A critical review'. *International Journal of Computer Applications* (2012), vol. 39(17): pp. 35–48. DOI: 10.5120/4915-7484.
27. HALGAMUGE, MALKA N et al.: 'An estimation of sensor energy consumption'. *Progress in Electromagnetics Research* (2009), vol. 12: pp. 259–295. DOI: 10.2528/PIERB08122303.
28. SOUA, RIDHA et al.: 'A survey on energy efficient techniques in wireless sensor networks'. *2011 4th Joint IFIP Wireless and Mobile Networking Conference (WMNC 2011)*. IEEE. 2011: pp. 1–9. DOI: 10.1109/WMNC.2011.6097244.
29. KANOUN, OLFA et al.: 'Next Generation Wireless Energy Aware Sensors for Internet of Things: A Review'. *2018 15th International Multi-Conference on Systems, Signals & Devices (SSD)*. IEEE. 2018: pp. 1–6. DOI: 10.1109/SSD.2018.8570695.
30. NGUYEN, NGOC-TU et al.: 'An efficient minimum-latency collision-free scheduling algorithm for data aggregation in wireless sensor networks'. *IEEE Systems Journal* (2018), vol. 12(3): pp. 2214–2225. DOI: 10.1109/JSYST.2017.2751645.
31. AHMAD, AASEM et al.: 'An energy efficient schedule for IEEE 802.15. 4/zigbee cluster tree WSN with multiple collision domains and period crossing constraint'. *IEEE Transactions on Industrial Informatics* (2017), vol. 14(1): pp. 12–23. DOI: 10.1109/TII.2017.2725907.

32. DBIBIH, IMANE et al.: 'Collision avoidance and service differentiation at the MAC layer of WSN designed for multi-purpose applications'. *2016 2nd International Conference on Cloud Computing Technologies and Applications (CloudTech)*. IEEE. 2016: pp. 277–282. DOI: 10.1109/CloudTech.2016.7847710.

33. TAMURA, NAOKI et al.: 'Low-overhead Wake-up Control for Wireless Sensor Networks employing Wake-up Receivers'. *IEICE Transactions on Communications* (2018), vol. DOI: 10.1587/transcom.2018SEP0008.

34. LAKSHMI, M PRASANNA et al.: 'Minimizing the maximum sender interference by deploying additional nodes in a wireless sensor network'. *Electronic Journal of Graph Theory and Applications (EJGTA)* (2019), vol. 7(1): pp. 169–182. DOI: 10.5614/ejgta.2019.7.1.13.

35. CHEN, ZHIHONG et al.: 'Interference-free Clustering Protocol for Large-Scale and Dense Wireless Sensor Networks'. *KSII Transactions on Internet & Information Systems* (2019), vol. 13(3). DOI: 10.3837/tiis.2019.03.007.

36. GUIDARA, AMIR et al.: 'Energy-Efficient On-Demand Indoor Localization Platform based on Wireless Sensor Networks using Low Power Wake up Receiver'. *Ad Hoc Networks* (2019), vol.: p. 101902. DOI: https://doi.org/10.1016/j.adhoc.2019.101902.

37. RASUL, ARAM et al.: 'The extra-bit technique for reducing idle listening in data collection'. *International Journal of Sensor Networks* (2017), vol. 25(1): pp. 31–44. DOI: 10.1504/IJSNET.2017.086788.

38. HAN, KAI et al.: 'Algorithm design for data communications in duty-cycled wireless sensor networks: A survey'. *IEEE Communications Magazine* (2013), vol. 51(7): pp. 107–113. DOI: 10.1109/MCOM.2013.6553686.

39. KHRIJI, SABRINE et al.: 'Redundancy Elimination for Data Aggregation in Wireless Sensor Networks'. *2018 15th International Multi-Conference on Systems, Signals & Devices (SSD)*. IEEE. 2018: pp. 28–33. DOI: 10.1109/SSD.2018.8570459.

40. HOUSSAINI, DHOUHA EL et al.: 'Distance measurement correction based on feedback filter for RSSI localisation technique in WSNs'. *International Journal of Space-Based and Situated Computing* (2018), vol. 8(3): pp. 160–168. DOI: https://doi.org/10.1504/IJSSC.2018.097293.

41. SHABANEH, ARAFAT AA et al.: 'Review of energy conservation using duty cycling schemes for IEEE 802.15. 4 wireless sensor network (WSN)'. *Wireless personal communications* (2014), vol. 77(1): pp. 589–604. DOI: https://doi.org/10.1007/s11277-013-1524-y.

42. AZIZ, AZRINA ABD et al.: 'A survey on distributed topology control techniques for extending the lifetime of battery powered wireless sensor networks'. *IEEE communications surveys & tutorials* (2012), vol. 15(1): pp. 121–144. DOI: 10.1109/SURV.2012.031612.00124.

43. ADAM, MOHAMMED SANI et al.: 'An Adaptive Wake-Up-Interval to Enhance Receiver-Based Ps-Mac Protocol for Wireless Sensor Networks'. *Sensors* (2019), vol. 19(17): p. 3732. DOI: 10.3390/s19173732.

44. KAUR, PARDEEP et al.: 'Recent Advances in MAC Protocols for the Energy Harvesting Based WSN: A Comprehensive Review'. *Wireless Personal Communications* (2019), vol. 104(1): pp. 423–440. DOI: 10.1007/s11277-018-6028-3.

45. KAUR, TARUNPREET et al.: 'TDMA-based MAC protocols for wireless sensor networks: A survey and comparative analysis'. *2016 5th International Conference on Wireless Networks and Embedded Systems (WECON)*. IEEE. 2016: pp. 1–6. DOI: 10.1109/WECON.2016.7993426.

46. KHAN, SAMIULLAH et al.: 'Effect of Increasing Number of Nodes on Performance of SMAC, CSMA/CA and TDMA in MANETs'. *INTERNATIONAL JOURNAL OF ADVANCED COMPUTER SCIENCE AND APPLICATIONS* (2018), vol. 9(2): pp. 294–299. DOI: 10.14569/IJACSA.2018.090241.

47. YANG, XIN et al.: 'Energy Efficiency TDMA/CSMA Hybrid Protocol with Power Control for WSN'. *Wireless Communications and Mobile Computing* (2018), vol. 2018. DOI: 10.1155/2018/4168354.

48. DEEPA, S et al.: 'Energy conservative data transmission using Z-MAC technique in wireless sensor network for environmental monitoring'. *2016 IEEE Technological Innovations in ICT for Agriculture and Rural Development (TIAR)*. IEEE. 2016: pp. 194–199. DOI: 10.1109/TIAR.2016.7801237.

49. FAHMY, HOSSAM MAHMOUD AHMAD: 'Energy Management Techniques for WSNs (2): Data-Driven Approach'. *Wireless Sensor Networks*. Springer, 2020: pp. 259–398. DOI: 10.1007/978-3-030-29700-8_5.

50. CHENG, HONGJU et al.: 'Data prediction model in wireless sensor networks based on bidirectional LSTM'. Vol. 2019. 1. Springer, 2019: p. 203. DOI: 10.1186/s13638-019-1511-4.

51. ZHENG, J. et al.: 'Work in progress: Data compression of wireless sensor network employing Kalman filter and QC-LDPC codes'. *9th International Conference on Communications and Networking in China*. 2014: pp. 18–21. DOI: 10.1109/CHINACOM.2014.7054251.

52. SPARKA, H. et al.: 'Effective Lossless Compression of Sensor Information in Manufacturing Industry'. *2017 IEEE 42nd Conference on Local Computer Networks (LCN)*. 2017: pp. 480–488. DOI: 10.1109/LCN.2017.89.

53. YOON, IKJUNE et al.: 'Adaptive data aggregation and compression to improve energy utilization in solar-powered wireless sensor networks'. *Sensors* (2017), vol. 17(6): p. 1226. DOI: 10.3390/s17061226.

54. FENG, JUAN et al.: 'An energy-efficient and adaptive data collection scheme for multisensory wireless sensor networks'. *International Journal of Distributed Sensor Networks* (2019), vol. 15(4). DOI: 10.1177/1550147719846017.

55. FAHMY, HOSSAM MAHMOUD AHMAD: 'Energy Management Techniques for WSNs'. *Wireless Sensor Networks*. Springer, 2020: pp. 103–108. DOI: 10.1007/978-3-030-29700-8_3.

56. BHUSHAN, BHARAT et al.: 'Routing protocols in wireless sensor networks'. (2019), vol.: pp. 215–248. DOI: 10.1007/978-3-662-57277-1_10.

57. GULERIA, KALPNA et al.: 'Comprehensive review for energy efficient hierarchical routing protocols on wireless sensor networks'. *Wireless Networks* (2019), vol. 25(3): pp. 1159–1183. DOI: https://doi.org/10.1007/s11276-018-1696-1.

58. WOODROW, EDWARD et al.: 'SPIN-IT: a data centric routing protocol for image retrieval in wireless networks'. *Image Processing. 2002. Proceedings. 2002 International Conference on*. Vol. 3. IEEE. 2002: pp. 913–916. DOI: 10.1109/ICIP.2002.1039121.

59. INTANAGONWIWAT, CHALERMEK et al.: 'Directed diffusion: A scalable and robust communication paradigm for sensor networks'. *Proceedings of the 6th annual international conference on Mobile computing and networking*. ACM. 2000: pp. 56–67. DOI: 10.1145/345910.345920.

60. BRAGINSKY, DAVID et al.: 'Rumor routing algorthim for sensor networks'. *Proceedings of the 1st ACM international workshop on Wireless sensor networks and applications*. ACM. 2002: pp. 22–31. DOI: 10.1145/570738.570742.

61. KANG, BYUNGSEOK et al.: 'An energy-efficient routing scheme by using GPS information for wireless sensor networks'. *International Journal of Sensor Networks* (2018), vol. 26(2): pp. 136–143. DOI: 10.1504/IJSNET.2018.089264.

62. YU, YAN et al.: 'Geographical and energy aware routing: A recursive data dissemination protocol for wireless sensor networks'. (2001), vol. DOI: 10.1.1.21.8533.

63. KARP, BRAD et al.: 'GPSR: Greedy perimeter stateless routing for wireless networks'. *Proceedings of the 6th annual international conference on Mobile computing and networking*. ACM. 2000: pp. 243–254. DOI: https://doi.org/10.1145/345910.345953.

64. MURTHY, SHREE et al.: 'An efficient routing protocol for wireless networks'. *Mobile Networks and applications* (1996), vol. 1(2): pp. 183–197. DOI: https://doi.org/10.1007/BF01193336.

65. CHIANG, CHING-CHUAN et al.: 'Routing in clustered multihop, mobile wireless networks with fading channel'. *proceedings of IEEE SICON*. Vol. 97. 1997. 1997: pp. 197–211.

66. PERKINS, CHARLES E et al.: 'Highly dynamic destination-sequenced distance-vector routing (DSDV) for mobile computers'. *ACM SIGCOMM computer communication review*. Vol. 24. 4. ACM. 1994: pp. 234–244. DOI: https://doi.org/10.1145/190314.190336.

67. JACQUET, PHILIPPE et al.: 'Optimized link state routing protocol for ad hoc networks'. *Multi Topic Conference, 2001. IEEE INMIC 2001. Technology for the 21st Century. Proceedings. IEEE International*. IEEE. 2001: pp. 62–68. DOI: 10.1109/INMIC.2001.995315.

68. PERKINS, CHARLES et al.: *Ad hoc on-demand distance vector (AODV) routing*. Tech. rep. 2003. DOI: 10.1109/MCSA.1999.749281.

69. TOH, CHAI-KEONG: 'Associativity-based routing for ad hoc mobile networks'. *Wireless Personal Communications* (1997), vol. 4(2): pp. 103–139. DOI: https://doi.org/10.1023/A:1008812928561.

70. ZHANG, DE-GAN et al.: 'Novel dynamic source routing protocol (DSR) based on genetic algorithm-bacterial foraging optimization (GA-BFO)'. *International Journal of Communication Systems* (2018), vol. 31(18): e3824. DOI: https://doi.org/10.1002/dac.3824.

71. DUBE, ROHIT et al.: 'Signal stability-based adaptive routing (SSA) for ad hoc mobile networks'. *IEEE Personal communications* (1997), vol. 4(1): pp. 36–45. DOI: 10.1109/98.575990.

72. GODOI, FABRICIO N et al.: 'Reliability enhancement of packet delivery in multi-hop wireless sensor network'. *Computer Networks* (2019), vol. 153: pp. 86–91. DOI: 10.1016/j.comnet.2019.02.013.

73. ADITYA, DN et al.: 'An Intruders Attack Towards Each Layer in Wireless Networks'. *Journal of Computational and Theoretical Nanoscience* (2018), vol. 15(5): pp. 1769–1773. DOI: 10.1166/jctn.2018.7386.

74. IZADI, DAVOOD et al.: 'A new energy efficient cluster-head and backup selection scheme in WSN'. *2013 IEEE 14th International Conference on Information Reuse & Integration (IRI)*. IEEE. 2013: pp. 408–415. DOI: 10.1109/IRI.2013.6642500.

75. MARWAN, MBAREK et al.: 'Protecting medical data in cloud storage using fault-tolerance mechanism'. *Proceedings of the 2017 International Conference on Smart Digital Environment*. ACM. 2017: pp. 214–219. DOI: 10.1145/3128128.3128161.

76. HANDY, MJ et al.: 'Low energy adaptive clustering hierarchy with deterministic cluster-head selection'. *4th international workshop on mobile and wireless communications network*. IEEE. 2002: pp. 368–372. DOI: 10.1109/MWCN.2002.1045790.

77. HEINZELMAN, WENDI RABINER et al.: 'Energy-efficient communication protocol for wireless microsensor networks'. *System sciences, 2000. Proceedings of the 33rd annual Hawaii international conference on*. IEEE. 2000: 10–pp. DOI: 10.1109/HICSS.2000.926982.

78. MILLER, MATTHEW J et al.: 'A MAC protocol to reduce sensor network energy consumption using a wakeup radio'. *IEEE Transactions on mobile Computing* (2005), vol. (3): pp. 228–242. DOI: 10.1109/TMC.2005.31.

79. ZHU, JIN et al.: 'On the energy-efficient organization and the lifetime of multi-hop sensor networks'. *IEEE Communications letters* (2003), vol. 7(11): pp. 537–539. DOI: 10.1109/LCOMM.2003.820097.

80. MEDAGLIANI, PAOLO et al.: 'Clustered Zigbee networks with data fusion: Characterization and performance analysis'. *Ad Hoc Networks* (2011), vol. 9(7): pp. 1083–1103. DOI: 10.1016/j.adhoc.2010.10.009.

81. FÖRSTER, ANNA et al.: 'Optimal cluster sizes for wireless sensor networks: An experimental analysis'. *International conference on ad hoc networks*. Springer. 2009: pp. 49–63. DOI: 10.1007/978-3-642-11723-7_4.

82. AMINI, NAVID et al.: 'Cluster size optimization in sensor networks with decentralized cluster-based protocols'. *Computer communications* (2012), vol. 35(2): pp. 207–220. DOI: 10.1016/j.comcom.2011.09.009.

83. ALRAJEI, NANCY et al.: 'A survey on fault tolerance in wireless sensor networks'. *2014 American Society For Engineering Education North Central Section Conference ASEE NCS Conference April*. Vol. 4. 2014. DOI: 10.1109/ICGCIoT.2015.7380451.

84. SRIVASTAVA, VIKAS et al.: 'Energy efficient optimized rate based congestion control routing in wireless sensor network'. *Journal of Ambient Intelligence and Humanized Computing* (2020), vol. 11(3): pp. 1325–1338. DOI: https://doi.org/10.1007/s12652-019-01449-1.

85. SHYAMA, M et al.: 'Fault-Tolerant Techniques for Wireless Sensor Network—A Comprehensive Survey'. *Innovations in Electronics and Communication Engineering*. Springer, 2019: pp. 261–269. DOI: 10.1007/978-981-13-3765-9_27.

86. JIA, SHUANG et al.: 'Fault Detection Modelling and Analysis in a Wireless Sensor Network'. *Journal of Sensors* (2018), vol. 2018. DOI: https://doi.org/10.1155/2018/7935802.

87. MAHAPATRO, ARUNANSHU et al.: 'Fault diagnosis in wireless sensor networks: A survey'. *IEEE Communications Surveys & Tutorials* (2013), vol. 15(4): pp. 2000–2026. DOI: 10.1109/SURV.2013.030713.00062.

88. KATRE, VARSHA et al.: 'Cluster Head Failure Detection and Correction Algorithm for WSN'. *2018 Second International Conference on Intelligent Computing and Control Systems (ICICCS)*. IEEE. 2018: pp. 1859–1862. DOI: 10.1109/ICCONS.2018.8663030.

89. MOSCHITTA, ANTONIO et al.: 'Power consumption assessment in wireless sensor networks'. *ICT-energy-concepts towards zero-power information and communication technology*. IntechOpen, 2014. DOI: 10.5772/57201.

90. RILEY, GEORGE F et al.: 'The ns-3 network simulator'. *Modeling and tools for network simulation*. Springer, 2010: pp. 15–34. DOI: https://doi.org/10.1007/978-3-642-12331-3_2.

91. LEVIS, PHILIP et al.: 'TOSSIM: Accurate and scalable simulation of entire TinyOS applications'. *Proceedings of the 1st international conference on Embedded networked sensor systems*. ACM. 2003: pp. 126–137. DOI: https://doi.org/10.1145/958491.958506.

92. JEMAI, A et al.: 'Study of key pre-distribution schemes in wireless sensor networks: case of BROSK (use of WSNet)'. *Applied Mathematics & Information Sciences* (2011), vol. 5(3): pp. 655–667.

93. ANTONOPOULOS, CH et al.: 'Experimental evaluation of a WSN platform power consumption'. *2009 IEEE International Symposium on Parallel & Distributed Processing*. IEEE. 2009: pp. 1–8. DOI: 10.1109/IPDPS.2009.5161185.

94. MILENKOVIC, ALEKSANDAR et al.: 'An environment for runtime power monitoring of wireless sensor network platforms'. *Proceedings of the Thirty-Seventh Southeastern Symposium on System Theory, 2005. SSST'05.* IEEE. 2005: pp. 406–410. DOI: 10.1109/SSST.2005.1460946.

95. MCCORMACK, MICHAEL et al.: *Current measuring probe and electrical energy meter for use therewith*. US Patent 6,825,650. 2004.

96. BIRCHER, WILLIAM LLOYD et al.: 'Runtime identification of microprocessor energy saving opportunities'. *ISLPED'05. Proceedings of the 2005 International Symposium on Low Power Electronics and Design, 2005.* IEEE. 2005: pp. 275–280. DOI: 10.1145/1077603.1077668.

97. *Keysight Technologies*. http://literature.cdn.keysight.com/litweb/pdf/5992-0731EN.pdf?id=2612931. access. May 2019.

98. JIANG, XIAOFAN et al.: 'Micro power meter for energy monitoring of wireless sensor networks at scale'. *2007 6th International Symposium on Information Processing in Sensor Networks*. IEEE. 2007: pp. 186–195. DOI: 10.1109/IPSN.2007.4379678.

99. SORO, STANISLAVA et al.: 'Prolonging the lifetime of wireless sensor networks via unequal clustering'. *Parallel and Distributed Processing Symposium, 2005. Proceedings. 19th IEEE International*. IEEE. 2005: 8–pp. DOI: https://doi.org/10.1155/2018/8035065.

100. KIM, JUNG-HWAN et al.: 'PRODUCE: a probability-driven unequal clustering mechanism for wireless sensor networks'. *22nd International Conference on Advanced Information Networking and Applications-Workshops (aina workshops 2008)*. IEEE. 2008: pp. 928–933. DOI: 10.1109/WAINA.2008.116.

101. LEE, SUNGRYOUL et al.: 'LUCA: An energy-efficient unequal clustering algorithm using location information for wireless sensor networks'. *Wireless Personal Communications* (2011), vol. 56(4): pp. 715–731. DOI: 10.1007/s11277-009-9842-9.

102. LI, CHENGFA et al.: 'An energy-efficient unequal clustering mechanism for wireless sensor networks'. *IEEE International Conference on Mobile Adhoc and Sensor Systems Conference, 2005.* IEEE. 2005: 8–pp. DOI: 10.1109/MAHSS.2005.1542849.

103. LAI, WEI KUANG et al.: 'Arranging cluster sizes and transmission ranges for wireless sensor networks'. *Information Sciences* (2012), vol. 183(1): pp. 117–131. DOI: https://doi.org/10.1016/j.ins.2011.08.029.

104. ISLAM, NAZMUL et al.: 'Energy-Balancing Unequal Clustering Approach to Reduce the Blind Spot Problem in Wireless Sensor Networks (WSNs)'. *Sensors* (2018), vol. 18(12): p. 4258. DOI: 10.3390/s18124258.

105. LI, HUAN et al.: 'COCA: Constructing optimal clustering architecture to maximize sensor network lifetime'. *Computer Communications* (2013), vol. 36(3): pp. 256–268. DOI: https://doi.org/10.1016/j.comcom.2012.10.006.

106. GULERIA, KALPNA et al.: 'Meta-heuristic Ant Colony Optimization Based Unequal Clustering for Wireless Sensor Network'. *Wireless Personal Communications* (2019), vol. 105(3): pp. 891–911. DOI: 10.1007/s11277-019-06127-1.

107. RUAN, DANWEI et al.: 'A PSO-Based Uneven Dynamic Clustering Multi-Hop Routing Protocol for Wireless Sensor Networks'. *Sensors* (2019), vol. 19(8): p. 1835. DOI: 10.3390/s19081835.

108. GARG, NITIKA et al.: 'Cluster Head Selection Using Genetic Algorithm in Hierarchical Clustered Sensor Network'. *2018 Second International Conference on Intelligent Computing and Control Systems (ICICCS)*. IEEE. 2018: pp. 511–515. DOI: 10.1109/ICCONS.2018.8662914.

109. PANDA, SATYASEN et al.: 'Performance analysis of wireless sensor networks using artificial bee colony algorithm'. *2018 Technologies for Smart-City Energy Security and Power (ICSESP)*. IEEE. 2018: pp. 1–5. DOI: 10.1109/ICSESP.2018.8376711.

110. PRASAD, D RAJENDRA et al.: 'Metaheuristic techniques for cluster selection in WSN'. *2017 International Conference on Algorithms, Methodology, Models and Applications in Emerging Technologies (ICAMMAET)*. IEEE. 2017: pp. 1–6. DOI: 10.1109/ICAMMAET.2017.8186745.

111. GUILOUFI, AWATEF BEN FRADJ et al.: 'An energy-efficient unequal clustering algorithm using 'Sierpinski Triangle'for WSNs'. *Wireless Personal Communications* (2016), vol. 88(3): pp. 449–465. DOI: https://doi.org/10.1007/s11277-015-3137-0.

112. XIA, HUI et al.: 'Energy-efficient routing algorithm based on unequal clustering and connected graph in wireless sensor networks'. *International Journal of Wireless Information Networks* (2016), vol. 23(2): pp. 141–150. DOI: https://doi.org/10.1007/s10776-016-0304-5.

113. GUPTA, VRINDA et al.: 'An improved energy aware distributed unequal clustering protocol for heterogeneous wireless sensor networks'. *Engineering Science and Technology, an International Journal* (2016), vol. 19(2): pp. 1050–1058. DOI: https://doi.org/10.1016/j.jestch.2015.12.015.

114. BARANIDHARAN, B et al.: 'DUCF: Distributed load balancing Unequal Clustering in wireless sensor networks using Fuzzy approach'. *Applied Soft Computing* (2016), vol. 40: pp. 495–506. DOI: https://doi.org/10.1016/j.asoc.2015.11.044.

115. GAJJAR, SACHIN et al.: 'FAMACROW: Fuzzy and ant colony optimization based combined mac, routing, and unequal clustering cross-layer protocol for wireless sensor networks'. *Applied Soft Computing* (2016), vol. 43: pp. 235–247. DOI: https://doi.org/10.1016/j.asoc.2016.02.019.

116. SAAKIAN, ARTEM: *Radio wave propagation fundamentals*. Artech House, 2011.

117. MAZUMDAR, NABAJYOTI et al.: 'Coverage-aware unequal clustering algorithm for wireless sensor networks'. *Procedia Computer Science* (2015), vol. 57: pp. 660–669. DOI: https://doi.org/10.1016/j.procs.2015.07.437.

118. SUHARJONO, A. et al.: 'Hop distances optimization for balancing the energy consumption of multi-hop clustered Wireless sensor Networks'. *2013 International Conference on Computer, Control, Informatics and Its Applications (IC3INA)*. 2013: pp. 49–52. DOI: 10.1109/IC3INA.2013.6819147.

119. KUMAR, SANTOSH et al.: 'On k-coverage in a mostly sleeping sensor network'. *Proceedings of the 10th annual international conference on Mobile computing and networking*. ACM. 2004: pp. 144–158. DOI: https://doi.org/10.1145/1023720.1023735.

120. AMINDOUST, ATEFEH et al.: 'Sustainable supplier selection: A ranking model based on fuzzy inference system'. *Applied Soft Computing* (2012), vol. 12(6): pp. 1668–1677. DOI: https://doi.org/10.1016/j.asoc.2012.01.023.

121. NAYAK, PADMALAYA et al.: 'A fuzzy logic-based clustering algorithm for WSN to extend the network lifetime'. *IEEE sensors journal* (2015), vol. 16(1): pp. 137–144. DOI: 10.1109/JSEN.2015.2472970.

122. MIRZAIE, MOSTAFA et al.: 'MACHFL-FT: a fuzzy logic based energy-efficient protocol to cluster heterogeneous nodes in wireless sensor networks'. *Wireless Networks* (2018), vol.: pp. 1–13. DOI: 10.1007/s11276-018-1757-5.

123. HEINZELMAN, W. R. et al.: 'Energy-efficient communication protocol for wireless microsensor networks'. *Proceedings of the 33rd Annual Hawaii International Conference on System Sciences*. 2000: 10 pp. vol.2-. DOI: 10.1109/HICSS.2000.926982.

124. MAO, SONG et al.: 'An improved fuzzy unequal clustering algorithm for wireless sensor network'. *Mobile Networks and Applications* (2013), vol. 18(2): pp. 206–214. DOI: 10.1007/s11036-012-0356-4.

125. NGUYEN, CHINH D et al.: 'Flexible and efficient wireless sensor networks for detecting rainfall-induced landslides'. *International Journal of Distributed Sensor Networks* (2015), vol. 11(11): p. 235954. DOI: https://doi.org/10.1155/2015/235954.

126. SASIDHAR, KALYAN et al.: 'A WSN lifetime improvement algorithm reaping benefits of data aggregation and state transitions'. *2014 IEEE Global Humanitarian Technology Conference-South Asia Satellite (GHTC-SAS)*. IEEE. 2014: pp. 201–205. DOI: 10.1109/GHTC-SAS.2014.6967583.

127. HILL, JASON et al.: 'System architecture directions for networked sensors'. *ACM SIGOPS operating systems review*. Vol. 34. 5. ACM. 2000: pp. 93–104. DOI: 10.1145/378993.379006.

128. *Micro (AAA)-Batterie Alkali-Mangan Conrad energy LR03 1.5 V*. http://www.produktinfo.conrad.com/datenblaetter/650000-674999/658010-da-01-en-CONRAD_ENERGY_ALKALINE_MICRO.pdf. access. May 2019.

129. MAHAPATRA, RANJAN KUMAR et al.: 'Topology Control in Wireless Sensor Networks: A Survey'. (2019), vol.: pp. 335–346. DOI: https://doi.org/10.1007/978-981-10-8204-7_34.

130. *CC1101 Low-Power Sub-1 GHz RF Transceiver*. http://www.ti.com/lit/ds/symlink/cc1101.pdf. access. Dec. 2019.

131. *BS170 Small Signal MOSFET*. http://www.onsemi.com/pub/Collateral/BS170-D.PDF. access. May 2019.

132. *LT1637*. https://www.analog.com/media/en/technical-documentation/data-sheets/1637fd.pdf. access. May 2019.

133. HOUSSAINI, D. EL et al.: 'Wireless sensor networks in agricultural applications: Technology, Components and System Design'. *Energy Harvesting for Wireless Sensor Networks*. DE GRUYTER, 2018: pp. 323–342. ISBN: 978-3-11-044505-3. DOI: 10.1515/9783110445053-017.

134. STERGIOU, CHRISTOS et al.: 'Secure integration of IoT and cloud computing'. *Future Generation Computer Systems* (2018), vol. 78: pp. 964–975. DOI: https://doi.org/10.1016/j.future.2016.11.031.

135. MEHMOOD, RASHID et al.: 'UTiLearn: a personalised ubiquitous teaching and learning system for smart societies'. *IEEE Access* (2017), vol. 5: pp. 2615–2635. DOI: 10.1109/ACCESS.2017.2668840.

136. DEHURY, CHINMAYA KUMAR et al.: 'Design and implementation of a novel service management framework for IoT devices in cloud'. *Journal of Systems and Software* (2016), vol. 119: pp. 149–161. DOI: https://doi.org/10.1016/j.jss.2016.06.059.

137. ASGHARI, PARVANEH et al.: 'Internet of Things applications: A systematic review'. *Computer Networks* (2019), vol. 148: pp. 241–261. DOI: https://doi.org/10.1016/j.comnet.2018.12.008.

138. REDDY, AALA SANTHOSH: 'Reaping the Benefits of the Internet of Things'. *Cognizant Reports, May* (2014), vol.

139. OBILE, W: 'Ericsson mobility report'. *Nov* (2016), vol.

140. DEHKORDI, SOROUSH ABBASIAN et al.: 'A survey on data aggregation techniques in IoT sensor networks'. *Wireless Networks* (2020), vol. 26(2): pp. 1243–1263. DOI: https://doi.org/10.1007/s11276-019-02142-z.

141. JAWAD, HAIDER MAHMOOD et al.: 'Energy-Efficient wireless sensor networks for precision agriculture: A review'. *Sensors* (2017), vol. 17(8): p. 1781. DOI: 10.3390/s17081781.

142. BAYNE, KAREN et al.: 'The internet of things—wireless sensor networks and their application to forestry'. *New Zealand Journal of Forestry* (2017), vol. 61(4): pp. 37–41.

143. BARKUNAN, SR et al.: 'Smart sensor for automatic drip irrigation system for paddy cultivation'. *Computers & Electrical Engineering* (2019), vol. 73: pp. 180–193. DOI: 10.1016/j.compeleceng.2018.11.013.

144. CHAUDHRY, SMITA et al.: 'Smart Irrigation Techniques for Water Resource Management'. *Smart Farming Technologies for Sustainable Agricultural Development*. IGI Global, 2019: pp. 196–219. DOI: 10.4018/978-1-5225-5909-2.ch009.

145. SALES, NELSON et al.: 'Wireless sensor and actuator system for smart irrigation on the cloud'. *2015 IEEE 2nd World Forum on Internet of Things (WF-IoT)*. IEEE. 2015: pp. 693–698. DOI: 10.1109/WF-IoT.2015.7389138.

146. MONICA, M et al.: 'Iot based control and automation of smart irrigation system: an automated irrigation system using sensors, GSM, bluetooth and cloud technology'. *2017 International Conference on Recent Innovations in Signal processing and Embedded Systems (RISE)*. IEEE. 2017: pp. 601–607. DOI: 10.1109/RISE.2017.8378224.

147. VAISHALI, S et al.: 'Mobile integrated smart irrigation management and monitoring system using IOT'. *2017 International Conference on Communication and Signal Processing (ICCSP)*. IEEE. 2017: pp. 2164–2167. DOI: 10.1109/ICCSP.2017.8286792.

148. HAQUE, MD SHADMAN TAJWAR et al.: 'Design and Implementation of an IoT based Automated Agricultural Monitoring and Control System'. *2019 International Conference on Robotics, Electrical and Signal Processing Techniques (ICREST)*. IEEE. 2019: pp. 13–16. DOI: 10.1109/ICREST.2019.8644212.

149. GUTIERREZ, JOAQUIN et al.: 'Automated irrigation system using a wireless sensor network and GPRS module'. *IEEE transactions on instrumentation and measurement* (2013), vol. 63(1): pp. 166–176. DOI: 10.1109/TIM.2013.2276487.

150. KAMIENSKI, CARLOS et al.: 'Swamp: an iot-based smart water management platform for precision irrigation in agriculture'. *2018 Global Internet of Things Summit (GIoTS)*. IEEE. 2018: pp. 1–6. DOI: 10.1109/GIOTS.2018.8534541.

151. PHAM, MANH LINH et al.: 'A Benchmarking Tool for Elastic MQTT Brokers in IoT Applications'. *International Journal of Information and Communication Sciences* (2019), vol. 4(4): pp. 70–78. DOI: 10.11648/j.ijics.20190404.11.

152. AGGARWAL, SHALABH: *Flask framework cookbook*. Packt Publishing Ltd, 2014.

153. *SparkFun Soil Moisture Sensor*. https://www.sparkfun.com/products/13637. access. 2019.

154. *DS18B20 Datasheet*. https://datasheets.maximintegrated.com/en/ds/DS18B20.pdf. access. 2019.

155. LARMO, ANNA et al.: 'Impact of coap and mqtt on nb-iot system performance'. *Sensors* (2019), vol. 19(1): p. 7. DOI: 10.3390/s19010007.

156. *Lighttpd*. https://www.lighttpd.net/. access. May 2019.

157. *Nginx*. https://www.nginx.com/. access. May 2019.

158. *L298: DUAL FULL-BRIDGE DRIVER*. https://www.sparkfun.com/datasheets/Robotics/L298_H_Bridge.pdf. access. 2020.

159. ABBASI, ABU ZAFAR et al.: 'A review of wireless sensors and networks' applications in agriculture'. *Computer Standards & Interfaces* (2014), vol. 36(2): pp. 263–270. DOI: https://doi.org/10.1016/j.csi.2011.03.004.

160. ATANASOV, SVETOSLAV: 'An overview of wireless communication technologies used in wireless sensor networks'. *International Scientific Conference eRA-8*. 2013. DOI: 10.3390/s90906869.

161. ZADEH, LOTFI A: 'Fuzzy logic systems: Origin, concepts, and trends'. *Science* (2004), vol. 80: pp. 16–18.

162. ZADEH, LOFTI A: 'Fuzzy logic, neural networks, and soft computing'. *Communications of the ACM* (1994), vol. 37(3): pp. 77–85. DOI: https://doi.org/10.1145/175247.175255.

163. MELIN, PATRICIA et al.: 'Basic Theory for the Type-2 Fuzzy Sugeno Integral'. *Extension of the Fuzzy Sugeno Integral Based on Generalized Type-2 Fuzzy Logic*. Springer, 2020: pp. 5–27. DOI: https://doi.org/10.1007/978-3-030-16416-4_2.

164. CHEN, YANG et al.: 'Forecasting by designing Mamdani general type-2 fuzzy logic systems optimized with quantum particle swarm optimization algorithms'. *Transactions of the Institute of Measurement and Control* (2019), vol. 41(10): pp. 2886–2896. DOI: https://doi.org/10.1177/0142331218816753.

165. FAJRI, DINY MELSYE NURUL et al.: 'Optimization of FIS Tsukamoto using particle swarm optimization for dental disease identification'. *2017 International Conference on Advanced Computer Science and Information Systems (ICACSIS)*. IEEE. 2017: pp. 261–268. DOI: 10.1109/ICACSIS.2017.8355044.

166. ISSARIYAKUL, TEERAWAT et al.: 'Introduction to network simulator 2 (NS2)'. *Introduction to network simulator NS2*. Springer, 2009: pp. 1–18. DOI: 10.1007/978-1-4614-1406-3_2.

167. RILEY, GEORGE F. et al.: 'The ns-3 Network Simulator'. *Modeling and Tools for Network Simulation*. Ed. by WEHRLE, KLAUS et al. Berlin, Heidelberg: Springer Berlin Heidelberg, 2010: pp. 15–34. ISBN: 978-3-642-12331-3. DOI: 10.1007/978-3-642-12331-3_2. URL: https://doi.org/10.1007/978-3-642-12331-3_2.

168. VARGA, ANDRÁS et al.: 'An overview of the OMNeT++ simulation environment'. *Proceedings of the 1st international conference on Simulation tools and techniques for communications, networks and systems & workshops*. ICST (Institute for Computer Sciences, Social-Informatics and ... 2008: p. 60. DOI: 10.1145/1416222.1416290.

169. SIMULATOR, QUALNET NETWORK: 'Scalable network technologies'. *Inc.[Online]. Available: www. qualnet. com* (2011), vol.: p. 33.

170. HIGHAM, DESMOND J et al.: *MATLAB guide*. SIAM, 2016.

171. SOBEIH, AHMED et al.: 'J-sim: A simulation environment for wireless sensor networks'. *38th Annual Simulation Symposium*. IEEE. 2005: pp. 175–187. DOI: 10.1109/ANSS.2005.27.

172. CHEN, MIN et al.: 'Introduction to OPNET Network Simulation'. *OPNET IoT Simulation*. Singapore: Springer Singapore, 2019: pp. 77–153. ISBN: 978-981-32-9170-6. DOI: 10.1007/978-981-32-9170-6_2. URL: https://doi.org/10.1007/978-981-32-9170-6_2.

List of Figures

List of Tables

List of Algorithms

Scientific Reports on Measurement and Sensor Technology

1. Bouchaala, Dhouha (2016)
Investigation of Current Excitation for Personal Health and Biological Tissues Monitoring
ISBN 978-3-941003-96-9
Volltext: http://nbn-resolving.de/urn:nbn:de:bsz:ch1-qucosa-204801

2. Heidary Dastjerdi, Maral (2016)
Ein Beitrag zur Verbesserung der Eigenschaften magnetisch-induktiver Tastspulen
ISBN 978-3-944640-98-3
Volltext: http://nbn-resolving.de/urn:nbn:de:bsz:ch1-qucosa-207628

3. Guermazi, Mahdi (2016)
In-Vitro Biological Tissue State Monitoring based on Impedance Spectroscopy
ISBN 978-3-96100-003-6
Volltext: http://nbn-resolving.de/urn:nbn:de:bsz:ch1-qucosa-206710

4. Viehweger, Christian (2017)
Modellbasiertes Energiemanagement für die intelligente Steuerung solarversorgter drahtloser Sensorsysteme
ISBN 978-3-96100-022-7
Volltext: http://nbn-resolving.de/urn:nbn:de:bsz:ch1-qucosa-224040

5. Gerlach, Carina (2017)
Dispersionsoptimierung von Kohlenstoffnanoröhren für die Herstellung von Polymer-Komposit-Drucksensoren
ISBN 978-3-96100-025-8
Volltext: http://nbn-resolving.de/urn:nbn:de:bsz:ch1-qucosa-226222

6. Sanli, Abdulkadir (2018)
Synthesis and Characterization of Strain Sensitive Multi-walled Carbon Nanotubes/ Epoxy based Nanocomposites
ISBN 978-3-96100-047-0
Volltext: http://nbn-resolving.de/urn:nbn:de:bsz:ch1-qucosa-233763

7. Weber, Christian (2018)
Entwicklung eines Verfahrens zur Anhaftungserkennung und Trennung von Einflussgrößen bei kapazitiven Näherungsschaltern mit Hilfe der Impedanzspektroskopie
ISBN 978-3-96100-056-2
Volltext: http://nbn-resolving.de/urn:nbn:de:bsz:ch1-qucosa2-234856

8. Benchirouf, Abderrahmane (2018)
Carbonaceous Nanofillers and Poly (3,4- ethylenedioxythiophene) Poly(styrenesulfonate) Nanocomposites for Wireless Sensing Applications
ISBN 978-3-96100-068-5
Volltext: http://nbn-resolving.de/urn:nbn:de:bsz:ch1-qucosa2-319037

9. Naifar, Slim (2019)
Model based Design of a Magnetoelectric Vibration Converter from Weak Kinetic Sources
ISBN 978-3-96100-079-1
Volltext: https://nbn-resolving.org/urn:nbn:de:bsz:ch1-qucosa2-327748

10. Bouhamed, Ayda (2019)
Investigation of Stress Distribution and Adhesion Effects of Strain Sensitive Epoxy/MWCNT Nanocomposite Films
ISBN 978-3-96100-080-7
Volltext: https://nbn-resolving.org/urn:nbn:de:bsz:ch1-qucosa2-327817

11. Bradai, Sonia (2019)
Design and Modelling of a Novel Hybrid Vibration Converter based on Electromagnetic and Magnetoelectric Principles
ISBN 978-3-96100-081-4
Volltext: https://nbn-resolving.org/urn:nbn:de:bsz:ch1-qucosa2-327874

12. Kallel, Bilel (2019)
Design of Inductive Power Transmission System for Low Power Application With Movable Receiver and Large Air Gap
ISBN 978-3-96100-083-8
Volltext: https://nbn-resolving.org/urn:nbn:de:bsz:ch1-qucosa2-329759

13. Chaour, Issam (2019)
Efficiency Improvement of RF Energy Transfer by a Modifier Voltage Multiplier RF DC Converter
ISBN 978-3-96100-079-1
Volltext: http://nbn-resolving.de/urn:nbn:de:bsz:ch1-qucosa2-327748

14. Fendri, Ahmed (2020)
Impedimetric Sensor System for Edible Oil Quality Assessment
ISBN 978-3-96100-107-1
Volltext: https://nbn-resolving.org/urn:nbn:de:bsz:ch1-qucosa2-371733

15. Götz, Martin (2020)
Subthreshold Leakage Voltage Supervisor für den wartungsfreien Betrieb umgebungsenergieversorgter Sensorknoten
ISBN 978-3-96100-115-6
Volltext: https://nbn-resolving.org/urn:nbn:de:bsz:ch1-qucosa2-384055

16. Kheriji, Sabrine (2021)
Design of an Energy-Aware Unequal Clustering Protocol based on Fuzzy Logic for Wireless Sensor Networks
ISBN 978-3-96100-130-9
Volltext: https://nbn-resolving.org/urn:nbn:de:bsz:ch1-qucosa2-733031